# BIODIESEL PRODUCTION FROM MICROALGAE BIOMASS USING CAPROLACTAM-BASED IONIC LIQUIDS

BY

RANIA AWAD NAIYL MUSTAFA

A THESIS SUBMITTED IN PARTIAL FULFILLMENT OF THE REQUIREMENTS FOR THE DEGREE OF DOCTOR OF PHILOSOPHY IN ANALYTICAL CHEMISTRY OF THE DEPARTMENT OF CHEMISTRY AND BIOCHEMISTRY, MOI UNIVERSITY

2023

# DECLARATION

## Declaration by the Candidate

This thesis is my original work and has not been presented for a degree in any other University. No part of this thesis may be reproduced without the prior written permission of the author and/or Moi University.
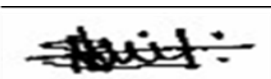
Signature_____ Date    22/12/2022

**Rania Awad Naiyl**

**PHD/ACH/03/18**

## Declaration by the Supervisors

This thesis has been submitted for examination with our approval as the university

supervisors.    _____

Signature_____ Date    07/12/2022

**Prof. Fredrick Orori Kengara**

School of Pure and Applied Sciences

Bomet University College, Bomet, Rift Valley, Kenya

Signature _____ Date   21/12/2022

**Prof. Kirimi Kiriamiti**

Department of Chemical and Process Engineering

School of Engineering,

Moi University, Eldoret, Kenya.

Signature _____ Date   22/12/2022

**Prof. Yousif Ali Ragab**

Department of Chemistry

Faculty of Engineering and Technology

University of Gezira, Sudan

# DEDICATION

I dedicate this thesis to my mother (Zienab Abdelrahman), my father (Awad Naiyl). Without their endless love and encouragement, I would never have been able to complete my academic journey. I love you both and appreciate everything you have done for me. This thesis is also dedicated to my brother (Amar Awad Naiyl) and my sister (Rimaz Awad Naiyl), who supported me in times of difficulty; they deserve my wholehearted thanks. All my relatives, my friends who encourage and support me, and all the people in my life who touch my heart. Thank you so much for being by my side and supporting this wonderful thesis.

# ABSTRACT

Biodiesel (fatty acids methyl esters, FAMEs) is a clean form of energy that could replace petroleum-diesel. Whereas microalgae is a promising renewable and sustainable lipid source for biodiesel production, the main limitation of this process is lack of inexpensive and efficient lipid extraction methods. Lately, the eco-friendly protic ionic liquids (PILs) such as caprolactam ionic liquids (CPILs) and its sulphonic-functionalized form (SO$_3$-bCPILs), have gained prominence in lipids extraction and biodiesel production. This is because of their lower cost relative to common ionic liquids, but they are rarely synthesized or applied. The aim of this study was to investigate the capacity of CPILs and SO$_3$-bCPILs for lipid extraction and biodiesel production from *Spirulina platensis* microalgae. Specifically, the study aimed to synthesize and characterize the CPIL/SO$_3$-CPIL. To extract lipids from both dry and wet algae using a conventional method and synthesized ionic liquids. To study direct and indirect conversion of the triglycerides (lipids) to the corresponding free fatty acids methyl esters (FAMEs-biodiesel). To characterize biodiesel products. To investigate the reusability of these compounds. Nine CPILs/SO$_3$-CPIL, namely, caprolactam chloride (CPHA), caprolactam methylsulphonate (CPMS), caprolactam trifluoromethane sulfonate (CPTFS), sulfonic-butyl caprolactam chloride (SO$_3$-bCPHA), sulfonic-butyl caprolactam methyl sulphonate (SO$_3$- bCPMS), caprolactam acetate (CPAA), caprolactam hydrogen sulphate (CPSA), caprolactam trifluoromethane acetate (CPTFA), and sulphonic-butyl caprolactam hydrogen sulphate (SO$_3$-bCPSA), were prepared through neutralization of caprolactam cations with different Brønsted acids. Lipid extraction from microalgal was performed under reflux at 95 °C for 2 h using pure CPILs, mixtures of CPILs/methanol and SO$_3$-CPILs/methanol in a ratio of 1:1 (w/w), and the control (Hexane: Methanol 54: 46, v/v, 10 h), with a dry/wet microalgae biomass: solvent ratio of 1:19 (w/w). The synthesized SO$_3$- bCPILs/CPILs and lipid/biodiesel extracts were characterized by techniques including Fourier transform infrared (FTIR), Raman, and UV/VIS spectroscopy, thermogravimetric analysis (TGA), gas chromatography-flame ionization detector (GC-FID), the biomass surface by scanning electron microscope (SEM) analysis and predictive methods to estimate the physicochemical properties of biodiesels. Characteristic absorption bands of caprolactam such as N-H (3296, 3209.33 and 3074.32 cm$^{-1}$), C=O (1658 cm$^{-1}$), in FTIR spectra and C-N (1485 cm$^{-1}$) and N-H (697 cm$^{-1}$), in Raman spectra, showed a large change in position/intensity, indicating successful formation of the ionic liquids. The first five of the synthesized compounds are novel. The TGA of SO$_3$-bCPIL/CPILs showed their stability between 108 - 221 °C. The extracted lipids yield was 9.5%/4.1% (dry/wet biomass, control), and 14.2%/13%/11% (CPAA/CPHA/CPTFA, dry biomass, methanol mixtures, P < 0.05). SO$_3$- bCPMS/methanol and SO$_3$-bCPSA/methanol mixtures showed no significant difference compared from control, for wet/dry biomass. SEM analysis showed the absence of intact microalgae cells after extraction by CPAA/CPHA. FTIR spectra of the CPILs/Methanol extracts showed characteristic peaks of FAMEs (C=O, 1739 and 1741 cm$^{-1}$), indicating direct conversion of lipids to biodiesel, and confirming that CPILs act as both solvents and catalysts. GC-FID analysis of the CPIL/methanol and SO$_3$- bCPIL/methanol extracts showed the presence of major FAMEs components found in biodiesel, including palmitic, palmitoleic and oleic acids, except for CPAA, which had the lowest acidity strength - and hence least catalytic activity. The biodiesel yield from indirect conversion using conventional (H$_2$SO$_4$) catalyst was 31%, whereas that of the synthesized compounds with high catalytic activity was 60 – 80%. The physicochemical properties results showed that the quality characteristics of produced biodiesels were in a good agreement with the specifications of international biodiesel standards (ASTM D6751 and EN 14214). The reusability of selected SO$_3$-bCPIL/CPILs (based on yield and extract clarity) was investigated, and there were insignificant differences over six runs. Therefore, the SO$_3$-bCPIL/CPILs method is simple, cost-effective, and faster and has higher or comparable lipid/biodiesel yields to the conventional method and it is recommended that the SO$_3$-bCPIL/CPILs be used as green solvents/catalysts for biodiesel production from other microalgae species.

## Table of content

# LIST OF TABLES

# LIST OF FIGURES

## LIST OF ABBREVIATIONS, ACRONYMS AND SYMBOLS

| | |
|---|---|
| B&D | Bligh and Dyer |
| C2mim | 1-ethyl-3-methylimidazolium |
| CO2 | Carbon dioxide |
| CP | Caprolactam |
| CPIL | Caprolactam ionic liquid |
| $Et_2PO_4$ | Ethyl phosphate |
| EtSO4 | Ethyl sulfate |
| FAMEs | Free fatty acid methyl esters |
| FT-IR | Fourier transform infrared |
| GC-FID | Gas chromatography-flame ionization detector |
| IL | Ionic liquid |
| KBr | Potassium bromide |
| $MeSO_4$ | Methyl sulfate |
| MPa | Mega Pascal |
| NLs | Neutral lipids |
| PIL | Protic ionic liquid |
| SEM | Scanning electron microscopy |
| SHS | switchable hydrophilicity solvents |
| $SO_3$-bCP | Sulphonic butyl-functionalized caprolactamium |
| $SO_3$-bCPIL | Sulphonic butyl-functionalized caprolactamium ionic liquid |
| SPS | switchable polarity solvents |
| TGA | Thermogravimetric analysis |
| UV-VIS | Ultra violate-Visible spectrometer |

# ACKNOWLEDGEMENT

## CHAPTER 1: INTRODUCTION

**1.1 Background of the study**

Energy security has grown to be a critical international issue and much research is being conducted to find environmentally friendly and cost-effective alternatives. Environmental issues associated with the combustion as well as the expected depletion of fossil fuels will limit their future use (Atabani et al., 2012). There are therefore compelling reasons to seek for alternative fuels that are technically feasible, environmentally friendly, economically competitive and readily available to replace fossil fuels. The most important reason is the increasing demand for fossil fuels due to human activities such as transportation, power generation, industrial processes, and domestic consumption. In fact, global energy consumption doubled between 1971 and 2001 and global energy demand will increase by 53% by 2030. (Selaimia et al., 2015). The second reason is that fossil fuels are non-renewable and will be exhausted within 40 to 60 years if the rate of consumption stays constant. (Andreani & Rocha, 2012). Finally, the volatility of petroleum fuel prices is seen as a serious threat to countries with limited economic and financial resources (Isahak et al., 2011)

Extensive research has been carried out on the development of renewable and sustainable energy in the last two decades such as solar energy (Lewis, 2007), tidal energy (Khojasteh et la., 2018), wind energy (Carvalho et al., 2017) and biofuels (bioethanol, biodiesel) (Leung et al., 2010; Molino et al., 2018). One of the most promising renewable green fuels for road and transportation is biodiesel, which is served as a substitute to fossil diesel. The American Society for Testing and Materials (ASTM) describes biodiesel as a mono-alkyl ester produced commonly from renewable sources such as edible/non-edible plant oils or

animal fats (Hameed, Lai, & Chin, 2009). Biodiesel is also known as fatty acid methyl ester (FAME) and fatty acid ethyl ester (FAEE) because it is made by converting vegetable oil with methanol and ethanol, respectively. However, methanol is the most commonly used due to its availability and relatively low cost (Gopinath et al., 2015). It is an energy efficient fuel has gained wide attention and global acceptance due to its non-toxicity, biodegradability and environmental friendliness (Lam & Lee, 2012). However, the economic potential of using biodiesel is currently constrained by the high price of common lipid feed stocks, which constitute between 70% and 85% of the total biodiesel production cost (Olkiewicz et al., 2014). Furthermore, the use of edible and non-edible plants such as palm oil and Jatropha oil, respectively, pose serious challenges such as food shortage, high cost, and lack of consistent supply (Popp et al., 2014).

Nowadays, the prospects of producing biofuels from microalgae appear promising and is considered a more sustainable and cleaner fuel. This is because of their unique attributes such as suitability for growing in open ponds – hence does not require land for production, high $CO_2$-sequestering capability, simple structures, and high photosynthetic efficiency - with a growth doubling time as short as 24 h (Wu et al., 2012). They also have the ability to grow in wastewater /seawater/brackish water, non-interference with the food chain and high-lipid productivity, which enables large-scale biodiesel production (Chisti, 2008; Arumugam et al., 2013). Moreover, microalgae can be grown all year round. The richness of species and biodiversity of microalgae in a wide range of climates and geographies make seasonal and geographical constraints much less of a concern than other lipid feed stocks (Wu et al., 2012). For example, worldwide, more than 50,000 species of microalgae exist in the aquatic as well as terrestrial environments, indicating widespread availability (Deng,

Li, & Fei, 2009). Approximately 4000 species have been identified and can be divided into several groups, including blue-green algae (Cyanophyceae), green algae (Chlorophyceae), diatom (Bacillariophyceae), yellow-green algae (Xanthophyceae), and golden algae (Chrysophyceae), red seaweed (Rhodophyceae), brown algae (Phaeophyceae), dinoflagellates (Dinophyceae) and "Picoplankton" (Prasinophyceae and Eustigmatophyceae) (Deng et al., 2009). Among them, diatoms and green algae are relatively common. The lipid content of most common microalgae is 20-75% by weight of dry biomass (Akubude, Nwaigwe, & Dintwa, 2019) as shown in Table 1.1. There are all potential sources of biodiesel production, as biodiesel yield depends on the lipid content of each cell, which varies greatly between microalgal types as described above (Krasowska et al., 2013). Among the various lipid classes, triacylglycerols (TAGs) are the most important targets for biodiesel production due to their low degree of unsaturation compared to other lipid fractions. Therefore, microalgae with high lipid content and relatively low amount of neutral lipids (TAGs) cannot be considered potential candidates for biodiesel. Microalgae, such as *Chlorella sp*., *Scenedesmus sp*. and *Nannochloropsis sp*., have been considered as the potential species for biodiesel production (Sati et al., 2019). Abubakar et al., (2011) investigated the high oil yielding algae species abundantly distributed naturally in the Kenyan aquatic environment and they found that *Chlorella* species showed the highest yields, followed by *Euglena* and *Nitzschia*. The total lipid content ranged between 1.5 and 10.5% of algal biomass. Although *Spirulina sp* is known for its nutritional benefits with very low lipid content. However, among all other algae, *S. platensis* is the most easy to cultivate due to its inherent resistance to contamination and environmental changes (Baunillo, Tan, Barros, & Luque, 2012). Furthermore, microalgae can be the source of

several types of biofuels such as methane - produced during anaerobic digestion of algae biomass (Krasowska et al., 2013), renewable gasoline and jet fuel and hydrogen- produced photobiologically under anaerobic conditions.

However, the main process limitation in microalgae-based biofuel technology is the efficient and cost-effective extraction of lipids. Conversion of microalgae lipid into biodiesel typically involves the following steps (Figure1.1): cultivation of algae, cell harvesting, lipid extraction, and esterification of lipids (Tripathi & Kumar, 2017). Concerns on flammability and high toxicity of organic solvents, necessitated the search for alternative technologies that are less hazardous to human beings and the environment. In latest years, ionic liquids (ILs) have received considerable attention as an environmentally friendly substitute for harmful volatile organic solvents, due to their non-volatile properties, good chemical and thermal stability, potential recovery and design ability (Zhao & Baker, 2013).

Table 1.1. Lipid content of some microalgae species

| No | Microalgae species | Lipid content (% dry wt.) | Group | References |
|---|---|---|---|---|
| 1 | Anabaena cylindrica | 4–7 | Blue green | Singh et al., 2011 |
| 2 | Ankistrodesmus sp. | 24–41 | Green algae | Kumar, et al. 2015 |
| 3 | Botryococcus braunii | 25–80 | Green algae | Deng et al. 2009 |
| 4 | Chlamydomonas reinhardtii | 21 | Green algae | Singh et al., 2011 |
| 5 | Chlorella emersonii | 28–32 | Green algae | Wu, et al. 2012 |
| 6 | Chlorella minutissima | 57 | Green algae | Kumar, et al. 2015 |
| 7 | Chlorella protothecoides | 57.9 | Green algae | Wu, et al. 2012 |
| 8 | Chlorella pyrenoidosa | 2 | Green algae | Singh et al., 2011 |
| 9 | Chlorella sp | 28–32 | Green algae | Deng et al. 2009 |
| 10 | Chlorella vulgaris | 14–22 | Green algae | Singh et al., 2011 |
| 11 | Crypthecodinium cohnii | 20–51 | Dinoflagellates | Deng et al. 2009 |
| 12 | Cylindrotheca sp | 16–37 | Diatom | |
| 13 | Dunaliella bioculata | 8 | Green algae | Singh et al., 2011 |
| 14 | Dunaliella primolecta | 23 | Green algae | Deng et al. 2009 |
| 15 | Dunaliella salina | 6 | Green algae | Singh et al., 2011 |
| 16 | Dunaliellat ertiolecta | 35.6 | Green algae | Singh et al., 2011b |
| 17 | Euglena gracilis | 14–20 | Dinoflagellates | Singh et al., 2011 |
| 18 | Hormidium sp. | 38 | Green algae | Singh et al., 2011b |
| 19 | Isochrysis sp | 7–33 | Dinoflagellates | Deng et al. 2009 |
| 20 | Monallanthus salina | 20-22 | N/V | |
| 21 | Nannochloris sp. | 30–50 | Green algae | Singh et al., 2011b |
| 22 | Nannochloropsis sp | 12-53 | Diatom | Deng et al. 2009 |
| 24 | Neochloris oleabundans | 29- 65 | Green algae | |
| 25 | Nitzschia sp | 45–47 | Diatom | |
| 26 | Phaeodactylum tricornutum | 18-57 | Diatom | Deng et al. 2009 |
| 27 | Pleurochrysis carterae | 30–50 | N/A | Singh et al., 2011b |
| 30 | Porphyridium cruentum | 9–14 | Red algae | Singh et al., 2011 |
| 31 | Prymnesium parvum | 22–38 | Golden algae | |
| 32 | Scenedesmus dimorphus | 16–40 | Green algae | |
| 33 | Scenedesmus obliquus | 12–14 | Green algae | |
| 34 | Schizochytrium sp | 50–77 | Diatom | Deng et al. 2009 |
| 35 | Spirogyra sp. | 11–21 | Green algae | Singh et al., 2011b |
| 36 | Spirulina maxima | 6–7 | Blue green | |
| 37 | Spirulina platensis | 4–9 | Blue green | |
| 38 | Synechoccus sp. | 11 | Blue green | |
| 39 | Tetraselmis maculate | 8 | Green algae | |
| 40 | Tetraselmis suecica | 15–23 | Green algae | Singh et al., 2011b |
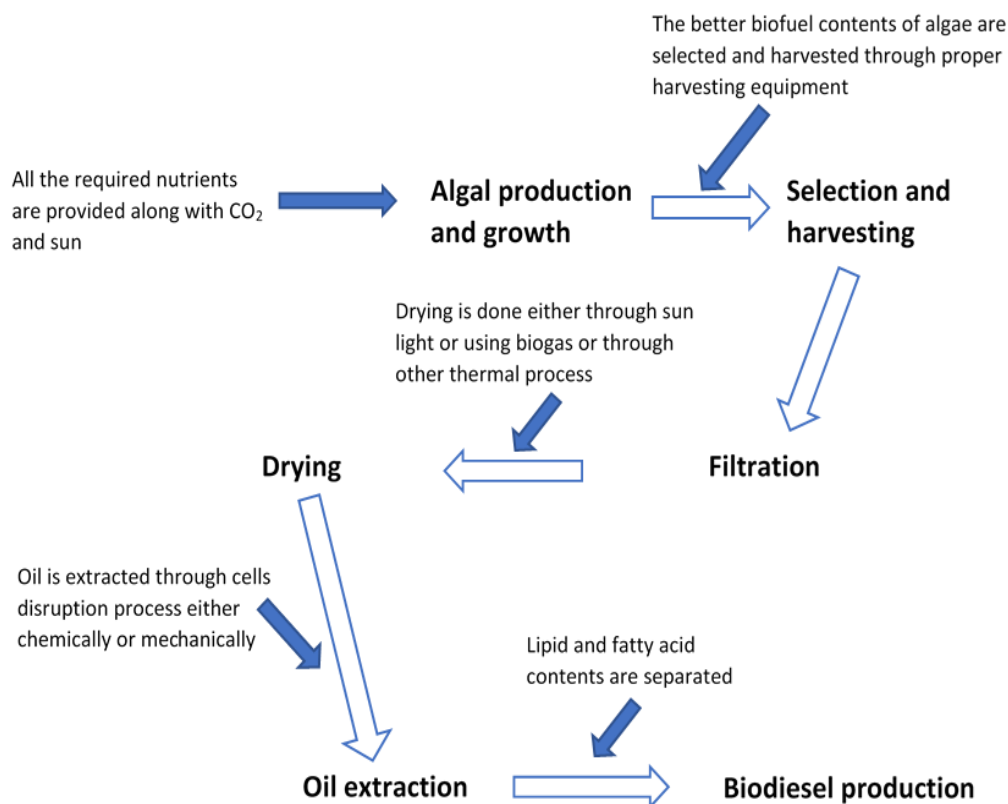
Figure 1.1. The main steps in biodiesel production from microalgae, bold

arrow indicates the addition to specific steps, which have been highlighted

with bold letters and full lined arrows

## 1.2 Ionic liquids

Ionic liquids (ILs) are a group of compounds that have been known for more than a century

(Wilkes, 2002), and have attracted substantial attention in science and technology in the

last two decades. Ionic liquid is an organic salt that melts below 100 °C (some of them are

liquids at room temperature), which is lower than the melting point of ordinary salts such

as Sodium chloride (NaCl), for example, which melts at 801 °C. The earliest discovery of

ionic liquids (ILs) was in the mid-nineteenth-century when a low melting organic salt was

observed as red oil. This oil was generated as a by-product in the Friedel Crafts reaction of

benzene alkylation with aluminum chloride as a catalyst (Wilkes, 2002). The red oil known as chloroaluminate, σ-complex as shown in Figure 1.2. It had remained unidentified until the discovery of the nuclear magnetic resonance technique.
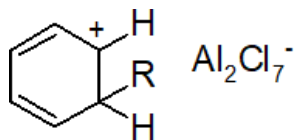


Figure.1.2. Chloroaluminate, σ-complex (red oil)

Ionic liquids are composed entirely of ions (Torimoto et al., 2010): a cation which is normally a bulky organic structure with low symmetry (such as imidazolium, pyridinium, pyrrolidinium, ammonium and phosphonium), and an anion which could be organic or inorganic (such as a halogen ($Cl^-$) , tetrafluoroborate, hexafluorophosphate, triflate, bis[(trifluoromethyl)sulfonyl]imide) as illustrated in Figure 1.3. The forces operating between the cation and anion of an ionic liquid are hydrogen bonds, coulombic interactions, and weak dispersion forces ( Singh et al., 2016). There are three basic chemical reactions for synthesis of ILs, namely metathesis reaction, reaction of imidazole carbenes and acid-base neutralization, which are very simple and inexpensive (Sarf, 2019).

Ionic liquids are divided into two main classes: aprotic ionic liquids and protic ionic liquids. There are possess several superior properties including extremely low vapor pressure, non-flammability, excellent thermal and chemical stabilities, catalytic properties, good solvating potential for a wide range of substrates, and potential recoverability (Zhao & Baker, 2013). Protic ionic liquids (ILs) have attracted considerable attention as a new technology for lipid extraction from microalgae and biodiesel production (Kim et al., 2012; Kim et al., 2013; Choi et al., 2014; Chiappe et al., 2016).
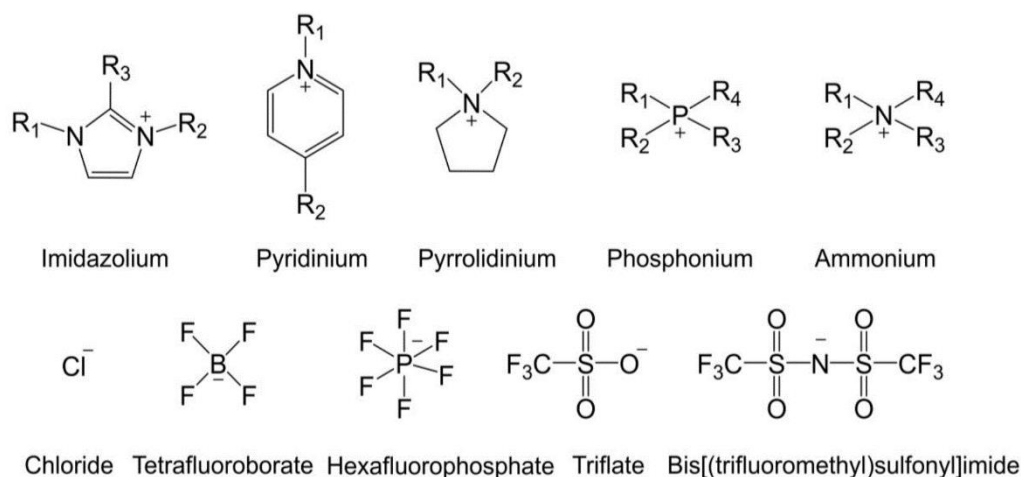
Figure 1.3. Common cations and anions of IL

Protic ionic liquids (PILs) can be synthesized by neutralizing selected bases with protic acids under mild conditions and are therefore significantly cheaper than common ILs (Greaves & Drummond, 2008; Hayes et al., 2015); Xu & Angell, 2003). Besides, protic ionic liquids are known to have low toxicity (Shankar et al., 2017; Shankar et al., 2019) and form strong hydrogen bonds due to labile protons. (Chhotaray & Gardas, 2014). Ionic liquids are also referred to as "designer solvents" because their polarity and hydrophilicity/hydrophobicity can be tuned by an appropriate combination of cation and anion (Ratti, 2014). Thus, different properties such as melting point, viscosity, density and water solubility of the target molecule can be obtained for a particular application (Andreani & Rocha, 2012). Furthermore, while anions are currently used to control solubility in water, cations can also influence hydrophobicity or hydrogen-bonding ability (Huddleston et al., 2001). Therefore, ILs are utilized in a variety of applications such as extractions, separation processes (Ventura et al., 2017), (Xiao, Chen, & Li, 2018) and organic synthesis (Qureshi et al., 2014). In particular, depending on their cation and anionic structures, they can

dissolve important biopolymers such as cellulose and lignin and, thus, disturb the cell structure of algae or change the permeability of the cell wall (Cevasco & Chiappe, 2014). Since the hydrogen bonds of the microalgal cell wall are affected by ions from the ionic liquid, enhancement of lipid extraction due to cell wall modification is expected. Additionally, ILs have found useful applications in sensors, solar cells, solid state photocells, batteries, and as thermal fluids, lubricants, hydraulic fluids, ionogels, fuels and electrolytes in thermoelectrochemical cells due to their wide electrochemical windows and good conductivities (Sarf, 2019; Hayes et al., 2015; Wasserscheid & Welton, 2003; Endres & Zein El Abedin, 2006; Rogers & Seddon, 2003; Plechkova & Seddon, 2008 and Greaves & Drummond, 2008).

**1.2.1 Role of ionic liquids in the transesterification reaction**

Biodiesel production is the process of producing biofuel (biodiesel) through the transesterification chemical reaction. This involves lipids or oils being reacted with an alcohol such as methanol. The ability of ionic liquids to act as catalysts in biodiesel production has received considerable attention due to their "green" catalytic potential (Ab Rani et al., 2011). Interestingly, the solubility, polarity, and acidity/basic properties of ionic liquids can be tailored for specific applications by choosing the cation/anion or its substitution pattern suitably (Chiappe et al., 2009). Both acidic and basic ionic liquids have been extensively studied as catalysts for transesterification reactions in biodiesel production. Replacing conventional catalysts such as sulfuric acid and sodium hydroxide with ionic liquids offers various advantages in terms of reactions, such as low corrosiveness, easy separation, recyclability, and less wastewater (Ishak et al., 2017). Basic ionic liquids have been used as catalysts in the transesterification reaction of biodiesel

(Fang et al., 2013), (Luo et al., 2013). Figure (1.4) illustrates the basic ionic liquid-catalyzed transesterification mechanism in biodiesel production, which proposed by Ishak et al. (2017). The methoxy group of MeOH (1) is deprotonated by the negatively charged anion of the ionic liquid (2). The activated methoxy group is attacked by the electrophilic center (electron deficient center) of the carbonyl carbon of the triglyceride (3). This center is bonded subsequent to two electronegative oxygen atoms. The intermediate (4) is converted to a diglyceride group (5) which produces a fatty acid methyl ester (FAME-biodiesel) (6) or each step of the transesterification reaction is reversible when the alcohol is in excess. Therefore, it is reverted into starting materials. The catalytic activity of basic ionic liquids depends on the anion's ability to activate methoxy groups due to the basicity of the anion and the miscibility between the reactants (Fang et al., 2013). The ionic liquid and the ester product form a separate phase that takes up water formed in the esterification reaction.
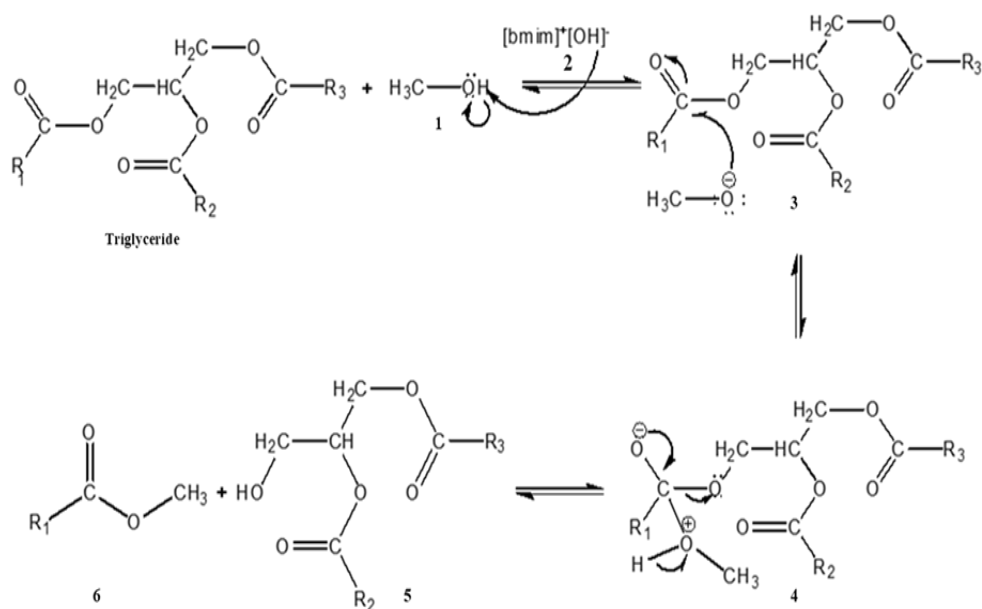


Figure 1.4. Proposed mechanism of basic ionic liquid-catalyzed transesterification reaction for biodiesel production (Ishak et al. 2017)

Similar to the basic ionic liquid mechanism, the acidic anion (1) catalyzes the reaction by donating a proton to the carbonyl group, becoming a stronger electrophile (Figure 1.5). This proton binds to the carbonyl group of triglycerides (2) to form a carbocation intermediate (3), which then reacts with MeOH (4) via a nucleophilic substitution reaction (5) to finally form molecules of a diglyceride (6), FAME-biodiesel (7), and a proton to catalyze the reaction as illustrated in figure 1.5 (Ishak et al. 2017).
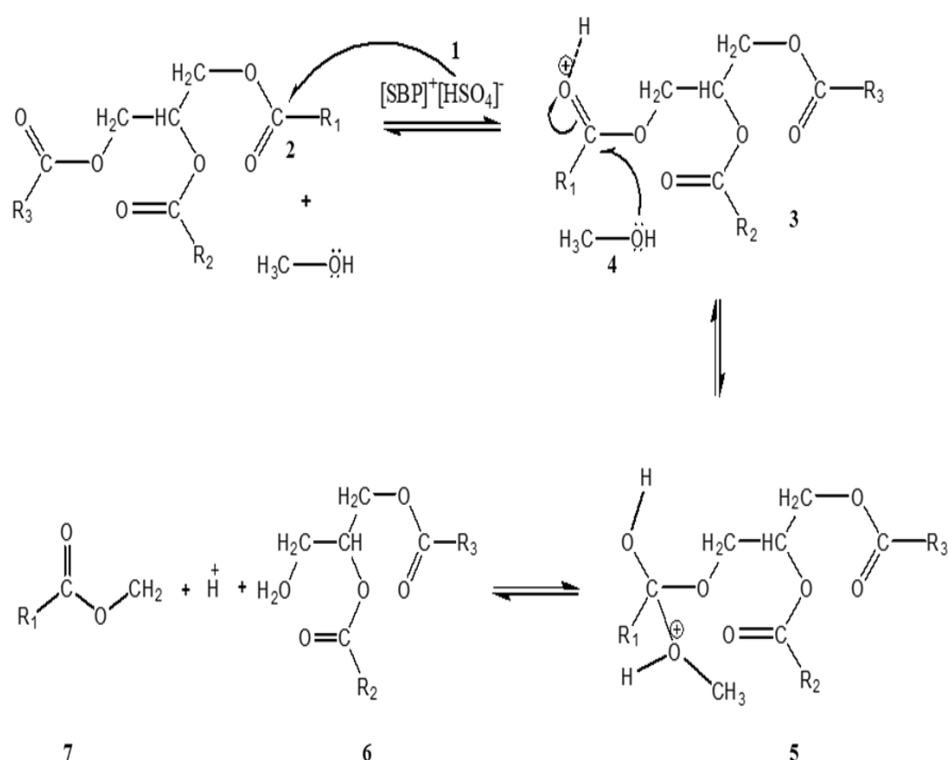


Figure 1.5. Proposed mechanism of acidic acidic ionic liquids catalyzed-transesterification reaction for biodiesel production (Ishak et al. 2017).

## 1.3 Problem statement

The major limitation in microalgal biofuel production is the lack of cost-effective and efficient extraction of lipids. Although higher lipid yields have been recorded after using

methods such as cell disruption (Halim et al., 2012), supercritical $CO_2$ (Crampon et al., 2013 ; Soh & Zimmerman, 2011), liquid $CO_2$, gas expanded liquids (Paudel et al., 2015) the additional energy required makes these processes economically unfeasible. Moreover, conventional lipid extraction methods also require reflux with highly toxic and flammable organic solvents.

The homogenous (sulfuric acid [$H_2SO_4$], or sodium hydroxide [NaOH]), heterogeneous (calcium oxide [CaO], or magnesium oxide [MgO]) and bio-catalysts were used to convert lipids to biodiesel through transesterification reaction ( Zhang et al., 2010; Tran et al., 2012; Kim et al., 2013; Park et al., 2017; Martínez et al., 2017;  & Qasim, 2019). Among them, the homogenous catalysts are relatively cheap. Nevertheless, they have drawbacks, such as high corrosion, difficult of separation, non-recyclability, and a large amount of waste water is generated due to purification of the products (Kim et al., 2013). Therefore, there is an increasing need to research alternative microalgal lipid processing methods that are simpler, cheaper, and more environmentally friendly. Through the analysis of data generated in the reviewed studies, it can be confirmed that ionic liquids have great potential as solvents for extraction of microalgae lipids and as catalysts for biodiesel production. . Despite this great potential of ILs, they present a number of challenges, such as low-cost production of IL, easy recovery, and the ability to reuse the catalyst over multiple biodiesel production cycles. , may limit their suitability and availability for this purpose. Recently, the use of ionic liquids, based on caprolactam cation, a kind of amine derivative as shown in  Figure 1.6, has been identified as promising solution to the problems listed above (Luo et al., 2017; Shankar et al., 2017; Shankar et al., 2019). In spite of the many potential advantages that caprolactam-based ionic liquids could confer, they are rarely synthesized

and hence their application in lipids extraction and biodiesel production remains limited. Therefore, the current focus of ILs research is on developing new types of caprolactam-based ionic liquids that can act as green solvents and catalysts, and thereby improve the long-term viability and sustainability of biodiesel production process from microalgae.
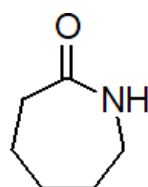


Figure 1.6. Caprolactam

## 1.4 Justification of the study

Among renewable energies, carbon neutral biofuels derived from microalgae seem to be a promising sustainable and cleaner fuels due to their high $CO_2$-sequestering capability, high productivity of lipid and ease of cultivation in an open pond and waste/marine/brackish water (Kumar et al., 2017) . In addition, microalgae considered to be the only renewable biodiesel source that can meet global transportation fuel demand  because they are grown on non-arable areas and require less land than other biofuel crops as well (Sati et al., 2019; Piemonte et al., 2015). Cheng & Timilsina, (2011) reported that if microalgae oil were used to produce biodiesel, it would take about 1.0-2.5% of the current US arable land to provide 50% of US transportation fuel needs, which is much more feasible than current oilseed crops. For instance, annual oil production from oil-rich microalgae ranges from 58,700 to 136,900 liters per hectare per year, which is higher than that of the next best crop, palm with the yield of 5,950 liters per hectare per year (Atabani et al., 2012). Moreover, microalgae have much faster growth-rates than terrestrial crops. Their rapid growth offers opportunities for continuous production of lipid biomass, and thus, insuring the

sustainability of biodiesel production (Velasquez et al., 2016).

 Microalgae showed more benefits over other feedstock such as waste oil and sludge. For example, it can be converted into biodiesel, bio-ethanol, bio-oil, bio-hydrogen and bio-methane by thermochemical and biochemical processes. Furthermore, microalgae can add value by absorbing the gases that emitted by burning of fossil fuels (or other processes) such as $CO_2$, $NO_2$, and $SO_2$, which are released into the atmosphere with impacts on the environment (climate change), economy and health (Chiappe et al., 2016; Majewski & Jaaskelainen, 2004).

Protic ionic liquids (PILs) have gained growing interest in science and technology. The PILs are normally simpler and less costly to prepare than other classes of ILs - due to the absence of byproducts (Du et al., 2005). Therefore, the use of PILs as novel green solvents for lipid extraction that can replace flammable and highly toxic volatile solvents (such as hexane and chloroform) has attracted significant attention. Lactams, particularly caprolactam (CP) are relatively cheaper, have lower intrinsic toxicity (hence safer to use) (Luo et al., 2017), and is available in large quantities from industry (i.e. used in the textile industry to produce polyamide 6) (Du et al., 2005).

All previous studies, where ionic liquids were used as solvents, focused on anionic hydrogen bonds that permeate algal cell structures. However, the utilization of caprolactam-based ionic liquid (which can be easily synthesized through acid-base neutralization reaction) could introduce a cation that possesses hydrogen-bonding capabilities. As shown in Figure 1.6 above, carbonyl groups added to lactams can provide specific functionality when these lactam-based ionic liquids are used as solvents or catalysts.

**1.5 Objectives of the study**

**1.5.1 Main objective**

To establish whether the long-term viability and sustainability of lipid extraction processes from *Spirulina platensis* microalgal biomass and their direct and indirect conversion to biodiesel (FAMEs) can be improved using caprolactam-based ionic liquids.

**1.5.2 Specific objectives**

To accomplish the main objective of the study; the following specific objectives were achieved:

1. To synthesize and characterize caprolactam-based ionic liquids.

2. To extract and characterize lipids from both dry and wet algae using a conventional organic solvent method and the synthesized ionic liquids.

3. To investigate direct and indirect conversion of the lipids to the corresponding fatty acid methyl esters (FAMEs-biodiesel).

4. To evaluate the quality of the produced biodiesels.

5. To investigate the reusability of the ionic liquids.

**1.5.3 Research Questions**

i. Will ionic liquids be synthesized successfully?

ii. Will ionic liquids extract the lipids from wet and dry algae biomass?

iii. Will ionic liquids catalyze direct and indirect transesterification reaction for biodiesel production?

iv. Will the transesterification reaction products contain fatty acid methyl esters (FAMEs-biodiesel)?

v. Will ionic liquids be easily recovered and reused many times?

## CHAPTER 2: LITERATURE REVIEW

Algae have received considerable attention in recent years as one of the most promising sustainable biomass sources for biodiesel production. Biodiesel production from microalgal oil has been previously demonstrated in the literature using conventional methods. In these methods, lipids are extracted from microalgal biomass and subsequently converted to FAMEs by chemical transesterification reactions (Montes et al., 2011). The efficient lipid extraction from microalgae biomass is the most important process in biodiesel production because it is associated with cell destruction (Halim et al., 2012). Therefore, lipid extraction has been identified as one of the most energy-intensive steps in the production of biodiesel from microalgae (Khoo et al., 2011).

### 2.1 Cell disruption of microalgae

Microalgal cell membranes are rigid and frequently require cell disruption to permit the discharge of intracellular lipids. Thus, various cell disruption methods have been investigated to improve the mass transfer efficiency of extraction with organic solvents (Halim et al., 2012). Theoretically, cell disruption increases the surface area of the interface between the lipid and the organic solvent, thus shortening the extraction time (Halim et al., 2012). However, many cell disruption methods can be energy intensive, thus, any increase in lipid extraction effectiveness must be substantial to justify their use. The cell disruption techniques used for microbial cells differ significantly from those used on oilseeds due to the much smaller size of microalgae, bacteria and yeasts (Orr, 2016). Cell disruption can be applied before or simultaneously with the lipid extraction step by mechanical, chemical or biological methods. Mechanical disruption can rupture most biomass membranes by physical forces. These include bead mills, presses, high pressure homogenization,

ultrasound, freeze drying and microwave (Lee et al., 2010; Zheng et al., 2011; Halim et al., 2012; Aguirre & Bassi, 2014; Kumar et al., 2015). Among the mechanical cell disruption methods, bead milling seems to be the most appropriate for large-scale application due to its low operating cost  (Halim et al., 2012).

Chemical disruption techniques typically include detergents, acids, bases, solvents, osmotic shock (Lee et al. 2010; Zheng et al. 2011; Halim et al., 2012; Kumar et al., 2015). Most chemical disruption techniques destroy the membrane/cell wall by intermolecular force. Chemical disruption is often performed concurrently with lipid extraction, most commonly using polar and/or non-polar solvents. (Orr, 2016).

Biological disruption processes involve the use of enzymes that degrade membrane polysaccharides and/or proteins. The use of enzymes offers high selectivity and the mildest reaction conditions. However, they are so expensive that their implementation has so far been limited. Mechanical and chemical disruption methods destroy microalgae in a non-selective manner. Mechanical disruption damages all species present in solution, and chemical disruption may involve side reactions with triacylglycerides (TAG) and free fatty acids (FFA) from microalgal cells. Biological methods can selectively target which bonds need to be broken in order to salvage lipids without side reactions or completely destroy them all (Orr, 2016). Advantages and disadvantages of these pretreatments are presented in Table 2.1.

## 2.2 Lipid extraction of microalgae

Cell disruption can effectively release microalgal lipids from biomass for microalgal biofuel production, but requires an extraction step to separate valuable neutral lipids and fatty acids from the cell matrix. Extraction can be done from dry biomass powder or

directly from wet concentrated biomass (Xu et al., 2011). Solvents play an important role in both methods by facilitating cell disruption and increasing the efficiency of lipid extraction by enhancing the mass transport properties of biomass (Ehimen et al., 2012). However, traditional solvent-based methods for lipid extraction are difficult to meet economic and environmental requirements.

Most studies have explored extraction methods that based on alternative solvents such as supercritical $CO_2$ (Crampon et al., 2013; Soh & Zimmerman, 2011), liquid $CO_2$, gas expanded liquids (Paudel et al., 2015) ionic liquids (ILs) (Orr, 2016), switchable solvents (Boyd et al., 2012) and deep eutectic solvents (Zhao & Baker, 2013). Below is a brief summary of the rationale for each method, as well as recent advances in the field and the challenges faced by the technology.

Table 2.1.The pretreatment technologies for cell disruption

| Method | Advantages | Disadvantages | References |
|---|---|---|---|
| Bead-milling | Work with difficult to lyse species | Difficult scale up Energy intensive High equipment costs | Halim et al., 2012 |
| Acid/alkaline hydrolysis | Low cost of equipment Low energy | Neutralization of waste needed Possible products degradation | Halim et al., 2012 |
| Steam explosion | Short processing time | Energy intensive High equipment costs Possible products degradation Potential | Halim et al., 2012 |
| Microwave-irradiation | Short processing time | Energy intensive High equipment costs. Possible products degradation. | Lee et al. 2010 |
| Ultrasonication | Short processing time | Energy intensive High equipment costs | Kumar et al., 2015 |
| Osmotic shock | Low energy. Mild conditions. Low cost of materials and equipment. | Long treatment time | Halim et al., 2012 |
| Enzymatic lysis | Low cost of equipment. Low energy. Mild conditions. | High cost of enzyme Long treatment of enzyme | Zheng et al. 2011 |
| Surfactant-assisted extraction | Mild condition low energy | The recovery process is often difficult | Halim et al., 2012 |

## 2.2.1 Traditional organic solvent and co-solvent extractions

Early methods of microalgal lipid extraction based on traditional organic solvents. The ideal solvent for this process is neutral lipid (NL) specific, highly volatile, and can

minimize energy distillation costs in separating the lipids from the solvent after extraction (Grima et al., 2013). Lipid extraction from microalgal biomass can be achieved using polar organic solvents such as methanol, acetone and ethanol and less polar organic solvents such as hexane, benzene, toluene, diethyl ether, ethyl acetate and chloroform. Low-polarity organic solvents alone cannot effectively extract NLs because they are inaccessible to those that form strong hydrogen bonds with polar lipids in the cell wall (Tang et al., 2016). To access these NLs, polar organic solvents must be combined with less polar organic co-solvents. Polar organic solvents are designed to disrupt neutral-polar lipid complexes and less polar organic solvents are designed to solubilize intracellular NLs. Therefore, a solvent system containing a mixture of low-polarity and polar organic solvents generally maximizes the extraction efficiency of NLs (Tang et al., 2016).

In 1957, Folch used a 2:1 (v/v) mixture of chloroform:methanol for lipid extraction from animal tissues; this is known as the Folch method (Folch, Lees and Stanley, 1957). This method was developed by Bligh and Dyer in 1959 using 2:1:0.8 by volume of chloroform: methanol: water for total lipid extraction and purification (Bligh & Dyer, 1959). A single-phase system is observed when the wet tissue is homogenized with a mixture of chloroform and methanol. However, the addition of water creates a two-phase system in which the chloroform layer contains the lipids and the methanol-water layer contains the non-lipids. These two methods are considered standard for conventional organic solvent extraction of microalgal lipids.

A recent study by Hidalgo et al., (2016) found that a 1:3 v:v mixture of chloroform: methanol was able extract 98.9 % of esterifiable lipids from *Botrycoccus braunii*, whereas a 3:1 mixture of methanol: diethyl ether could extract 96.9 % of esterifiable lipids without

the use of halogenated solvent. Unfortunately, diethyl ether is highly flammable and, like chloroform, is industrially unacceptable. Some researchers also found that adding formic acid increased total lipid yield. Kuan et al., (2016) studied the extraction of lipids from dried *Chlorella protothecoidesis*. The highest lipid yield of 42% (w/w) was obtained using a solvent mixture consist of 70% dichloromethane, 20% formic acid, and 10% methanol, with a FAME yield of 89% (w/w). There are several major barriers associated with conventional organic solvent extraction-based methods. The costs associated with large-scale lipid extraction from microalgae using conventional solvent systems are unlikely to make these processes economically viable. Solvent loss due to evaporation presents a defect both from an environmental and an economic point of view. Although conventional organic and co-solvent extraction methods are effective in extracting lipids from dried microalgae biomass, they face significant limitations, including the use of halogenated organic solvents and inefficiencies encountered during lipid extraction from wet microalgae (Viner, 2017). Halogenated organic solvents are unlikely to be used industrially due to health and environmental concerns, such as ozone depletion, groundwater contamination and carcinogenic potential. In addition, most organic and co-solvent extraction methods require large volumes of chlorinated, flammable and/or volatile solvents to obtain high lipid yields, which can have significant environmental impacts, including water-borne waste stream pollution and solvent-related impacts (Viner, 2017). Residual water in the microalgal slurry impedes the mass transfer of lipids from the microalgal cells and reduces the efficiency of lipid extraction. To avoid this problem, energy-intensive drying is usually performed (Chen, Chang, & Lee, 2015). Therefore, it is

important to develop more environmentally friendly extraction processes to improve the overall technical and economic feasibility of algal biofuel production.

### 2.2.2 Supercritical $CO_2$ extraction method

Supercritical fluid extraction (SFE) is emerging as an alternative to traditional organic solvent-based extraction methods due to health and safety concerns and the environmental impact of organic solvents (Santana et al., 2012). "A supercritical fluid (SCF) is a compound, mixture, or element that is above its critical temperature and pressure, but below the pressure required to condense into a solid" (Jessop & Leitner, 2007). SCF has many attractive properties as an extraction solvent, such as the tunable dissolving power of the liquid. In particular, $CO_2$ has a very low polarity, allowing NL to be preferentially extracted (Mendes et al., 2003). The most common liquid used in SFE studies reported to date is supercritical $CO_2$ ($scCO_2$). It has many advantages over Soxhlet extraction and conventional organic solvent extraction, including higher selectivity, shorter extraction time, low toxicity, minimal oxidation or thermal decomposition of extracts, fast penetration through the cell matrix, high diffusivity and easy product/solvent separation (Y.Li et al., 2014). Therefore, $scCO_2$ extraction is a greener and promising extraction technology, usually performed at 50–80°C, high pressure 200–300 bar, for 80 min (Santana et al., 2012). There are a number of studies recently published on improving the extraction technique of $scCO_2$. Taher et al., (2014) investigated the extraction of $scCO_2$ lipids from Scenedesmus sp. for biodiesel production. The best results were obtained at 50 MPa, 53°C and a continuous $scCO_2$ flow of 1.9 g/min, yielding a lipid extraction efficiency of 7.4% wt. This study also compared $scCO_2$ extraction with Soxhlet, chloroform/methanol, n-hexane extract as well as n-hexane/isopropanol extraction and the optimized $scCO_2$ method

showed the highest yields of total lipids and triacylglycerols (Taher. et al., 2014). McKennedy et al., (2016) investigated the effect of $scCO_2$ and co-solvent extraction conditions on the distribution of recovered FAMEs. The authors have shown that $scCO_2$ with co-solvents such as methanol and hexane can efficiently extract fats without excessive heat. Viguera et al., (2016) described the effects of operating conditions and water content on the extraction of $scCO_2$ lipids from C. protothecoides. At 30 MPa $CO_2$, 70°C and a flow rate of 72 kg CO2/h.kg biomass, the maximum lipid yield achieved was 21% (w/w), which is one of the highest values reported for microalgae. Although $scCO_2$ avoids the use of environmentally harmful organic solvents, it still requires high capital costs to build and operate equipment under high pressure conditions. As a result, the economical production of biodiesel from microalgal lipids is limited by the energy and capital costs associated with the extraction techniques described. An ideal extraction process would not require the use of high pressure and would also avoid the need for a distillation step. Gas expansion liquid extraction provides a potential solution to these challenges.

### 2.2.3 Gas-expanded liquid extraction method

A gas-expanded liquid is made by dissolving a compressible gas, such as $CO_2$ or light olefins, in the conventional liquid phase at moderate pressures (tens of bar) (Subramaniam, 2010). When $CO_2$ is used as an expansion gas, the resulting liquid phase is called $CO_2$ expansion liquid (CXL). CO2-expanded liquid (CXL) has been used in a variety of applications including extractions, separations, and reactions (Scurto, Hutchenson, & Subramaniam, 2009; Lin et al., 2013). The Life Cycle Assessment (LCA) has determined that the environmental impact of microalgal oil extraction using CXL is only one-tenth that of other extraction methods including chloroform/methanol, dichloromethane/methanol,

isopropanol/hexane, $scCO_2$ and $CO_2$ expansion ethanol. , especially regarding inhalation toxicity and climate change impacts (Wang et al., 2016). Moreover, another LCA performed by Collotta et al., (2017) compared the extraction system based on the common solvents (chloroform: methanol), non-expanded methanol and $CO_2$- expanded methanol (CXM). $CO_2$-expanded methanol (CXM) showed the lowest environmental impact of all categories tested. Furthermore, CXM has recently been considered an effective method for the extraction of triglycerides from the microalgae biomass of Botryococcus braunii, as it requires much less pressure than supercritical $CO_2$ extraction. However, normalized extraction compared to the standard Folch extraction procedure only recovered 50% of the available oil (Paudel et al. 2015). Additionally, CXL provides environmental benefits over conventionl organic solvents, including significant replacement of organic solvents with eco-friendly $CO_2$ and process safety benefits such as reduced flammability related to the presence of $CO_2$ in the vapor phase (Subramaniam, 2010). Further work will be needed to evaluate the limitations of this technology.

### 2.2.4 Extraction method of Liquid $CO_2$

The high capital cost of $scCO_2$ is mainly due to the need of high pressure equipment (Liau et al., 2010) and is a major obstacle of this technology. Liquid $CO_2$ extraction has considered as a viable alternative requiring lower temperatures and pressures than $scCO_2$ extraction while avoiding the toxic or flammable organic solvents used in conventional solvent extraction. For example, to obtain a density of 0.8 g/mL is high enough for an acceptable solubilizing power. $scCO_2$ at 50 °C requires a pressure of 21 MPa, while $lCO_2$ at 25 °C requires only 9 MPa (Viner, 2017). $lCO_2$ is less polar than most organic solvents, exhibits high selectivity over neutral lipids, which are most desirable for biodiesel

production, and can minimize co-extraction of less desirable polar lipids in biodiesel production (Crampon et al.,. Unfortunately, there are limited studies on the topic of $lCO_2$ extraction. Paulel et al. (2015) found that $CO_2$ extraction performed on lyophilized *B. braunii* at 6.8 MPa and 25°C resulted in a lipid yield of 19% (w/w). Chen et al., (2013) investigated that high yields could be provides with $lCO_2$ in a continuous lipid extraction from a slurry of pre-dried commercial microalgae rich in docosahexaenoic acid (DHA; an omega-3 fatty acid) under pressures of up to 20 MPa. While these initial results are encouraging, more experimental results are needed to evaluate the effectiveness of $lCO_2$ technology.

## 2.2.5 Ionic liquids extraction

Since the cell walls of microalgae are mainly composed of cellulose, ionic liquids are considered effective solvents to dissolve microalgae. Therefore, the role of ionic liquids in lipid extraction from microalgae, is to use their ability to destroy the cellular structure of microalgae by dissolving biomass simultaneously, as well as displacing organic solvents (Choi, Oh, et al., 2014; Kim et al. 2013). Most of the ionic liquids studied so far have focused on imidazolium-based ionic liquids, probably because they are commercially available. A few publications described the use of pyridinium, ammonium, phosphonium, quanidinium and caprolactamium based ionic liquids (Fauzi & Amin, 2012; Olkiewicz et al. 2015; Orr, 2016; Yang et al., 2017; Chiappe et al. 2016; Shankar et al., 2017; Shankar et al., 2019). *Chlorella vulgaris* is probably the most studied microalgae for ionic liquid extraction, as it is known to be one of the most difficult species to dissolve (Orr, 2016).

## 2.2.5.1 Ionic liquids extraction using dry microalgae

Orr, (2016) reviewed that all the ionic liquids described to date were hydrophilic and water-

soluble ionic liquids, except of 1-ethyl-3-methylimidazolium bis (trifluoromethylsulfonyl) imide [$C_2$mim][$NTf_2$]. Dialkylimidazolium cations can be widely used in combination with alkyl ester sulfates or phosphate. [$C_2$mim] in combination with either [$EtSO_4$], [$MeSO_4$], or [$Et_2PO_4$] generally resulted in higher lipid yields (>70%) compared to conventional solvent extraction methods. One of the most commonly known ionic liquids is 1-ethyl-3-methylimidazolium chloride [$C_2$mim][Cl], which has also exhibited high lipid extraction efficiency, whereas other dialkylimidazolium chlorides worked poorly. Interesting 1-hexyl-imidazolium showed moderate capacity (53.4%) to extract lipids at room temperature even when the ionic liquid water content was 30% (Orr, 2016). Acidic ionic liquids consisting of carboxylate anions also exhibited some lipid extraction capacity, which increased with increasing processing temperature and decreased with increasing carboxylic acid chain length. There are few reports of pyridinium, ammonium, and phosphonium based ionic liquids for lipid extraction. However, ammonium and phosphonium-based ionic liquids can be significantly cheaper to synthesize than their imidazolium-based ones (Olkiewicz, 2015; Shankar et al., 2017; Shankar et al., 2019). Similar to dialkylimidazolium ionic liquids studied to date, methyl-triethyl ammonium methyl sulphate [$N_{1\ 2\ 2\ 2}$] [$MeSO_4$] exhibited good lipid recovery, as did ammonium or phosphonium cations that combined with carboxylic acids. Lastly, only three pyridinium based ionic liquids were tested at room temperature, however, 1-butyl-3-methylpyridinium bromide[$C_4$mβpy][Br], exhibited significant disruption of the microalgal cell structure, allowing recovery of 100% of available lipids (Orr, 2016). Choline amino acid-based ILs is made up of bioavailable compounds (bio-based ILs), which can be considered as greener solvents as well as catalysts (Hulsbosch et al., 2016), which also considered as low cost IL

compared to imidazolium ILs. Based on a variety of choline amino acid-based ILs investigated for lipid extraction from microalgae in the study of To et al., (2018), choline arginine [Ch][Arg] gave higher extraction performance (up to 51.1% of total lipids) than glycine, lysine, phenylalanine anions based ILs. Using aqueous solutions (65% IL- 35% water) instead of pure ILs and mild pretreatment conditions (70 °C, 3h). However, the used of the concentrated hydrochloric acid in order to convert fatty acids to their neutral form that is more soluble in hexane to achieve high efficient extraction would be a major challenge in this process.

Reaction conditions can play an important role in the success of screening studies using ionic liquids. Lower temperatures are generally desirable to minimize the energy required for the overall process. However, because many ionic liquids exhibit high viscosity at low temperatures, most studies have focused on the treatment of algal biomass at temperatures between 100 and 120°C. Viscosity also can be decreased to some extent by using a co-solvent such as methanol. The ability to extract lipids using a mixture of an ionic liquid and a polar organic solvent has been demonstrated. In general, methanol was found to have little effect on lipid yield compared with ionic liquids alone, while hexane was found to decrease lipid extraction and chloroform increased it (Choi, Oh, et al., 2014). Acetone has also emerged as a promising co-solvent for [C$_2$mim][MeSO$_4$] (Young et al., 2010).

A study by (Kim et al., 2012) monitored several IL-methanol co-solvents for lipid extraction from the microalgae *Chlorella vulgaris* to determine their effectiveness compared with the commonly used Bligh and Dyer method. The ILs used include 1-butyl-3-methylimidazolium methyl sulfate [BMIm][MeSO$_4$], 1-ethyl- l-3-methylimidazolium methyl sulfate [EMIm][MeSO$_4$], and 1-butyl-3-methylimidazolium methyl sulfate triflate

[BMIm] [CF$_3$SO$_3$] with extraction yield of 11.84%, 11.88% and 12.54%, respectively, achieving higher yields than the 10.6% extraction method of Bligh and Dyer. This indicated that the lipid extraction efficiency was affected by the anionic structure and the hydrophobic or hydrophilic properties of the IL. In addition, Choi, Oh, et al., (2014) compared the effect of 12 ILs on the lipid extraction yield of *Chlorella vulgaris* microalgae. The results showed that ILs with organic solvents and IL mixtures, generally had higher lipid yields due to synergistic influences with various anions. For instance, the mixture of hydrophilic ionic liquid 1-ethyl-3-methylimidazolium acetate [C2mim][Ac] and the hydrophobic ionic liquid [C$_2$mim][NTf$_2$] increased the extraction efficiency from 76.3 and 59.5% with each ionic liquid alone respectively, to 87.5% together compared to Bligh & Dyer extraction. Moreover, the yield improvement effects of mixing of molten salt with ionic liquid were investigated. Among the three molten salts zinc nitrate hexahydrate (Zn(NO$_3$)$_2$·6H$_2$O), Magnesium perchlorate hexahydrate (Mg(ClO$_4$)$_2$·6H$_2$O), and ferric chloride hexahydrate (FeCl$_3$·6H$_2$O), FeCl$_3$·6H$_2$O increased overall [C$_2$mim][Ac] extraction efficiency up to 70% of available FAMEs (Choi, Lee et al., 2014; Choi, Jung, et al., 2014).

### 2.2.5.2 Ionic liquid extraction using wet microalgae

One of the largest cost factors in lipid extraction from microalgae is the dehydration and drying process. Therefore, the extraction of lipids from wet algal biomass by ionic liquids has received much attention. Salvo et al., (2011), Salvo et al., (2013) and Teixeira, (2012), have demonstrated the disruption of predominantly *Chlorella sp* structures using wet culture. Several species have been dissolved within one hour at temperatures above 100 °C, mostly using imidazolium chloride-based ionic liquids. Soon after, the wet disturbance

of the cyanobacterium *Synechocystis sp*. was performed using 1-ethyl-3-methylimidazolium methylphosphite $[C_2mim]$ $[MeO(H)PO_2]$ and 1-ethyl-3-methylimidazolium acetate $[C_2mim]$ $[O_2CMe]$ at room temperature for 30 min (Fujita et al., 2013). It has also been reported that hydrophobic ionic liquids $[C_2mim][NTf_2]$ and 1-ethyl-3-methylimidazolium tetrafluoroborate $[C_2mim][BF_4]$ were ineffective but has since shown some ability to extract lipids (Kim et al. 2012; Choi, Oh, et al., 2014). More recent reports have provided a better analytical understanding of extraction efficiency and the role of water in ionic liquid-based lipid extraction. Lipids were successfully extracted from fresh *N. oculata* biomass containing 71.7% water using phosphonium-based ionic liquid $[P(CH_2OH)_4]Cl$ (Olkiewicz, 2015). About 75% of the available lipids were extracted using the ionic liquid based method when compared to the B&D method. Both methods exhibited a higher tendency to extract short-chain fatty acids when wet biomass was used. The ionic liquid $[C_2mim][EtSO_4]$ in combination with the co-solvent methanol has also been shown to successfully extract lipids from wet biomass (Orr, 2016). This study also demonstrated that at water contents above 82% wt., the extraction efficiency decreased significantly and the solids loading factor and methanol to ionic liquid ratio dropped above or below 2:1 (Methanol:IL). In both studies, room temperature ionic liquids could be processed in less than an hour, and these ionic liquids were successfully reused up to four times.

Other reports have recently been reviewed that combined ionic liquid extraction from wet biomass with other methods of disruptions. For example, ultrasound or microwave irradiation combined with ionic liquid extraction using 1-ethyl-3-methylimidazolium hydrogensulfate $[C_4mim][HSO_4]$ increased yields over ionic liquids alone , which was not compared with the theoretical maximum yield from dried biomass-extracted lipids (Pan et

al., 2016). In addition, previous studies using the related ionic liquid [C$_2$mim][HSO$_4$] showed very poor extraction of lipids from dry biomass (less than 15% of total available lipids) (Choi, Lee, et al., 2014; Choi, Oh, et al. ., 2014) and microwave irradiation and ultrasound are known to enhance the disruption of wet algae. It is difficult to discern whether the ionic liquid actually assisted this process, as no microwave irradiation or ultrasound negative controls were performed without the presence of the ionic liquid using the same extraction procedure. In another report using ultrasonication, again, no extraction was performed without the presence of ionic liquid using the same conditions as the IL extraction (for example the same solvents) and the total lipid content of the algae biomass produced was less than 3% (w/w). Using the B&D method indicating that either the control extractions worked poorly, or there was no neutral lipids present in the biomass used (Wahidin et al., 2016). Finally, in a report involving the use of tri-etylammonium hydrogen sulfate [N$_{0\ 2\ 2\ 2}$] [HSO$_4$] in combination with high-pressure extraction (1 MPa) for 1 h at 110°C resulted in the extraction of extraction of all available lipids. However, again, no negative controls were used to distinguish the role of ionic liquids from the role of extraction conditions at temperature and High pressure is used (Chen, Hu, et al., 2015; Zhuanni et al., 2016). In addition, the ionic liquid concentrations used in this study was 1% in water, were extremely low and thus these ionic liquids would be present mainly in dissociated form, which will greatly reduce their unique solvent properties.

Recently, a novel protic IL (PIL) has been investigated for microalgal cell disruption and lipid extraction (Shankar et al., 2017; Shankar et al., 2019). The applicability of some PILs with butyrolactam, caprolactam, propylammonium and hydroxypropylammonium cations in combination with formate, acetate and hexanoate anions for cell disruption and lipid

extraction from microalgae was evaluated in these studies. The results showed that the lipid yield of formate and hexanoate-PIL anions was statistically comparable and/or superior to that of the B&D control. Furthermore, both studies explain the promising ability of these inexpensive green solvents, especially PIL containing formate and hexanoate anions, to be used for a relatively energy efficient and one-step cell disruption and lipid extraction process from wet microalgae.

**2.2.5.3 Switchable solvents**

Switchable solvents are a subclass of ionic liquids that can be divided into two categories: switchable polar solvents (SPS) or switchable hydrophilic solvents (SHS) (Orr, 2016). There are also called 'reversible' or 'smart' solvents that can reversibly change their properties when a 'trigger' is applied or removed. (Jessop, 2015). SPS invented by Jessop, (2015), switch from low polarity to high polarity IL upon $CO_2$ (the trigger) exposure (Figure 2.1). Solvent polarity can be reversed by removing $CO_2$. This can be accomplished by heating the solution or aerating it with a non-acidic gas such as air, $N_2$, or Ar gas. Thus, SPS can extract lipids in one form and then separate the lipids from the solvent in the most polar form (Samorì et al., 2010; Samorì et al., 2013). N,N-Dimethylcyclohexylamine mixed with octanol has been shown to be effective in extracting lipids from the wet biomass of *Nannochloropsis gaditana* and *Tetracermis suecica*, *Desmodesmus communis* compared to 1,8-diazabicyclo-[5.4.0]-undec-7ene (DBU) octanol extraction of *Botryococcus braunii*, however it is difficult to ascertain whether this was due to differences in these microalgae species. Although this process can provide a unique method for lipid separation, the process is time consuming and can take 24 hours or more to lyse *D. communis*. In addition to the use of 1,8-diazabicyclo[5.4.0]undec-7-ene [HDBU] cation, Chiappe et al., (2016) was also

reported the use of switchable solvent based on tetramethylguanidinium and [HTMG] cation. The results showed extraction efficiencies similar to organic solvents at 80 ˚C for 1 hour in presence of methanol. Furthermore, (Du et al., 2019) evaluated two switching processes for energy requirement of lipid recovery from microalgae with N-ethylbutylamine. The processes are $CO_2$ and temperature switching processes and the results showed that the total energy requirement of lipid recovery using $CO_2$ switching is 61.7 MJ/kg lipid, while, the cost of the lipids that recovered by temperature switching is only 12.4 MJ/kg lipid. Thus, the temperature switching process is a promising method for extracting lipids from algae and using them for energy applications.



Low polarity form
(N-ethylbutylamine)

high polarity form
(IL)
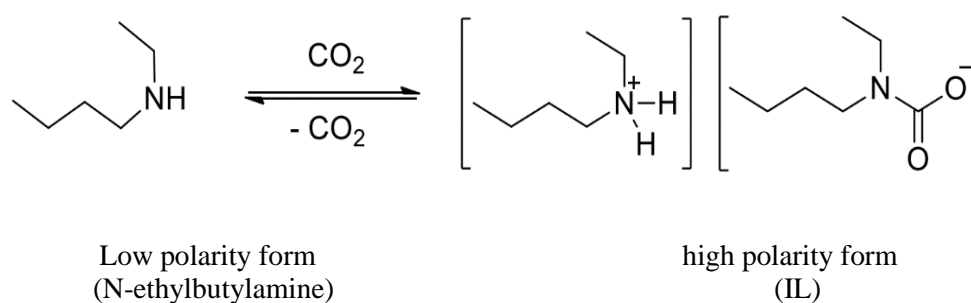
Figure 2.1. The formation of SPS: change from a low polarity to a high

polarity IL when exposed to $CO_2$

A SHS can be reversibly switched between a hydrophobic form that forms a two phasic mixture with water and a hydrophilic form that is miscible with water. In the case of lipid extraction from microalgae, a hydrophobic SHS will extract the lipid from the microalgae, which will then convert to a hydrophilic form upon addition of carbonated water (Figure 2.2) (Jessop et al., 2010). ; Jessop et al., 2011). Boyd et al., (2012) used N,N-dimethylcyclohexylamine, an SHS, to extract lipids from lyophilized *B. braunii*. The crude lipid fraction contained high concentrations of long chain TAG without phospholipids.

N,N-Dimethylcyclohexylamine extracted up to 22 % crude lipid on a microalgae dry mass basis.
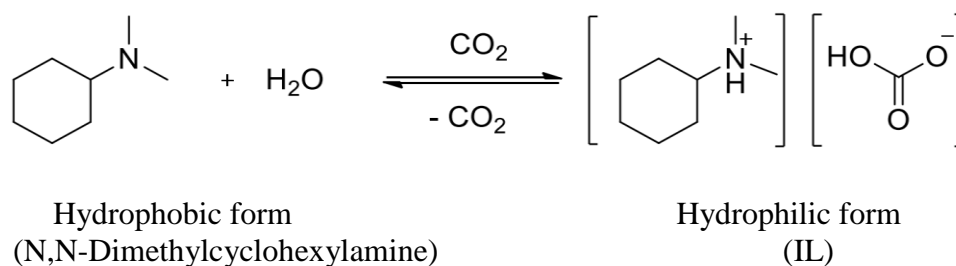


Figure 2.2. The formation of SHS: convertion from a hydrophobic to a

hydrophilic IL when exposed to $CO_2$

Overall, extraction with SHS does not require solvent drying, so using SHS is preferred over using SPS. However, the amount of lipids remaining in the recovered SHS needs to be lowered before this technique is considered viable. Although results using switchable solvents are promising, there are still many challenges to overcome before the use of convertible solvents for lipid extraction from microalgae becomes an economically viable commercial process. Further technological improvements are needed in extraction equipment technology, increasing solvent recovery efficiency, preventing environmental pollution and further reducing treatment costs.

**2.2.5.4 Deep Eutectic Solvents**

The latest generation of ILs, known as deep eutectic solvents (DES), have attracted considerable interest in recent years as solvents (Connor et al., 2020). DES is generally composed of an organic salt (such as choline chloride, choline acetate, quaternary ammonium or phosphonium salts) and a hydrogen bond donor (HBD) (such as an amide, amine, alcohol, or carboxylic acid, etc.). There are stable in hydrogen bond interactions form,

with a melting point much lower than its constituents (Durand et al., 2013). Abbott et al., (2004) was the first, who explained such solvents by reporting that a series of DES from a mixture of solid organic salts and a complexing agent could form liquids at temperatures below 100°C. Figure 2.3 depicts some of the most common DESs used today (Farrán et al., 2015). The combination of DES and α-cellulose, hemicellulose, creates new hydrogen bonds that can damage microalgal cells to improve lipid extraction. Three different aqueous DESs, namely choline chloride-oxalic acid (Ch-O), choline chloride-ethylene glycol (Ch-EG) and urea-acetamide (U-A), were used for *Chlorella sp.* pretreatment and biomass lipid recovery rates were evaluated. The results showed that the lipid recovery rate increased from 52.0% of the blank control group to 80.9, 66.9 and 75.3% of the biomass treated with Ch-O, Ch-EG and U-A, respectively (Lu et al. 2016). A consistent conclusion was obtained when DES was treated on wet (water content 65-67%) and unbroken biomass of *Chlorella sp.* and *Chlorococcum sp.* (GN38) through one and two-step methods (Pan et al., 2017). From the above studies it is clear that DES contributes significantly to improve the overall lipid extraction process.. However, the high cost the DESs could limit their sustainability. Another weakness is the high viscosity, which hampers with mass transfer kinetics and leads to poor performance (Connor et al., 2020).

**Halide**  **Hydrogen Bond Donors**



HO—⟍_N^+ Cl^-
Choline chloride

HO—⟍_N^+ Cl^-
*N*-ethyl-2-hydroxy-*N*,*N*-
dimethylethanaminium chloride

O=⟨_Cl O—⟍_N^+
2-[(chlorocarbonyl)oxy]-*N*,*N*,*N*-
trimethylethanaminium

H₂N—C(=O)—NH₂
urea

CH₃—C(=O)—NH₂
acetamide

NH—C(=O)—NH₂
1-methylurea

NH—C(=O)—NH
1,3-dimethylurea

N—C(=O)—NH₂
1,1-dimethylurea

HO—⟍—OH
ethane-1,2-diol
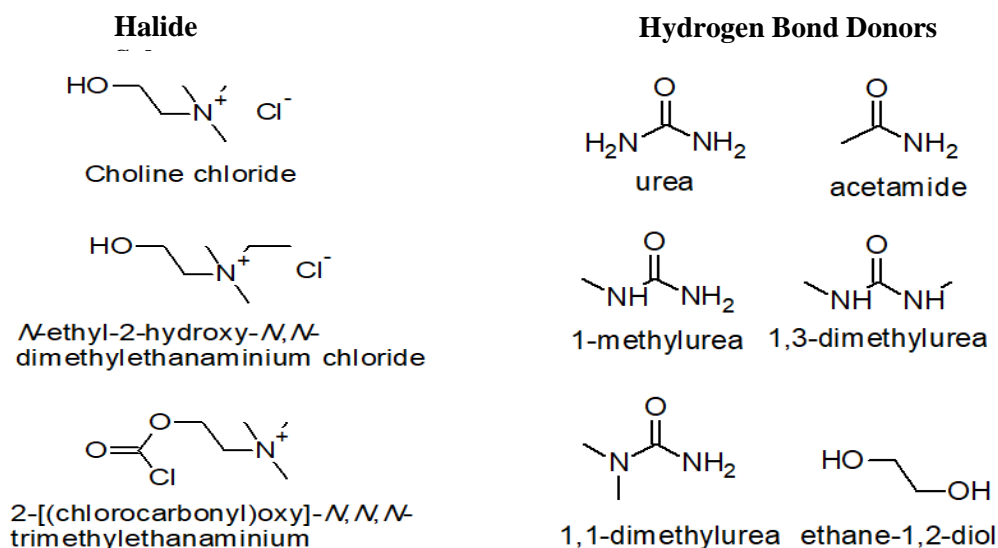
Figure. 2.3. The common deep eutectic solve (Farrán et al., 2015)

## 2.3 Biodiesel production from microalgal lipids

As mentioned earlier, biodiesel is made from alkyl esters of fatty acids and is made from natural oils, such as vegetable or animal fats. Several techniques have developed to efficiently produce biodiesel including pyrolysis (Hsu, 2012; Harman-Ware et al., 2013), micro emulsification (Attaphong & Sabatini, 2013), and transesterification of oil (Farooq, Amin, & Abdullah, 2013). Pyrolysis is a thermochemical process that heats biomass (400-500°C) in the absence of oxygen to produce bio-oils similar to crude oil. This bio-oil is then converted into a transportation fuel by hydro treating, where hydrogen reacts with the bio-oil to remove sulfur and oxygen, followed by hydrocracking, where the treated bio-oil reacts with hydrogen to produce smaller chain hydrocarbons that meet the specifications of diesel fuels (Hsu, 2012). Micro-emulsification involves reducing the viscosity of vegetable oils and improving the miscibility of the polar and oil phases in the biodiesel production process. (Attaphong & Sabatini, 2013; Ekkpowpan  et al., 2014). The

transesterification or alcoholization of triglycerides (TAGs) by short chain alcohols in the presence of a catalyst is commonly used to produce biodiesel. This process has been widely adopted, as it can achieve high yields at a relatively low cost.

## 2.3.1 Transesterification of lipids

The transesterification involves the reaction of triglyceride molecules with alcohol in the presence of a catalyst to yield glycerol and esters of mono-alkylated fatty acids (Bucy et al., 2012). Common factors affecting transesterification efficiency involve reaction temperature, methanol/oil ratio, reaction time, catalyst type and concentration, FFA content, and water content of the oil (Khan et al., 2020). Non-catalytic transesterification can also produce biodiesel with high conversion, but is usually carried out under extreme conditions of temperature (200 - 400 ∘C) and pressure (10 - 25 MPa), reduces the economic feasibility of the process (Da Silva & Oliveira, 2014; Bhatia et al., 2021). For instance, environmentally friendly catalyst-free methods have been reported involving the use of supercritical alcohols at high temperature and pressure that can convert lipids in the presence of water, to biodiesel efficiently and/or rabidly (Srivastava, Paul, & Goud, 2018; Felix et al., 2019; Rathnam et al., 2020). Therefore, catalysts are frequently used to convert lipids to biodiesel under milder conditions. The catalysts utilized in transesterification/esterification processes could be homogeneous such as potassium hydroxide (KOH), sodium hydroxide (NaOH), or sulfuric acid ($H_2SO_4$), or heterogeneous catalysts such as calcium oxide (CaO) and magnesium oxide (MgO) (Park et al., 2017); Kim et al., 2013; Martínez et al., 2017). Commercially, homogeneous catalysts have been used for the transesterification reaction. Although commercial catalysts are relatively cheap and widely available, their hazardous and non-green properties make them unsustainable

for the environment. (Muhammad et al., 2015). These catalysts also generate large amounts of wastewater during post-treatment steps and are not recyclable, making them energy-intensive processes (Aleman-Ramirez et al., 2021). Additionally, the catalyst is partially miscible with biodiesel, creating problems in separating the product from the reaction mixture (Tan et al., 2019).

The use of enzymes as catalysts for these reactions eliminates most of the obstacles associated with acid or base catalysis; however, enzymes are quite expensive and in the presence of FFAs and short-chain alcohols, there are tend to denature (Tran et al., 2012; Teo et al., 2014; Rodriguez et al., 2016; Rangel-Basto et al. events, 2018; Sanchez-Bayo., 2019). Overall, the desire to use greener methods with low energy consumption, low capital costs and environmental friendliness has prompted researchers to investigate the use of IL as an alternative catalyst.

### 2.3.2 Ionic liquids as a catalyst in biodiesel synthesis

The properties of ionic liquids as green catalysts can be emphasized by their properties of having either acidic or basic properties. Their properties can be tuned by changing the combination of cations and anions. For example, some cationic bases are combined with alkyl substituents, such as the addition of functional groups that provide acidic properties such as sulfonic acid [-SO3H] and carboxylic acid [-COOH] (Olivier-Bourbigou et al. 2010). Therefore, ionic liquids can be divided into two groups: (a) acidic ionic liquids (AILs) and (b) basic ionic liquids (BILs).

### 2.3.2.1 Acidic ionic liquids

Acidic ionic liquids (AILs) can be classified into three main categories: (i) Lewis Acidic Ionic Liquids (LAIL), (ii) Brønsted Acidic Ionic Liquids (BAIL), and (iii) Brønsted-Lewis

Acidic Ionic Liquids (BLAIL) ( Ishak et al. 2017; Tiong et al., 2018). Lewis acidic ionic liquids (LAILs) have Lewis acidic sites and thus accept lone pairs from Lewis bases. Brønsted acidic ionic liquids (BAILs) have one or more Brønsted acid sites that transfer protons to Brønsted bases, depending on the number of acid sites on the IL. Brønsted-Lewis acidic ionic liquids (BLAILs) have both Brønsted and Lewis acidic sites and exhibit stronger acidity because both acidic sites act simultaneously to promote catalytic activity. Researchers have explored many AILs as potential catalysts in biodiesel production. Transesterification of microalgae lipids to biodiesel through AIL catalysts provides a better conversion process. Sun et al., (2017) reported that hydrogen sulfate anion based ILs ([BMIM][HSO$_4$]), were used as an extractant for lipid extraction and acid catalyst for in-situ transesterification in *Nannochloropsis sp*. with biodiesel yield up to 95.3% in a short time of 30 min. However, this highest yielding reaction required a reaction temperature of 200 °C. Combined with methanol and KOH, the IL, 1-ethyl-3-methyl- imidazolium ethyl sulphate [C$_2$mim][EtSO$_4$] has also been investigated for the direct trans- esterification of intracellular lipids in the wet biomass of the oleaginous yeast *Rhodosporidium diobovatum* (Ward et al., 2017). In this process, low temperature (65 °C) and short reaction time (2.5 h) were used to recover more than 97% of FAMEs in fresh yeast biomass containing up to 80% water by weight. However, whereas IL was easily recovered, the homogeneous catalyst used in this study (KOH) was not. Moreover, Lee et al., (2015) used 1-butyl-3-methylimidazolium trifluoromethane sulfonate ([BMIM][CF$_3$SO$_3$]) for the one-step lipid extraction and transformation to biodiesel with a moderate yield of 54%.

Another study performed the in-situ transesterification of two species of microalgae (*Duniella* and *Chlorella*) using 1-ethyl-3-methylimidazolium methyl sulfates [C$_2$C$_1$IM]

[C$_1$SO$_4$] ionic liquid and methanol co-solvent to facilitate the acid-catalyzed (HCl) direct transformation of lipids to biodiesel (Young et al., 2011) . The results showed that higher biodiesel yield were obtained from Chlorella (36%). The use of switchable ionic liquids based on [HTMG]- and 1,8- [HDBU cations and methyl formate/hydrogen carbonate [MeOCO$_2$/HCO$_3$] anion were also explored in direct seperation of fatty acid methyl esters (FAMEs-biodiesel) from *Scenedesmus obliquus* biomass  (Chiappe et al., 2016). Their proposed process allows: (i) the use of milder temperature conditions, (ii) simplicity of operation, and (iii) the recyclability of IL.

Other AIL which has received considerable attention as a catalyst in the production processes of biodiesel is 1-(4-sulfonic) butylcaprolactamium hydrogen sulfate ([SO$_3$-bCPL] [HSO$_4$]), which was examined only by Luo et al. (2017). With this catalyst, 95% biodiesel yield was achieved from jatropha oil under optimal conditions (oil/methanol/IL = 1:9:0.25 [molar ratio] at 80 °C for 1h). This ionic liquid showed many benefits, such as the low cost, simple synthesis process as well as good reusability.

**2.3.2.2 Basic ionic liquids (BILs)**

In addition to acidic ILs, basic ILs such as imidazolium- and choline-based ILs have also been used in biodiesel synthesis. (Luo et al., 2013; Ren et al., 2014). Basic ionic liquids are alkaline ILs with high thermal stability and low decomposition temperature. (Hajipour & Rafiee, 2009; Gadilohar & Shankarling, 2017). Other benefits include having characteristics similar to inorganic bases, being stable in air and water, having high catalytic efficiency, being simple to separate, and being reusable. (Hajipour & Rafiee, 2009).

Nonetheless, when compared to AILs, reports on the use of BILs in biodiesel production

from microalgae are scarce in published research. One such study was conducted by (Malekghasemi et al., 2021) who investigated the use of phosphonium carboxylate ionic liquid catalysts in direct transesterification of lipids from wet microalgae to biodiesel. Four ILs, namely, tetrabutylphosphonium formate ($[P_{4444}][For]$), tetrabutylphosphonium acetate ($[P_{4444}][Ace]$), tetrabutylphosphonium propionate ($[P_{4444}][Prop]$), and tetrabutylphosphonium butyrate ($[P_{4444}]$ [Buty]) have been tested at 102 ˚C for 4h. The leading candidate IL catalyst, ($[P_{4444}][For]$), showed significant catalytic activity and allowed recovery of 98 % of biodiesel. The major limitations of this method is the cost effective in term of IL high price and energy saving.

## 2.3.2.3 Ionic liquid-assisted enzymatic production biodiesel from microalgae

Normally, the transesterification of lipid extracted from microalgae catalyzed by lipase-enzymes to produce biodiesel is carried out with or without organic solvents. The production of biodiesel through lipase-catalyzed transesterification of lipids extracted from microalgae is a viable and environmentally friendly substitute to its chemical counterparts requiring acids or alkalis as the catalyst (Vyas et al., 2010). However, the use of organic solvents has some significant limitations, including low conversion, difficulty in product separation, and difficulty in recovering and reusing lipases due to impeding their activation by methanol and increasing concentration of glycerol (a by-product). As a potential alternate for volatile organic solvents, ionic liquids (ILs) are often used as effective reaction media for bio-catalytic processes with many advantages, such as: improved conversion rate, improved optical selectivity, better enzyme activity and thermal stability, in addition to better recovery and recycling (Moniruzzaman et al., 2010). In particular, ILs have been shown to have beneficial effect on lipase activity and stability (both free and immobilized)

(Moniruzzaman et al., 2010; Lozano et al., 2020). The first study on the use of IL in enzymatic conversion of lipids extracted from microalgae into biodiesel was reported by (Lai et al., 2012). Enzyme-catalyzed esterification of oil from *Botryococcus braunii* (two strains, BB763 and BB764), *Chlorella vulgaris*, and *Chlorella pyrenoidosa* was carried out using two immobilized lipases, *Penicillium expansum* lipase and *Candida antarctica* lipase B (Novozym 435) in an IL [bmim][PF$_6$] (1-butyl-3-methylimidazolium hexafluorophosphate). The authors studied the effects of the methanol/oil molar ratio, reaction temperature, solvent volume, and water content to optimize the yield. Both lipases produced significantly higher yields of FAME in the IL system than in tert-butanol, an organic solvent system commonly used in production of biodiesel. Based on these results, it is reasonable to conclude that IL [BMIM][PF$_6$] or other hydrophobic ILs can be used as suitable solvent candidates for lipase-catalyzed microalgal biodiesel production. Bauer et al., (2017) reported a one-pot IL-assisted microalgae conversion to biodiesel. This integrated procedure combines the extraction of oil from a mixture of whole-cell microalgae followed by lipase-catalyzed transesterification to biodiesel in water using zwitterion IL as a co-catalyst. In this study, the authors combined lyophilized whole-cell microalgae with deionized water, MeOH, lipase (*Candida antarctica* lipase B (Novozyme 435), and IL. In this method, the blends were vortexed and heated in a rotary hybridization furnace at 60 $^{\circ}$C for 65 h. The authors selected two ILs, 1- octyl-3(propyl-3-sulfonyl) imidazolium (Oct-PrSO$_3$) and 1- decyl-3(propyl-3-sulfonyl) imidazolium (Dec-PrSO$_3$), which have specific surfactant properties to verify their effect on microalgal biodiesel production. The addition of IL significantly improved the selectivity of biodiesel production, but overall oil conversion was not affected. In fact, IL interacts with enzymes,

making them less reactive but more selective. More importantly, ILs are oil soluble due to their surfactant properties, increasing substrate availability for lipase (Bauer et al., 2017). Lozano and coworkers were also developed one-pot systems based on binary mixtures of ionic liquids and immobilized enzyme, appropriate for the direct extraction and bio-catalytic convertion of algal oil to biodiesel without previous separation. These blends were based on a mixture of spongy ionic liquids (e.g. 1- hexadecyl-3-methylimidazolium bis (trifluoromethylsulfonyl) imide, [C16 mim][NTf2]) with the IL 1-butyl-3-methylimidazolium chloride ([Bmim][Cl]) (Lozano et al. 2020). The finding showed that 100 % of biodiesel yield was given after 2 h of reaction at 60ºC.  Although, these methods enabled rapid and efficient biodiesel synthesis, their sustainability, however, could be limited because of the high cost of both the ILs and the enzymes. Moreover, immobilization requires additional time, equipment and materials so is more expensive to set up (Basso & Serban, 2019; Poppe et al., 2015).

## 2.4 Conclusion and research gab

Microalgal biodiesel is considered a potential alternative to petroleum-based fuels. Numerous methods have been utilized to extract microalgal lipids. Mechanical, chemical, and biological pretreatment techniques have been sought to reduce the use of organic solvents and decrease extraction times. Each pretreatment method has specific advantages and limitations (Table 2.1). Due to the limited literature available, it is difficult to provide an optimal method that works for all microalgal strains. Mechanical support is energy intensive, while chemical support suffers from restrictions such as bio-toxicity, equipment corrosion, long extraction times, lipid degradation. Similarly, enzymatic lysis (biological procedure) requires longer extraction times and proper optimization of reaction conditions

to increase the process efficiency. In addition to efforts to streamline biodiesel production costs and increase energy efficiency, it is also important to ensure that all processes, materials and techniques involved are environmentally friendly. A promising alternative to toxic organic solvents and inorganic catalysts was the development of various green techniques such as supercritical fluids, gas expansion liquid extraction, and liquid $CO_2$ extraction. However, the major constraints of these procedures are represented by the high energy consumption and capital costs associated with various downstream processes. As a "green" tunable solvent, ILs have great potential in biodiesel production process. This review shows that ILs have already shown potential as extraction solvents, co-solvents and catalysts in biodiesel production. Ionic liquids introduce some unique properties compared to traditional solvent. There are offer significant advantages such as high product yield, recyclability, and the ability to degrade wet microalgal biomass faster than organic solvent extraction processes under mild conditions.

Apart from that, the high cost of most ILs in terms of commercial feasibility remains a major obstacle to their application on an industrial scale and an obstacle to commercialization (George et al., 2015). Therefore, there is a need to improve current IL techniques through developing new IL methods that are inexpensive, environmentally friendly and sustainable. In recent years, the use of potentially cheaper cations to synthesis ILs have been proposed to increase efficiency and yields of lipid extraction and biodiesel production while reducing costs. As such, speculation on the use of caprolactam cation-based ILs could be an option for achieving greener and more sustainable biodiesel production routes. The caprolactam-based ionic liquids have shown many benefits including availability in large-scale, low cost, simple preparation process as well as good

reusability (Du et al., 2005;  Fauzi & Amin, 2012; Luo et al., 2017; Shankar et al., 2017; Shankar et al., 2019). Despite these potential advantages, caprolactam-based ILs are rarely synthesized and therefore their application is limited. In particular, biodiesel production from microalgae using this class of ionic liquids has not yet been reported in the literature. Therefore, this study aims to investigate, for the first time, the feasibility of caprolactam-based ILs to produce biodiesel from microalgae, as a potentially energy-saving and green system.

## CHAPTER 3: METHODOLOGY

### 3.1 Materials and methods

The microalgae species used in this study was *Spirulina platensis*. Nine ILs were synthesized and characterized using FTIR and RAMAN techniques (for chemical structure), UV/VIS spectrometer (for acidity strength), and TGA for thermal analysis. Besides, density and viscosity were determined through pycnometer and viscometer, respectively. Lipid extraction from dry and wet biomass was performed using conventional methods such as Soxhlet extraction using hexane: methanol mixture and methanol as positive and negative control, respectively. Pure ILs and with co-organic solvent were investigated for lipid extraction and direct biodiesel production. Extracts yields were determined gravimetrically and characterized via FTIR and GCMS analysis to identify the presence of FAMEs. Microalgae biomass surface changed before and after lipids extraction was identified by SEM analysis. Catalytic activity of the ILs was studied through the indirect biodiesel production process and evaluated via determination of the produced biodiesel yields gravimetrically. Predictive methods were used to estimate the physicochemical properties of the produced biodiesel. Lastly, the recovery and reusability of synthesized ILs were investigated though determination of yield percentage of the extract after each cycle.

### 3.1.1 Sources of microalgae, chemicals and reagents

*Spirulina platensis* dried biomass was obtained from an algae cultivation pond at Masinde Muliro University of Science and Technology (coordinates: 0.5947° N, 34.7803° E), Kenya. Caprolactam (CP, 99 %), 1,4-butane sultone (99 %), Methane sulphonic acid ($CH_3SO_3H$, 99 %), Trifluoromethanesulphonic acid ($CF_3SO_3H$, 99 %) and n-hexane were

supplied by Sigma-Aldrich (Germany). Hydrochloric acid (HCl, 37 %), Sulfuric acid ($H_2SO_4$, 98 %), Trifluoroacetic acid ($CF_3CO_2H$, 98 %) and Methanol ($CH_3OH$, 99.8 %) were supplied by Labo Chem PVT (India), (Toluene, 99.6 %) was supplied by VWR (China) and Acetic acid ($CH_3COOH$, 99.6 %) was obtained from M&B (England).

## 3.2 Synthesis of Ionic Liquids

### 3.2.1 Synthesis of Caprolactam-based ionic liquids

Six Caprolactam-based ionic liquids (CPILs) (Table 3.1), namely, Caprolactam chloride (CPHA), Caprolactam methyl sulphonate (CPMS), Caprolactam acetate (CPAA), Caprolactam hydrogen sulphate (CPSA), Caprolactam trifluoromethane- acetate (CPTFA), and Caprolactam trifluoromethane sulfonate (CPTFS) were prepared using the method reported by (Huang et al., 2014). The synthesis was carried out by adding equimolar amounts of caprolactam (CP) and a Brønsted acid (hydrochloric (HCl), methane sulphonic ($CH_3SO_3H$), acetic ($CH_3COOH$), sulfuric ($H_2SO_4$), tri-fluoroacetic ($CF_3CO_2H$) and tri-fluoromethane sulphonic ($CF_3SO_3H$). As a typical example, the synthesis procedure of CPHA is described here: 10 mL of water was added to a 100-mL flask containing 11.32 g of Caprolactam (0.1 mol) and stirred. Then 3.65 g of hydrochloric acid (0.1 mol) was added slowly into the flask, within 30 min, in an ice bath. The flasks were left to stand for 24 h at room temperature (r.t) (23 ˚C). Then water was evaporated by vacuum distillation and the mixture was washed with toluene, followed by drying at 80 $^o$C in a vacuum oven, and the resultant percentage yields were calculated. The same procedure was conducted to synthesize the other CPILs. The preparation of CPILs is illustrated in Figure (3.1) and the synthesized ILs were listed in Table (3.1).
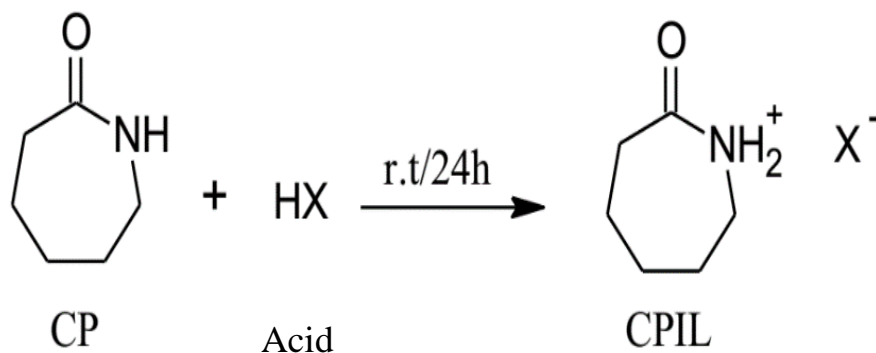
Figure 3.1: Preparation of CPILs **(1)** X= Cl (CPHA); **(2)** X= CH$_3$SO$_3$

(CPMS); **(3)** X= CH$_3$COO (CPAA); **(4)** X= HSO$_4$, (CPSA); **(5)** X = CF$_3$CO$_2$

(CPTFA) & **(6)** X = CF$_3$SO$_3$ (CPTFS).

### 3.2.2 Synthesis of sulfonic butyl -functionalized Caprolactam Ionic Liquids

Three sulfonic butyl-functionalized Caprolactam ionic liquids (SO$_3$-bCPIL), namely sulfonic-butylcaprolactamium hydrogen sulfate (SO$_3$-bCPSA), was reported by (Luo et al., 2017), sulfonic-butylcaprolactamium chloride (SO$_3$-bCPHA), and sulfonic-butylcaprolactamium methyl sulfonate (SO$_3$-bCPMS) were prepared according the described procedure of (Luo et al., 2017). Caprolactam was stirred, solvent-free, with equal-moles (0.1 mol) of 1,4-butane sultone for 10 h at 60 °C. The reaction mixture was then washed three times with toluene (5 ml) to remove unreacted reactants and impurities, and dry evaporated under vacuum (80 °C), to yield a white precipitate of sulfonic butyl-functionalized caprolactam (zwitterion). Afterwards, equimolar concentrated sulfuric acid was added dropwise to the zwitterion, and the mixture was vigorously stirred at 800 rpm at 80 °C for about 8 h until the zwitterion was dissolved. The obtained viscous oil was washed thoroughly with toluene (5 ml) and dry evaporated under vacuum (80 °C). The same procedure was performed to synthesize (SO$_3$-bCPHA) and (SO$_3$-bCMS) by adding

HCl and $CH_3SO_3H$, respectively, instead of $H_2SO_4$. The chemical reaction is illustrated in Figure (3.2) and the synthesized ILs were listed in Table (3.1).
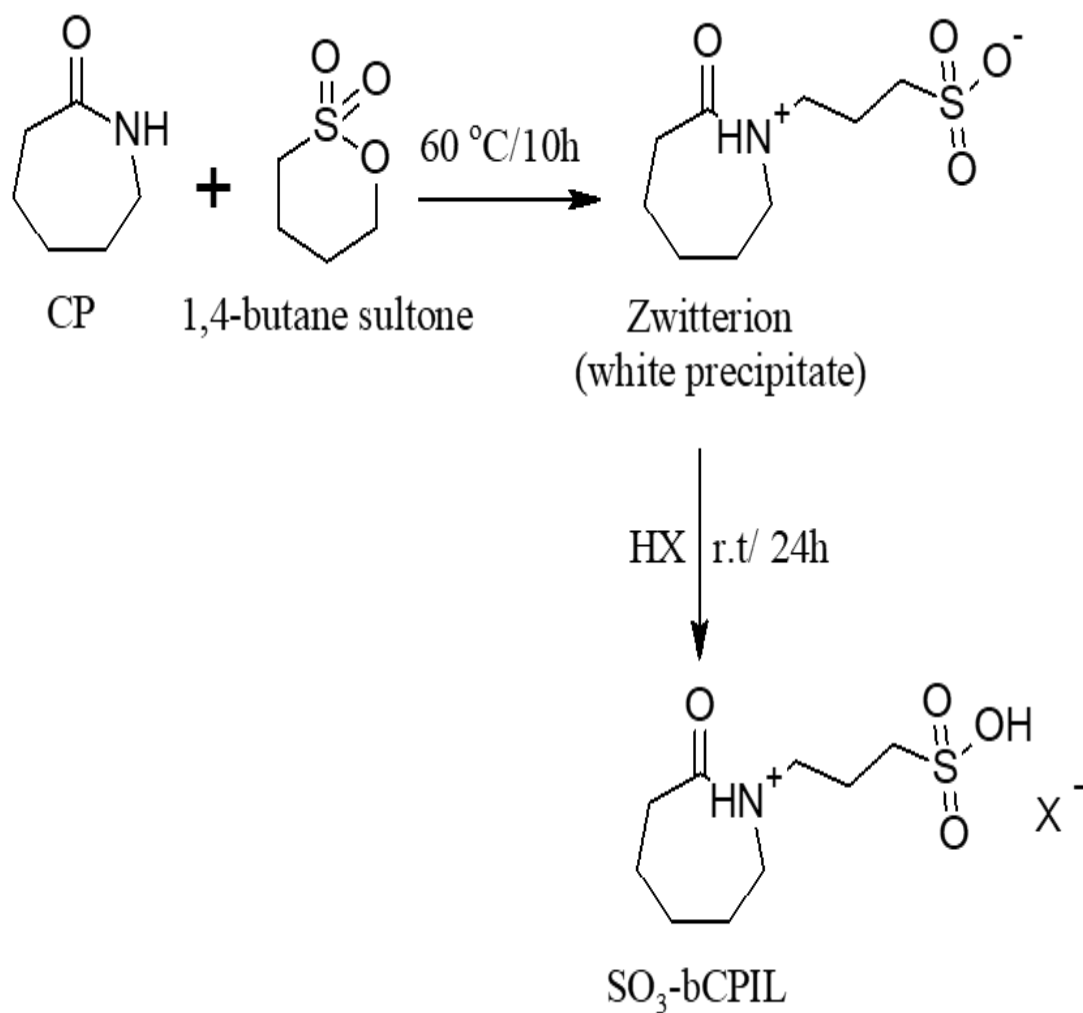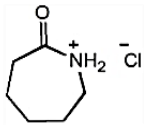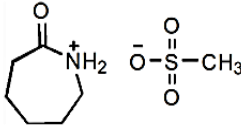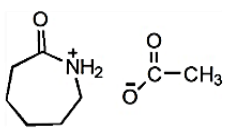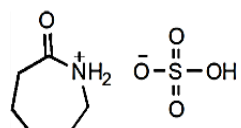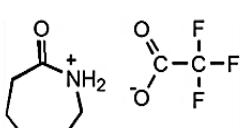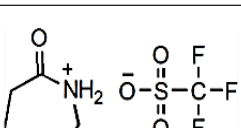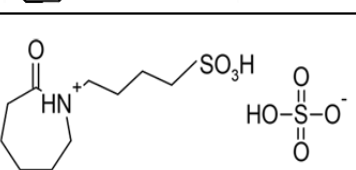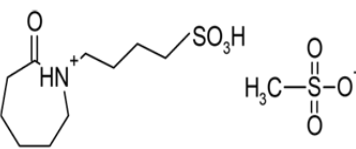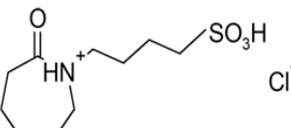


Figure 3.2: Preparation of $SO_3$-bCPILs, **(7)** $X^- = HSO_4^-$ ($SO_3$-bCPSA); **(8)** $X^-$

$= CH_3SO_3^-$ ($SO_3$-bCPMS) & **(9)** $X^- = Cl^-$ ($SO_3$-bCPHA)

Table 3.1. The synthesized CPIL and SO$_3$-bCPIL

| No | CPILs | Abbreviation | Structural formula | Molecular formula |
|---|---|---|---|---|
| 1 | Caprolactamium chloride | CPHA |  | C$_6$H$_{12}$ClNO |
| 2 | Caprolactamium methanesulphonate | CPMS |  | C$_7$H$_{15}$NO$_4$S |
| 3 | Caprolactamium acetate | CPAA |  | C$_8$H$_{15}$NO$_3$ |
| 4 | Caprolactamium hydrogen sulphate | CPSA |  | C$_6$H$_{13}$NO$_5$S |
| 5 | Caprolactamium trifluoromethane acetate | CPTFA |  | C$_8$H$_{12}$F$_3$NO$_3$ |
| 6 | Caprolactamium trifluoromethane sulphonate | CPTFS |  | C$_7$H$_{12}$F$_3$NO$_4$S |
| 7 | sulfonic-butylcaprolactamium hydrogen sulphate | SO$_3$-bCPSA |  | C$_{10}$H$_{21}$NO$_8$S$_2$ |
| 8 | sulfonic-butylcaprolactamium methyl sulfonate | SO$_3$-bCPMS |  | C$_{11}$H$_{23}$NO$_7$S$_2$ |
| 9 | sulfonic-butylcaprolactamium chloride | SO$_3$-bCPHA |  | C$_{10}$H$_{20}$ClNO$_4$S |

**3.3 Characterization of the synthesized ionic liquid**

**3.3.1 Characterization of chemical structures**

The chemical structures of the synthesized CPILs and SO$_3$-bCPILs were characterized using Fourier transform infrared (FT-IR) spectroscopy and Raman spectroscopy. The FT-IR spectra were recorded using a Shimadzu IRTracer –100 spectrometer (Japan), through the use of a KBr liquid cell or by dilution with thoroughly dried KBr followed by pressing into pellets, in the range of 500 to 4000 cm$^{-1}$. Raman spectra were obtained using a Raman Spectrometer (CBEx 2.0, USA) at room temperature, in small glass tubes, by using laser light of 785 nm in the range of 400 to 2200 cm$^{-1}$.

**3.3.2 Determination of density**

The density ($\rho$) expresses the mass per unit of volume. All densities were determined using a Pycnometer (weight method) (see Figure 3.3), following ISO 4787 standard (Gülüm & Bilgin, 2015). First, the empty pycnometer (25ml) was weighed. Then the pycnometer filled with the IL and reweighed. The mass of IL was a subtract value of the two weighings. The density was calculated by the following formula:

$$\rho = m/v \qquad (1)$$

Where m is the mass of the IL, v is the volume of the pycnometer (25 ml).



Figure 3.3. Pycnometer

### 3.3.3 Determination of viscosity

Viscosity ($\eta$) is the resistance of a fluid to flow. The dynamic viscosities were determined following DIN 53015 standard. Measurements was made by capillary viscometer (Oswald) as depicted in Figure 3.4 (Gülüm & Bilgin, 2016). The viscosity was calculated using the following formula:

$$\eta_2 = \frac{\rho_2 t_2}{\rho_1 t_1} \times \eta_1 \qquad (2)$$

Where $\eta_2$ = viscosity of sample, $\rho_1$ = density of water, $\rho_2$ = density of sample, $\eta_1 = 0.85 \times 10^{-3}$, $t_1$ = mean time of flow of water from A to B, $t_2$ = mean time of flow of sample from A to B.
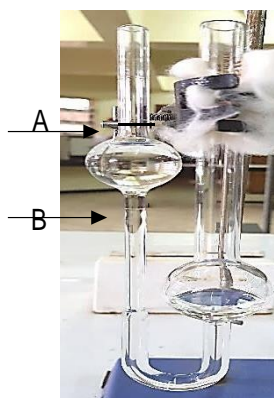


Figure 3.4. Capillary viscometer (Oswald)

### 3.3.4 Thermogravimetric analysis

Thermogravimetric analysis (TGA) was performed using a Simultaneous Thermal Analyzer (STA 6000, The Netherlands). Samples ($\sim$ 20-30 mg) were heated from room temperature to 600 °C under a nitrogen atmosphere, at a scan rate of 10 °C/ min. The percentage purity of the $SO_3$-bCPIL/CPIL were determined from the mass losses of TGA thermogram using the following equation:

$$\text{Purity \%} = \frac{100 \times \text{W (mg)}}{\text{W \%}} \bigg/ \text{W}_{\text{initial}} \qquad (3)$$

Where W is total weight loss of the SO$_3$-bCPIL/CPIL. W$_{\text{initial}}$ is the initial weigh of sample.

### 3.3.5 Determination of the acidity strength

The Brønsted acidity of SO$_3$-bCPIL/CPIL was evaluated from the determination of the Hammett functions ($H_0$) by UV-visible spectroscopy (Chiappe et al., 2013). The indicator 4-nitroaniline and the CPILs were dissolved in distilled water at concentrations of 10 mg/L and 10 mmol/L, respectively. The UV–vis spectra of the solutions were then recorded on a Beckman coulter- DU 720 (US), UV-vis spectrophotometer at room temperature, both in the absence (2 ml of indicator solution mixed with 3 ml water) and in the presence of IL (2 ml of indicator solution mixed with 3 ml of ionic liquid solution) after standing for 6 h. The Hammett acidity function was calculated by the following formula:

$$H_0 = pK(I)aq + \log([I]/[IH]^+) \qquad (4)$$

Where $H_0$ is Hammett function, pK(I)aq is the pKa value of the indicator (0.99 for 4-nitroaniline), and [I] and [IH$^+$] are the molar concentrations of the unprotonated and protonated forms, respectively, of the indicator in the solvent. A low value of $H_0$ indicates that the IL has a strong acidity. According to Lambert–Beer's Law, the value of [I] and [HI+] were calculated from the UV–vis spectra, on the basis of the absorbance values at 380 nm (absorption maximum) (Chiappe et al., 2013).

### 3.4 Determination of algae water content

For water content determination, 10 g of algal biomass was placed in a conventional oven at 40°C for 24 h and then at 105°C overnight, to obtain constant weight (Chiappe et al.

2016).

## 3.5 Lipid extraction using the conventional Hexane: Methanol method

As described by (Chiappe et al., 2016) a hexane-methanol mixture (54:46, v/v, 150 ml) was used to extract lipids from wet (80 %) and dry microalgae (3.0 g) using the Soxhlet extraction method, which has three main compartments. 250 ml round bottom flask containing the solvent, extraction chamber and condenser. First, the sample was placed in a porous thimble, the flask was heated, and then the solvent was evaporated and transported to the condenser, where it was converted to a liquid and collected in the extraction chamber containing the sample. As the solvent passed through the sample, the lipids were extracted and carried to the flask. This process lasted 10 hours. After extraction, the solvent was evaporated using a rotary evaporator. The extracted lipids fraction was transferred into a weighed beaker and dried to constant weight in an oven at 60 ˚C. The experiments were performed in duplicate and the crude lipids extraction yield was then calculated using the following formula:

$$R_{lipid}\% = \frac{W_{lipid}}{W_{biomass}} \times 100 \qquad (5)$$

Where the $R_{lipid}$ and $W_{lipid}$ are the recovery and the weight of lipid extracts, respectively. $W_{biomass}$ is the initial dry biomass weight (g) (Chiappe et al., 2016).

## 3.6 Lipid extraction using ionic liquids

### 3.6.1 The effect of reaction time and temperature on lipid extraction.

Three caprolactam ionic liquids, CPAA, CPHA, and CPSA were utilized for lipid extraction at 75 $^o$C for 5 h and at 95 $^o$C for 2 h using reflux method (150 ml round bottom flask fitted with a condenser). Take into consideration the fact that these conditions were modified from a study reported by Choi, Oh et al., (2014), who extracted lipids using

imidazolium-based ILs at 65 ℃ for 18h and 120 ℃ for 2h . The microalgae dry biomass

was mixed with the ionic liquid in a ratio of 1:19 (w/w, 0.5 g of biomass, and 9.5 g of IL)

under magnetic stirring. After extraction, the upper lipid phase could not be easily

recovered due to the small scale of the experiment, and therefore the mixture was treated

with n-hexane (10 ml) or a mixture of hexane: methanol 2:1 (v/v, 10 ml) to ascertain the

actual lipid yield. The recovered n-hexane phase was washed two times with water to

remove polar compounds. The lipid fraction was dried in a thermostat oven at 60 °C to a

constant weight, and the residue was weighed to measure the gravimetric yield using

formula (1). The overall process of the lipid extraction is shown in Figure 3.5.

## 3.6.2 Lipid extraction using pure ionic liquids

Lipid extraction using the six-caprolactam ionic liquids was carried out at 95 ℃ for 2 h.

Afterwards, lipids were extracted from the ionic liquids according to the same procedure

described above (section 3.6.1). In the case of CPSA, CPMS, and CPHA, hexane: methanol

2:1 (v/v) was used, rather than hexane because there were solidified after mixing with

hexane. The solidification happened, due to the fact that, CPHA and CPMS are solid at

room temperature, whereas CPSA is highly viscous. Thus, when hexane was added at room

temperature (in our case this ranged from 18 - 20 ˚C), and being immiscible with the ILs,

there was a decrease in temperature which led to solidification of the mixture. Therefore,

methanol was added because it is miscible with the ILs, to ease their transfer to centrifuge

tubes.

## 3.6.3 The effect of organic co-solvents on ionic liquid extraction of lipids

Lipids were extracted using mixtures of $SO_3$-CPIL/CPIL and methanol as co-solvent (1:1

w/w). Methanol (MeOH) was also used separately as a negative control. The microalgae

dry biomass (0.5 g) was mixed with 4.8 g each of ionic liquid and methanol in a ratio of 1:19 in a round- bottomed flask (150 ml) fitted with a condenser. The extraction was conducted at 95 °C for 2 h under magnetic stirring at 600 rpm. Thereafter, lipids were collected with hexane (2 × 5 ml). To facilitate the faster separation of layers, the mixture was further centrifuged at 4000 rpm for 30 min.
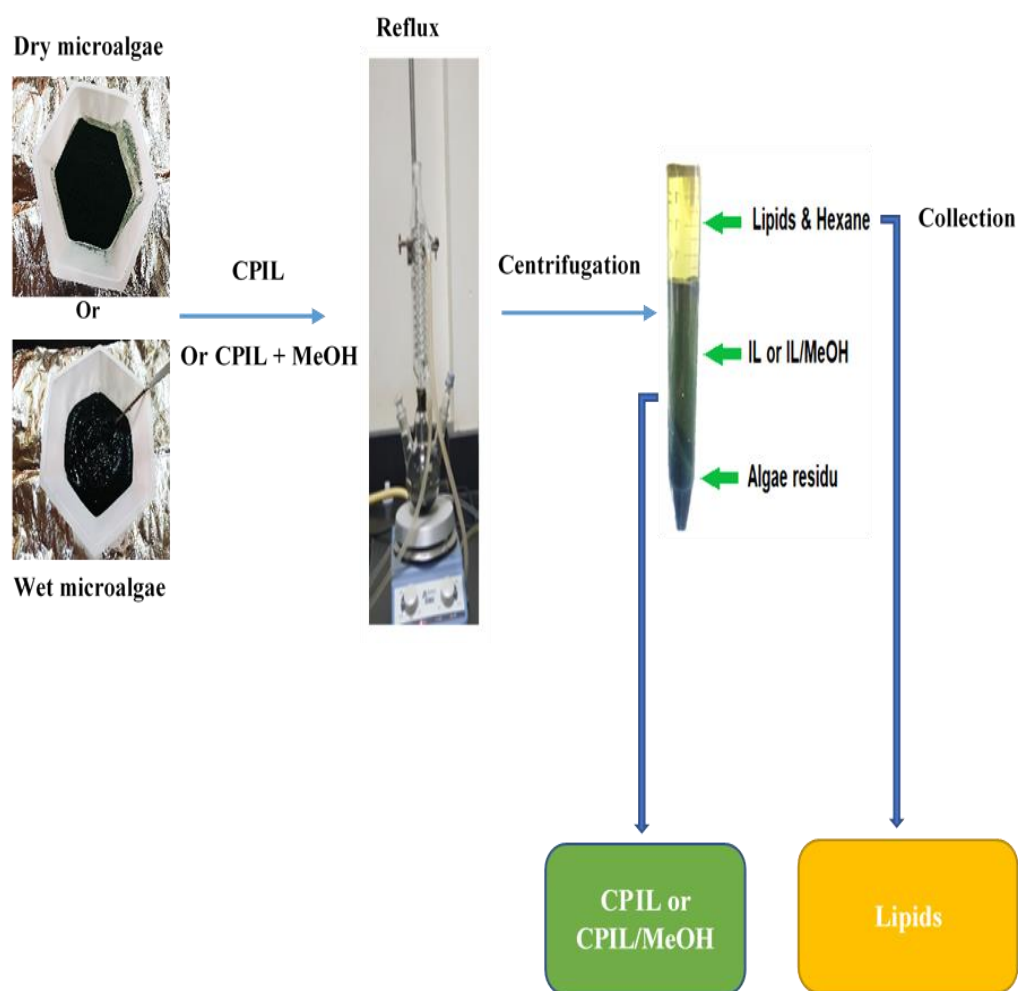


Figure 3.5. A schematic presentation of the lipid extraction process

**3.6.4 Extraction of lipids from wet biomass**

To find out the effect of water content on lipids extracted from microalgae, 4 g of distilled

water was added to 1 g dried *Spirulina platensis* biomass, to form wet biomass with water

content of 80 %. The lipids extraction was performed using mixtures of $SO_3$-CPIL/CPIL

with methanol (1:1 w/w) to dry weight equivalent wet microalgae biomass at the ratio of

19:1 at 95 $^{\circ}$C for 2h, following the procedure in section 3.6.1

**3.7 Characterization of biomass and extracted Lipids**

**3.7.1 Characterization of Spirulina platensis biomass surface ultrastructures**

The cell wall and surface ultrastructures of microalgae cells were determined by scanning

electron microscopy (SEM) (TESCAN Vega3 SBU, Czech), at an acceleration voltage of

10 kV.

**3.7.2 Characterization of extracted Lipids**

**3.7.2.1 FTIR analysis**

The FT-IR spectra of extracted lipids were recorded in the spectral range of 4000 – 400

$cm^{-1}$ using a FT/IR- 6600 spectrometer (Japan). For sample preparation, the same

procedure in section 3.3.1 was used.

**3.7.2.2 Gas Chromatography analysis of free fatty acid methyl esters (FAMEs)**

The recovered FAMEs were analyzed using Gas chromatograph (MRC GC3420A,

Germany) fitted with a flame ionization detector (FID), Agilent CP-Sil 88 capillary column

(60m×0.25mm×0.20µm, Netherlands), with nitrogen as carrier gas and other gases were

hydrogen and air. The FID and the injector port temperatures were maintained at 260 $^{\circ}$C

and 240 $^{\circ}$C, respectively. The injection volume was 0.5 µL and the gas flow rate was 100

ml/min. The temperature program was held at 150$^{\circ}$C for 1 min, increased to 220 $^{\circ}$C at  10

°C/min and held for 2 min, then increased to 240 °C at 3 °C/min, and finally maintained at 240 °C for 8 min. For external calibration, a 37-component FAMEs standard mixture was used.

## 3.8 Indirect transesterification of extracted lipids

Variable quantities of extracted lipids (10–70 mg) were transesterification to FAMEs-biodiesel through acid/catalysed esterification/transesterification, using a method reported by (Christie & Han, 2012). Lipids were dissolved in hexane (1 ml) in a stoppered tube, and 1% sulfuric acid or $SO_3$-CPIL/CPIL in methanol (2 ml) was added. The mixture was left to stand overnight at 50 °C. Water (5 ml) containing sodium chloride (5 %) was added and the required esters were extracted with hexane (2 × 5 ml), using Pasteur pipettes to separate the layers. The hexane layer was washed with water (4 ml) containing potassium bicarbonate (2 %) and dried over anhydrous sodium sulfate. The solution was filtered and the solvent evaporated (Figure 3.6). The yield of biodiesel was calculated using the following formula:

$$\text{The yield of Biodiesel \%} = \frac{\text{FAME (g)}}{\text{Lipids (g)}} \times 100 \qquad (6)$$
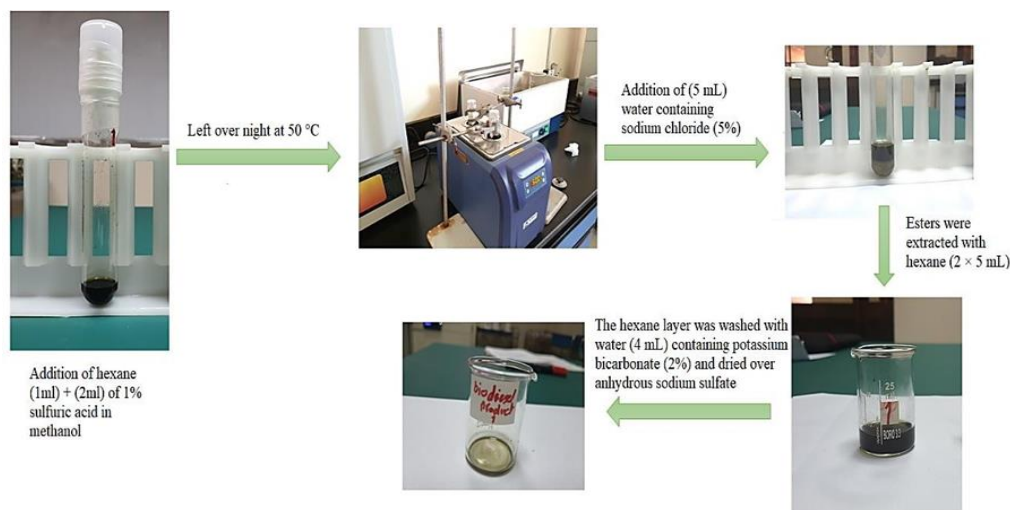


Figure 3.6: Indirect biodiesel production

**3.9 Prediction of physicochemical properties of FAMEs**

Eight mathematical models that have been reported in the literature (Sarin et al., 2009; Sarin et al., 2010; Ramírez-verduzco et al., 2012; Su et al., 2011),were used to estimate the physicochemical properties of the produced biodiesels in this study. The physicochemical properties include cloud point (CP), pour point (PP), cold filter plugging point (CFPP), cetane number (Ø), kinematic viscosity (η), density (ρ), flash point (FP) and higher heating value (calorific value, δ) of fatty acid methyl esters.

A set of predictive equations for the CP, the PP and the CFPP based on the composition of palmitic fatty acid methyl ester (PFAMEs) (in weight percentages) were developed by Sarin et al., 2009 and Sarin et al., 2010 as follow:

$$CP = 0.526_{(PFAME)} - 4.992 \ (0\% < PFAME < 45\%) \qquad (7)$$

$$PP = 0.571_{(PFAME)} - 12.24 \ (0\% < PFAME < 45\%) \qquad (8)$$

$$CFPP = 0.511_{(PFAME)} - 7.823 \ (0\% < PFAME < 45\%) \qquad (9)$$

The cetane number, density, and higher heating value of FAMEs were calculated using predictive equations obtained by Ramírez-verduzco et al., (2012); . In these mathematical models, $M_i$ represents the molecular weight of each FAME, and N is the number of double bonds in a given FAME.

The cetane number of each fatty acid methyl ester is obtained from

$$Ø_i = -7.8 + 0.302 \times M_i - 20 \times N \qquad (10)$$

Where $Ø_i$ is the cetane number of each FAME.

The density of each FAME can be calculated from

$$\rho_i = 0.8463 + (4.9/M_i) + 0.0118 \times N \qquad (11)$$

Where $\rho_i$ is the density at 20 ˚C of each FAME in kilogram per cubic meter (kg/m$^{3)}$).

The expression for higher heating value (calorific value) of each FAME is:

$$\delta_i = 46.19 - (1794/M_i) - 0.21 \times N \qquad (12)$$

Where $\delta_i$ is the higher heating value of the ith FAME in mega joule per kilogram

(MJ/kg).

Then the physical properties of biodiesel produced by $SO_3$-CPIL/CPIL were estimated

from the individual physical properties of FAMEs using the mixing rule that reported by

(Ramírez-verduzco et al., 2012). The following general expression was used:

$$f\text{b} = \sum_{i=1}^{n}(x_i \cdot f_i) \qquad (13)$$

Where $f$b is a function that represents any physical property (the subscripts b and $i$ refer

to the biodiesel and the individual FAME, respectively), $x_i$ is the mole fraction of the $i$

FAME. The function $f$b must be interchanged by the variables $\emptyset_b$, $\rho_b$ and $\delta_b$ in order to

specify the cetane number, density and calorific value of biodiesels, whereas the function

$f_i$ must be replaced by the variables $\emptyset$i, $\rho_i$ and $\delta_i$ in order to specify the properties of the

individual $i$FAME.

The mole fraction $(x_i)$ of individual FAME was estimated from its mass fraction $(w_i)$

composition using equation (14):

$$x_i = \frac{\frac{w_i}{M_i}}{\sum_{i=1}^{n}\frac{w_i}{M_i}} \qquad (14)$$

Whereas, the mass fraction was calculated using the following formula

$$w_i = \frac{A_i}{\sum A} \qquad (15)$$

Where $A_i$ is the peak area for individual FAME, $\sum A$ is the total peak areas of FAMEs

composition in each biodiesel product.

The flash point and viscosity properties for each biodiesel product was predicted using the method that has been reported by (Su et al., 2011) as shown below:

$$FP = 23.362N_C + 4.854N_{DB} \qquad (16)$$

$$\eta = 0.235N_c - 0.468N_{DB} \qquad (17)$$

Where FP and $\eta$ refer to the flash point and viscosity, respectively. $N_C$ is the weighted-average number of carbon atoms and $N_{DB}$ is the weighted-average number of double bonds. The comparison between the experimental value and the calculated value of the physical properties of biodiesel was carried out using the means of the average absolute deviation (AAD) as reported by Ramírez-verduzco et al., (2012) and Su et al., (2011) using the following formula:

$$AAD = \left(\frac{1}{n}\right)\left(\sum_{j=1}^{n}\left|\frac{f_{j,exp}-f_{j,cal}.(100)}{f_{j,exp}}\right|\right) \qquad (18)$$

Where n is the number of experimental points that are being compared, whereas $f_{j,\,exp}$ and $f_{j,\,cal}$ are functions that represent the experimental and calculated biodiesel physical property.

### 3.10 Recoverability and reusability of the SO₃-bCPIL/CPILs

After extraction of the *S. plastensis* lipids, a tri-phasic system was obtained by centrifugation. The top phase contained FAMEs, the middle phase contained SO₃-CP/CPILs with methanol, and the bottom phase contained the algae residue. The top phase was collected by pasteurization, and the supernatant containing the ionic liquid and methanol was evaporated to remove methanol. The extraction of lipids using recycled ionic liquid was tested according to the same procedure in section 3.6.3.

## 3.11 Analysis of data

The analysis was achieved in duplicate and the provided data was expressed as (Mean $\pm$ SD). T-test was used to compare results with controls, and an effect was considered to be significant when $P \leq 0.05$. The data analyzed using Microsoft excel.

## CHAPTER 4: RESULTS AND DISCUSSION

### 4.1 Physical properties of synthesized ionic liquids

All of the $SO_3$-CPILs/CPILs were prepared with high yields of 60.4 - 99.6 % as depicted in

Table (4.1). Among them, CPAA, CPSA, CPTFA, CPTFS, $SO_3$-CPSA, $SO_3$-CPHA and

$SO_3$-CPMS were colorless with excellent fluidity at room temperature, whereas CPMS and

CPHA were white solids (Figure 4.1). $SO_3$-CPILs/CPILs were moisture stable, as attested

by the consistent weigh measurements at various time intervals at 25 ˚C. All the $SO_3$-

CPILs/CPILs were insoluble in hexane and revealed high miscibility with water and

methanol, confirming that those ILs are hydrophilic.

Table 4.1: The yield percentage of the synthesized ILs

| IL | Yield % |
|----|---------|
| **CPAA** | 83.3 |
| **CPHA** | 80.7 |
| **CPSA** | 91 |
| **CPMS** | 99 |
| **CPTFA** | 92.4 |
| **CPTFS** | 99.6 |
| **$SO_3$-CPHA** | 60.4 |
| **$SO_3$-CPMS** | 75 |
| **$SO_3$-CPSA** | 95.6 |

(A)                                          (B)
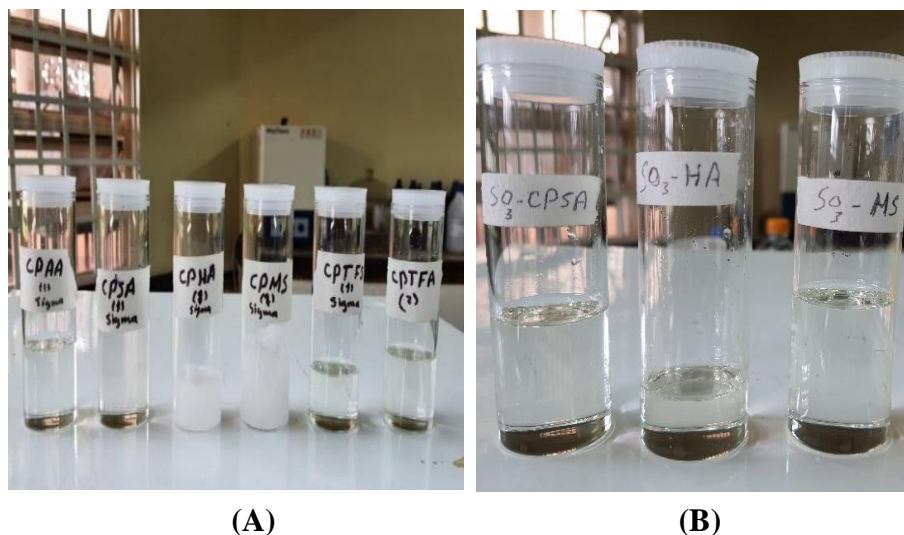
Figure 4.1. The synthesized ionic liquids, (A) CPILs: from left to right,

CPAA, CPSA, CPHA, CPMS, CPTFS and CPTFA. (B) SO$_3$-CPILs: from

left to right, SO$_3$-CPSA, SO$_3$- CPHA and SO$_3$-CPMS

## 4.2 Characterization of the Synthesized Ionic Liquids

The synthesized ILs were characterized by identifying their chemical structure (the functional groups of each IL) using FTIR and RAMAN techniques, determination of density and viscosity, which are important properties for solvents and catalyst. The acidity strength and thermal stability of the ILs were determined via UV/VIS and TGA analysis, respectively.

### 4.2.1 Characterization of chemical structures

### 4.2.1.1 FTIR analysis of caprolactam

Garbuzova & Lokshin, (2004) reported that solid caprolactam is present in dimeric hydrogen- bonded form as shown in Fig.4.2a. Therefore, the peaks at 3296.12, 3209.33 and 3074.32 cm$^{-1}$ correspond to N–H in hydrogen bonding as shown in Fig 4.2b. The observed peaks at 2929.67 and 2856.38 cm$^{-1}$ were assigned to the vibration of asymmetrical and symmetrical stretching, respectively, of the –CH$_2$- group from cyclic lactam. The peak

at 1487 cm$^{-1}$ corresponds to a hydrogen bond formed between C=O and N–H. The band at

1440.73 cm$^{-1}$ relates to the scissoring vibration in the – CH$_2$– group and the band located

at 1417.58 cm$^{-1}$ was assigned to the bending vibrations in the same group. The bands at

1365.51, 1290.29, 1257.50, and 1197.71 cm$^{-1}$ correspond to the amide group bonded with

the alkyl group (– NH–CH$_2$–). The C=O bond, related to lactam was observed at 1658.67

cm$^{-1}$ and was confirmed by the bands at 865.98 and 690.47 cm$^{-1}$. The band located at 823.55

cm$^{-1}$ relates to out of plane bending vibration of the NH bond. Both bands at 582.46 and

505.31 cm$^{-1}$ correspond to the amide group of lactam ring (Garbuzova & Lokshin, 2004);

(Farias-Aguilar et al., 2014). Moreover, according to a study reported by Huang et al.

(2014), the characteristic peaks of caprolactam-based ionic liquids at 1441 – 1445 cm$^{-1}$ and

2930 - 2941 cm$^{-1}$ may relate to N-H and N-C-H, respectively.



(a)

**(b)**
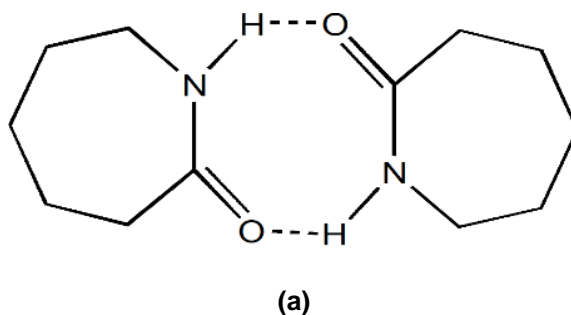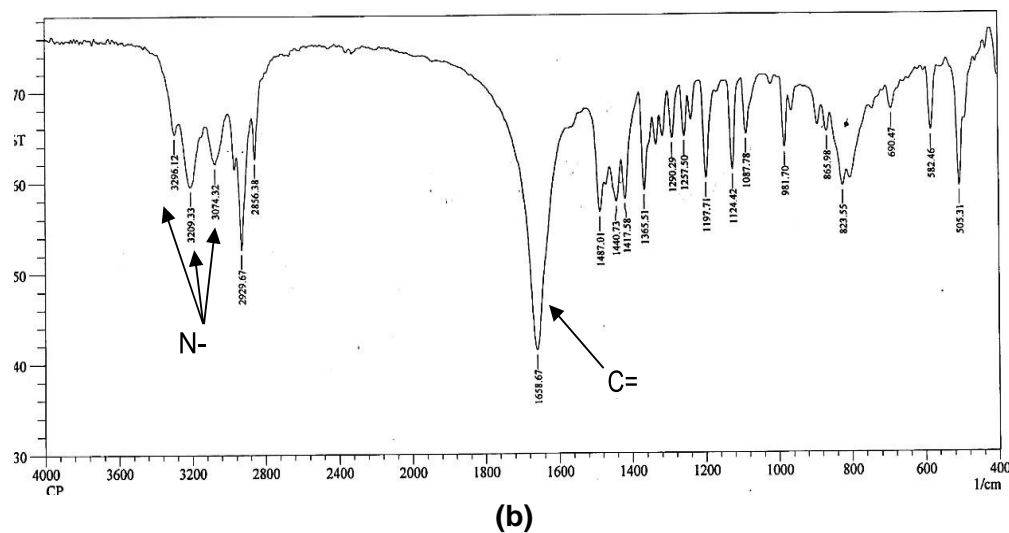
Figure 4.2. (a) Solid caprolactam dimer showing hydrogen

bonding between two amide groups, (b) FTIR spectrum of

Caprolactam

### 4.2.1.2 FTIR analysis of the synthesized caprolactam ionic liquids (CPIL)

The characteristic IR absorption peaks of the ILs are shown in Figure 4.3 and Table 4.2. A

significant change was observed in the caprolactam IR spectrum after reaction with HCl,

$CH_3SO_3H$, $CF_3SO_3H$, $CH_3CO_2H$, $CF_3CO_2H$, and $H_2SO_4$ acids to produce ionic liquids.

This modification resulted in the loss of three N–H hydrogen-bonded peaks, and new peaks

at different frequencies appear due to the interaction between the cation and the anion.

Furthermore, the decrease in intensities of the C=O peak observed in most spectra is

attributed to the loss of double bond character in the caprolactam units due to the formation

of hydrogen bonds (Shakeela, Sinduri, & Rao, 2017).

Functional groups were assigned to the characteristic IR absorption peaks for each

synthesized CPIL (Fig. 4.3a – 4.3f). CPAA (Fig. 4.3a): N-$H_2^+$ (3286.48 cm$^{-1}$); $CH_3$

asymmetric stretch (3041.53 cm$^{-1}$) related to acetate ion; CH stretching (2929.67, 2858.31

cm$^{-1}$); C=O (1708.81, 1662.52 cm$^{-1}$); CO…H (1485.09 cm$^{-1}$); CH bending vibration

(1440.73, 1357.79 cm$^{-1}$).   CPHA (Fig.  4.3b):  N-H$_2^+$  (2970.17 cm$^{-1}$); asymmetric and symmetric CH stretching (2929.67 and 2860.24 cm$^{-1}$), respectively; C=O (1645.17cm$^{-1}$); CO…H (1483.16 cm$^{-1}$); CH scissor vibration (1440.73, 1357.79 cm$^{-1}$). CPMS (Fig. 4.3c): N-H$_2^+$(3404.13); CH$_3$ asymmetric stretch (3049.25 cm$^{-1}$) related to methylsulphonate ion; CH asymmetrical stretching (2937.38 cm$^{-1}$); C=O (1704.96, 1623.95 cm$^{-1}$); CO…H (1502.44 cm$^{-1}$); CH bending vibrations (1413.72 cm$^{-1}$); –NH–CH$_2$– (1332.72 cm$^{-1}$); the broad and sharp peak located at (1191.93 cm$^{-1}$) may be due to overlapping of the symmetric stretching SO$_3$ and (–NH–CH$_2$–), whereas the peak at (1043.42 cm$^{-1}$) may correspond to S-O-H bend or SO$_3$ symmetric stretch (associated). The peaks at 781.12, 599.82 and 557.39 cm$^{-1}$ may indicate free and associated stretch (C-S) and the peak at 536.17 cm$^{-1}$ may be related to SO$_3$ symmetric bend (Zhong et al., 2018; Chackalackal & Stafford, 1966). CPSA (Fig 4.3d): N-H$_2^+$ (3045.39 cm$^{-1}$): CH asymmetrical stretching (2935.46 cm$^{-1}$); C=O (1681.81, 1633.59 cm$^{-1}$): the band at (1512.09 cm$^{-1}$) may be related to CO…H or scissoring H-C-H ); CH bending vibrations (1438.80 cm$^{-1}$); overlapping of symmetric stretch SO$_3$ and –NH–CH$_2$– at (1193.85 cm$^{-1}$). The peak that may be related to the S-O-H bend or SO$_3$ symmetric stretch (associated) is located at (1054.99 cm$^{-1}$). The two peaks at (879.48 and 852.48 cm$^{-1}$) may indicate an associated and monomeric stretch of (S-OH) (Chackalackal & Stafford, 1966); stretch C-S at (781.12 cm$^{-1}$); SO$_3$ symmetric bend (580.53 cm$^{-1}$). CPTFA (Fig. 4.3e): N-H$_2^+$ (3047.32 cm$^{-1}$); CH stretching (2939.31, 2866.02 cm$^{-1}$; C=O (1676.03, 1627.81cm$^{-1}$); CH scissor vibrations (1438.80 cm$^{-1}$) or may also be related to symmetric vibration in CO$_2$, and the one at (1336.58 cm$^{-1}$) associated to –NH– CH$_2$- or may also attributed to symmetric vibration in CF$_3$. Broadband at (1178.43 cm$^{-1}$) may indicate vibrational in F-CF$_2$ and symmetrical CF$_3$ stretch. The peaks located at (798.47, 721.33, 601.75, and 514.96 cm$^{-1}$) may be associated to symmetric CO$_2$ scissor and umbrella,

bending and asymmetric vibrations in $CF_3$, respectively (Christe & Naumann, 1973). CPTFS (Fig. 4.3f): $N-H_2^+$ (3242.12 cm$^{-1}$); CH asymmetrical stretching (2941.24 cm-$^1$); C=O (1638.74 cm$^{-1}$); CO…H or scissor H-C-H at (1514.02 cm$^{-1}$); CH bending vibrations (1450.37 cm$^{-1}$). A broad overlapping band at (1251.72 and 1170.71 cm$^{-1}$) indicates –NH–CH$_2$-, asymmetrical $SO_3$ stretching and symmetrical $CF_3$ stretching (Singh et al., 2016). The peak located at (761.83 cm$^{-1}$) may be attributed to symmetric FCF scissor and C-S stretch. The bands observed at 638.39, 578.60 and 518.82 cm$^{-1}$ may be attributed to SO bond oscillation, symmetric (OSO) scissor & (FCF) scissor and asymmetric (OSO) scissor & (FCF) scissor, respectively (Singh et al., 2016).

The observable split carbonyl bands in CPAA and CPTFA are related to carbonyl groups in acetate and caprolactamium ions at the higher and lower frequencies, respectively. Nevertheless, the same split exists in each of CPSA, CPMS, and CPTFS, and this phenomenon was explained by Winston & Kemper, (1971), as resulting from coupled stretching vibrations of the O=C-C group in acyclic structures, through symmetric asymmetric modes. Furthermore, there is a significant change in the fingerprint regions in IR spectra of all ILs except CPHA, which showed slight differences compared to the caprolactam spectrum. This may infer the presence of more interactions between caprolactamium cation and the anions.
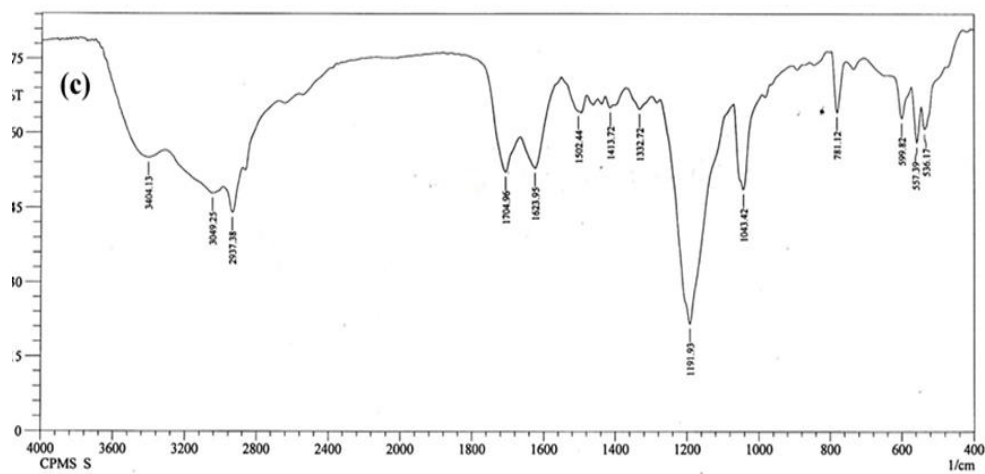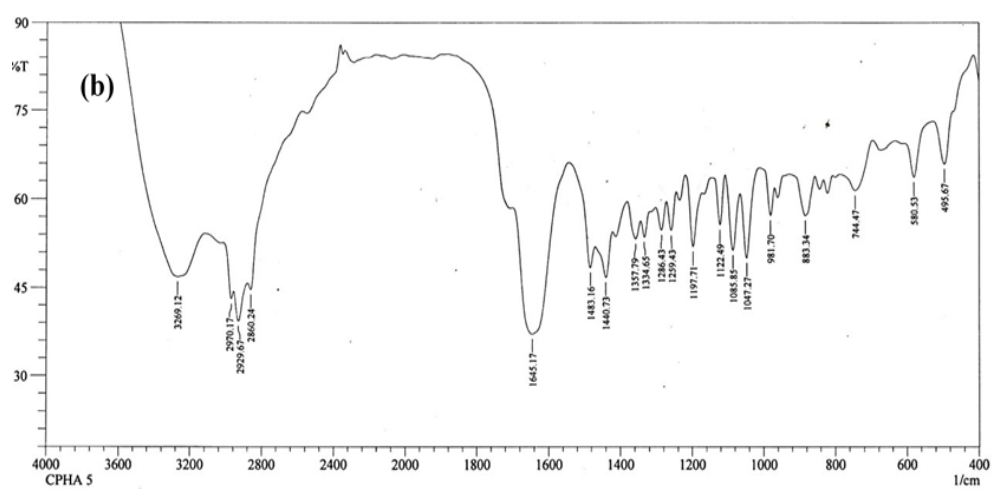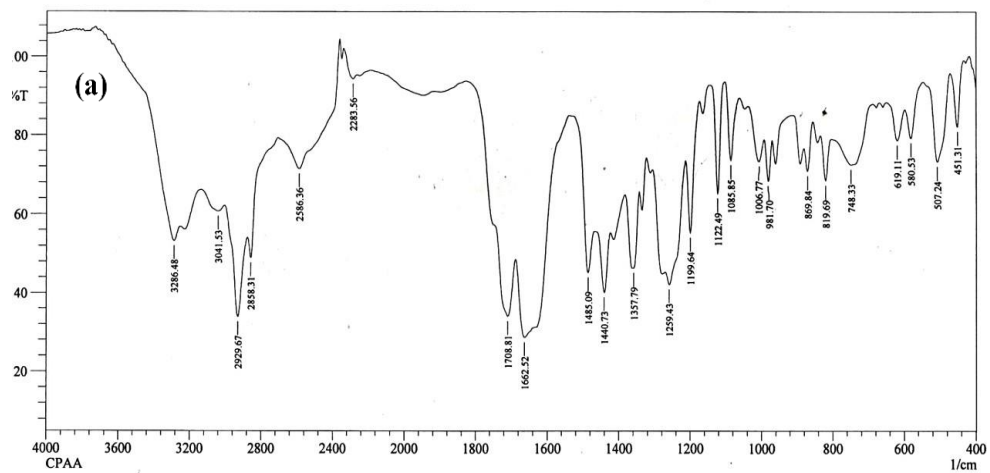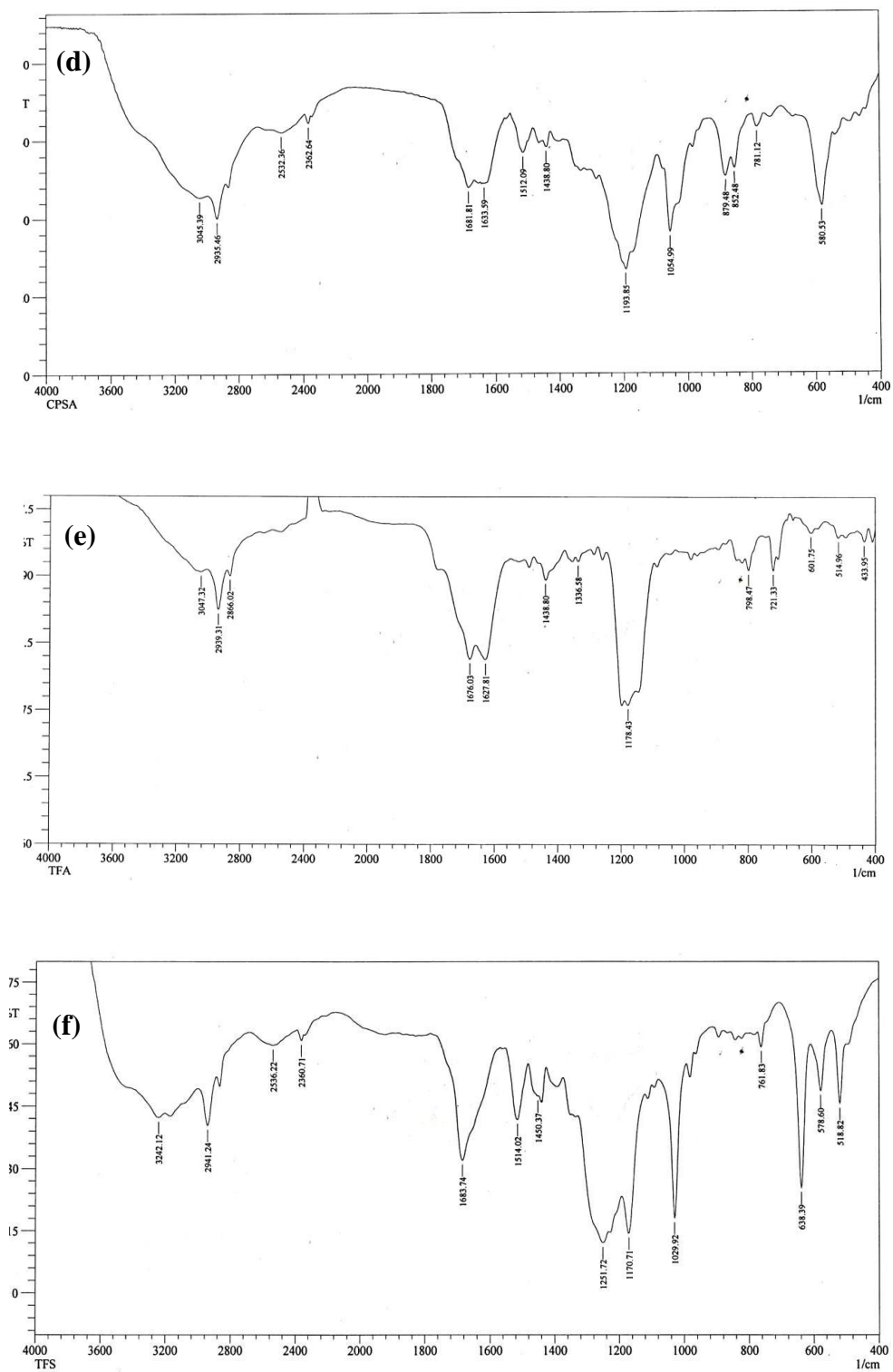
Figure 4.3. FTIR spectra of (a) CPAA, (b) CPHA (c) CPMS, (d) CPSA,

(e) CPTFA and (f) CPTFS

Table 4.2. FT-IR Spectroscopy vibrational wavenumbers and mode assignments of CP and CPILs (in cm$^{-1}$)

| Wavenumbers cm$^{-1}$ | | | | | | | Band assignment | Functional groups |
|---|---|---|---|---|---|---|---|---|
| CP [a] | CPAA | CPHA | CPMS | CPSA | CPTFA | CPTFS | | |
| 3296.12, 3209.33, 3074.32 | 3286.48 | 3269.12 | 3404.13 | 3045.39 | 3047.32 | 3242.12 | νN-H, N-H$^+$ | Amine group of lactam and protonated amine of ILs |
| - | 3041.53 | - | 3049.25 | - | - | - | ν$_{as}$CH3 | CH3 methyl group of the methylsulphonate |
| 2929.67 | 2929.67 | 2929.67, | 2937.38 | 2935.46 | 2939.31, | 2941.24 | ν$_{as}$CH2 | CH2 methylene groups from cyclic lactam or alkyl group |
| 2856.38 | 2858.31 | 2860.24 | - | | 2866.02 | - | ν$_s$CH2 | |
| 1658.67 | 1708.81, 1662.52 | 1645.17 | 1704.96, 1623.95 | 1681.81, 1633.59 | 1676.03, 1627.81 | 1638.74 | ν$_s$C=O | The carbonyl group of the lactam |
| 1487 | 1485.09 | 1483.16 | 1502.44 | 1512.09 | - | 1514.02 | C=O….N-H | hydrogen bond formed between carbonyl and amine groups of lactam |
| 1440.73, 1417.58 | 1440.73, | 1440.73, | -1413.72 | 1438.8 | 1438.8 | -1450.37 | sciCH2 δCH2, | CH2 methylene groups from cyclic lactam |
| 1365.51, 1290.29, 1257.50, | 1357.79, 1259.43 | 1357.79, 1334.65, 1286.43, 1259.43 | 1332.72 | - | 1336.58 | 1363.58 | (–NH–CH2) | The amide group bonded with the alkyl group |
| 1197.71 | - | 1197.71 | 1191.93 | 1193.85 | - | - | Overlapping of (–NH–CH2–) and ν$_s$SO$_3$$^b$ | The amide group bonded with the alkyl group & sulphonate group |
| - | - | - | - | - | 1178.43 | 1251.72, 1170.71 | Overlapping of (–NH–CH2–), ν$_{as}$SO$_3$ and ν$_s$CF$_3$$^c$ | The amide group bonded with the alkyl, sulphonate and trifluoro groups |
| - | - | - | 1043.42 | 1054.99 | - | - | δ S-O-H$^b$ or ν$_s$ SO$_3$$^b$ | The sulphate or sulphonate group |
| - | - | - | - | 879.48, 852.48 | - | - | ν S-OH$^b$ | |
| - | - | - | 781.12, 599.82, 557.39 | 781.12 | - | 761.83 | Free and associated (vC-S$^c$) | The methanesulphonate group |
| - | - | - | 536.17 | 580.53 | - | - | δsSO$_3$$^c$, δ SO$_4$ | The sulphonate or sulphate group |
| - | - | - | - | - | 514.96 | 638.39, 578.6, 518.82 | scis (OSO)& sci(FCF)$^c$ scis$_{as}$(OSO) & sci(FCF)$^c$ | The sulphonate and trifluoro groups |
| 865.98, 690.47 | 869.84, 619.11 | - | - | - | 721.33 | - | δC=O | The carbonyl group of the lactam |
| 823.55 | 819.69 | - | - | - | 798.74 | - | δN-H | Amine group |
| 582.46, 505 | 580.53, 507.24 | 580.53, 495.67 | - | - | - | 578.6, 518.82 | OC-NH | Amide group |

ν= stretching, ν$_S$= symmetric stretching, ν$_{as}$ = asymmetrical stretching, δ = deformation (bend), δs = symmetric, deformation (bend), sci = scissor, sci$_s$ = symmetric scissor, sci$_{as}$ = asymmetric scissor. Band assignments are taken from references, [a] (Garbuzova & Lokshin, 2004), [b] (Zhong et al. 2018) & (Chackalackal & Stafford, 1966); [c] (Singh et al. 2016).

**4.2.1.3 FTIR analysis of sulfonic butyl-functionalized caprolactam IL (SO$_3$-bCPIL)**

Compared to the caprolactam spectrum, there was similar observation on the loss of the three N–H hydrogen-bonded peaks, due to addition of the sulfonic-butyl (SO$_3$ C$_4$H$_8$) group, and the new peaks appeared at 3295, 3231 and 3090 cm$^{-1}$ (Figure 4.4a). The peak of (N-H$^+$C$_4$H$_8$-SO$_3$-) was located at 3394 cm$^{-1}$. The peaks at 2929 and 2857 cm$^{-1}$ were assigned to the vibration of asymmetrical and symmetrical stretching, respectively, of the –CH$_2$-group from cyclic lactam and butyl chains. The peak at 1477 cm$^{-1}$ corresponds to a hydrogen bond formed between C=O and N–H. The band at 1438 cm$^{-1}$ relates to the scissoring vibration in the – CH$_2$– group. The two sharp bands at 1348 and 1167 cm$^{-1}$ correspond to asymmetrical and symmetrical stretching vibration of S=O group, respectively, and confirm the presence of the sulfonic group. The C=O peak, related to lactam ring showed no shift, compared to the caprolactam peak at 1658 cm$^{-1}$. However, the C-O bend vibration was shifted to 706.6 cm$^{-1}$. The peak at 907 cm$^{-1}$ may related to the amide group bonded with the alkyl group (–NH–C$_4$H$_8$–) of the butyl chain (Kiefer, Stuckenholz, & Rathke, 2018), or to the S-OH stretching (Zhong et al., 2018). The bands located at 826.2 and 779.3 cm$^{-1}$ relate to out of plane bending vibration of the NH and C-S symmetric stretch, respectively. The bands at 579.4 cm$^{-1}$ correspond to the amide group of lactam ring (Garbuzova & Lokshin, 2004); (Farias-Aguilar et al., 2014). The sharp band located at 502.5 cm$^{-1}$ was assigned to SO$_3$ asymmetric bend (Zhong et al., 2018).

The major observation in SO$_3$-bCPILs is the appearance of a broad peak at (2700-3300 cm$^{-1}$), which may be attributed to the OH group of S-OH (Figure 4.4b, c, d). The peak of (N-H$^+$C$_4$H$_8$-SO$_3$$^-$) was not detected in all spectra, and that may due to overlap with the OH broad band. The decrease in intensities of the C=O peak was also observed in all spectra,

as explained previously. Additionally, the symmetrical stretching vibration of S=O of sulfonic group appeared as a broad band in all spectra, and this may attributed to the formation of hydrogen bond between sulfonic groups.

Figures (4.4b– 4.4d) and Table (4.3) shows the functional groups that were assigned to the characteristic IR absorption peaks for each synthesized $SO_3$-bCPIL. $SO_3$ bCPHA (Fig. 4.4b): asymmetric and symmetric CH stretching (2930 and 2865 cm$^{-1}$), respectively; C=O (1721, 1625 cm$^{-1}$); CO…H (1521cm$^{-1}$); CH bending vibration (1439 cm$^{-1}$); asymmetrical and symmetrical S=O stretching (1351 and 1151 cm$^{-1}$), respectively; –NH–$C_4H_8$- (910 cm$^{-1}$); out of plane bending vibration of the NH and C-S symmetric stretch (827.1 and 782.9) cm$^{-1}$, respectively; the amide group of lactam ring underwent a big shift (598.6 cm$^{-1}$); $SO_3$ asymmetric bend (503.6 cm$^{-1}$). $SO_3$-bCPMS (Fig. 4.4c): asymmetric and symmetric CH stretching (2937 and 2863 cm$^{-1}$), respectively; C=O (1727, 1672 cm$^{-1}$); CO…H (1515cm$^{-1}$); CH bending vibration (1438 cm$^{-1}$); asymmetrical and symmetrical S=O stretching (1348 and 1167 cm$^{-1}$), respectively; –NH–$C_4H_8$- (906.5 cm$^{-1}$); out of plane bending vibration of the NH and C-S symmetric stretch (826.4 and 775.3) cm$^{-1}$, respectively; the C-O bend vibration (707.1 cm$^{-1}$); the amide group of lactam ring (580.5 cm$^{-1}$); $SO_3$ asymmetric bend (502.9 cm$^{-1}$). $SO_3$-bCPSA (Fig. 4.4d): asymmetric and symmetric CH stretching (2939 and 2864 cm$^{-1}$), respectively; C=O (1678 cm$^{-1}$); CO…H (1516 cm$^{-1}$); CH bending vibration (1438 cm$^{-1}$); asymmetrical and symmetrical S=O stretching (1346 and 1166 cm$^{-1}$), respectively; –NH–$C_4H_8$- (906.4 cm$^{-1}$); out of plane bending vibration of the NH and C-S symmetric stretch (826.2 and 781.9 cm$^{-1}$), respectively; the C-O bend vibration (707.9 cm$^{-1}$); the amide group of lactam ring underwent a big shift (571.8 cm$^{-1}$); $SO_3$ asymmetric bend (503.2 cm$^{-1}$).

The split carbonyl band also appeared in the spectra of $SO_3$-bCPHA and $SO_3$-bCPMS. To

explain the presence of the intense peak at 1034 cm$^{-1}$ and the absence of the C-O bend in SO$_3$-bCPHA, we need more structural interactions' study. A more detailed assessment of band assignments for SO$_3$-bCP and SO$_3$-bCPILs is given in Table 4.3



(a)



(b)
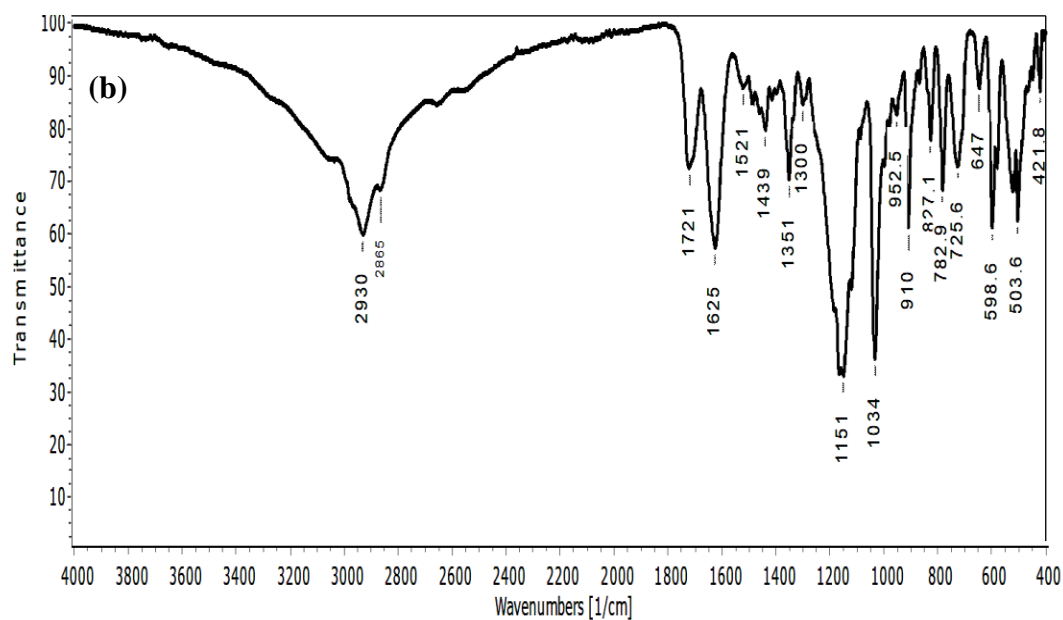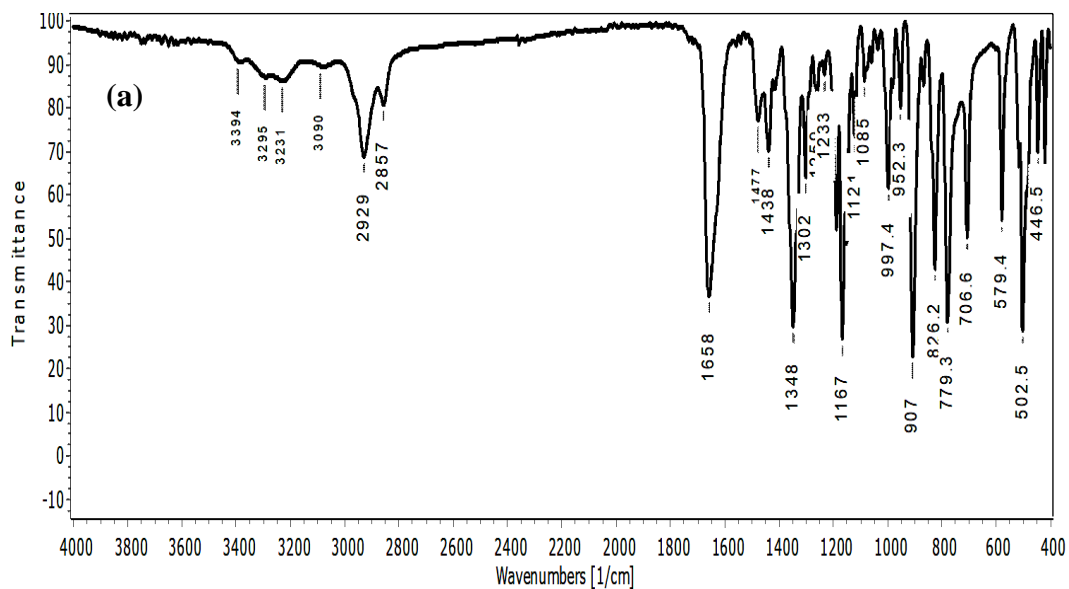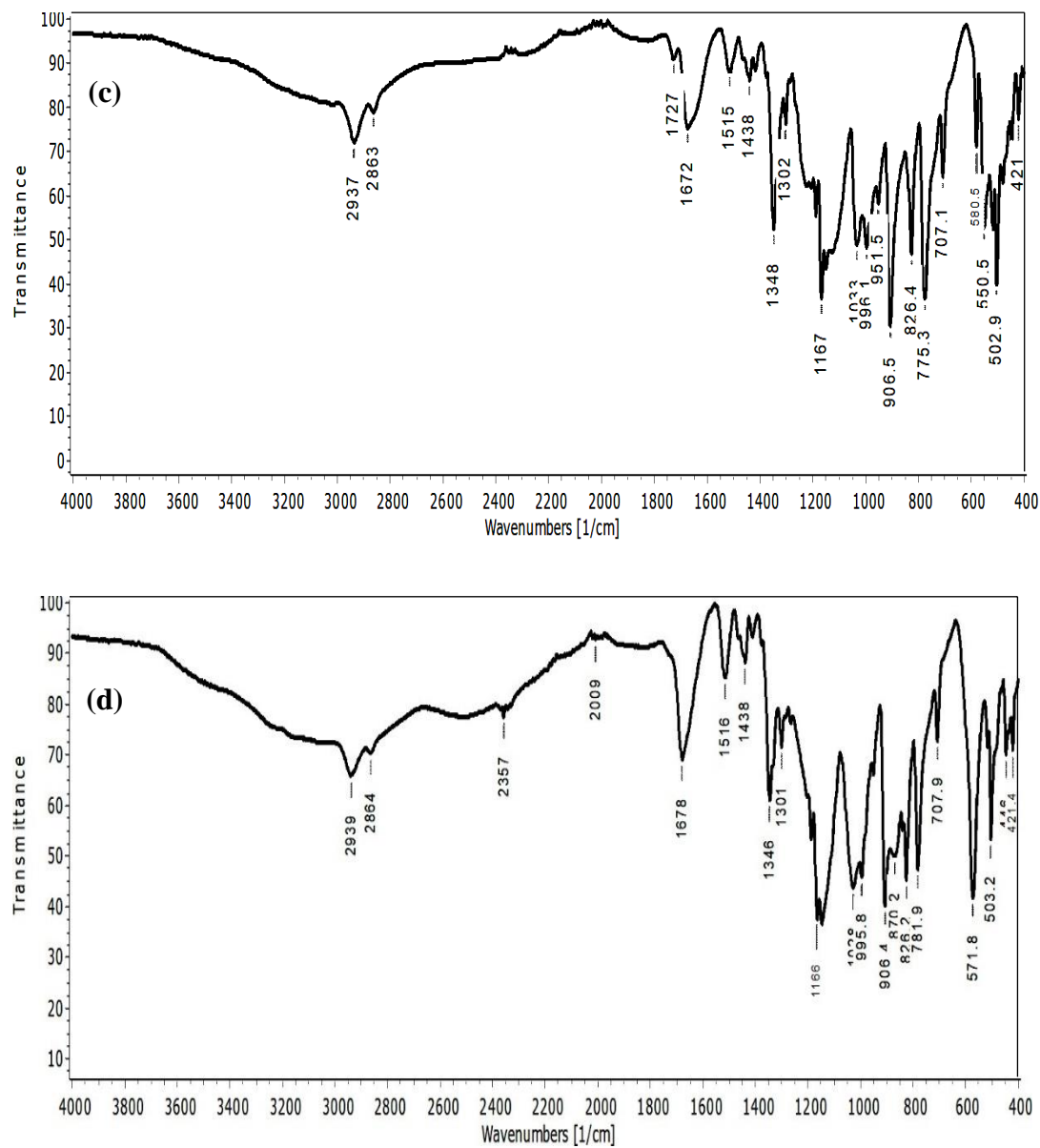
Figure 4.4. FTIR spectra of (a) $SO_3$-bCP, (b) $SO_3$-bCPHA, (c) $SO_3$-bCPMS, (d) $SO_3$-bCPSA

Table 4.3. FT-IR Spectroscopy vibrational wavenumbers and mode assignments of $SO_3$-bCP and $SO_3$-CPILs (in $cm^{-1}$)

| Wavenumbers $cm^{-1}$ | | | | Band assignment | Functional groups |
|---|---|---|---|---|---|
| $SO_3$–bCP [a] | $SO_3$–bCPHA | $SO_3$–bCPMS | $SO_3$–bCPSA | | |
| 3295, 3231, 3090 | 3286.48 | 3269.12 | 3404.13 | $\nu$N-H, | Amine group of sulphonic-functionalized-lactam |
| 3394 | - | - | - | N-H$^+$C$_4$H$_8$-SO$_3$ | Protonated amine of ILs |
| - | 3041.53 | - | 3049.25 | $\nu_{as}$CH$_3$ | CH$_3$ methyl group of the methylsulphonate |
| 2929 | 2930 | 2937 | 2939 | $\nu_{as}$CH$_2$ | CH$_2$ methylene groups from cyclic lactam and butylsulphonate chain |
| 2857 | 2865 | 2863 | 2864 | $\nu_s$CH$_2$ | |
| 1658 | 1721, 1625 | 1727, 1672 | 1678 | $\nu_s$C=O | The carbonyl group of the lactam |
| 1477 | 1521 | 1515 | 1516 | C=O….N-H | hydrogen bond formed between carbonyl and amine groups of lactam |
| 1438 | 1439 | 1438 | 1438 | sciCH$_2$ $\delta$CH$_2$, | CH$_2$ methylene groups from cyclic lactam |
| 1348, | 1351, | 1348, | 1346, | $\nu_{as}$S=O, | S=O of butyl sulphonate group |
| 1167 | 1151 | 1167 | 1166 | $\nu_s$S=O | |
| 1348, 1302 | 1351, 1300 | 1348, 1302 | 1346, 1301 | –NH–CH$_2$–$^a$ | The amide group bonded with the alkyl group in lactam ring |
| 907 | 910 | 906.5 | 906.4 | –NH–C$_4$H$_8$–$^b$, $\nu$ S-OHc | The amide group bonded with the alkyl group in lactam ring with the butyl chain, or the sulphonate group |
| 1058 w | 1034 sh | 1033 w | 1029 | $\delta$ S-O-H or $\nu_s$SO$_3$ | The sulphonate group |
| 779.3 | 782.9 | 775.3 | 781.9 | Free and associated $\nu_s$ C-S $^d$ | The butylsulphonate group |
| - | - | - | 536.17 | $\delta_s$SO$_3$ d | The sulphate group |
| 706.6 | - | 707.1 | 707.9 | $\delta$C=O | The carbonyl group of the lactam |
| 826.2 | 827.1 | 826.4 | 826.2 | $\delta$N-H | Amine group |
| 579.4 | 598.6 | 580.5 | 571.8 | OC-NH | Amide group of the lactam ring |
| 502.5 | 503.6 | 502.9 | 503.2 | $\delta_{as}$SO$_3$ | SO$_3$ asymmetric bend of sulphonic group |

$\nu$= stretching, $\nu_s$= symmetric stretching, $\nu_{as}$ = asymmetrical stretching, $\delta$ = deformation (bend), $\delta$s = symmetric, deformation (bend), sci = scissor, sci$_s$ = symmetric scissor, sci$_{as}$ = asymmetric scissor, sh = sharp, w = weak.

Band assignments are taken from references, [a] (Garbuzova & Lokshin, 2004), [b](Kiefer et al., 2018), [c] (Zhong et al. 2018); [d] (Singh et al. 2016).

**4.2.1.4 Raman analysis of the synthesized caprolactam-based ILs**

Figure 4.5 shows Raman spectra of the original caprolactam and its ionic liquids (CPILs) in the region 400 - 2200 $cm^{-1}$. The caprolactam (CP) spectrum shows two main absorption peaks. Compared to a previous study by (Triggs et al., 1993), the two peaks correspond to the vibrations of the C=O stretch between 1600 – 1700 $cm^{-1}$ and C-N stretch between 1480 - 1580 $cm^{-1}$. Other peaks appeared in the spectrum for the bending vibration of C=O (579.75, 865.56 $cm^{-1}$), and at 696.59 $cm^{-1}$ which may be assigned to vibration of N-H. In the 739.59 - 1438.98 $cm^{-1}$ region of the CP Raman spectra, the absorptions may be attributed to methylene sequences ($CH_2$ rock, wag, twist, and scissor) (Schmidt & Hendra, 1994).

Similar absorption peaks were observed in CPAA and CPHA, with a slight shift in position and/or a difference in band areas and intensities. In particular, the C=O stretch on CPAA was located at 1618.73 $cm^{-1}$ (for Caprolactamium cation) and 1708.61 $cm^{-1}$ (for acetate anion), whereas on CPHA it was located at 1625.92 $cm^{-1}$ (for Caprolactamium cation). The lower frequencies of C-O bend on CP, CPAA and CPHA appeared at 579.7, 619.3 and 577.96 $cm^{-1}$. The observable change in absorption peak intensities occurred in the region of C-N stretch and N-H vibration, which provide evidence for the generation of new interactions due to the formation of the ILs. Moreover, there is a band that appears at 879.94 $cm^{-1}$, which may relate to symmetric C-C stretch in the acetate ion (Yang, Tripathy, Li, & Sue, 2005). In CPSA, CPMS, and CPTFS spectra, a sharp and intense peak occurred between 1000 - 1100 $cm^{-1}$, and was assigned to asymmetric vibration of $SO_4$ and symmetric $SO_3$ stretch (Rull & Sobron, 1994; Singh et al., 2016; Zhong et al., 2018). Whereas the peaks that appeared at 542, 544 and 572.5 $cm^{-1}$ in CPMS, CPSA and CPTFS spectra may

be attributed to the S-O wag, as reported by (Chackalackal & Stafford, 1966), they also seemed to overlap with C-Obend frequencies. The strong peak at 742 cm$^{-1}$ in the CPTFA spectrum may be attributed to the presence of a C-F bond (Shartsaa et al., 1998), although the vibration of CH$_2$ rock may overlap it. Moreover, a significant change was revealed by the intensities and positions, as well as the disappearance, of the main characteristic peaks such as C=O, C-N, and N-H. Specifically, the missing carbonyl band in each of CPTFA and CPTFS spectra, may be explained by the presence of fluorine groups, which may generate more interactions with caprolactamium cations through the H- bond, due to protonation of the carbonyl group as illustrated in Figure 4.6 (Fábos et al., 2008). The summary of all absorption bands is presented in Table 4.4.
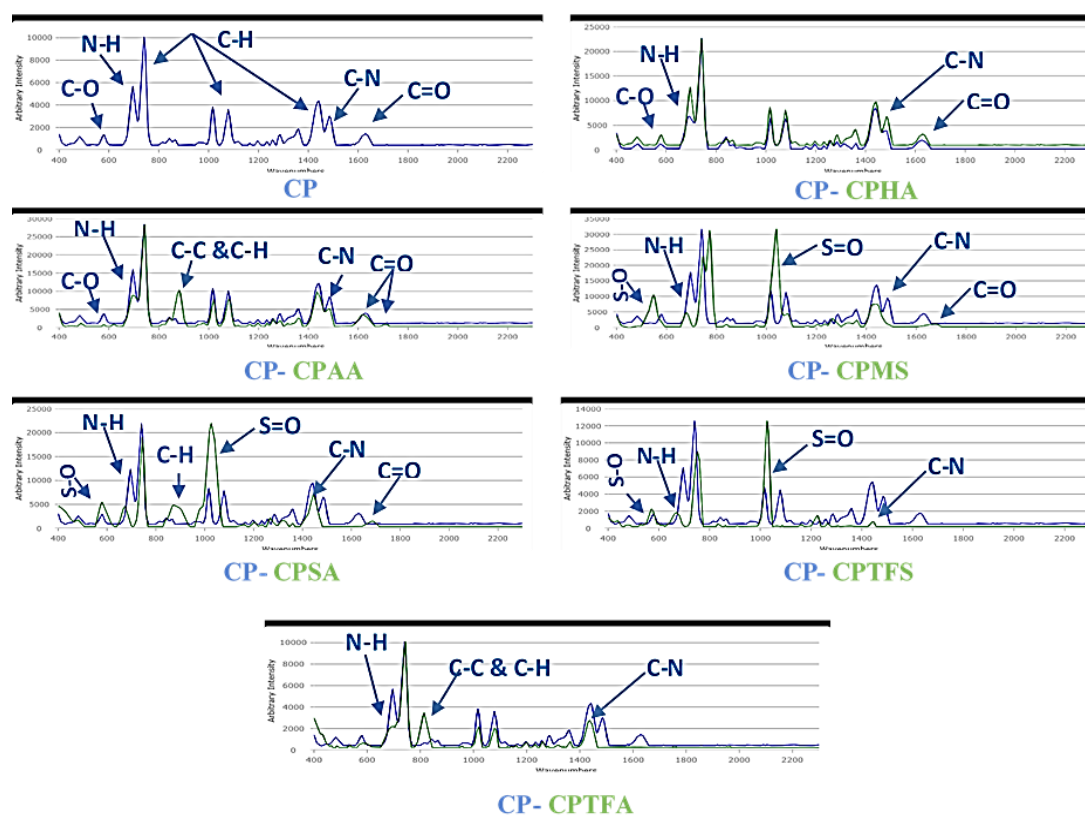


Figure 4.5. Comparison of Raman spectra of caprolactam (CP, blue) and its ionic liquids (green)
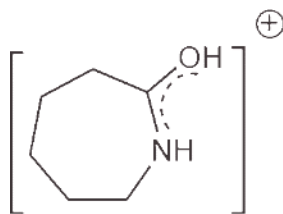
Figure 4.6. Protonation of ε-caprolactam

**4.2.1.5 Raman analysis of the sulfonic butyl-functionalized caprolactam ILs**

Figure 4.7 shows the Raman spectra of sulfonic butyl-functionalized caprolactam ($SO_3$-bCP) and its ionic liquids. Compared to the caprolactam spectrum, the $SO_3$-bCP showed the appearance of peaks that may assigned to the butyl sulphonic group, such as C-C and C-H in and out of plane bending at 782.9, 1072, 1165.8 $cm^{-1}$ and 1439 $cm^{-1}$; symmetric $SO_3$ stretch at 1000.4 $cm^{-1}$. The band at 506.7 $cm^{-1}$ may be attributed to S-O wag (Chackalackal & Stafford, 1966). The peak located at 1359 $cm^{-1}$ may be assigned to $SO_2$ asymmetric stretching (Chackalackal & Stafford, 1966) or C-C stretching mode (Singh et al., 2014). This is besides the observable shift in frequencies and intensities in the main characteristic peaks in caprolactam that was mentioned previously.

In $SO_3$-CPHA spectrum, there is a peak at 646 $cm^{-1}$, which may represent a hydroxyl in S-OH group. The intense reduction of C-H band at 740 $cm^{-1}$ may be explained by the formation of hydrogen bonds between methylene groups in the butyl chain and chloride ions. The N-H at 706 and 707 $cm^{-1}$ in $SO_3$-bCPMS and $SO_3$-bCPSA spectra appear as very intense peaks, which are different from other ILs. For demonstration of this phenomenon, more understanding of structural interactions will be needed. Moreover, the overlapping that was observed in C-H and $SO_4$/$SO_3$ regions of 700-1300 $cm^{-1}$ and 1000-1100 $cm^{-1}$, respectively (more observable in $SO_3$-bCPMS), may due to the sources of these groups:

from methyl sulphonate, hydrogen sulphate and the sulphonic butyl chain. Another intense peak was observed at 773.8 cm$^{-1}$ and overlapped with C-H at 750.5 cm$^{-1}$ in SO$_3$-bCPMS spectrum, and may be attributed to S-C stretch (Chackalackal & Stafford, 1966). The summary of all absorption bands of SO$_3$-bCPIL/ CPIL is presented in Table (4.4).
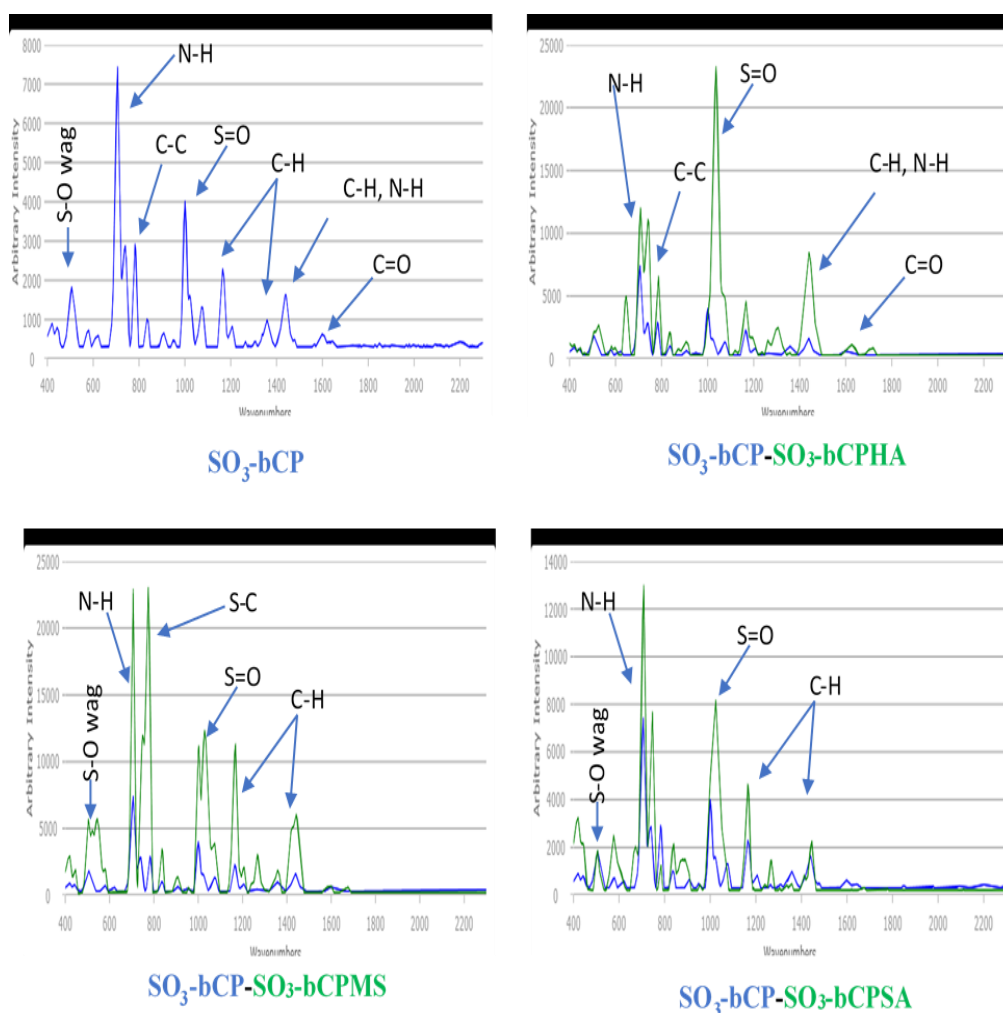


Figure 4.7. Comparison of Raman spectra of sulfonic butyl-functionalized caprolactam (SO$_3$-bCP, blue) and its ionic liquids (green)

Table 4.4. Raman vibrational wavenumbers and mode assignments of $SO_3$-bCPIL/ CPIL (in $cm^{-1}$)

| ILs | vsC=O | vC-N | vN-H | δC=O | Methylene sequences CH2 | vsC-C | vas S=O in SO4 | vs & δ S=O in SO3 | vsS-OH or S-Ow |
|---|---|---|---|---|---|---|---|---|---|
| CP | 1627.53 | 1485.71 | 696.59 | 577.96 | 741.5,str 1016&1077,r 1284.31 &1358.09,w& tw. 1438.98 sci | - | - | - | - |
| CPAA | 1618.73, 1708.61 | 1482.12 | 696.59 | 579.75 | 1018 & 1081r 1359.89,w& tw 1437.16 sci | 879.94 | - | - | - |
| CPHA | 1625.92 | 1487.52 | 694.8 | 574.36 | 1016.56,1075.88r 1358.09 w & tw, 1438.98 sci | - | - | - | - |
| CPMS | 1689.79 | - | 745.13 | - | 1305.52, w & tw 1431.84 sci, 942.6, CH3 r | - | - | 1035.11, vs; 544.1,δ | - |
| CPSA | 1685.24 | - | 671.43 | 579.75 | 1268.21& 1320.34, w & tw, 1446.17, sci | - | 1025.54 | - | 878.15 |
| CPTFA | - | - | 693 sho | 588.74 | 1016.56 & 1079, r; 1261.02& 1363.48, w & wt; 1437.18, sci | 813.43 | - | - | - |
| CPTFS | - | - | 667.83 | 572.56 | 1221.48, w & tw ; 1442.27, sci | - | - | 1027.34 | - |
| SO3-bCP | 1600 | - | 706 | 576.1 | 738;1074.2 r; 1358.9; w & tw; 1439, sci | 782.5; 1165 | - | 1001.3 | 506.7; S-Ow |
| SO3- bCPHA | 1625.9 | - | 709.1 | | 739.7, 1263, 1302.4, 1440.8 | 786.5, 1166 | - | 1036.3 | 506.1, S-O; 525.8, S-OH |
| SO3-bCPMS | 1672.7 | - | 705.6 | | 750.5r,1072.2,1266.4, 1358.1, 1440.8 | 836.8, 1166 | - | 1002.1; 1029.1 | 506.1, 543.8 |
| SO3- bCPSA | - | - | 707.4 | 576.2 | 745.1, 1266.4, 1444.4 | 782.9, 838.6, 1166 | 1023.8 | 1023.8 | 504.3 |

$v_s$ =symmetric stretch; $v_{as}$= Asymmetric stretch δ= Asymmetric bend; r = rock, w=wag; tw= twist; sci= scissor; sho= shoulder. Band assignments are taken from references (Chackalackal & Stafford, 1966) and (H. Singh et al., 2014)

**4.2.2 Density and Viscosity of CPILs and SO₃-bCPILs**

The densities ($\rho$) and dynamic viscosities ($\eta$) of CPAA, CPSA, CPTFA, and CPTFS were measured at 20 °C without further drying, and the results are presented in Table 4.5. The $\eta$ and $\rho$ magnitudes of CPAA were the lowest. These values are different from $\eta$ and $\rho$ at 20 °C (39.81 mPa.s and 1.06 g/ml), respectively, reported by (Chhotaray et al., 2014) with water content of 3872 µg/g. The viscosity and density of CPTFA (Table 4.5) are almost similar in magnitude to the values of 28 mPa.s and 1.24 g/ml reported at 25 °C by (Du et al., 2005). The CPSA exhibited a higher viscosity value (3549.63 mPa.s), however, the findings of (Fábos et al., 2008) showed that the viscosity was unmeasurable at 80 °C. The viscosity value of CPTFS has not yet been reported in literature. In contrast, the density of CPSA (1.358g/ml) is lower than the density of CPTFS (1.375g/ml). (Fábos et al., 2008) also reported that the density of CPSA was (1.372g/ml) at 50 °C. The differences in the viscosities and densities from literature can be explained by the presence of water impurities (Grishina et al., 2013). Moreover, given that viscosity and density depend on molecular weight (Mw) of the anions - as in the case of CPAA, CPTFA, and CPTFS - then it follows that the two properties increase with increase in Mw (Seki et al., 2010). However, CPSA is structurally dependent on density and viscosity, findings that have been reported for imidazolium-based ILs by Ullah et al., (2015) who demonstrated that the phenomena is due to strong interactions, and less steric hindrance, of cationic and anionic structures. We propose that the interaction between [HSO₄]⁻ and Caprolactamium cation results in hydrogen bonding between the [HSO₄]⁻ ion dimers and the acidity hydrogen of the amide group on the caprolactam (Figure 4.8). Ko1lle & Dronskowski, (2004) investigated and showed the bridge of two [HSO₄]⁻ anions by two short hydrogen bonds to form dimers, as well as the formation of hydrogen bonding between the dimer and the acidity hydrogen on

the imidazolium ring.

Table 4.5. Density and Viscosity of CPILs and SO$_3$-bCPILs at 20 °C

| Ionic liquid | Molecular weight (Mw, mol/g) | Density ($\rho$) (g/ml) | Viscosity ($\eta$) (mPa.s) | Water content (w/w %) |
|---|---|---|---|---|
| CPAA | 137.212 | 1.042 | 13.69 | 4.52 |
| CPSA | 211.239 | 1.358 | 3,549.63 | 1.21 |
| CPTFA | 224.18 | 1.249 | 24.81 | 0.65 |
| CPTFS | 263.24 | 1.375 | 144.76 | 1.53 |
| SO$_3$-bCPHA | 285.788 | 1.218 | Unmeasurable[*] | 0.29 |
| SO$_3$-bCPMS | 345.43 | 1.26 | 180.5[*] | 0.65 |
| SO$_3$-bCPSA | 347.409 | 1.405 | Unmeasurable[*] | 1.28 |

*At 40 °C. Unmeasurable = couldn't be determined using viscometer method
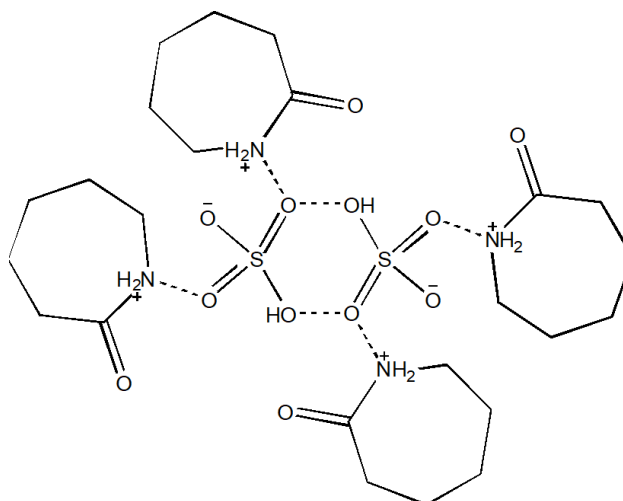


Figure 4.8. Proposed hydrogen bond interaction in CPSA

Similar observations have been reported for the SO$_3$-bCPILs. For instance, the densities

follow the increasing order, SO$_3$-bCPSA > SO$_3$-bCPMS > SO$_3$-bCPHA, and this indicates

their dependency on molecular weight (Mw) of the anions. Thus, density increases with

increase in Mw as shown in Table 4.5, while viscosity seems to be structurally dependent.

We would also like to point out that the viscosity and density measurements of these ionic

liquids have not yet been reported in literature.

On the other hand, when the comparison of density and viscosity was performed for all CPILs and $SO_3$-bCPILs together, they were found to be follow the increasing order, $SO_3$-bCPSA > CPTFS > CPSA > $SO_3$-bCPMS > CPTFA > $SO_3$-bCPHA > CPAA, while the Mws of these compounds followed the order, $SO_3$-bCPSA > $SO_3$-bCPMS > $SO_3$-bCPHA > CPTFS > CPTFA > CPSA > CPAA. Therefore, it was obvious that these properties are only dependent on cation-anion interactions. Hence, a deeper understanding of the structure interactions of these compounds is necessary.

### 4.2.3 Determination of thermal stability and purity of $SO_3$-bCPIL/CPIL

Thermogravimetric analysis (TGA) of $SO_3$-bCPIL/CPIL was performed to determine the thermal stability and the percentage purity of CPILs and $SO_3$-CPILs. The thermograms of the two classes of CPILs demonstrated that there are three or more observable weight loss (in mg) regions, as presented in Figure (4.9 I) and Table (4.6). The exact temperature at which a weight loss occur has been determined from the $1^{st}$ derivative of the TGA curve in the form of endothermic peaks for each IL, as demonstrated in TGA curve of CPTFS and its derivative (Figure 4.9 II). Initially, there are slight mass losses of 2 to 7 % between 41 - 177 $^oC$, which may be corresponded to the loss of physically bound water and breakup of hydrogen- bonded networks (Elavarasan et al., 2015). The decomposition of the ILs occurred then with the increase of temperature. The weight loss from 108 - 440 $^oC$, with mass loss ranges of 4 – 63 % may be attributed to the loss of low molecular weight compounds (Ojha & Das, 2017) such as acetate and halides (chloride & fluoride), and to combustion of –$SO_3H$ (Li et al., 2021) present in $SO_3$-CPILs and CPMS, CPSA and CPTFS, as well. The final step of thermal decomposition for the all ILs were occurred

between 167 ºC and 541 ºC, with mass losses of 9 – 44 %, which may be ascribed to decomposition of the C-H bonds of the cyclic ring of caprolactam.

To insure that the weight losses in TGA curve for each IL belong to evaporation of water, loss of low molecular weight compounds, combustion of –SO$_3$H and C-H bonds decomposition, X-ray diffraction studies should be performed after each weight loss step. Moreover, the sulphonic acid functional group in SO$_3$-CPMS lowers the thermal stability of the ionic liquids compared to their corresponding CPMS. Amarasekara & Owereh, (2011) reported similar findings, when they demonstrated the effect of sulphonic groups on the thermal stability of imidazolium-based ionic liquids. However, on the contrary, the sulphonic acid functional group in each of SO$_3$-CPSA and SO$_3$-CPHA significantly increased their thermal stability compared to their corresponding CPSA and CPHA, respectively.
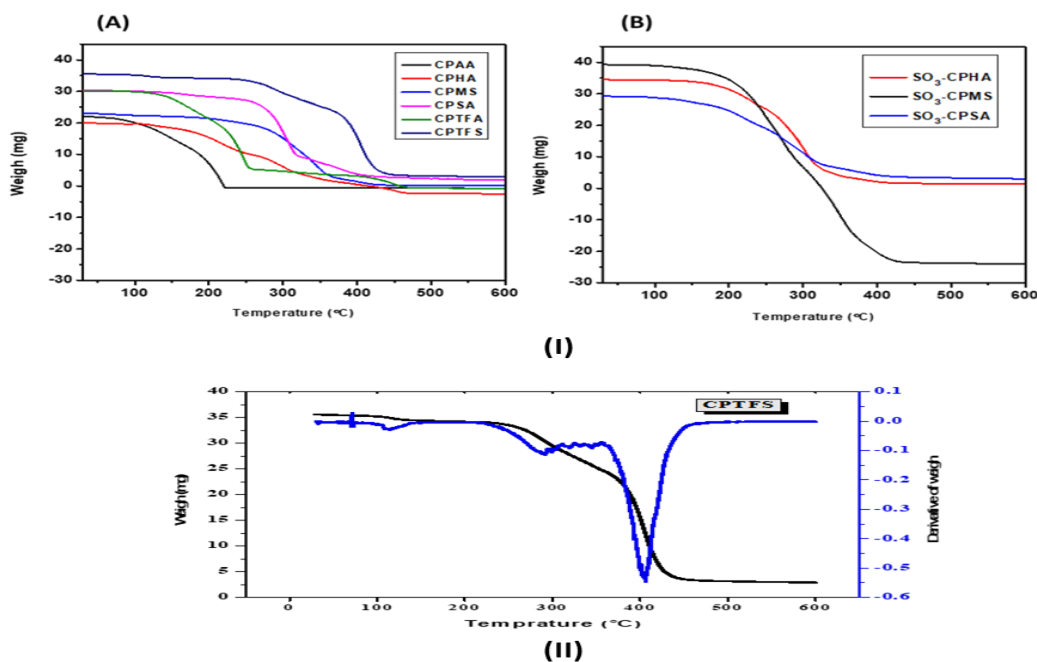


Figure 4.9 Thermogravimetric analysis (TGA) of: (I) CPILs, (A) and SO$_3$-functionalized CPILs (B). (II) TGA curve and its derivative for CPTFS

The TGA of the $SO_3$-bCPIL/CPIL shows that they are stable in the range of 108 °C to 221 °C as depicted in Table 4.6 and their thermal stability followed an increasing sequence of CPTFS > CPMS > $SO_3$-bCPMS > $SO_3$-bCPHA > $SO_3$-bCPSA > CPSA > CPTFA > CPHA > CPAA. Du et al., (2005) reported a similar result for CPTFA (up to 135 °C). Therefore, TGA confirmed that all $SO_3$-bCPIL/CPIL that we prepared had excellent thermal stability (CPAA, recorded the minimum), and can therefore be used as catalysts for trans-esterification of lipids, even at high temperature.

Table 4.6. Thermal decomposition (Td/ °C) stages of CPILs and $SO_3$ -functionalized CPILs

| $SO_3$-CP/ CPILs | Evaporation of water | Low Mwt compounds and / or -$SO_3H$ group combustion | Final step in the thermal decomposition of $SO_3$-CP/ CPILs |
|---|---|---|---|
| CPAA | 60 – 108 | 108-167 | 167 – 223 |
| CPHA | 105 -128 | 128-254, 254-318, 318-409 | 409 - 479 |
| CPMS | 41 – 177 | 177 - 223, 223 - 353 | 353 - 446 |
| CPSA | 102 – 156 | 156 - 240, 240-307, 307 - 440 | 440 - 541 |
| CPTFA | 72– 135 | 135 – 197, 197 – 251, 251 - 386 | 386 - 478 |
| CPTFS | 81 – 127 | 221 – 355 | 355 - 465 |
| $SO_3$-CPHA | 76 – 166 | 166 – 236, 236 - 327 | 327 - 463 |
| $SO_3$-CPMS | 92 – 174 | 174 – 300 | 300 – 483 |
| $SO_3$-CPSA | 81 – 162 | 162 – 245, 245 – 318, 318 - 351 | 351 - 515 |

The percentage purity of the $SO_3$-bCPIL/CPIL were also determined from the mass losses in TGA curve using equation as shown in Table (4.7) and Appendix (A). The results revealed that all the synthesized ILs were prepared with high purity (100 %).

Table 4.7: The percentage purity of $SO_3$-CP/ CPILs

| $SO_3$-CP/ CPILs | $W_{initial}$ (mg) | Total W loss % | Total W loss (mg) | Purity % |
|---|---|---|---|---|
| CPAA | 30.58 | 74.01 | 22.64 | 100.01 |
| CPHA | 28.66 | 77.67 | 22.55 | 101.00 |
| CPMS | 31.65 | 72.47 | 22.94 | 100.00 |
| CPSA | 38.82 | 73.05 | 28.36 | 99.99 |
| CPTFA | 38.93 | 79.59 | 31.12 | 100.40 |
| CPTFS | 44.20 | 73.5 | 32.41 | 99.76 |
| $SO_3$-CPHA | 43.17 | 76.89 | 33.19 | 99.99 |
| $SO_3$-CPMS | 47.88 | 99.95 | 47.88 | 100.05 |
| $SO_3$-CPSA | 37.75 | 69.2 | 26.12 | 99.99 |

**4.2.4 Determination of $SO_3$-bCPIL/CPILs acidity strength**

The role of $SO_3$-bCPIL/CPIL acidity in the trans-esterification reaction is carried out by determining the Hammett acidity function ($H_0$) of $SO_3$-bCPIL/CPIL, which also indicates their catalytic activity.

The maximum absorbance of the indicator in its unprotonated form was observed at 380 nm in water as depicted in Figure (4.10), and this is consistent with previously reported values (Kore & Srivastava, 2011). When an acidic CPIL was added, the indicator was protonated by the acid and thus the absorbance of unprotonated 4-nitroaniline was reduced

as follows: CPAA > CPTFA ≈ SO$_3$-bCPHA > CPHA > SO$_3$-bCPMS ≈ CPSA > H$_2$SO$_4$ > CPMS > CPTFS >SO$_3$-bCPSA (Figure 4.10). The [I]/[IH+] ratio was determined by measuring the difference in absorbance after the addition of SO$_3$-bCPIL/CPIL, and Hammett's acidity of SO$_3$-bCPIL/CPIL was calculated using Equation (4):

$$H_0 = pK(I)aq + \log \left([I]/[IH]^+\right)$$

Therefore, when a SO$_3$-bCPIL/CPIL with stronger acidity was added, a lower H$_0$ value would be obtained. According to the data reported in Table (4.8), acidity increases in the following order: CPAA ≈ CPTFA ≈ SO$_3$-bCPHA ≈ CPHA < SO$_3$-bCPMS ≈ CPSA < H$_2$SO$_4$ < CPMS < CPTFS < SO$_3$-bCPSA, which is the reverse of the absorbance trend. Findings with a similar trend of CPSA < H$_2$SO$_4$ < SO$_3$-bCPSA has been reported by (Luo et al., 2017).
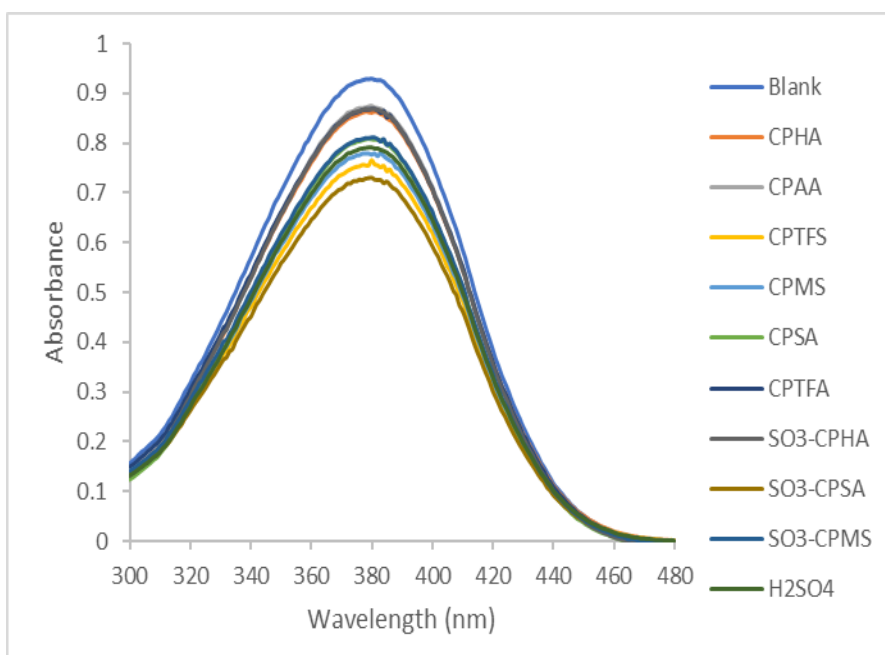


Figure 4.10. Absorption spectra of 4-nitroaniline for various SO$_3$-bCPILs/CPILs in distilled water

Table 4.8. Hammett acidity ($H_0$) values of the $SO_3$-bCPIL/CPIL at room temperature.

| $SO_3$-bCPIL/CPIL | $A_{max}$ | [I]% | [IH$^+$]% | $H_0$ |
|---|---|---|---|---|
| Blank | 0.928 | 100 | 0 | - |
| CPAA | 0.876 | 94.4 | 5.6 | 2.23 |
| CPTFA | 0.870 | 93.8 | 6.3 | 2.16 |
| $SO_3$-bCPHA | 0.870 | 93.8 | 6.3 | 2.16 |
| CPHA | 0.860 | 92.7 | 7.3 | 2.09 |
| $SO_3$-bCPMS | 0.810 | 87.3 | 12.7 | 1.827 |
| CPSA | 0.809 | 87.2 | 12.8 | 1.823 |
| $H_2SO_4$ | 0.790 | 85.1 | 14.9 | 1.747 |
| CPMS | 0.776 | 83.6 | 16.4 | 1.697 |
| CPTFS | 0.757 | 81.6 | 18.4 | 1.637 |
| $SO_3$-bCPSA | 0.730 | 78.7 | 21.3 | 1.558 |

As stated above, the acidity of CPIL clearly depends on the anion structure, as CPTFS shows stronger acidity while CPAA shows lower acidity. On the other hand, the $SO_3$-bCPILs, such as $SO_3$-bCPSA, showed observable increase in acidity compared to their corresponding unfuctionalized CPILs (CPSA). In contrast, $SO_3$-bCPMS had a lower acidity value than that of CPMS, whereas $SO_3$-bCPHA had an acidity strength almost similar to CPHA. This finding is inconsistent with the report of (Luo et al., 2017), who demonstrated that the acidity of $SO_3$-functional caprolactam-based ionic liquids is stronger than that of sulfone-free caprolactam-based ionic liquids. Therefore, we can conclude that the acidity of $SO_3$-bCPIL/CPIL depends on the intra molecular interactions between the cation and anion. Thus, additional study on the structure of these compounds will be

required.

## 4.3 Extraction of lipids from microalgae biomass

## 4.3.1 Optimization of lipid extraction time and temperature

Figure 4.11 depicted a comparison of lipid yield between 5 h at 75 ˚C and 2 h at 95 ˚C

extractions of three selected CPILs. Thus, long period/low temperature and short

period/high temperature were compared in order to minimize reaction time. There was no

significant difference in lipid extraction yields (P-value = 0.23) of CPHA, CPAA and

CPSA at 75 ˚C for 5 h and at 95 ˚C for 2 h. As a result, lipids were extracted using synthetic

ionic liquids at 95 ˚C for 2 h.
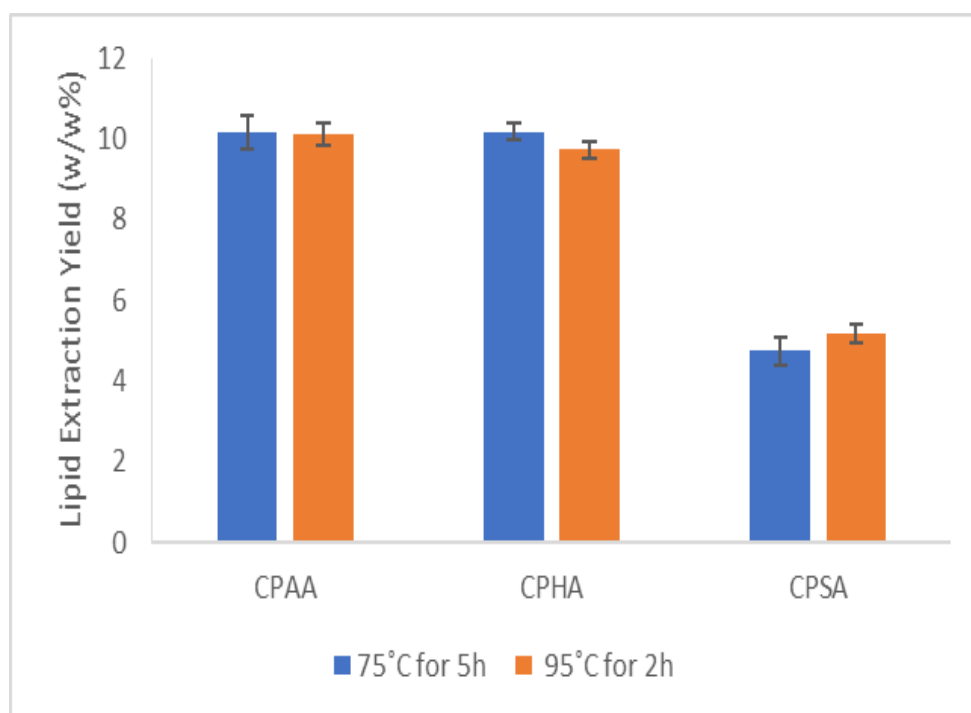


Figure 4.11. The yield of extracted Lipids by ionic liquids at 75 ℃ for 5 h

and 95 ℃ for 2 h

**4.3.2 Extraction of lipids by a conventional method and pure CPILs**

The extraction yields of the synthetic CPILs from dried biomass (with moisture content of 11.2 ± 0.005 %) as well as the total recovered lipids obtained by conventional Soxhlet extraction using hexane- MeOH as solvents (control) (Derakhshan et al., 2015), are shown in Figure 4.12. The yield from the conventional organic solvent extraction method (control) was 9.5 ± 0.23 %, which is comparable to the yield obtained by Mandal et al., (2013), under the following conditions: Chloroform: methanol (2:1), 6 h at r.t. 8.60 % lipids from *Spirulina* algae biomass was also reported by Nautiyal et al., (2014) using Bligh and Dyer traditional method for lipid estimation. The extraction yields of three of the CPILs did not differ significantly from the control experiment (P > 0.05). CPAA, CPTFA, and CPHA, in particular, had lipid yields of 10.1 0.28% (P-value = 0.153), 10.1 0.25% (P-value = 0.159), and 9.3 0.1% (P-value = 0.326). This is in contrast to previous research on lipid extracts from dried and dehydrated marine *Nannochloropsis oculata*, *Chlorella salina*, and *Chlorococcum sp* microalgae, which found that using CPAA for extraction resulted in lower yields compared to the control (Shankar et al., 2017; Shankar et al., 2019). The reason for this can be due to the fact that the cell wall structures of microalgae, which contain cellulose, glycoprotein, silica, and peptidoglycan (Zhou et al., 2019), may vary from one type to another. As a result, various ILs may have varying levels of cell wall penetration. Therefore, CPAA may have a greater impact on the wall structure of *S. platensis*. On the other hand, lower yields (circa. 5%) were obtained using CPSA (*P*-value = 0.003), CPTFS (*P*-value = 0.031), and CPMS (*P*-value = 0.01). Overall, the CPILs containing sulphate and sulphonate anions yielded the least amount of lipids when compared to the control experiment. To et al., 2018 studied lipid extraction from *S.*

*platensis* utilizing choline and amino acid based ILs for efficient lipid extraction from *S. platensis*. A high lipid extraction yield up to 51.1% of total lipids was obtained after 3h at 70 °C when choline argininate was used.  Although choline and amino acid based ILs, have similar potential properties of the caprolactam such as easily preparation and low toxicity, however, economic concerns usually limit their application for large scale biodiesel production due to high material cost compare to caprolactam-based ILs.
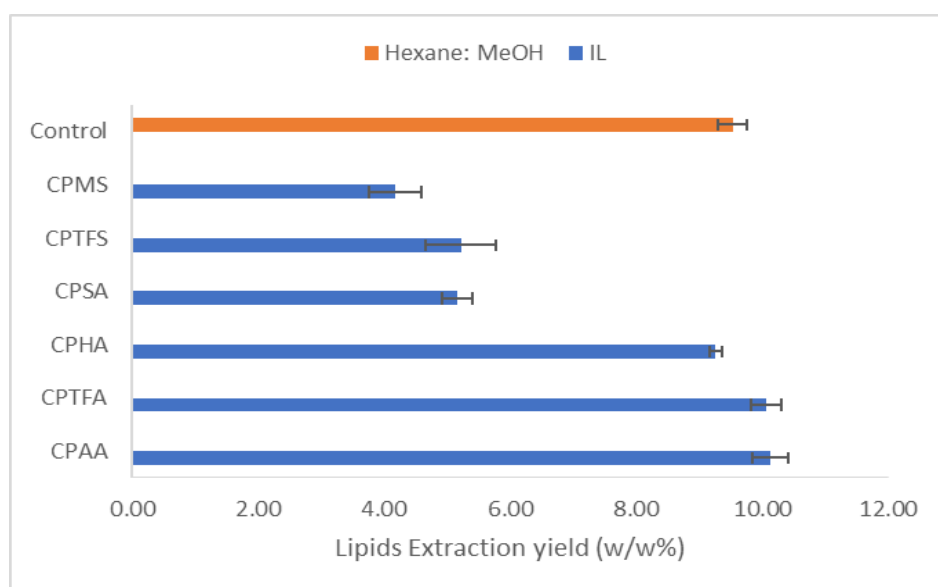


Figure 4.12. The influence of pure ionic liquids on lipid extraction

**4.3.3 The effect of organic co-solvents on CPILs extraction of lipids**

Figure 4.13 depicts the yields for lipid extraction from dry biomass using ionic liquid and methanol mixtures (as co-solvent). Methanol (MeOH) was also used separately as an extraction solvent (negative control) for comparison purposes, yielding 1.31 0.27% lipids. The highest yields were 14.2 0.11% (P-value = 0.007) for the CPAA/ MeOH mixture and 13.1 0.1% (P-value = 0.02) for the CPHA/ MeOH mixture. In this case, a significant increase (P < 0.05) was observed over pure CPAA and CPHA. However, the lipid yield of

the CPTFA/ MeOH mixture was 11.1 0.13% (P-value = 0.028), which was slightly higher than the pure one but still significantly different from the control experiment (P < 0.05). This is due to a variety of interaction mechanisms between IL-IL, IL-methanol and lipids-IL-methanol such as van der Waals Electrostatic, London forces, hydrogen bonds, and hydrophobic bonding (Cooney et al., 2009; Singh et al., 2016; Halim et al., 2012). Therefore, the three CPIL/MeOH mixtures are better than organic solvents in the extraction of lipids from algae biomass, and hence they can be used as alternative green solvents.

On the other hand, the mixtures of methanol with CPSA, CPTFA, and CPMS showed an enhancement of around 6% in lipid yield. The co-solvent effect can be explained by the action of polar methanol on microalgae cell disruption, which improves the efficiency of lipid extraction from biomass (Halim et al., 2012; Dong et al., 2016). The reason behind this is that some non-polar lipids are found in the cytoplasm as a complex with polar lipids. This complex is strongly bound to proteins in the cell membrane via hydrogen bonds. Therefore, polar solvents (CPILs and MeOH), can disrupt lipid-protein associations by forming hydrogen bonds with the polar lipids of the complex (Halim et al., 2012). As a result, methanol speeds up the precipitation of lipids from the cell, whereas CPILs improve the permeability of the cell wall (Zhou et al., 2019). It is also hypothesized that the action of the ionic liquid – methanol system creates a more hydrophobic environment, which makes lipid transfer easier (Zhou et al., 2019). The same author has also claimed that the addition of methanol may reduce the viscosity of ionic liquids, increasing the possibility of hydrogen bonds forming between fibers on the microalgae cell wall and ionic liquids. Moreover, the different intramolecular interactions of these ionic liquids appear to be the primary factor for their ability to form hydrogen bonds with microalgae cell walls, and thus

lead to the differences in their effectiveness for lipid extraction.
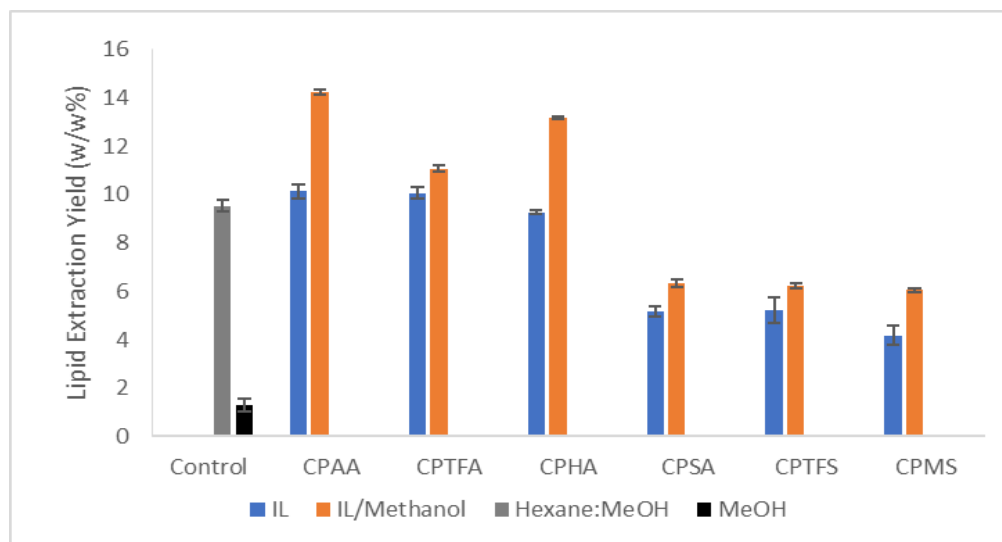


Figure 4.13. Comparison of lipid extraction yields by CPILs and mixtures of

CPIL/MeOH (1:1)

### 4.3.4 The effect of CPIL/MeOH mixture on lipid extraction from wet biomass

In order to reduce the cost of extraction of lipids from microalgae, we have also investigated the potential of these CPILs to extract lipids from wet biomass, thereby avoiding the drying stage, which is thought to be a key contributing factor to the high cost of biodiesel production. In this study, three mixtures of CPAA/ MeOH, CPTFA/ MeOH and CPHA/ MeOH were used, and the highest lipid yields recorded were from dry biomass. The control sample of wet *S. platensis* biomass (80%) provided a lipid yield of $4.1 \pm 0.06$ %. The findings indicated that the CPAA/ MeOH mixture produced the highest yield of 8.07 0.09 % (P-value = 0.001), followed by the CPTFA/ MeOH at 6.1 0.1% (P-value = 0.005), and the CPHA/ MeOH mixture at 5.1 0.08 % (P-value = 0.008). As can be seen, the three mixtures offered a higher yield (P< 0.05) than the control (Figure 4.14). On the other hand, the lipids yield of CPAA is nearly identical (*P*-value = 0.047) to that of the

control sample from dry biomass ($9.5 \pm 0.23\%$). Therefore, from an economic point of view, CPAA could be the most promising CPIL for production of biodiesel from *S. platensis* biomass—in terms of energy and cost savings, when compared to conventional extraction processes.
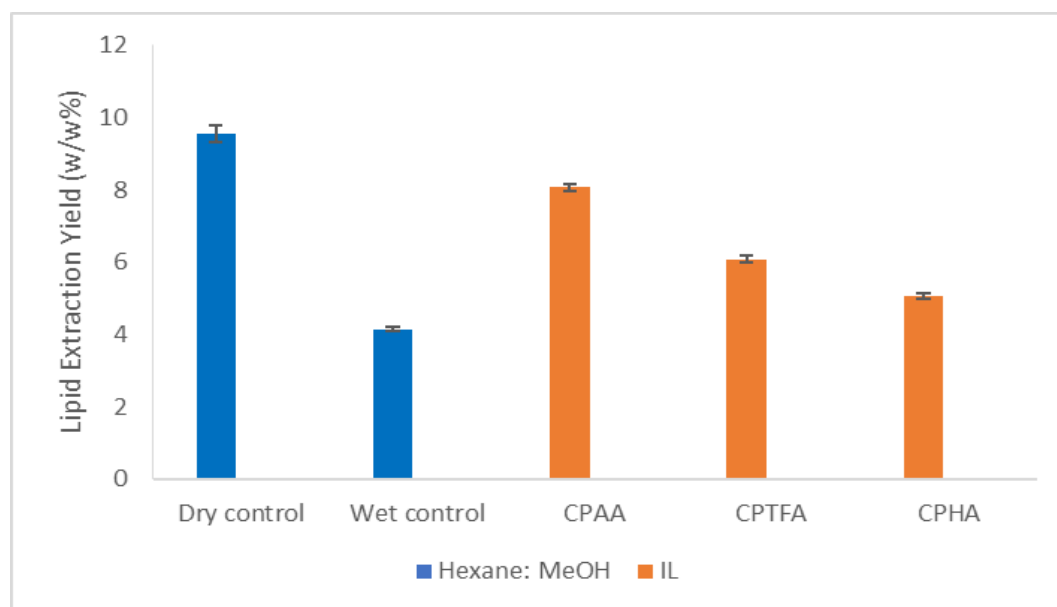


Figure 4.14. Lipid extraction yields from wet *Spirulina platensis* biomass

### 4.3.5 Extraction of lipids by SO₃-bCPIL/MeOH form dry and wet biomass

The use of $SO_3$-functionalized ionic liquids have been widely reported in the literature, but only in their use as catalysts (Fan et al., 2017; Keshavarz et al., 2019; Li et al., 2021; Ong et al., 2021). Particularly, $SO_3$ butyl-functionalized caprolactam-based ionic liquids were used to catalyze biodiesel production from Jatropha oil (Luo et al., 2017). Thus, this study provides a chance to highlight the utilization of these compounds as solvents, too. Figure (4.15) depicted the lipid extraction yields for mixtures of methanol with $SO_3$-bCPSA, $SO_3$-bCPHA and $SO_3$-bCPMS, from both dry and wet microalgae biomass. The findings demonstrated that there was no discernible variation in extraction yields from dry biomass,

when each of the three mixtures was compared to the control i.e. $9.0 \pm 1.41$ % ($P = 0.69$), $9.8 \pm 0.35$ % ($P = 0.56$) and $8 \pm 0.00$ % ($P = 0.07$), for $SO_3$-bCPSA, $SO_3$-bCPHA and $SO_3$-bCPMS mixtures, respectively. For wet biomass, both $SO_3$-bCPSA and $SO_3$-bCPMS showed no significant difference in extraction yields ($8 \pm 0.00$ %, $P = 0.07$). However, $SO_3$-bCPHA recorded a low yield of $2.5 \pm 0.71$ ($P = 0.03$).

Consequently, from an economic perspective, $SO_3$-bCPSA and $SO_3$-bCPMS when compared to conventional extraction processes, could be the most promising ionic liquids for producing biodiesel from *S. platensis* biomass in terms of energy and cost savings.
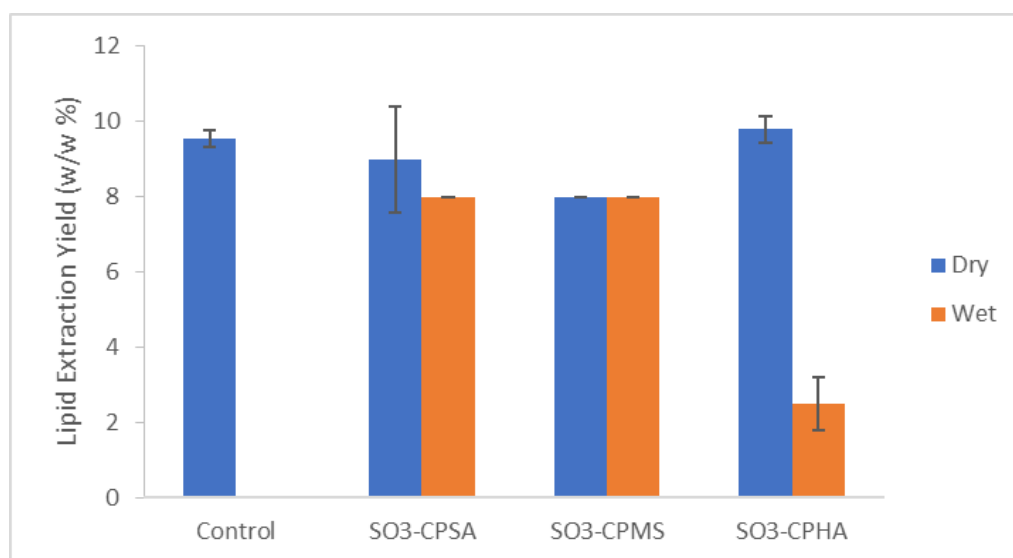


Figure 4.15. Lipid extraction yields from dry and wet *Spirulina platensis* biomass by $SO_3$-CPILs

## 4.4 Characterization of Biomass and Lipids

### 4.4.1 SEM analysis of Biomass

Here, structural analysis with SEM was carried out to thoroughly examine the extraction procedures. Figure 4.16 depicted the changes in the surface of microalgae cells before and after lipid extraction by CPIL/MeOH, which recorded the highest lipids yield, in two

different magnifications. Fig. 4.16(A) depicts the images of microalgae biomass before extraction, whereas Fig. 4.16 (B) and (C) depict the images of microalgae biomass after lipids extraction by CPAA and CPHA, respectively. The biomass image in Fig. 4.16 (A) showed the presence of intact cells (not damaged cells) of *S. platensis* algae, which have irregular shape with an uneven surface. In contrast, Fig. 4.16 (B) and (C) are distinguished by the absence of any intact cells and appears to be primarily composed of aggregates of *S. platensis* cellular debris. It was also noticed that a portion of the cell barrier structure of the cell was disrupted, although the cell wall structure was not altered. The findings suggested that ionic liquids primarily act on the dissolution of cell wall polysaccharides (cellulose and hemicellulose analogs), allowing lipids to be released from cells more easily. These results are consistent with previous research, which found that imidazolium-based ILs were effective for cell wall disruption and lipid extraction from *Chlorella sp*., *Scenedesmus sp*., and *Neochloris oleoabundans* (Teixeira, 2011; Zhuanni et al., 2016; Zhou et al., 2019). The ILs contact the cell and lyses, dissolves, or solvates the cell wall polysaccharides (cellulose, lignocellulose and lignin) and thus, the cell lipids are releases to the surrounding liquid (Teixeira, 2011; Zhou et al., 2019). In addition, the ILs that are hydrophilic in nature showed a higher lipid extraction efficiency than the one that is hydrophobic (Kim et al., 2012).
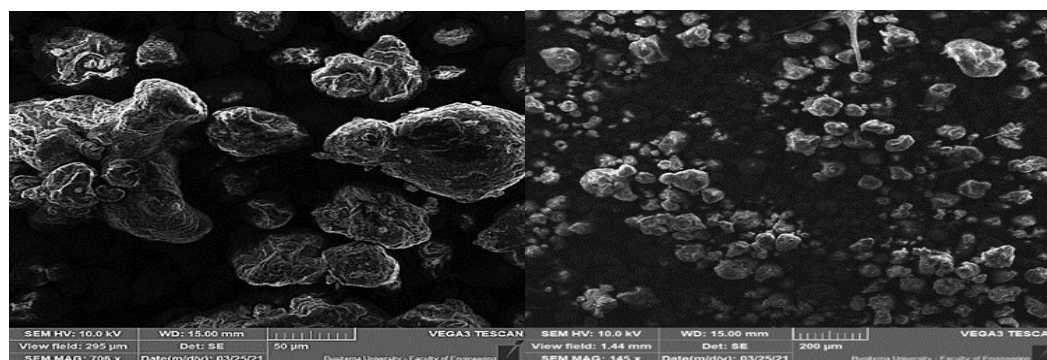


**(A)**
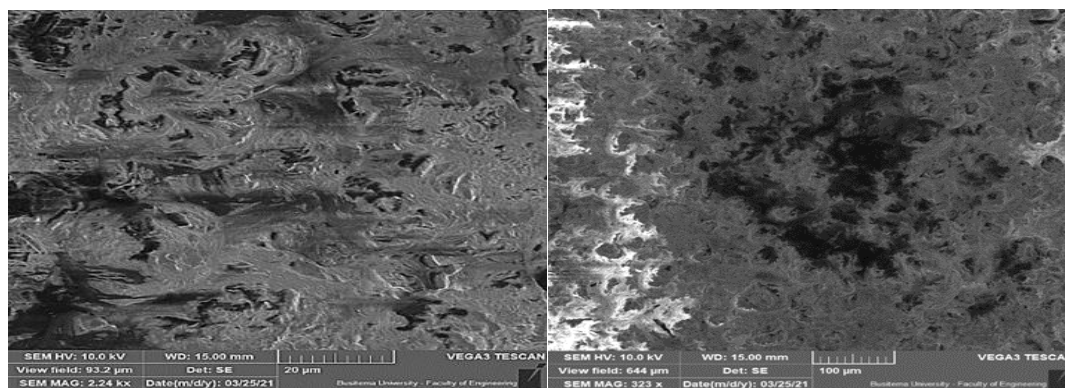
**(B)**
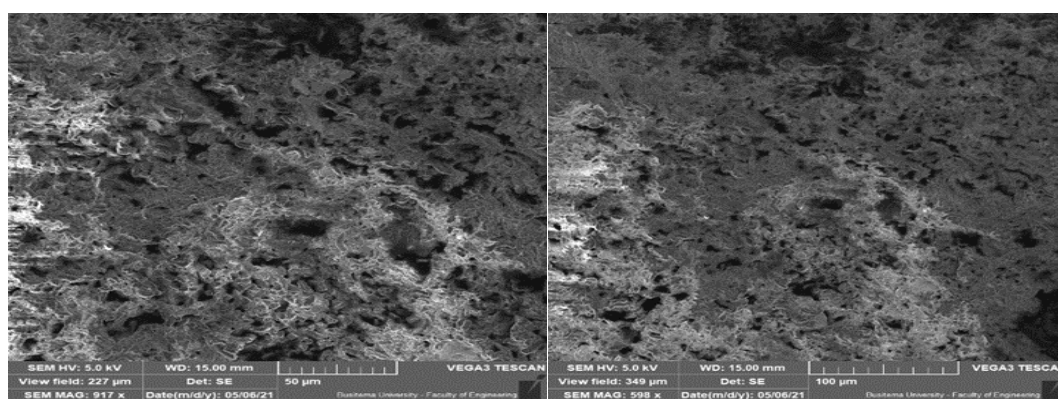


**(C)**

Figure 4.16. SEM images of *S. platensis* biomass before (A) and after (B)

lipid extraction by CPAA, and (C) by CPHA

## 4.4.2 FT-IR Characterization of the lipids extracts

Infrared spectra (FT-IR) of the lipid extracts from *S. platensis* biomass using CPIL/MeOH

mixtures are shown in Fig. 4.17. All spectra showed bands related to the hydrocarbon

chain, where the main absorption bands at the regions 2922.47 - 2925.88 $cm^{-1}$ and 2852.52

- 2853.54 $cm^{-1}$, refer to the asymmetric and symmetric vibration stretching of the saturated

carbon-carbon bonds, respectively. More interestingly, the recovered lipids showed a direct

transformation of the fatty acids and triglycerides into the corresponding free fatty acid

methyl ester (FAMEs-biodiesel), as indicated by the presence of peaks at 1739.67, 1740.49,

1741.60 cm$^{-1}$, which were identified as C=O bonds of ester groups (Dean et al., 2010; Nautiyal et al., 2014). The maximum shift of 1704.96 cm$^{-1}$, that related to the ester C=O bond in the CPAA and CPTFA spectra, may be caused by the presence of hydrogen bonding (Blume, 1996), or may be attributed to the keto C=O bond of chlorophyll. The bands at 1666, 1645 and 1633 cm$^{-1}$ for CPAA, CPTFA, and CPMS (very weak), respectively, are associated with the C=C in chlorophyll and its derivatives (Xiaoli et al., 2018), which are responsible for the dark green color. However, the corresponding bands were not detected in the spectra of CPHA, CPSA and CPTFS, which can be explained by the reduction of these pigments in their lipids extracts. The bands in the region 1000 - 1320 cm$^{-1}$ are related to the stretching vibration of the ester C- O groups (Fattah et al., 2020). Otherwise, the patterns of band distribution and peaks obtained for the other ILs were found to be similar for all the lipid extracts, with closely matching peaks. A more detailed assessment of band assignments for the recovered lipids is given in Table 4.9.

More evidence for the above findings was given in Figure 4.18, which shows the FTIR analysis of lipids extracts, from *S. platensis*, of the control (Hexane: MeOH) before (4.18A) and after (4.18B) conversion to biodiesel. As can be seen in Figure 4.18(A), there is absence of carbonyl group absorption bands in the spectra of the lipids extract. Similar observations of the invisibility of the carbonyl group frequency in the spectra of lipids extracts from *S. platensis* and *C. vulgaris* were detected in Zhang et al., (2018) and Mathimani et al., (2016) studies, respectively. Therefore, extracts of the control require an additional transesterification step for biodiesel production, as indicated in Figure 4.18B.

Table 4.9. Comparison of the main IR absorption bands for extracts (cm$^{-1}$) of the control and CPIL/MeOH mixtures

| Wavenumbers cm$^{-1}$ | | | | | | | Band assignment | Functional groups |
|---|---|---|---|---|---|---|---|---|
| Control | CPAA | CPHA | CPSA | CPMS | CPTFA | CPTFS | | |
| ~3400 | 3288.40 | ~3400 | - | - | - | ~3400 | O-H, NH stretching | FFA, fatty acid amides, and N-containing heterocyclic |
| | 3228.62 | | - | - | - | | | |
| 2926.01 | 2925.81 | 2925.81 | 2923.88 | 2923.88 | 2923.88 | 2922.47 | $v_{as}$CH2-CH3 | CH2 and CH3 methyl & methylene groups |
| 2854.65 | 2852.52 | 2852.52 | 2852.52 | 2852.52 | 2852.52 | 2853.54 | $v_s$CH2-CH3 | |
| - | - | - | - | 2360.71 | 2360.71 | - | Triple bonds or cumulative double | Unsaturated compounds |
| 1741.72 | 1704.96 | 1741.60 | 1741.60 | 1739.67 | 1704.96, 1739.67 | 1740.49 | $v$C=O | Ester of lipids and fatty acids |
| - | 1666.38 | - | - | 1633.59 | 1645.17 | - | $v$C=C | Unsaturated hydrocarbon |
| 1460.11 | 1438.80 | 1461.94 | 1461.94 | 1460.01 | 1460.01 | 1461.64 | $\delta_{as}$CH2, $\delta_{as}$CH3 | The bending (scissoring) of the CH2 |
| 1369.46 | 1361.65 | 1375.15 | 1375.15 | 1363.58 | 1363.58 | 1363.67 | $\delta_s$CH2, | The bending (scissoring) of the CH3 |
| - | 1284.50 | - | - | - | - | | $v_{as}$P=O | Phosphodiester of nucleic acids and phospholipids |
| 1199.72 | 1197.71 | 1195.78 | - | 1191.93 | 1197.71 | 1199.56 | C-O-C | The stretching vibration of the ester groups |
| 1170.79 | 1122.49 | 1170.71 | 1168.78 | 1116.71 | 1170.71 | 1170.54 | | |
| - | 1085.85 | - | 1093.95, 1020.27 | 1058.85 | - | 1086.65 | | |
| - | 979.77 | - | - | - | - | 981.6 | P-O-P | Polyphosphate |
| 719.45 | 723.26 | 723.26 | - | 723.26 | 721.33 | 722.2 | $\gamma$(CH2)n | CH2-rocking |
| 657.73 | 503.39 | - | 665.40 | 669.25 | 669.25 | - | C-H | Aromatic |

$v_s$= symmetric stretching, $v_{as}$ = asymmetrical stretching, $\delta$ = symmetric deformation (bend), $\delta_{as}$ = asymmetric deformation (bend).Band assignments are taken from references (Gomez et al., 2011), (Forfang et al., 2017), (Pohndorf et al., 2016), and (Mayers et al., 2013)
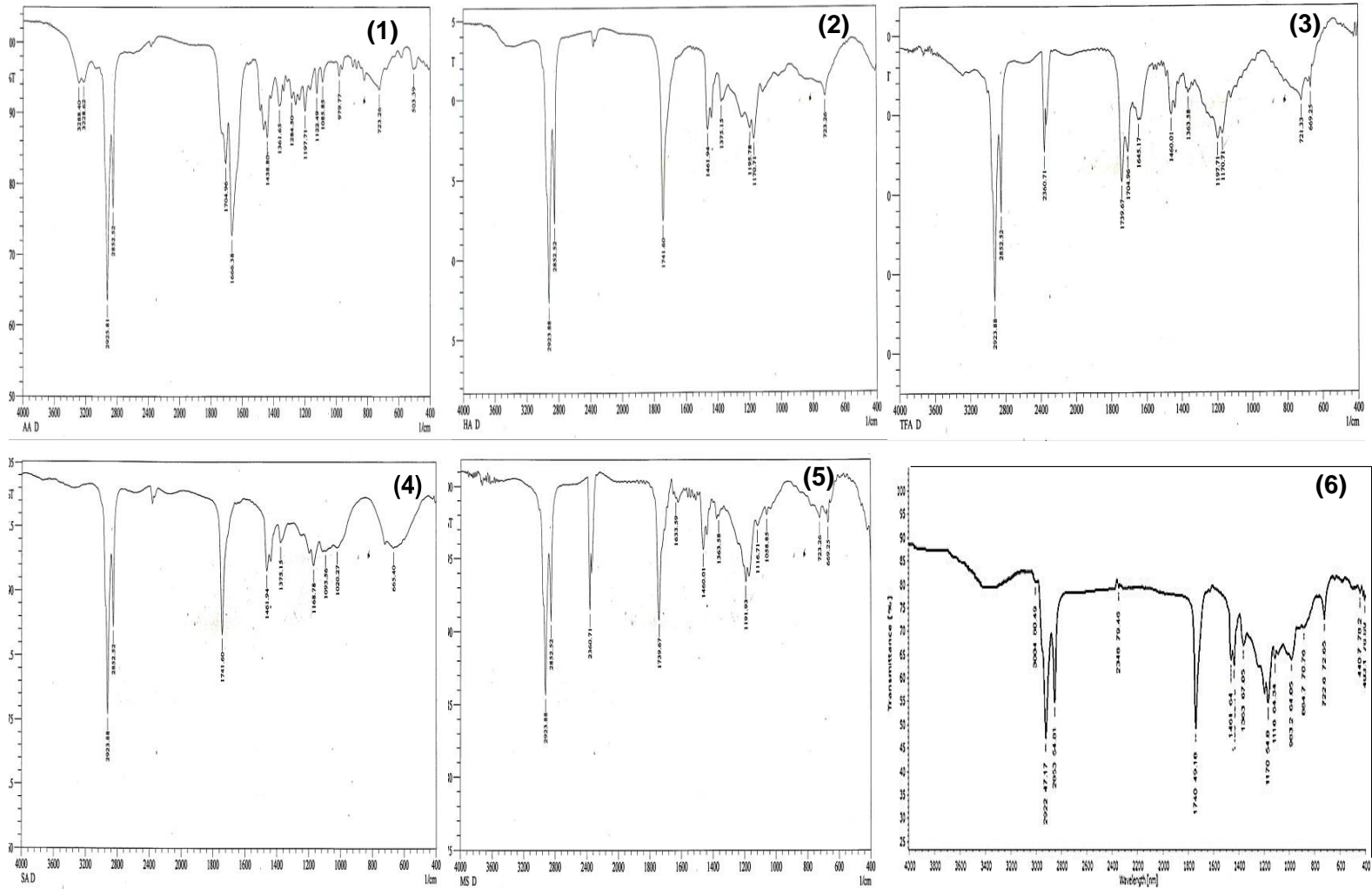
Figure 4.17. FT-IR spectra of the lipid extracts by 1) CPAA, 2) CPHA, 3) CPTFA, 4) CPSA, 5) CPMS, and 6) CPTFS
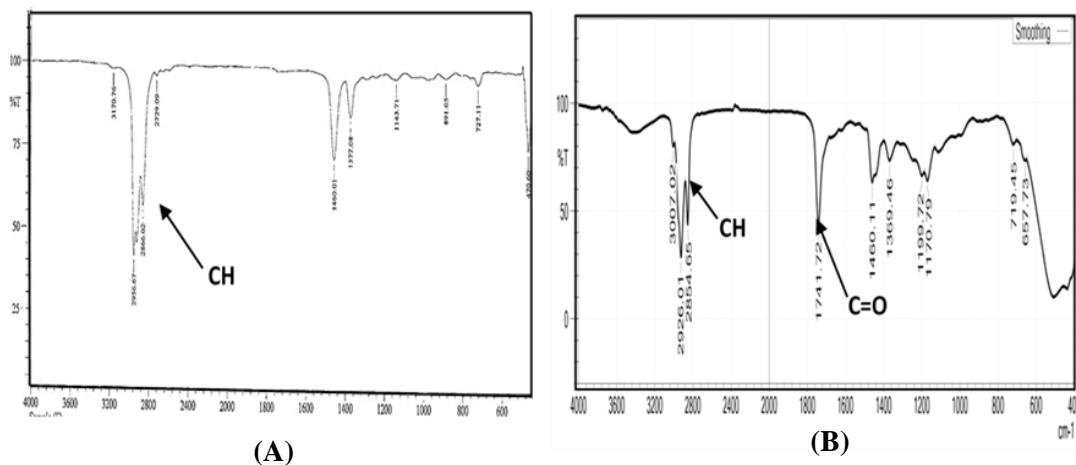
Figure 4.18. The FT-IR spectra of lipid extracts from S. platensis of the

control before (A), and after (B), conversion to biodiesel.

### 4.4.3 The influence of SO₃-CPIL/CPIL on the color of the lipid fractions

The green color of plant-derived lipids is caused by the unfavorable presence of lipid-soluble carotenoids and chlorophyll (Shankar et al., 2019). Because of the high intensity of the color, the number and length of biodiesel production processes would increase, resulting in less sustainable economics. Figure 4.19 (A and B) displays equal lipid fractions (w/w), produced by CPIL and SO₃-CPIL (dry and wet biomass) with methanol, respectively, and diluted in hexane to enable color observation. The lipids extracted by CPTFA, CPHA, and CPMS in Figures 4.19 (A2), (A3), and (A5), respectively, appear to have substantially lighter color intensities than the lipids extracted by CPAA and SO₃-CPHA in Figures 4.19 (A1) and (B1). The change of color to brown, as shown in Figure 4.20a, indicates the degradability of chlorophyll in microalgae biomass (Chiappe et al., 2016). On the other hand, CPSA and CPTFS, in addition to dry and wet biomass extracts of SO₃-bCPSA and SO₃-bCPMS (Figures 4.19: A4, A6, B2, B3, B4 and B5), respectively, showed yellow extracts - indicating the absence of pigments, and the biomass residues

remained stable as indicated by the bright green color (Figure 4.20b). This finding was confirmed by the presence of characteristic functional groups in FT-IR spectra of CPAA, CPTFA and CPMS (very weak), as explained previously in section 4.4.2. Thus, the utilization of the CPILs and $SO_3$-bCPIL (except for CPAA, CPTFA and $SO_3$-bCPHA), causes pigments' deterioration, which is a desirable consequence and might reduce the number of processes needed to produce biodiesel.



(A)                                    (B)
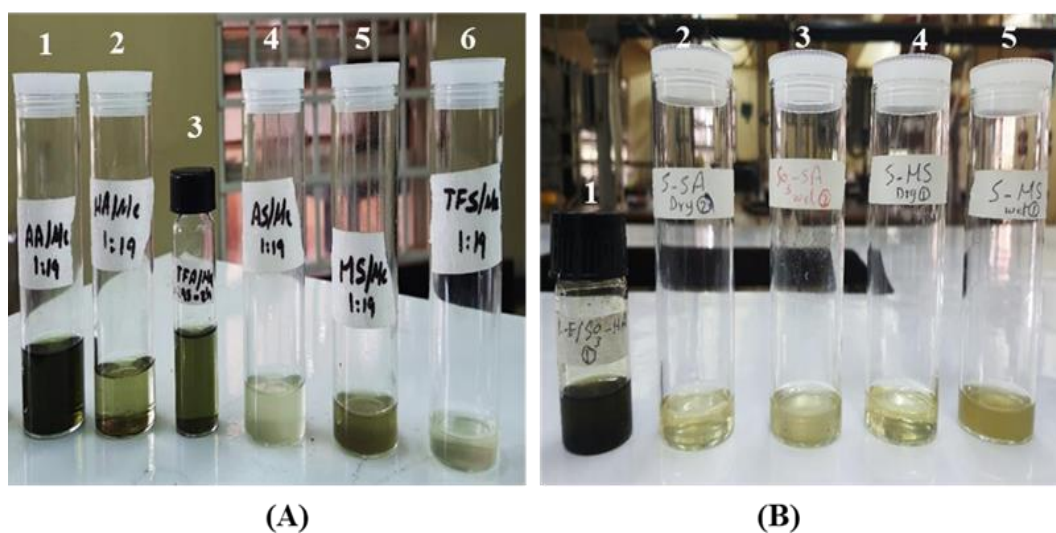
Figure 4.19. Extracted lipid samples by CPIL/MeOH (A), and $SO_3$-CPIL/MeOH (B).



(a)                                    (b)
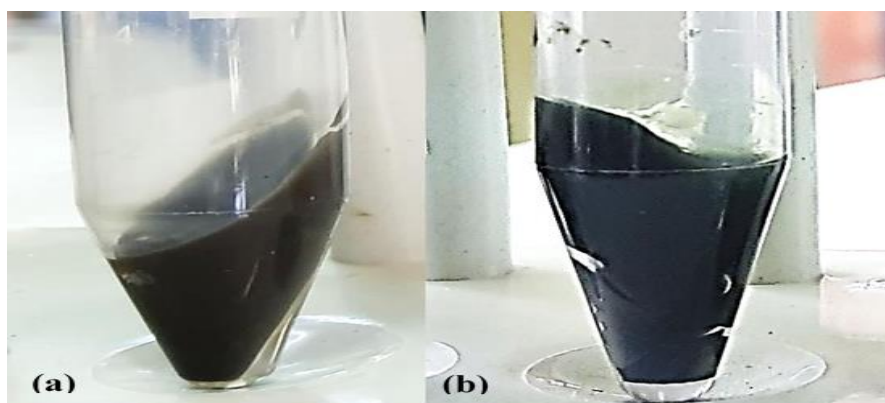
Figure 4.20. The biomass residues after extraction showing, (a) degradability (brown colour) and (b) stability (bright green) of the chlorophyll pigments

**4.5 Direct and indirect transesterification of recovered lipids of CPIL/MeOH and SO$_3$-CPIL/MeOH**

Two procedures for producing biodiesel from *S. platensis* biomass through transesterification process were performed as follow: (1) direct transesterification, which involves the simultaneous extraction of lipids and the transesterification process, where the SO$_3$-CP/CPIL act as solvents and catalysts at the same time. (2) Indirect transesterification, the two-stage method, which involves separating the lipids from the microalgae biomass and then transesterifying the extracted lipids. In this process the SO$_3$-CP/CPIL were used as catalysts for transesterification of lipids in order to provide more evidence to their catalytic activity that were exhibited in the direct transesterification process.

**4.5.1 Identification of the FAMEs profile produced by conventional method**

The identification and quantification of FAMEs that were produced by the conventional method (Christie & Han, 2012) was done through comparison of the extracts with the FAMEs standard mixture, whose GC (FID) profile and retention times are presented in Appendix (B) and Table 4.10.

The percentages of FAMEs in the biodiesel produced from the lipid extracts of *Spirulina platensis* microalgae, using the conventional method (for comparison purpose) are shown in Appendix (C) and Table 4.11. Among all FAMEs, palmitic acid (C16:0) methyl ester was the most abundant (61%), followed by caprylic (C8:0, 9%), oleic (C18:1, 6%) and linoleic (C18:2, 5%) acid methyl esters. Fattah et al. 2020 investigated the FAME compositions derived from *Chlorella sp.* and *Spirulina sp.* via enzymatic synthesis. Their findings revealed that palmitic (C16:0) and stearic (C18:0) acids were the major components for both *Chlorella sp*. and *Spirulina sp*. biodiesel. Nautiyal et al., (2014) also

reported that palmitic (C16:0, 41.21%), linolenic (C18:3, 17.79 %), linoleic (C18:2, 12.64%), oleic (C18:1, 4.11%) and caprylic (C8:0, 3.90%) acids were the main FAME components in *S. platensis*. In a study by (Rahman et al., 2017), *S. maxima* showed the presence of palmitic acid (40.2%), linoleic (17.87%), linolenic acids (18.34%) as major fatty acids.

Table 4.10. The retention time of all the FAMEs components of the standard mixture

| Peak | FAMEs | Retention time (RT) (min) |
|------|-------|---------------------------|
| 1 | C6:0 Caproic acid | 4.612 |
| 2 | C8:0 Caprylic acid | 4.98 |
| 3 | C10:0 Capric acid | 5.589 |
| 4 | C11:0 Undecanoic acid | 6.007 |
| 5 | C12:0 Lauric acid | 6.505 |
| 6 | C13:0 Triundecanoic acid | 7.08 |
| 7 | C14:0 Myristic acid | 7.73 |
| 8 | C14:1 Myristoleic acid | 8.336 |
| 9 | C15:0 Pentadecanoic acid | 8.448 |
| 10 | C15:1 cis-10-Pentadecenoic acid | 9.107 |
| 11 | C16:0 Palmitic acid | 9.296 |
| 12 | C16:1 Palmitoleic acid | 9.844 |
| 13 | C17:0 Heptadecanoic acid | 10.204 |
| 14 | C17:1 cis-Heptadecenoic acid | 10.797 |
| 15 | C18:0 Stearic acid | 11.413 |
| 16,17 | C18:1 trans-9-Elaidic acid, C18:1 cis-9- Oleic | 11.837 |
| 18 | C18:2 trans-Linolelaidic acid | 12.358 |
| 19 | C18:2 cis- Linoleic acid | 12.718 |
| 20 | C18:3 γ-Linolenic | 13.473 |
| 21 | C18:3 α-Linolenic | 14.008 |
| 22 | C20:0 Arachidic acid | 15.137 |
| 23 | C20:1 cis-11-Eicosenoic | 16.127 |
| 24 | C20:2 cis-11,14-Eicosadienoic, C20:3 cis- 8,11,14-Eicosatrienoic | 17.396 |
| 25 | C22:0 Behenic | 19.192 |
| 26 | C22:1 Erucic acid, C22:2 cis-13,16- Docosadienoic, C23:0 Tricosanoic, C24:0   Lignoceric, C22:6 (cis-4,7,10,13,16,19-Docosahexaenoic), C24:1 Nervonic | 22.625 |

Cn = carbon chain length. Cn:0 = saturated FAME. Cn:1, 2 or 3 = unsaturated FAMEs

The predominant of palmitic acid in *S. platensis* lipids extracts was also stated in (Rahman & Nahar, 2016); (El-Shimi et al., 2013); (El-Shimi et al., 2015) and (Saeedi Dehaghani & Pirouzfar, 2018) researches, with percentage values between 38.9 and 59.3 %. However, Pradana et al., (2018) and Murad & Al-dawody, (2020) were reported different major components, which are oleic acid (45.10 %) and linoleic acid (39.92 %), respectively. If we take into account that all above studies used various methods (ILs not included) for FAMEs production from *S. platensis* biomass, thus, these variations may due to the method used for biodiesel production, as well as the different conditions of microalgae growth (Aratboni et al., 2019).

Moreover, a higher proportion of saturated fatty acids (79 %) relative to unsaturated fatty acids (21 %), could be advantageous because saturated FAMEs have superior burning qualities, whereas unsaturated FAMEs have better fluidity in cold temperatures (Knothe, 2005). Long-chain saturated fatty acids, in particular, palmitic (C16:0) and stearic acid (C18:0), are highly desirable (Hayyan et al., 2011), because biodiesel with a high saturated fatty acid content has a higher oxidation resistance. (Mostafa & El-Gendy, 2013). A data given by (Nautiyal et al., 2014) showed that about 50% saturated FAMEs and about 41% unsaturated FAMEs present in the *S. platensis* biodiesel, which revealed similar high proportion of saturated FAMEs. Palm oil, which consider the best crop for biodiesel production (Atabani et al., 2012), consists of about 43.4% saturated FAME and 56.6% unsaturated (Nautiyal et al., 2014). Therefore, the biodiesel produced in this study is more stable than biodiesel from palm due to its lower proportion of unsaturated fatty acids. Overall, structural features, namely hydrocarbon chain length, degree of saturation and branching, influence the structure of fatty acid esters. These have a direct effect on the

properties of biodiesel and thus on its properties and performance as an automotive fuel (Knothe, 2005). More details has been provided in section 4.6.

Table 4.11. Identification of the FAMEs composition produced by conventional method (indirect transesterification)

| Free fatty acid methyl esters (FAMEs) | Retention time (RT) (min) | FAME % (of total FAMEs) |
|---|---|---|
| C6:0 Caproic acid | 4.567 | 0.76 |
| C8:0 Caprylic acid | 5.166 | 9.27 |
| C12:0 Lauric acid | 6.492 | 0.16 |
| C13:0 Triundecanoic acid | 7.379 | 1.63 |
| C14:0 Myristic acid | 7.733 | 0.57 |
| C15:0 Pentadecanoic acid | 8.683 | 2.57 |
| C15:1 cis-10-Pentadecenoic acid | 8.996 | 1.46 |
| C16:0 Palmitic acid | 9.286 | 61.18 |
| C16:1 Palmitoleic acid | 9.818 | 3.27 |
| C17:1 cis-Heptadecenoic acid | 10.618 | 0.79 |
| C18:0 Stearic acid | 11.268 | 1.50 |
| C18:1 trans-9-Elaidic acid, C18:1 cis-9- Oleic | 11.662 | 5.81 |
| C18:2 trans-Linolelaidic acid | 12.175 | 0.31 |
| C18:2 cis- Linoleic acid | 12.690 | 4.74 |
| C18:3 γ-Linolenic | 13.423 | 1.84 |
| C20:1 cis-11-Eicosenoic | 16.109 | 2.96 |
| C22:0 Behenic | 20.477 | 1.18 |

Cn = carbon chain length. Cn:0 = saturated FAME. Cn:1,2 or 3 = unsaturated FAMEs

**4.5.2 Direct transesterification of recovered lipids by CPIL/MeOH**

To be able to confirm the occurrence of the direct production of biodiesel, which was indicated by FT-IR analysis (ester C=O bonds), GC analysis of the recovered lipids of

CPIL/MeOH was performed, and this gave more evidence of direct conversion of lipids to the corresponding FAMEs-biodiesel. Table 4.12 shows the composition of the FAMEs (only the major ones that have been reported in previous studies) of the obtained biodiesel for each CPIL, which identified through comparison with the FAMEs standard profile. The biodiesel of CPAA showed the total absence of the major FAME (palmitic acid, C16:0) that was found in the biodiesel produced by the conventional method. However, it was present in low percentages in each of CPHA (6%) and CPTFA (15%), which means that they have less catalytic activity to convert lipids to biodiesel. The biodiesel that was obtained from CPSA, CPMS and CPTFS showed conversions of palmitic acid of 54%, 44% and 50%, respectively, which is higher than the 29% and 41.21% that was stated by Fattah et al. (2020) and Nautiyal et al. (2014), respectively. Additionally, the CPAA seems to have selectivity toward eicosenoic acid (C20:1) as shown in Table 4.12, while the same acid was also dominant in each of CPHA and CPTFA. In order to investigate the thermal efficiency of the biodiesel that was obtained by the CPILs, the ratio of the saturated to unsaturated FAMEs was evaluated and the results are shown in Figure 4.21. As can be seen, CPAA, CPHA and CPTFA have a higher level of unsaturated FAMES, compared to saturated FAMEs, indicating the poor/lower thermal efficiency of the produced biodiesel. However, CPSA, CPMS and CPTFS recorded a higher saturated FAMEs than the unsaturated ones, indicating the good/higher thermal efficiency of the biodiesel produced. Therefore, the last three CPILs act as solvents with good catalytic activity; hence, they are more appropriate for the direct production of biodiesel from microalgae biomass.

From the above results, it is obvious that the direct conversion of the lipids (triglycerides) extracted by CPILs to the corresponding FAMEs was incomplete. Thus, the lipid extracts

were subjected to a further transesterification process, utilizing the approach described by (Christie & Han, 2012). An observable enhancement of the percentages of the main FAMEs occurred as depicted in Figure 4.22. In particular, the lipid profiles of the CPSA extracts produced palmitic of (81%), which is higher compared to the control (65%), followed by CPAA and CPMS (75%), while CPHA and CPTFS recorded 68 % and 66 %, respectively, which is nearly identical to the control. In contrast, the lipid yield produced by extraction with CPTFA was 55%, which was lower than the yield of the control.

Furthermore, the biodiesel obtained by the CPILs had a higher proportion of saturated fatty acids (80-93%) than unsaturated fatty acids (9-21%), as depicted in Figure 4.23. These results showed the excellent thermal and other properties of the produced biodiesel (Knothe, 2005).

Table 4.12. Percentage of FAME composition in obtained biodiesel using CPIL/MeOH

| Free fatty acid methyl esters (FAMEs) | FAME % | | | | | |
|---|---|---|---|---|---|---|
| | CPAA | CPHA | CPTFA | CPSA | CPMS | CPTFS |
| C16:0 Palmitic acid | - | 6 | 15 | 54 | 44 | 50 |
| C16:1 Palmitoleic acid | - | 1 | 2 | 3 | 1 | 3 |
| C18:0 Stearic acid | - | - | - | - | 0.5 | 0.9 |
| C18:1 trans-9-Elaidic acid, C18:1 cis-9- Oleic | - | 0.05 | 0.3 | 0.5 | 0.9 | 3 |
| C18:2 trans-Linolelaidic acid | - | - | - | 3 | - | - |
| C18:2 cis- Linoleic acid | - | 1 | 3 | - | 7 | 11 |
| C18:3 γ-Linolenic | - | - | 0.9 | 11 | 7 | 12 |
| C18:3 α-Linolenic | - | 1 | 1 | 11 | 0.5 | 0.9 |
| C20:1 cis-11-Eicosenoic | 92 | 89 | 73 | 8 | 24 | 9 |
| Others | 8 | 2 | 5 | 9 | 14 | 10 |
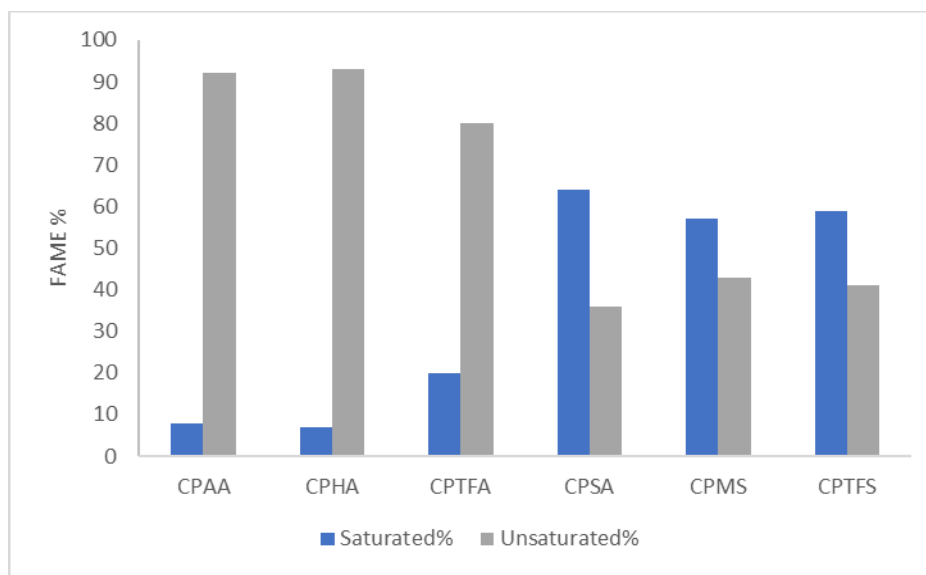
Figure 4.21. Saturated and unsaturated fatty acid methyl esters profile in

biodiesel produced by CPIL/MeOH
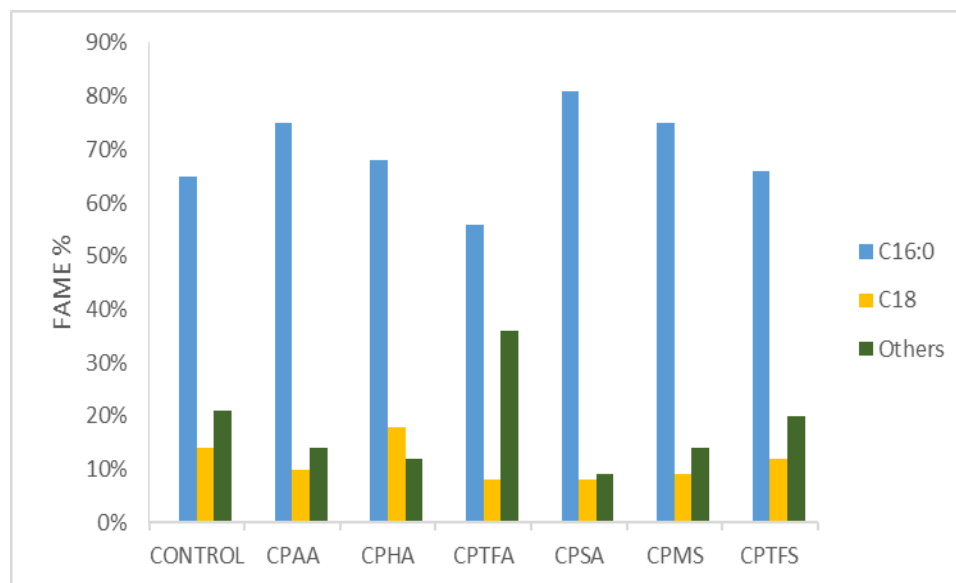


Figure 4.22. The FAMEs composition in the extracted lipids by CPIL/MeOH

after conducted to further transesterification process
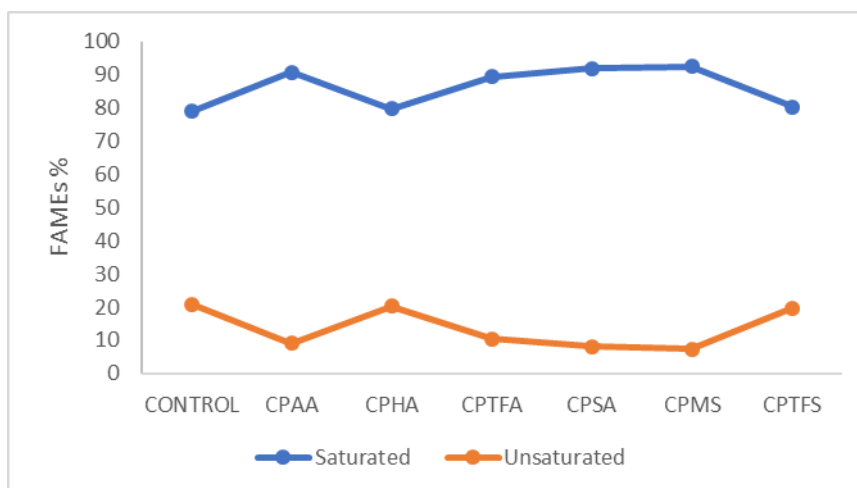
Figure 4.23. Saturated and unsaturated fatty acid methyl esters profile in

biodiesel produced by CPIL/MeOH after conducted to further

transesterification process

Based on the above information it can be concluded that the high efficiency of CPAA as solvents for extraction of lipids from microalgae, for biodiesel production, was confirmed by the higher percentages of main FAMEs composition that were detected by GC analysis - compared to the control, followed by CPHA and CPTFA. Despite their low extraction lipid yields, CPSA, CPMS and CPTFS also showed the presence of higher or similar percentages of FAMEs to that of the above three CPILs, assuming reduced extraction of unsaponifiable lipids such as hydrocarbons, ketones, sterols and pigments (Chiappe et al., 2016). This means that, apart from their good catalytic activity, these CPILs are also better than conventional solvents in the extraction of lipids from algae biomass, and hence, are a promising green technology for biodiesel production in a single step. Therefore, more optimization studies on the last three CPILs will be required to increase their effectiveness for the direct biodiesel production process.

**4.5.3 Direct transesterification of recovered lipids from dry and wet biomass using SO₃- bCPIL/MeOH**

As already discussed, the fatty acid composition of biodiesel has a significant impact on its characteristics. Thus, the FAMEs composition that was obtained from dry *S. platensis* biomass SO$_3$-bCPHA/MeOH, SO$_3$-bCPMS/MeOH and SO$_3$-bCPSA/MeOH, as well as from wet biomass using the last two solvent systems, was investigated, because the yield of their extracted lipids was similar to that of the control (Hexane: MeOH). As shown in Table 4.13, the fatty acid profile for SO$_3$-bCPIL/MeOH was dominated by palmitic acid (C16:0), except in case of SO$_3$-CPHA/MeOH, which was predominated by eicosenoic acid (C20:1), followed by palmitic acid.

On the other hand, an important difference could be observed in the FAME profile between the dry and wet biomass (Table 4.13). For instance, extraction of wet biomass using SO$_3$-bCPIL/MeOH mainly increased the amount of palmitic acid. However, there was no effect on the total content of saturated and unsaturated FAME content of the dry and wet biomass. The total saturated FAMEs content obtained from dry biomass for SO$_3$-bCPSA/MeOH and SO$_3$-bCPMS/MeOH was 60 % and 57 %, respectively, compared to 59 % and 56 % from wet biomass, while the total unsaturated FAMEs content produced from dry biomass was 40 % and 43 %, compared to 41 % and 44 % from wet biomass. In general, there was higher saturated than unsaturated FAMEs content in both dry and wet biomass, for SO$_3$-bCPSA/MeOH and SO$_3$-bCPMS/MeOH, and this is important for biodiesel properties, such as thermal efficiency, as discussed previously (Figure 4.24). Nevertheless, SO$_3$-CPHA/MeOH showed opposite results (higher unsaturated than saturated FAMEs content) and hence is not suitable for application in direct biodiesel production.

Table 4.13. Percentage of FAME composition in obtained biodiesel for SO$_3$-bC

PIL/MeOH

| Free fatty acid methyl esters (FAMEs) | FAME % | | | | |
|---|---|---|---|---|---|
| | SO$_3$-bCPHA-dry | SO$_3$-bCPMS-dry | SO$_3$-bCPMS-wet | SO$_3$-bCPSA-dry | SO$_3$-bCPSA-wet |
| C16:0 Palmitic acid | 9 | 27 | 47 | 43 | 51 |
| C16:1 Palmitoleic acid | 1 | 6 | 4 | 6 | 4 |
| C18:0 Stearic acid | 0.1 | - | 1 | 2 | 0.4 |
| C18:1 trans-9-Elaidic acid, C18:1 cis-9- Oleic | 0.3 | 1 | 3 | 3 | 3 |
| C18:2 trans-Linolelaidic acid | - | - | - | - | - |
| C18:2 cis-Linoleic acid | 1.0 | 5 | 11 | 13 | 13 |
| C18:3 γ-Linolenic | 1.2 | 6 | 11 | 13 | 13 |
| C18:3 α-Linolenic | 0.1 | - | - | - | - |
| C20:1 cis-11-Eicosenoic | 84 | 23 | 7 | 3 | 6 |
| Others | 3 | 34 | 14 | 17 | 9 |

In view of the foregoing results, it can be stated that in addition to their comparable lipid extraction efficiency to organic solvents, SO$_3$-bCPSA/MeOH and SO$_3$-bCPMS/MeOH also possess good catalytic activity for both dry and wet biomass. Moreover, considering that eliminating biomass drying from lipid extraction processes can result in significant energy, time and cost savings (Dejoye Tanzi et al., 2013), these ionic liquids are considerably an effective and efficient technology for simultaneous extraction and transesterification of lipids in single step process.
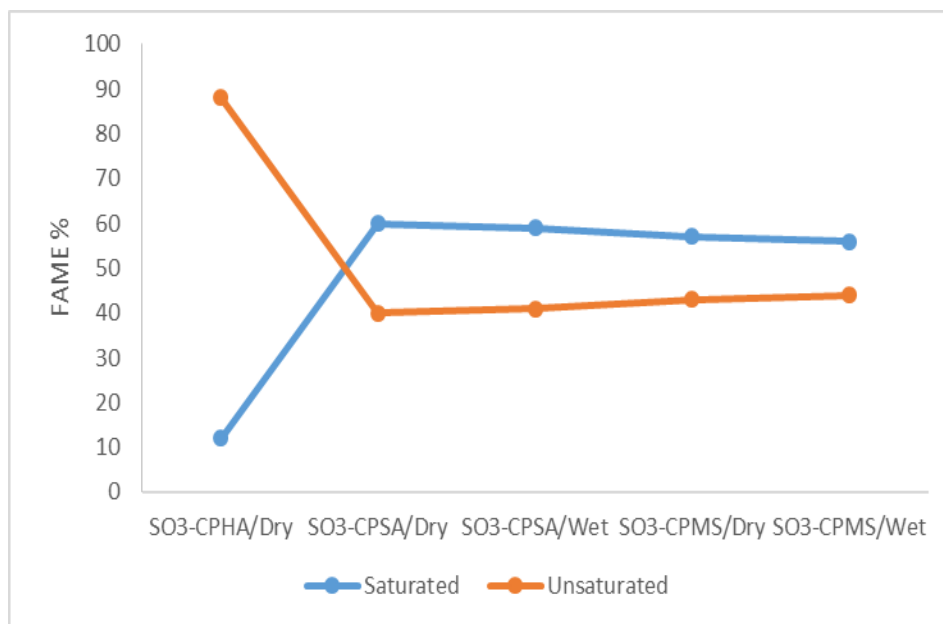
Figure 4.24. Saturated and unsaturated fatty acid methyl esters profile in biodiesel produced by $SO_3$-bCPIL/MeOH after conducted to further transesterification process

The fatty acids content in the resulting biodiesel of $SO_3$-bCPSA and $SO_3$-bCPMS from wet *S. platensis* biomass was also compared with that produced by other reported conventional catalysts such as sulphuric acid ($H_2SO_4$) and potassium hydroxide (KOH), as well as ionic liquids (Table 4.14). As can be seen, all resulting biodiesel were observed to be rich in palmitic methyl ester, except for the case of biodiesel that was produced using KOH (Pradana et al., 2018), which was rich in oleic acid methyl ester (unsaturated fatty acid), and this indicates poor biodiesel quality. Compared with biodiesel acquired using $H_2SO_4$ (El-Shimi et al., 2013) shorter reaction time was needed for $SO_3$-bCPSA and $SO_3$-bCPMS, and this could largely reduce energy consumption, with a similar or even better transformation rate of fatty acids. Compared with other ionic liquids such as 1-ethyl-3-methylimidazolium acetate [Emim] [OAc] and choline L-arginine [Ch] [ARG] ionic

liquids (To et al., 2018), a single step production process - with relatively milder operation conditions - was required for $SO_3$- bCPSA and $SO_3$-bCPMS. In summary, we propose that $SO_3$-bCPSA and our novel $SO_3$- bCPMS should be the best candidates for transesterification catalysis, given that there are easy-to-use catalysts for scaling purposes due to their low cost, relatively simple to separate, and their good catalytic performance. Moreover, such catalysts could far outperform other catalysts in terms of cost. For instance, the protic ionic liquids [HTMG] [$MeOCO_2/HCO_3$] and [HDBU] [$MeOCO_2/HCO_3$] reported by (Chiappe et al., 2016), and tetrakis(hydroxymethyl) phosphonium chloride [$P(CH_2OH)_4$]Cl reported by Olkiewicz, (2015), have been used for production of biodiesel from other microalgae species, and the starting material prices (according to the sigma Aldrich) for these ionic liquids are summarized in Table 4.15.

Table 4.14. Fatty acid content of biodiesel derived from *Spirulina platensis* produced by other reported catalysts and ionic liquids

| Method | Transesterification conditions | Palmitic (C16:0) | Palmitoleic (C16:1) | Stearic (C18:0) | Oleic (C18:1) | Linoleic (C18:2) | Linolenic (C18:3) |
|---|---|---|---|---|---|---|---|
| SO₃-bCPMS- wet | Algae: IL: MeOH, with ratio 1: 9.5: 9.5, 95°C for 2h | 47 | 4 | 1 | 3 | 11 | 11 |
| SO₃-bCPSA-wet | | 51 | 4 | 0.4 | 3 | 13 | 13 |
| H₂SO₄ | 100% H₂SO₄ concentration (wt./wt oil) at 65°C for 8 hr ,15 g of dry biomass and 80 ml of methanol | 48.35 | 2.66 | 2.02 | 2.41 | 5.37 | 7.84 |
| KOH | 0.2 g of KOH, 150 g of biomass, methanol-hexane (500 ml) were 3:7 at 50°C for 2h | 41.03 | - | 5.54 | 45.10 | 8.34 | - |
| [Emim] [OAc] | 1ˢᵗ step: Algae: IL, 1:5, at 70°C for 3h. 2ⁿᵈ step: addition of chloroform/ MeOH at 85 °C for1h | 36.6 | 9.3 | 0.5 | 1.2 | 17.2 | 18.7 |
| [Ch] [ARG] | | 64.3 | 0.9 | 0.4 | - | 7.3 | - |

Table 4.15. The price of starting materials for state-of-the art protic ionic liquids

| Ionic liquids | Starting material | Price in euro |
|---|---|---|
| This study | Caprolactam | 41.8/ kg |
| [Emim] [OAc] | Imidazole | 153/kg |
| [Ch] [ARG] | Choline hydroxide | 271/500 ml |
| [HTMG][MeOCO$_2$/HCO$_3$] | Tetramethylguanidinium | 427/ kg |
| [HDBU][MeOCO$_2$/HCO$_3$] | 1,8-diazabicyclo[5.4.0]undec-7-ene | ≈ 86/L |
| [P(CH$_2$OH)$_4$]Cl | Aluminum phosphate | 117/500 ml |

## 4.5.4 Indirect transesterification of recovered lipids from microalgae biomass using SO$_3$-CPIL

This study was performed to confirm the catalytic efficacy of SO$_3$-bCPIL/CPIL, which was observed in the investigation of direct transesterification of lipids. This was done by determining the maximum yield of biodiesel products, and comparing it with acidity strength measurements (section 4.2.3). Biodiesel was obtained via a two-step process of oil extraction using conventional method (Hexane: MeOH, 1:1, v/v) followed by transesterification using the CPSA, CPMS, CPTFS, SO$_3$-bCPSA, and H$_2$SO$_4$ as control. The biodiesel yield was expressed in the terms of relative weight of biodiesel obtained to that of extracted oil. It was observed that the SO$_3$-bCPSA resulted in high biodiesel yield (80 %), followed by CPTFS (78 %), CPMS (75 %), CPSA (60 %) and H$_2$SO$_4$ had the lowest yield of 31%. As can be seen, the biodiesel yield of the ionic liquids in these catalytic investigations followed the order, SO$_3$-bCPSA > CPTFS > CPMS > CPSA > H$_2$SO$_4$, which is consistent with the order of acidity measurements - using UV-VIS

spectroscopy - as shown in Table 4.8. The results demonstrated that higher acidity resulted in greater the catalytic activity because of the ease and readiness of the IL to donate a proton, $H^+$ (Xing et al., 2005; Zabeti et al., 2009), except for the case of $H_2SO_4$, whose activity was supposed to be higher or closer to CPSA. These differences may be due to the different conditions that were used in performing the experiments e.g., purity of the chemical.

These findings not only confirm the importance of acidity in catalytic transesterification of lipids using $SO_3$-bCPIL/CPIL, but also provide further evidence of the effectiveness of these ionic liquids as green catalysts for biodiesel production.

### 4.5.5 Transesterification reaction mechanism using SO₃-CPIL/CPIL

As was explained previously in section 1.3, and as has been reported by (Maaira et al., 2011), the transesterification reaction is made up of three reversible and stepwise reactions. In each step, the triglyceride is converted into a diglyceride, a monoglyceride (FAME), and finally a glycerol. In contrast to the mechanism that was suggested by Ishak et al. (2017), which proposed that the transesterification reaction was catalyzed by donation of a proton from the acidic anion of ionic liquids, Luo et al. (2017) proposed that a proton was donated by the acidic cation of $SO_3$-bCPSA ([$SO_3$-bCP] [$HSO_4$]), which contains a sulfonic group as depicted in Figure (4.25). Therefore, the same transesterification mechanism was used for all $SO_3$ bCPIL as follows: In the first step, the proton ($H^+$) supplied by the sulfonic group of the $SO_3$-bCPIL attacks the carbonyl group of the triglyceride, and the protonated carbonyl group generates a carbocation. Nucleophilic attack of methanol on carbocation produces intermediate adducts with H-bonds (Zaramello et al., 2012; Da Silva et l., 2014). Finally, the intermediate product is decomposed into FAME and the catalytic cycle ends. It

is obvious that the catalytic activity of SO$_3$-bCPIL in transesterification comes mainly from the sulfonic group, which can donate H protons.
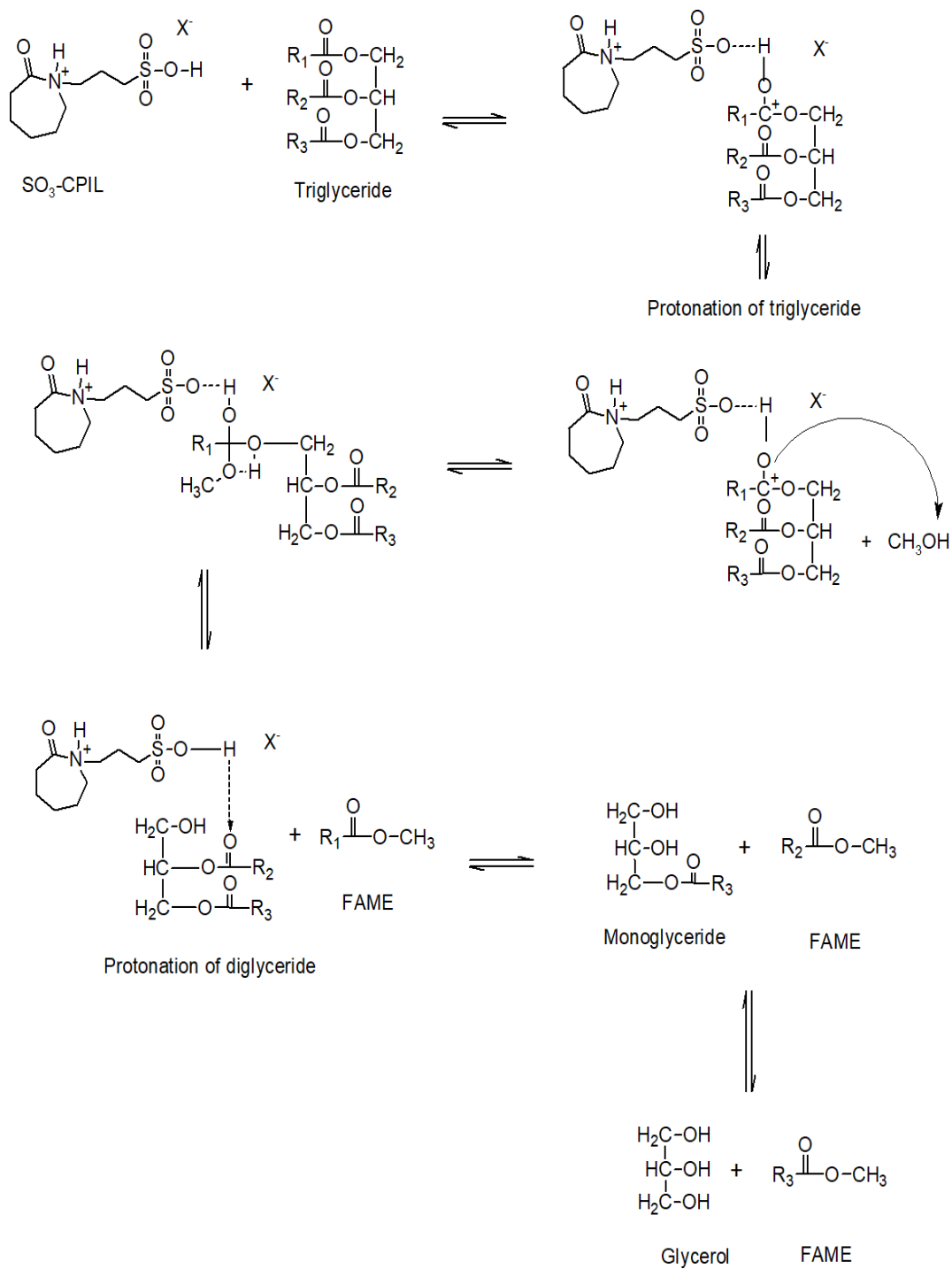


Figure 4.25. The transesterification mechanism in the presence of SO$_3$-bCPIL, X- is Cl$^-$, HSO$_4^-$, or CH$_3$SO$_3^-$

According to the above acid-catalyzed transesterification suggested by Ishak et al. (2017) and Luo et al. (2017), two possible transesterification reaction mechanisms in the presence of CPILs are depicted in Figure 4.26. In the first mechanism, the transesterification reaction is catalyzed via a proton that is donated from the acidic cation provided by the caprolactamium group, as in CPMS and CPTFS (Figure 4.26a). The second mechanism is catalyzed through donation of a proton from acidic anions, such as $HSO_4^-$ in CPSA, as shown in Figure 4.26b. Otherwise, a similar transesterification mechanism was followed as demonstrated in Figure 4.25.
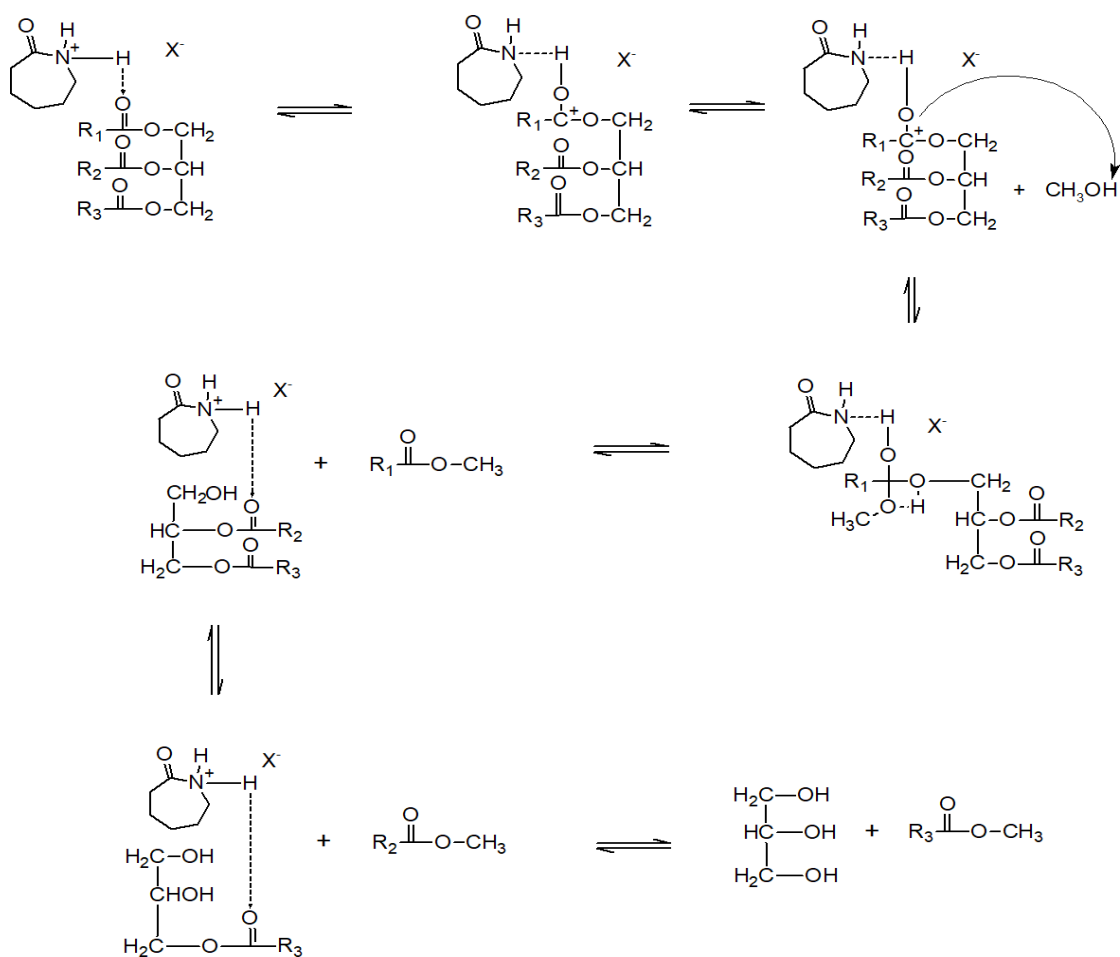


Transesterification mechanism (a)
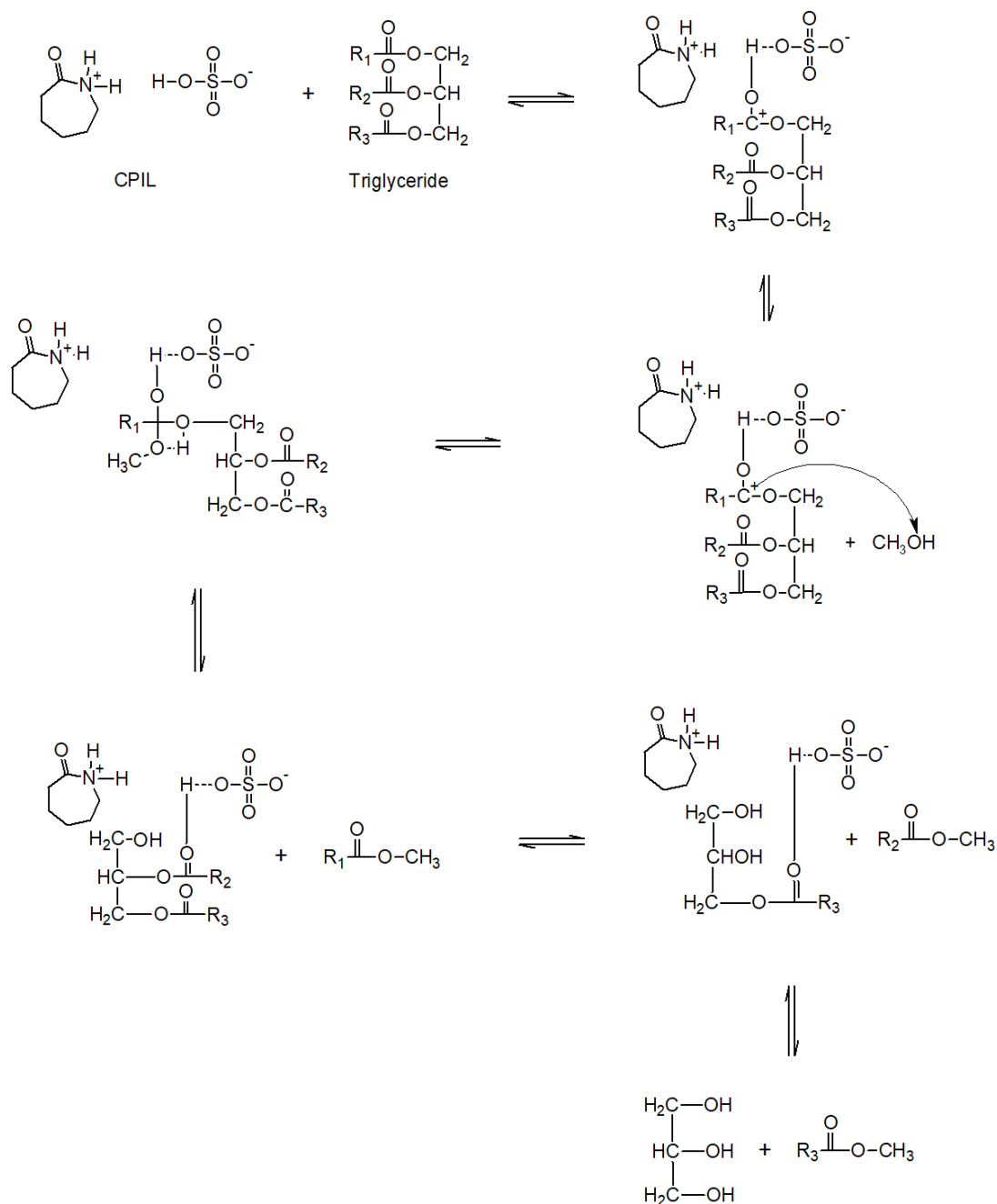
Transesterification mechanism (b)

Figure 4.26. Proposed transesterification mechanism in the presence of CPMS or
CPTFS, X⁻ is $CH_3SO_3^-$ or $CF_3SO_3^-$, respectively (a), and the transesterification
mechanism in the presence of CPSA (b)

## 4.6 Quality evaluation of the produced biodiesel

In addition to the structural configurations of the FAMEs as stated above, the physicochemical characteristics of each FAME have a significant impact on the qualities of biodiesel. In this work, predictive methods that have been reported by (Sarin et al., 2009; Sarin et al., 2010; Su et al., 2011 and Ramírez-verduzco et al., 2012) were used to estimate some of the important physicochemical properties of biodiesels that obtained by $SO_3$-CPIL/CPIL via direct transesterification, which influence the engine performance. The evaluation of produced biodiesels have been performed by comparison with the specifications of the international biodiesel standards prescribed by American Society for Testing and Materials (ASTM 6751) and European Standard (EN 14214) as shown in Table (4.16), and Table (4.17). Furthermore, comparison between experimental data that have been stated in the literature, which are close to the predicted data in this study was expressed as an average absolute deviation (AAD). The prediction of kinematic viscosity (ή), density (ρ), cloud point (CP), pour point (PP), cold filter plugging point (CFPP), cetane number (Ø), calorific value (δ ) and flash point (FP) were explained in details below.

## 4.6.1 Kinematic viscosity

Viscosity (ή) is an important characteristic of a fuel that indicates its ability to flow. Highly viscous fuels that are prone to forming huge droplets during injection may not be properly atomized during the spray, increasing engine deposits and necessitating additional energy. As a result, higher viscosity causes poor combustion as well as increased exhaust smoke and pollutants. In Table (4.16) and Table (4.17), the kinematic viscosity at 40 ˚C was provided for biodiesel samples that obtained from *S. platensis* via the direct transesterification by $SO_3$-CPIL/CPIL.

Table 4.16. The prediction of physicochemical properties for biodiesel produced by Control and CPILs compared to experimental data and standard biodiesel specifications

| Biodiesel property | Unit | Control | Predicted property | | | | | | Experimental data | Limits (ASTM D6751) | Limits (EN 14214) |
|---|---|---|---|---|---|---|---|---|---|---|---|
| | | | CPAA | CPHA | CPSA | CPMS | CPTFA | CPTFS | | | |
| ή@ 40 °C | mm$^2$/s | 0.96 | 4 | 4.1 | 3.4 | 3.5 | 3.9 | 3.5 | 12.4[a], 4.8[b], 5.7[c], 4.5[d], 5.8[e], 4.3[f], 4.5[g] | 1.9 - 6 | 3.5 - 5 |
| ρ@15 °C | kg m$^{-3}$ | 869 | 873 | 873 | 874 | 872 | 873 | 873 | 0.86[a], 0.89[b], 0.86[c], 0.86[d], 0.83[e], 0.87[f], 0.83[g] | 880 | 860 - 900 |
| CP | °C | -1.6 | -4.99 | 0.96 | -1.46 | -1.98 | 1.67 | -1.2 | -3[a], 5[b] | -3 to -12 | ---- |
| PP | °C | -8.56 | -12.24 | -5.79 | -8.39 | -8.97 | -5.01 | -8.13 | -9[a], -1[b], -18[c] | -15 to -16 | ---- |
| CFPP | °C | -4.53 | -7.82 | -2.05 | -4.39 | -4.90 | -1.35 | -4.14 | - | 5 max | ---- |
| Ø | ---- | 46.1 | 67.7 | 68.6 | 58.9 | 63.00 | 66.64 | 60.06 | 70[a], 60.73[b], 48[d], 49.85[f], 55[g] | 47 mini | 51 mini |
| δ | MJ/kg | 38.8 | 40 | 40.2 | 39.3 | 39.3 | 39.8 | 39.3 | 45.6[a], 41.36[c], 38.48[d], 38.92[f], 38.43[g], 40.5[h] | ---- | ---- |
| FP | °C | 350 | 444 | 457 | 382 | 383 | 430 | 381 | 189[a], 172[b], 130[c], 178[d], 145[e], 178[g] | 130 mini | 101 mini |

[a] (Mostafa & El-Gendy, 2013), [b] (Nautiyal et al., 2014), [c] (Rahman et al., 2017), [d] (El-Shimi et al., 2013), [e] (Hariram & Kumar, 2013), [f] (Murad & Al-dawody, 2020), [g] (Rahman & Nahar, 2016), [h] (Kenya Bureau of Standards (KEBS)

Table 4.17. Physicochemical properties for biodiesel produced by $SO_3$-CPILs compared to experimental data and standard biodiesel specifications

| Biodiesel property | Unit | Predicted property | | | | | Experimental data | Limits (ASTM D6751) | Limits (EN 14214) |
|---|---|---|---|---|---|---|---|---|---|
| | | $SO_3$-CPHA | $SO_3$-CPMS/dry | $SO_3$-CPMS/wet | $SO_3$-CPSA/dry | $SO_3$-CPSA/wet | | | |
| ή@ 40 °C | mm$^2$/s | 4.1 | 2.6 | 3.5 | 3.4 | 3.5 | 12.4[a], 4.8[b], 5.7[c], 4.5[d], 5.8[e], 4.3[f], 4.5[g] | 1.9 - 6 | 3.5 - 5 |
| ρ@15 °C | kg m$^{-3}$ | 873 | 840 | 873 | 873 | 873 | 0.86[a], 0.89[b], 0.86[c], 0.86[d], 0.83[e], 0.87[f], 0.83[g] | 880 | 860 - 900 |
| CP | °C | 0.76 | -1.15 | -1.78 | -1.98 | -1.7 | -3[a], 5[b] | -3 to -12 | ---- |
| PP | °C | -6.00 | -8.07 | -8.76 | -8.97 | -8.67 | -9[a], -1[b], -18[c] | -15 to -16 | ---- |
| CFPP | °C | -2.24 | -4.09 | -4.70 | -4.90 | -4.63 | - | 5 max | ---- |
| Ø | ---- | 68.7 | 49.4 | 60.27 | 58.52 | 59.55 | 70[a], 60.73[b], 48[d], 49.85[f], 55[g] | 47 mini | 51 mini |
| δ | MJ/kg | 40.2 | 35.1 | 39.4 | 39.2 | 39.3 | 45.6[a], 41.36[c], 38.48[d], 38.92[f], 38.43[g], 40.5[h] | ---- | ---- |
| FP | °C | 452 | 277 | 387 | 375 | 383 | 189[a], 172[b], 130[c], 178[d], 145[e], 178[g] | 130 mini | 101 mini |

[a](Mostafa & El-Gendy, 2013), [b] (Nautiyal et al., 2014), [c] (Rahman et al., 2017), [d](El-Shimi et al., 2013), [e] (Hariram & Kumar, 2013), [f] (Murad & Al-dawody, 2020), [g] (Rahman & Nahar, 2016), [h] (Kenya Bureau Of Standards (KEBS).

The prediction values of biodiesel viscosities that obtained by $SO_3$-CPIL/CPIL are in the range of 2.6 – 4.1 mm$^2$/s, which are fall within the minimum (1.9 mm$^2$/s) and maximum (6.0 mm$^2$/s) range required by the ASTM D6751 specification. Gopinath et al., (2015) have reviewed a number of research studies, which related the viscosity to the FAMEs composition. It has been found that the increases in the number of carbon atoms of FAME (chain length) and increasing degree of saturation leads to increase of the kinematic viscosity, whereas, it decreases with increasing degree of unsaturation. This fact is highly agreed with the finding in this study as stated previously, except in case of $SO_3$-CPMS, which have been used to synthesize biodiesel from wet biomass showed slightly lower viscosity than the minimum value that required by biodiesel standard. The reason may be that the cis double-bond configuration was dominant than the trans configuration, which can also affects the viscosity as stated by (Knothe & Steidley, 2005), resulting in lower viscosity.

On the other hand, when the experimental data of *S. platensis* biodiesel that have been provided in the literature was compared versus the predicted values of the viscosity in this study as shown in Table (4.16), Table (4.16) and Appendix(Y). The average absolute deviation (AAD) of 16.5% was obtained, which indicated to the high variation between the experimental and calculated values. Similar findings has been reported by (Mostafa & El-Gendy, 2013), who recorded a high viscosity of 12.4 mm$^2$/s, which was much higher than that of biodiesel standard and that of the other studies as depicted in Table (4.16) and Table (4.17). These variations may due to the fact that different cultivation conditions of microalgae is highly effected on the biomass composition, as the result, the changes in FAMEs composition could be observed (Barros et al., 2015; Japar et al., 2017).

**4.6.2 Density**

One of the main fuel qualities used to calculate how much fuel should be injected by the injection systems to ensure optimum combustion is density ($\rho$). Thus, fuel density can have a significant impact on engine performance and emissions. Additionally, correlation of density with nitrogen oxide (NOx) emissions was investigated, and it has been found that lower densities producing lower NOx emissions (McCormick et al., 2001).

From Table (4.16) and (4.17), it is obvious that the density of the majority of the biodiesel produced by $SO_3$-CPIL/CPIL was mostly in the range of 860 kg/m$^3$ to 900 kg/m$^3$ required by the ASTM D6751 and EN 14214 specifications. Pratas et al., (2010) have stated that the density increases with increasing the percentage of short chain of FAMEs (C4 –C16) and increasing unsaturation percentage (number of double bonds) whereas, Yuan et al., (2009) have investigated that the density decreases with increasing the percentage of long chain (from C17) and increases with decreasing saturation percentage. These facts are very consistent with our findings as depicted in Table (4.18). For example, the density value of 873 kg/m3 produced by $SO_3$-CPHA, CPAA, CPHA increased with increasing of unsaturation and decreasing of saturation, whereas, in case of CPMS, CPTFS, $SO_3$-CPMS/wet, $SO_3$-CPSA/dry, $SO_3$-CPSA/wet, increased with increasing the short chain percentage and decreasing the long chain percentage. The density of biodiesel produced by $SO_3$-CPMS/dry recorded the minimum value of 840 kg/m$^3$, and it seems that the density value was more effected with unsaturation than the short chain percentages, thus, it decreased with decreasing unsaturation. The reason behind the slightly higher and lower density values of 874 kg/m$^3$ and 872 kg/m$^3$, which recorded by CPTFA and CPSA, respectively, could not be explained by Pratas and Yuan findings. However, the effect of

cis and trans double-bond configuration could also be considered as mentioned previously. As can be seen in Appendix (Y), the AAD between experimental and estimated density values was 1.37 % with reproducibility of (± 1.2), indicated that there is excellent agreement between the experimental and calculated values.

Table 4.18. The percentage of saturation/short chain and unsaturation/ long chain of FAMEs in biodiesel products

| Biodiesel produced by IL | Saturation/Short chain % | Unsaturation/ long chain% |
|---|---|---|
| CPAA | 7.9 | 92 |
| CPHA | 8.1 | 93 |
| CPSA | 66.1 | 36 |
| CPMS | 59.1 | 43 |
| CPTFA | 21.9 | 80 |
| CPTFS | 62.2 | 40 |
| $SO_3$-CPHA | 11.9 | 89 |
| $SO_3$-CPMS/dry | 66.8 | 40 |
| $SO_3$-CPMS/wet | 62.5 | 39 |
| $SO_3$-CPSA/dry | 64.1 | 39.3 |
| $SO_3$-CPSA/wet | 63.2 | 41 |

### 4.6.3 Properties of low-temperature

One of the major issues associated with the use of biodiesel in a cold weather areas is poor cold-flow properties (Gopinath et al., 2015). Biodiesel's applicability is limited by its poor low-temperature flow characteristics. The formation of deposits in biodiesels at low temperatures might have serious effects for diesel fuel delivery systems. The metrics used to evaluate the low temperature qualities of biodiesel are the cloud point (CP), pour point (PP), and cold-filter plugging point (CFPP) (Gopinath et al., 2015; Sakthivel et al., 2018).

**4.6.3.1 Cloud point**

The lowest temperature at which the wax in the fuel initially crystallizes and takes on a cloudy appearance is known as the cloud point (CP) (Joshi & Pegg, 2007). Only the cloud point of biodiesel that produced by CPAA meet the required values for biodiesel (-4.99 ˚C) as shown in Table (4.16). The presence of cis unsaturation FAMEs increases the CP as reported by (Gopinath et al., 2015). This observation was detected in the biodiesel products that obtained by CPHA, CPTFA and $SO_3$-CPHA. Although the rest of the produced biodiesels in this study had higher values of cloud point (1.67 to -1.98 ˚C) than those of biodiesel standard specifications (-3 to -12 ˚C), better cold flow qualities are still being reported, which boosts the benefits of the produced biodiesel and makes it more suited for use in the majority of African countries. As can be seen in Table (16) and Table (4.17), limits are not given in European Standard (EN 14214), rather a report is required. For its seasonal classes (summer and winter), each country could select one of two possibilities (temperate or arctic climate), and may alter this specification in accordance with local meteorological information (Knothe, 2005).

On the other hand, a higher experimental value of cloud point (5 ˚C) was also reported by Nautiyal et al., (2014), indicated that the variation is a result of different FAMEs content as explained previously.

**4.6.3.2 Pour point**

The pour point (PP) of a fuel is the lowest temperature at which it loses its flow qualities (Joshi & Pegg, 2007). Pour point is also an important characteristic in cold flow operation because the fuel is only suitable for use above the pour point value. The prediction values of biodiesel pour points that obtained by $SO_3$-CPIL/CPIL, are between -5.01 and  -12.24

˚C, which are much higher than the range required by the ASTM D6751 specification (-15 to -16 ˚C). Mostafa & El-Gendy, (2013) and Nautiyal et al., (2014) were reported a relatively comparable observation of pour point values of -9 and -1 ˚C , respectively, which do not meet the ASTM D6751 specification. According to Su et al., (2011), the AAD of 4.83 % indicated that the predicted values of PP are close to the experimental values of Mostafa & El-Gendy, (2013). The excessive deviation of both predicted values in this study and experimental values from the requirements of the biodiesel standard is due to the fact that these biodiesel are particularly consist of saturated fatty acids. Longer saturated methyl ester than C12 increases both CP and PP (Gopinath et al., 2015).

### 4.6.3.3. Cold filter plugging point

The most crucial factor considered when assessing a fuel's capacity to operate in a cold flow is its cold filter plugging point (CFPP). It is the lowest temperature at which the production of crystal blocs causes the fuel to clog the filter device (Boshui et al., 2010). The filterability limit of the fuel can be precisely described by the CFPP more than CP; the cloud point (CP) value of the fuel is always less than its CP value (Sakthivel et al., 2018). Table (4.16) and Table (4.17) showed that all $SO_3$-CPIL/CPIL exhibits CFPP values in the range of maximum -1.35 ˚C (CPTFA) and minimum -7.82 ˚C (CPAA), which are into the range required by the ASTM 6751 specification (5 ˚C maximum). The CFPP determination of biodiesel produced from *S. platensis* has not been reported, as a result, the AAD could not be calculated.

### 4.6.4 Cetane number

One of the most important characteristics of biodiesel is its cetane number (Ø), which indicates the ignition quality of diesel fuel and influencing engine efficiency (Gerpen,

1996). Cetane number has a direct effect on the ignition delay period, which is the time from the injection of fuel into the combustion chamber to the onset of ignition. The shorter the ignition delay, the higher the cetane number, and vice versa (Atabani et al., 2012). Lower cetane number leads to knocking, increased engine emissions and excessive engine deposits due to incomplete combustion (Atabani et al., 2013). It should be noted that the cetane number of biodiesel increases as the chain length and degree of fatty acid saturation increases as stated by (Gopinath et al., 2015). The cetane number of biodiesel fuel is specified by ASTM D6751 (47 minimum) and EN 14214 (51 minimum) (Atabani et al., 2013; Sakthivel et al., 2018). The cetane number of biodiesel varies from 45 to 67 (Gerpen, 1996).

From Table (4.16) and Table (4.17), it is evident that all obtained biodiesels showed higher cetane number in the range of 49.4 and 68.7, which would result in higher combustion efficiency. Furthermore, the cetane number of biodiesel samples was predicted, and it is fairly close to the experimental values, because an AAD of 2.9 % was founded as shown in Appendix (Y).

### 4.6.5 Calorific value

Calorific value ($\delta$) or the heat of combustion of a fuel is the number of heat units (kJ or MJ) released after the complete combustion of one kilogram or one liter of fuel. A higher calorific value is hence preferable for internal combustion engines. Generally, calorific value of conventional diesel fuel is higher than calorific value of biodiesel fuel. ASTM D6751 and EN 14214 standards do not specify calorific value, but EN 14213 (Biodiesel for Heating) specifies a minimum value of 35 MJ/kg (Atabani et al., 2013; Sakthivel et al., 2018), whereas,  ASTM D 4868 specifies a minimum value of 40.5 MJ/kg according to

Kenya Bureau Of Standards (KEBS). From Table (4.16) and Table (4.17), the highest calorific value is 40.2 MJ/kg for biodiesel produced by CPHA and $SO_3$-CPHA and the least calorific value is 35.1 for $SO_3$-CPMS/dry, while the others were obtained calorific value values of (circa. 39 MJ/kg). The AAD between experimental, calculated and Kenyan standard high calorific values was 3.17 %, with reproducibility of ($\pm$ 1.6), which indicated to high accuracy of predicting and sufficient energy content as well.

### 4.6.6 Flash point

The flash point (FP) is the lowest temperature at which vapors of volatile fuel compounds ignite when they come into contact with an ignition source (Liaw & Chiu, 2003). It is one of the most significant flammability indices used to assess a liquid's risk of fire and explosion. The conventional petro diesel has a flash point less than the biodiesel. The flash point of biodiesel fuel is specified by ASTM D6751 (130 minimum) and EN 14214 (101 minimum) (Atabani et al., 2013; Sakthivel et al., 2018). Table (4.16) and Table (4.17) depicted the characteristics of the flash point of various biodiesels produced using $SO_3$-CPIL/CPIL. It can be noticeably observed that the flash point values lies between 277 and 457 ˚C, which indicated that the biodiesel obtained in this study are much less flammable fuel, making it much safer to handle, store, and transport. The maximum flash point value of 189 ˚C have been reported by (Mostafa & El-gendy, 2013). The high variation between estimated and experimental values may due to the fact that biodiesel with longer chain components has a higher flash point (Gopinath et al., 2015).

### 4.7 Recoverability and reusability study of the $SO_3$-bCPIL/CPIL

The possibility of ionic liquid recycling is also a critical problem for an energy-saving system, as it has the potential to considerably reduce the cost of biodiesel manufacturing.

Considering the low volatility of SO3-bCPIL/CPILs, they are often claimed to be readily recyclable. For these reasons, the recycling of the $SO_3$-bCPIL/CPILs for subsequent lipid extraction and biodiesel production was investigated. A great advantage of using $SO_3$-bCPIL/CPILs is that it is very easy to separate the final products by decanting, due to their hydrophilic nature and thus, reuse the supernatant in the next cycle. The $SO_3$- CPILs/CPILs appeared as a gel-like liquid in the middle layer after the extraction process (Figure 4.27).
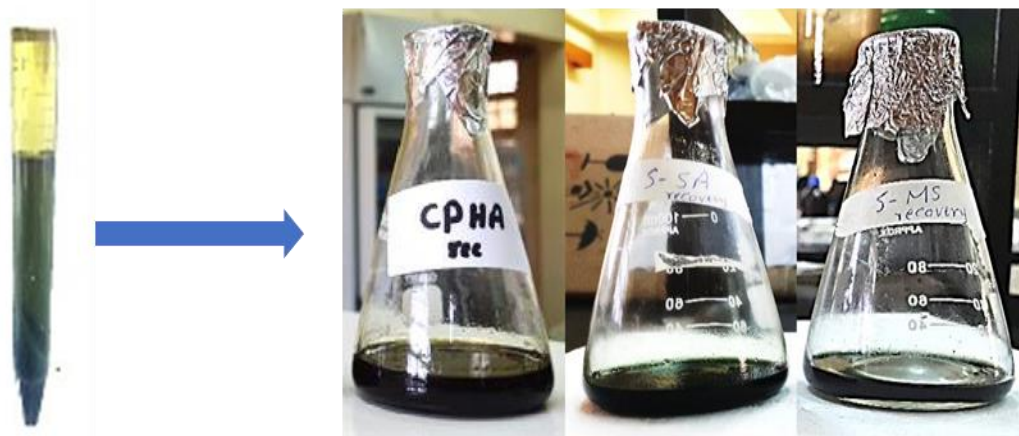


Figure 4.27. The recovered $SO_3$-bCPILs/CPILs

Extraction of lipids was done for up to six cycles (fresh extractan + five successive runs) using each of CPHA, $SO_3$-bCPMS and $SO_3$-bCPSA, due to their extraction efficiency and clear extraction products. More cycles were not performed, considering that there were weight losses and unpurification associated with the process of recovering CPIL. The yields of lipid extracts using these $SO_3$-bCPIL/CPILs in the six repeated runs are displayed in Figure 4.28. These observations point to a very slow inactivation of the efficacy of $SO_3$-bCPILs/CPILs. Further investigation will be required to demonstrate that $SO_3$-bCPIL/CPIL can be recycled without lowering the lipid and biodiesel efficiencies.
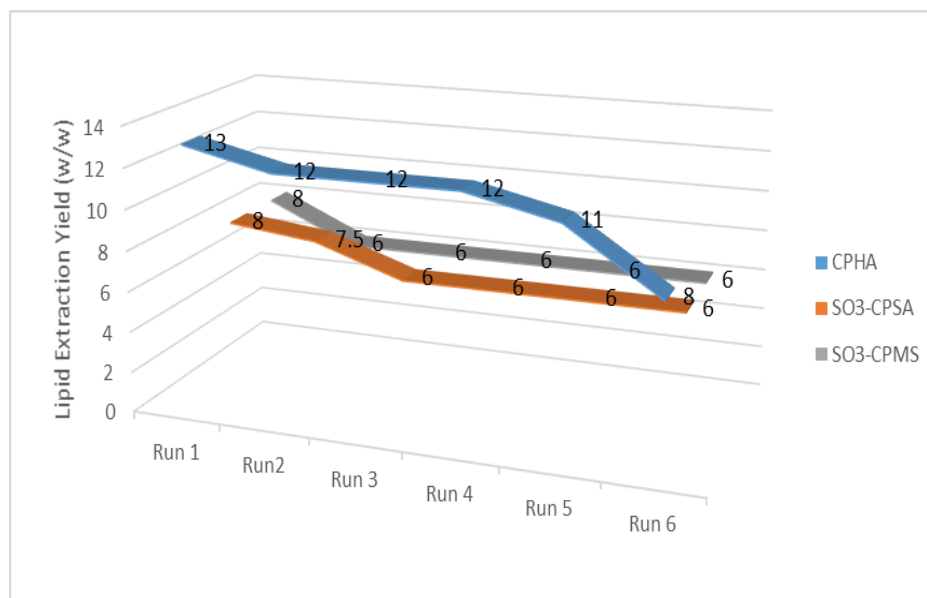
Figure 4.28. Reusability study of SO₃-CPIL/CPIL

## CHAPTER 5: CONCLUSION AND RECOMMENDATION

**5.1 Conclusion**

Nine CPILs and $SO_3$-bCPILs were synthesized successfully through a simple neutralization reaction using low-cost starting materials, and resultant yields were good. Characterization was done using FTIR and Raman spectroscopic techniques, density and viscosity measurements, thermal stability using TGA, and acidity strength using UV/VIS spectroscopy. The characteristic absorption bands in the FTIR and Raman spectra of the prepared compounds exhibited a significant shift in position and/or intensity (compared to caprolactam), indicating the successful formation of ionic liquids. Five of these compounds, namely, Caprolactam chloride (CPHA), Caprolactam methyl sulphonate (CPMS), Caprolactam trifluoromethane sulfonate (CPTFS), sulfonic-butylcaprolactamium chloride ($SO_3$- bCPHA) and sulfonic-butylcaprolactamium methyl sulfonate ($SO_3$-bCPMS) are novel. The results revealed that both density and viscosity values of CPILs/$SO_3$-bCPILs do not depend on their molecular weights, but only depend on intra molecular cation-anion interactions of the compounds. The TGA analysis showed that all $SO_3$-bCPIL/CPILs had good thermal stability, ranging between 108 ˚C and 221 ˚C (CPAA recorded the lowest value), and the compounds can therefore be used as catalysts for transesterification of microalgal lipids, even at high temperatures. The acidity strength of CPMS, CPTFS and $SO_3$-bCPSA was found to be higher than that of sulphuric acid ($H_2SO_4$), while lower acidity values were recorded for CPAA, CPTFA, CPHA, CPSA, $SO_3$-bCPHA and $SO_3$-bCPMS.

The pure forms of three of these CPILs - Caprolactamium acetate (CPAA), Caprolactamium chloride (CPHA), and caprolactam trifluoromethane acetate (CPTFA) -

showed comparable lipid recovery efficiency from dry biomass to the conventional organic solvent (hexane –methanol) extraction method, while their mixtures with methanol (CPIL/MeOH) were found to exhibit enhanced in lipid extraction relative to the control (9.5 %). A maximum lipid recovery of 14% and 8% from dry and wet biomass, respectively, was achieved with the use of CPAA/MeOH, followed by CPHA/MeOH (13 %) and CPTFA/MeOH (11 %) from dry biomass.

In respect of $SO_3$-bCPILs, results showed the lipids yield to be similar to the control, for both wet and dried microalgae biomass, except for $SO_3$-bCPHA, which recorded a lower lipid yield from wet biomass. The energy-intensive drying process employed in conventional organic solvent-based lipid extraction could be replaced by the utilization of wet biomass. SEM analysis revealed that the cell wall was weak, non-uniform, and likely non-intact, implying that the CPILs had a high dissolution capacity, resulting in the effective rupture of microalgae cell walls. The CPILs and $SO_3$-bCPILs also displayed the potential for direct transformation of lipids into the corresponding methyl esters, particularly CPSA, CPMS, CPTFS, $SO_3$-bCPSA, and $SO_3$-bCPMS. The conversion rate of fatty acids was similar or even better than that of the conventional method ($H_2SO_4$, KOH), and state of the art ionic liquids such as choline L-arginine [Ch] [ARG]. The CPAA, CPHA, CPTFA and $SO_3$-bCPHA showed less conversion rate of the major fatty acids, and thus poor biodiesel quality, due to their low acidity strength - and hence little catalytic activity. Catalytic activity of the ILs followed the order, $SO_3$-bCPSA > CPTFS > CPMS > CPSA > $H_2SO_4$, and was dependent on acidity strength.

In addition, all CPILs and $SO_3$-bCPILs (except CPAA and $SO_3$-bCPHA) minimized pigment co-extraction, and this could potentially reduce the number of steps involved in

biodiesel production.

Despite the effectiveness of CPMS, CPTFS and $SO_3$-bCPSA in direct transesterification of lipids, the extremely strong acidity (higher than $H_2SO_4$), and therefore corrosiveness, of these ionic liquids is a drawback. However, CPSA and $SO_3$-bCPMS have a lower acidity than that of $H_2SO_4$ and could thus be used as catalysts to avoid or minimize corrosivity. In particular, $SO_3$-bCPMS, which also exhibited efficacy with wet biomass, is a promising green technology for production of biodiesel in single step, with potential energy and cost savings.

The biodiesel quality characteristics provided in this study are largely in accord with the specifications of ASTM D6751 and EN 14214. Furthermore, the CPILs and $SO_3$-bCPILs were easily recovered and successfully recycled for up to six runs.

This thesis provided insights into the emergence of more environmentally friendly, simple and cost-effective technologies, that are faster and have higher or comparable lipid/biodiesel yields to conventional methods, and that can therefore replace fossil fuels, which contribute significantly to global warming.

## 5.2 Recommendations and further work

Some further important chemical structure characterization for the synthesized ionic liquids such as nuclear molecular resonance (NMR) and mass spectroscopy (MS) can be undertaken. The simultaneous lipid extraction and transesterification reaction of $SO_3$-bCPMS as well as CPSA, CPMS, CPTFS and $SO_3$-bCPSA that were carried out for biodiesel production at 95 $^o$C for 2 h could be improved. Therefore, future optimization experiments will be necessary for parameters such as the ratio of ionic liquid: methanol, as well as the temperature and time. For biodiesel characterization, some important additional studies need to be carried out, including physical properties such as acid value, alcohol

control, and cloud soak filtration, oxidation stability, Karl Fischer water, free and total Glycerin and the FAME profile and compared with the conventional fuels. This to assure the quality of the biodiesel produced, as well as the accurate yield determination of the biodiesel produced through direct transesterification of lipids using EN 14103:2011 standard test method. Analysis will also be needed to determine the quality of the produced biodiesel after reusability of the ILs. Furthermore, it is important to investigate the potential toxic effects of CPILs and $SO_3$-bCPILs, for safety in use and disposal considerations. Lastly, $SO_3$-bCPIL/CPIL can be used as an eco-friendly solvent/catalyst for biodiesel production from other microalgae species.

Eventually, these techniques, which have been investigated to enhance the conversion of microalgae lipids to biodiesel, can be scaled up, especially for uses in the transportation applications.

# REFERENCES

Ab Rani, M. A., Brant, A., Crowhurst, L., Dolan, A., Lui, M., Hassan, N. H., … Wilding, R. (2011). Understanding the polarity of ionic liquids. *Physical Chemistry Chemical Physics*, *13*(37), 16831–16840. https://doi.org/10.1039/c1cp21262a

Abbott, A. P., Boothby, D., Capper, G., Davies, D. L., & Rasheed, R. K. (2004). Deep Eutectic Solvents Formed between Choline Chloride and Carboxylic Acids: Versatile Alternatives to Ionic Liquids. *J. AM. CHEM. SOC*, *126*(29), 9142–9147. https://doi.org/10.1021/acssuschemeng.8b04255

Abubakar, L.U1., Mutie, A. M.1, Kenya, E. . (2011). Microalgae Species Biodiversity and Abundance and Their. *4th National Council Of Science & Technology National Conference*, *Nairobi*, *K*, 155–158.

Aguirre, A. M., & Bassi, A. (2014). Investigation of high pressure steaming (HPS) as a thermal treatment for lipid extraction from Chlorella vulgaris. *Bioresource Technology*, *164*, 136–142. https://doi.org/10.1016/j.biortech.2014.04.089

Akubude, V. C., Nwaigwe, K. N., & Dintwa, E. (2019). Materials Science for Energy Technologies Production of biodiesel from microalgae via nanocatalyzed transesterification process : A review. *Materials Science for Energy Technologies*, *2*(2), 216–225. https://doi.org/10.1016/j.mset.2018.12.006

Aleman-Ramirez, J. L., Moreira, J., Torres-Arellano, S., Longoria, A., Okoye, P. U., & Sebastian, P. J. (2021). Preparation of a heterogeneous catalyst from moringa leaves as a sustainable precursor for biodiesel production. *Fuel*, *284*(August 2020), 118983. https://doi.org/10.1016/j.fuel.2020.118983

Amarasekara, A. S., & Owereh, O. S. (2011). Thermal properties of sulfonic acid group functionalized Bro acidic ionic liquids. *J Therm Anal Calorim*, *103*, 1027–1030. https://doi.org/10.1007/s10973-010-1101-5

Andreani, L., & Rocha, J. D. (2012). Use of ionic liquids in biodiesel production: A review. *Brazilian Journal of Chemical Engineering*, *29*(1), 1–13. https://doi.org/10.1590/S0104-66322012000100001

Aratboni, H. A., Rafiei, N., Garcia-Granados, R., Alemzadeh, A., & Morones-Ramírez, J. R. (2019). Biomass and lipid induction strategies in microalgae for biofuel production and other applications. *Microbial Cell Factories*, *18*(1), 1–17. https://doi.org/10.1186/s12934-019-1228-4

Arumugam, M., Agarwal, A., Arya, M. C., & Ahmed, Z. (2013). Influence of nitrogen sources on biomass productivity of microalgae Scenedesmus bijugatus. *Bioresource Technology*, *131*, 246–249. https://doi.org/10.1016/j.biortech.2012.12.159

Atabani, A. E., Silitonga, A. S., Badruddin, I. A., Mahlia, T. M. I., Masjuki, H. H., & Mekhilef, S. (2012). A comprehensive review on biodiesel as an alternative energy resource and its characteristics. *Renewable and Sustainable Energy Reviews*, *16*, 2070–2093. https://doi.org/10.1016/j.rser.2012.01.003

Atabani, A. E., Silitonga, A. S., Ong, H. C., Mahlia, T. M. I., Masjuki, H. H., Badruddin, I. A., & Fayaz, H. (2013). Non-edible vegetable oils: A critical evaluation of oil extraction, fatty acid compositions, biodiesel production, characteristics, engine performance and emissions production. *Renewable and Sustainable Energy Reviews*, *18*, 211–245. https://doi.org/10.1016/j.rser.2012.10.013

Attaphong, C., & Sabatini, D. A. (2013). Phase behaviors of vegetable oil-based microemulsion fuels: The effects of temperatures, surfactants, oils, and water in ethanol. *Energy and Fuels*, *27*(11), 6773–6780. https://doi.org/10.1021/ef401441a

Barros, A. I., Gonçalves, A. L., Simões, M., & Pires, J. C. M. (2015). Harvesting techniques applied to microalgae: A review. *Renewable and Sustainable Energy Reviews*, *41*, 1489–1500. https://doi.org/10.1016/j.rser.2014.09.037

Basso, A., & Serban, S. (2019). Industrial applications of immobilized enzymes—A review. *Molecular Catalysis*, *479*(March), 110607. https://doi.org/10.1016/j.mcat.2019.110607

Bauer, G., Lima, S., Chenevard, J., Sugnaux, M., & Fischer, F. (2017). *Biodiesel via in Situ Wet Microalgae Biotransformation: Zwitter-Type Ionic Liquid Supported Extraction and Transesteri fi cation*. https://doi.org/10.1021/acssuschemeng.6b02665

Baunillo, K. E., Tan, R. S., Barros, R., & Luque, R. (2012). Investigations on microalgal oil production from Arthrospira platensis : towards more sustainable biodiesel production {. *RSC Advances*, *2*, 11267–11272. https://doi.org/10.1039/c2ra21796a

Bhatia, S. K., Bhatia, R. K., Jeon, J. M., Pugazhendhi, A., Kumar Awasthi, M., Kumar, D., … Yang, Y. H. (2021). An overview on advancements in biobased transesterification methods for biodiesel production: Oil resources, extraction, biocatalysts, and process intensification technologies. *Fuel*, *285*(April 2020), 119117. https://doi.org/10.1016/j.fuel.2020.119117

Bligh, E. G., & Dyer, W. J. (1959). A rapid method of total lipid extraction and purification. *Canadian Journal of Biochemistry and Physiology*, *37*(8), 911–917.

Blume, A. (1996). Properties of lipid vesicles : FT -IR spectroscopy and fluorescence probe studies. *Current Opinion in Colloid & Interface Science*, *1*(1), 64–77. https://doi.org/10.1016/S1359-0294(96)80046-X

Boshui, C., Yuqiu, S., Jianhua, F., Jiu, W., & Jiang, W. (2010). Cold flow properties and crystal morphologies of biodiesel blends. *Chemistry and Technology of Fuels and*

*Oils*, *46*(1). https://doi.org/10.1007/s10553-010-0185-8

Boyd, A. R., Champagne, P., McGinn, P. J., MacDougall, K. M., Melanson, J. E., & Jessop, P. G. (2012). Switchable hydrophilicity solvents for lipid extraction from microalgae for biofuel production. *Bioresource Technology*, *118*, 628–632. https://doi.org/10.1016/j.biortech.2012.05.084

Bucy, H. B., Baumgardner, M. E., & Marchese, A. J. (2012). Chemical and physical properties of algal methyl ester biodiesel containing varying levels of methyl eicosapentaenoate and methyl docosahexaenoate. *Algal Research*, *1*(1), 57–69. https://doi.org/10.1016/j.algal.2012.02.001

Carvalho, D., Rocha, A., Gómez-Gesteira, M., & Silva Santos, C. (2017). Offshore winds and wind energy production estimates derived from ASCAT, OSCAT, numerical weather prediction models and buoys – A comparative study for the Iberian Peninsula Atlantic coast. *Renewable Energy*, *102*, 433–444. https://doi.org/10.1016/j.renene.2016.10.063

Cevasco, G., & Chiappe, C. (2014). Are ionic liquids a proper solution to current environmental challenges? *Green Chemistry*, *16*(5), 2375–2385. https://doi.org/10.1039/c3gc42096e

Chackalackal, S. M., & Stafford, F. E. (1966). *Infrared Spectra of Methane-, Fluoro-, and Chlorosulfonic Acids*.

Chen, C. L., Chang, J. S., & Lee, D. J. (2015). Dewatering and Drying Methods for Microalgae. *Drying Technology*, *33*(4), 443–454. https://doi.org/10.1080/07373937.2014.997881

Chen, K. T., Cheng, C. H., Wu, Y. H., Lu, W. C., Lin, Y. H., & Lee, H. T. (2013). Continuous lipid extraction of microalgae using high-pressure carbon dioxide. *Bioresource Technology*, *146*, 23–26. https://doi.org/10.1016/j.biortech.2013.07.017

Chen, X., Hu, L., Xing, R., Liu, S., Yu, H., Qin, Y., … Li, P. (2015). Ionic liquid-assisted subcritical water promotes the extraction of lipids from wet microalgae Scenedesmus sp. *European Journal of Lipid Science and Technology*, *117*(8), 1192–1198. https://doi.org/10.1002/ejlt.201400189

Cheng, J. J., & Timilsina, G. R. (2011). Status and barriers of advanced biofuel technologies: A review. *Renewable Energy*, *36*(12), 3541–3549. https://doi.org/10.1016/j.renene.2011.04.031

Chhotaray, P. K., & Gardas, R. L. (2014). Thermophysical properties of ammonium and hydroxylammonium protic ionic liquids. *Journal of Chemical Thermodynamics*, *72*, 117–124. https://doi.org/10.1016/j.jct.2014.01.004

Chiappe, C., Malvaldi, M., & Pomelli, C. S. (2009). Ionic liquids: Solvation ability and polarity. *Pure and Applied Chemistry*, *81*(4), 767–776. https://doi.org/10.1351/PAC-CON-08-09-08

Chiappe, C., Mezzetta, A., Pomelli, S., & Iaquaniello, G. (2016). *microalgae using protic ionic liquids*. https://doi.org/10.1039/c6gc00923a

Chiappe, C., Rajamani, S., & D'Andrea, F. (2013). A dramatic effect of the ionic liquid structure in esterification reactions in protic ionic media. *Green Chemistry*, *15*(1), 137–143. https://doi.org/10.1039/c2gc35941c

Chisti, Y. (2008). Biodiesel from microalgae beats bioethanol. *Trends in Biotechnology*, *26*(3), 126–131. https://doi.org/10.1016/j.tibtech.2007.12.002

Choi, S. A., Jung, J. Y., Kim, K., Kwon, J. H., Lee, J. S., Kim, S. W., … Yang, J. W. (2014). Effects of molten-salt/ionic-liquid mixture on extraction of docosahexaenoic acid (DHA)-rich lipids from Aurantiochytrium sp. KRS101. *Bioprocess and Biosystems Engineering*, *37*(11), 2199–2204. https://doi.org/10.1007/s00449-014-1197-2

Choi, S. A., Lee, J. S., Oh, Y. K., Jeong, M. J., Kim, S. W., & Park, J. Y. (2014). Lipid extraction from Chlorella vulgaris by molten-salt/ionic-liquid mixtures. *Algal Research*, *3*(1), 44–48. https://doi.org/10.1016/j.algal.2013.11.013

Choi, S. A., Oh, Y. K., Jeong, M. J., Kim, S. W., Lee, J. S., & Park, J. Y. (2014). Effects of ionic liquid mixtures on lipid extraction from Chlorella vulgaris. *Renewable Energy*, *65*, 169–174. https://doi.org/10.1016/j.renene.2013.08.015

Christe, K. 0., & Naumann, D. (1973). Vibrational spectra of trifluoroacetates. *Spectmchimica Acta*, *29*, 2017–2024.

Christie, W. W., & Han, X. (2012). Preparation of derivatives of fatty acids. *Lipid Analysis*, 145–158. https://doi.org/10.1533/9780857097866.145

Collotta, M., Busi, L., Champagne, P., Romagnoli, F., Tomasoni, G., Mabee, W., & Alberti, M. (2017). Comparative LCA of Three Alternative Technologies for Lipid Extraction in Biodiesel from Microalgae Production. *Energy Procedia*, *113*, 244–250. https://doi.org/10.1016/j.egypro.2017.04.061

Connor, S. O., Connor, S. O., Pillai, S. C., Ehimen, E., & Bartlett, J. (2020). Production of Biodiesel Using Ionic Liquids. *Nanotechnology-Based Industrial Applications of Ionic Liquids, Nanotechnology in the Life Sciences*, (Switzerland), 246–264. https://doi.org/10.1007/978-3-030-44995-7

Cooney, M., Young, G., & Nagle, N. (2009). Extraction of Bio - oils from Microalgae. *Separation & Purification Reviews*, *38*(4), 291–325.

Crampon, C., Mouahid, A., Toudji, S. A. A., Lepine, O., & Badens, E. (2013). Influence of pretreatment on supercritical CO2 extraction from Nannochloropsis oculata. *Journal of Supercritical Fluids*, *79*, 337–344. https://doi.org/10.1016/j.supflu.2012.12.022

Da Silva, A. C. H., Dall'Oglio, E. L., De Sousa, P. T., Da Silva, S. C., & Kuhnen, C. A. (2014). DFT study of the acid-catalyzed ethanolysis of butyric acid monoglyceride: Solvent effects. *Fuel*, *119*(November), 1–5. https://doi.org/10.1016/j.fuel.2013.11.023

Da Silva, C., & Oliveira, J. V. (2014). Biodiesel production through non-catalytic supercritical transesterification: Current state and perspectives. *Brazilian Journal of Chemical Engineering*, *31*(2), 271–285. https://doi.org/10.1590/0104-6632.20140312s00002616

Dean, A. P., Sigee, D. C., Estrada, B., & Pittman, J. K. (2010). Using FTIR spectroscopy for rapid determination of lipid accumulation in response to nitrogen limitation in freshwater microalgae. *Bioresource Technology*, *101*(12), 4499–4507. https://doi.org/10.1016/j.biortech.2010.01.065

Dejoye Tanzi, C., Abert Vian, M., & Chemat, F. (2013). New procedure for extraction of algal lipids from wet biomass: A green clean and scalable process. *Bioresource Technology*, *134*, 271–275. https://doi.org/10.1016/j.biortech.2013.01.168

Deng, X., Li, Y., & Fei, X. (2009). Microalgae: A promising feedstock for biodiesel. *African Journal of Microbiology Research*, *3*(13), 1008–1014.

Derakhshan, M. V., Nasernejad, B., Abbaspour-Aghdam, F., & Hamidi, M. (2015). Oil extraction from algae: A comparative approach. *Biotechnology and Applied Biochemistry*, *62*(3), 375–382. https://doi.org/10.1002/bab.1270

Dong, T., Knoshaug, E. P., Pienkos, P. T., & Laurens, L. M. L. (2016). Lipid recovery from wet oleaginous microbial biomass for biofuel production: A critical review. *Applied Energy*, *177*, 879–895. https://doi.org/10.1016/j.apenergy.2016.06.002

Du, Y., Cyprichová, V., Hoppe, K., Schuur, B., & Brilman, W. (2019). Process evaluation data supporting studies on swing strategies to recover N-ethylbutylamine after wet lipid extraction from microalgae. *Data in Brief*, *26*. https://doi.org/10.1016/j.dib.2019.104416

Du, Z., Li, Z., Guo, S., Zhang, J., Zhu, L., & Deng, Y. (2005). Investigation of physicochemical properties of lactam-based Brønsted acidic ionic liquids. *Journal of Physical Chemistry B*, *109*(41), 19542–19546. https://doi.org/10.1021/jp0529669

Du, Z., Li, Z., Guo, S., Zhang, J., Zhu, L., Deng, Y., … Deng, Y. (2005). *Investigation of Physicochemical Properties of Lactam-Based Br ø nsted Acidic Ionic Liquids*

*Investigation of Physicochemical Properties of Lactam-Based Brønsted Acidic Ionic Liquids*. https://doi.org/10.1021/jp0529669

Durand, E., Lecomte, J., & Villeneuve, P. (2013). Deep eutectic solvents: Synthesis, application, and focus on lipase-catalyzed reactions. *European Journal of Lipid Science and Technology*, *115*(4), 379–385. https://doi.org/10.1002/ejlt.201200416

Ekkpowpan, P., Arpornpong, N., Charoensaeng, A., & Khaodhiar, S. (2014). Life Cycle Assessment of Biofuel from Microemulsion and Transesterification Processes. *International Conference on Advances in Engineering and Technology*, 610–614. https://doi.org/10.15242/iie.e0314051

El-Shimi, H.I.; Attia, N. K.; El-Sheltawy, S. T.; El-Diwani, G. I. (2013). Biodiesel Production from Spirulina-Platensis Microalgae by In-Situ Transesterification Process. *Journal of Sustainable Bioenergy Systems*, *3*, 224–233.

El-Shimi, H. I., Attia, N. K., Abd El Aal, A. A., El-Sheltawy, S. T., & Diwani, G. I. (2015). Quality Profile of Spirulina-platensis Oilgae Extraction for Biodiesel Production. *Indian Journal of Applied Research*, *5*(3), 16–21.

Elavarasan, P., Kondamudi, K., & Upadhyayula, S. (2015). *A Functionalized , Supported Ionic Liquid for Alkylation of p-Cresol with Tert-Butyl Alcohol Journal of Chemical Engineering &*. (August 2016). https://doi.org/10.4172/2157-7048.1000270

Endres, F., & Zein El Abedin, S. (2006). Air and water stable ionic liquids in physical chemistry. *Physical Chemistry Chemical Physics*, *8*(18), 2101–2116. https://doi.org/10.1039/b600519p

Fábos, V., Lantos, D., Bodor, A., Bálint, A. M., Mika, L. T., Sielcken, O. E., … Horváth, I. T. (2008). ε-caprolactamium hydrogen sulfate: An ionic liquid used for decades in the large-scale production of ε-caprolactam. *ChemSusChem*, *1*(3), 189–192. https://doi.org/10.1002/cssc.200700135

Fan, P., Xing, S., Wang, J., Fu, J., Yang, L., & Yang, G. (2017). Sulfonated imidazolium ionic liquid-catalyzed transesterification for biodiesel synthesis. *Fuel*, *188*, 483–488. https://doi.org/10.1016/j.fuel.2016.10.068

Fang, D., Jiang, C., & Yang, J. (2013). Preparation of Biodiesel from Castor Oil Catalyzed by Novel Basic Ionic Liquid. *Energy Technology*, *1*(2), 135–138. https://doi.org/10.1002/ente.201200026

Farias-Aguilar, J. C., Ramírez-Moreno, M. J., Téllez-Jurado, L., & Balmori-Ramírez, H. (2014). Low pressure and low temperature synthesis of polyamide-6 (PA6) using Na0 as catalyst. *Materials Letters*, *136*(December), 388–392. https://doi.org/10.1016/j.matlet.2014.08.071

Farooq, A., Amin, U. K., & Abdullah, Y. (2013). Transesterification of oil extracted from different species of algae for biodiesel production. *African Journal of Environmental*

*Science and Technology*, *7*(6), 358–364. https://doi.org/10.5897/ajest12.167

Farrán, A., Cai, C., Sandoval, M., Xu, Y., Liu, J., Hernáiz, M. J., & Linhardt, R. J. (2015). Green Solvents in Carbohydrate Chemistry: From Raw Materials to Fine Chemicals. *Chemical Reviews*, *115*(14), 6811–6853. https://doi.org/10.1021/cr500719h

Fattah, I. M. R., Noraini, M. Y., Mofijur, M., & Silitonga, A. S. (2020). Lipid Extraction Maximization and Enzymatic Synthesis of Biodiesel from Microalgae. *Applied Sciences*, *10*, 6103. https://doi.org/doi:10.3390/app10176103

Fauzi, A. H. M., & Amin, N. A. S. (2012). An overview of ionic liquids as solvents in biodiesel synthesis. *Renewable and Sustainable Energy Reviews*, *16*(8), 5770–5786. https://doi.org/10.1016/j.rser.2012.06.022

Felix, C., Ubando, A., Madrazo, C., Gue, I. H., Sutanto, S., Tran-Nguyen, P. L., … Chen, W. H. (2019). Non-catalytic in-situ (trans)esterification of lipids in wet microalgae Chlorella vulgaris under subcritical conditions for the synthesis of fatty acid methyl esters. *Applied Energy*, *248*(May), 526–537. https://doi.org/10.1016/j.apenergy.2019.04.149

Folch, J., Lees, M., & Sloane Stanley, G. H. (1957). A simple method for the isolation and purification of total lipides from animal tissues. *The Journal of Biological Chemistry*, *226*(1), 497–509. https://doi.org/10.1016/s0021-9258(18)64849-5

Forfang, K., Zimmermann, B., Kosa, G., Kohler, A., & Shapaval, V. (2017). FTIR Spectroscopy for Evaluation and Monitoring of Lipid Extraction Efficiency for Oleaginous Fungi. *PLoS ONE*, *12*(1), 1–17. https://doi.org/10.1371/journal.pone.0170611

Fujita, K., Kobayashi, D., Nakamura, N., & Ohno, H. (2013). Direct dissolution of wet and saliferous marine microalgae by polar ionic liquids without heating. *Enzyme and Microbial Technology*, *52*(3), 199–202. https://doi.org/10.1016/j.enzmictec.2012.12.004

Gadilohar, B. L., & Shankarling, G. S. (2017). Choline based ionic liquids and their applications in organic transformation. *Journal of Molecular Liquids*, *227*, 234–261. https://doi.org/10.1016/j.molliq.2016.11.136

Garbuzova, I. A., & Lokshin, B. V. (2004). Hydrogen bonding in ε-caprolactam dimer: A quantum-chemical study. *Russian Chemical Bulletin*, *53*(9), 1894–1902. https://doi.org/10.1007/s11172-005-0047-4

Gerpen, J. Van. (1996). Cetane Number Testing of Biodiesel. *Third Liquid Fuel Conference "Liquid Fuels and Industrial Products from Renewable Resources,"* 197–206.

Gomez, N. A., Abonia, R., Cadavid, H., & Vargas, I. H. (2011). Chemical and Spectroscopic Characterization of a Vegetable Oil used as Dielectric Coolant in Distribution Transformers. *J. Braz. Chem. Soc*, *22*(12), 2292–2303.

Gopinath, A., Sairam, K., Velraj, R., & Kumaresan, G. (2015). Effects of the properties and the structural configurations of fatty acid methyl esters on the properties of biodiesel fuel: A review. *Proceedings of the Institution of Mechanical Engineers, Part D: Journal of Automobile Engineering*, *229*(3), 357–390. https://doi.org/10.1177/0954407014541103

Gouveia, L., Marques, A. E., Da Silva, T. L., & Reis, A. (2009). Neochloris oleabundans UTEX #1185: A suitable renewable lipid source for biofuel production. *Journal of Industrial Microbiology and Biotechnology*, *36*(6), 821–826. https://doi.org/10.1007/s10295-009-0559-2

Greaves, T. L., & Drummond, C. J. (2008). ChemInform Abstract: Protic Ionic Liquids: Properties and Applications. *ChemInform*, *39*(18), 206–237. https://doi.org/10.1002/chin.200818249

Grima, E. M., González, M. J., & Giménez, A. G. (2013). Solvent Extraction for Microalgae Lipids. *Algae for Biofuels and Energy*, *20*, 491–515. https://doi.org/10.1007/978-94-007-5479-9

Grishina, E. P., Ramenskaya, L. M., Gruzdev, M. S., & Kraeva, O. V. (2013). Water effect on physicochemical properties of 1-butyl-3-methylimidazolium based ionic liquids with inorganic anions. *Journal of Molecular Liquids*, *177*(3), 267–272. https://doi.org/10.1016/j.molliq.2012.10.023

Gülüm, M., & Bilgin, A. (2015). Density, flash point and heating value variations of corn oil biodiesel-diesel fuel blends. *Fuel Processing Technology*, *134*, 456–464. https://doi.org/10.1016/j.fuproc.2015.02.026

Gülüm, M., & Bilgin, A. (2016). Two-term power models for estimating kinematic viscosities of different biodiesel-diesel fuel blends. *Fuel Processing Technology*, *149*, 121–130. https://doi.org/10.1016/j.fuproc.2016.04.013

Hajipour, A. R., & Rafiee, F. (2009). Iranian Chemical Society Basic Ionic Liquids . A Short Review. *Review Literature And Arts Of The Americas*, *6*(4), 647–678.

Halim, R., Danquah, M. K., & Webley, P. A. (2012). Extraction of oil from microalgae for biodiesel production : A review. *Biotechnology Advances*, *30*(3), 709–732. https://doi.org/10.1016/j.biotechadv.2012.01.001

Hameed, B. H., Lai, L. F., & Chin, L. H. (2009). Production of biodiesel from palm oil (Elaeis guineensis) using heterogeneous catalyst: An optimized process. *Fuel Processing Technology*, *90*(4), 606–610.

https://doi.org/10.1016/j.fuproc.2008.12.014

Hariram V. and G. Mohan Kumar. (2013). Combustion analysis of algal oil methyl ester in a direct injection compression ignition engine. *Journal of Engineering Science and Technology*, *8*(1).

Harman-Ware, A. E., Morgan, T., Wilson, M., Crocker, M., Zhang, J., Liu, K., … Debolt, S. (2013). Microalgae as a renewable fuel source: Fast pyrolysis of Scenedesmussp. *Renewable Energy*, *60*, 625–632. https://doi.org/10.1016/j.renene.2013.06.016

Hayes, R., Warr, G. G., & Atkin, R. (2015). Structure and Nanostructure in Ionic Liquids. *Chemical Reviews*, *115*(13), 6357–6426. https://doi.org/10.1021/cr500411q

Hayyan, A., Alam, M. Z., Mirghani, M. E. S., Kabbashi, N. A., Hakimi, N. I. N. M., Siran, Y. M., & Tahiruddin, S. (2011). Reduction of high content of free fatty acid in sludge palm oil via acid catalyst for biodiesel production. *Fuel Processing Technology*, *92*(5), 920–924. https://doi.org/10.1016/j.fuproc.2010.12.011

Hidalgo, P., Ciudad, G., & Navia, R. (2016). Evaluation of different solvent mixtures in esterifiable lipids extraction from microalgae Botryococcus braunii for biodiesel production. *Bioresource Technology*, *201*(November), 360–364. https://doi.org/10.1016/j.biortech.2015.11.031

Hsu, D. D. (2012). Life cycle assessment of gasoline and diesel produced via fast pyrolysis and hydroprocessing. *Biomass and Bioenergy*, *45*, 41–47. https://doi.org/10.1016/j.biombioe.2012.05.019

Huang, P., Gu, A., & Wang, J. (2014). *Efficient production of 5-hydroxymethylfurfural through the dehydration of sugars with caprolactam hydrogen sulfate ([ CPL ] HSO 4 ) ionic liquid catalyst solvent*. https://doi.org/10.1007/s11164-014-1633-6

Huddleston, J. G., Visser, A. E., Reichert, W. M., Willauer, H. D., Broker, G. A., & Rogers, R. D. (2001). Characterization and comparison of hydrophilic and hydrophobic room temperature ionic liquids incorporating the imidazolium cation. *Green Chemistry*, *3*(4), 156–164. https://doi.org/10.1039/b103275p

Hulsbosch, J., De Vos, D. E., Binnemans, K., & Ameloot, R. (2016). Biobased Ionic Liquids: Solvents for a Green Processing Industry? *ACS Sustainable Chemistry and Engineering*, *4*(6), 2917–2931. https://doi.org/10.1021/acssuschemeng.6b00553

Isahak, W. N. R. W., Ismail, M., Jahim, J. M., Salimon, J., & Yarmo, M. A. (2011). Transesterification of Palm Oil by using Ionic Liquids as a New Potential Catalyst. *Trends in Applied Sciences Research*, *6*(9), 1055–1062. https://doi.org/10.3923/tasr.2011.1055.1062

Ishak, Z. I., Sairi, N. A., Alias, Y., & Kheireddine, M. (2017). A review of ionic liquids as

catalysts for transesterification reactions of biodiesel and glycerol carbonate production. *Catalysis Reviews*. https://doi.org/10.1080/01614940.2016.1268021

Japar, A. S., Takriff, M. S., & Yasin, N. H. M. (2017). Harvesting microalgal biomass and lipid extraction for potential biofuel production: A review. *Journal of Environmental Chemical Engineering*, *5*(1), 555–563. https://doi.org/10.1016/j.jece.2016.12.016

Jessop, P. G. (2015). Switchable Solvents as Media for Synthesis and Separations. *Aldrichimica Acta*, *48*(1), 18–21.

Jessop, P. G., & Leitner, W. (2007). Supercritical Fluids as Media for Chemical Reactions. *Chemical Synthesis Using Supercritical Fluids*, 1–36. https://doi.org/10.1002/9783527613687.ch1

Joshi, R. M., & Pegg, M. J. (2007). Flow properties of biodiesel fuel blends at low temperatures. *Fuel*, *86*, 143–151. https://doi.org/10.1016/j.fuel.2006.06.005

Keshavarz, M., Iravani, N., & Parhami, A. (2019). *Novel SO 3 H-functionalized polyoxometalate-based ionic liquids as highly ef fi cient catalysts for esteri fi cation reaction*. *1189*, 272–278. https://doi.org/10.1016/j.molstruc.2019.04.027

Khan, M. F., Garg, A., Jain, S., Dwivedi, G., & Nath Verma, T. (2020). Optimization of low-temperature transesterification of low FFA blend of sunflower oil and algae oil. *Fuel*, *279*(April). https://doi.org/10.1016/j.fuel.2020.118459

Khojasteh, D., Khojasteh, D., Kamali, R., Beyene, A., & Iglesias, G. (2018). Assessment of renewable energy resources in Iran; with a focus on wave and tidal energy. *Renewable and Sustainable Energy Reviews*, *81*, 2992–3005. https://doi.org/10.1016/j.rser.2017.06.110

Khoo, H. H., Sharratt, P. N., Das, P., Balasubramanian, R. K., Naraharisetti, P. K., & Shaik, S. (2011). Life cycle energy and CO2 analysis of microalgae-to-biodiesel: Preliminary results and comparisons. *Bioresource Technology*, *102*(10), 5800–5807. https://doi.org/10.1016/j.biortech.2011.02.055

Kiefer, J., Stuckenholz, M., & Rathke, B. (2018). Influence of the alkyl chain on the vibrational structure and interionic interactions in 1-alkyl-3-methylimidazolium trifluoromethanesulfonate ionic liquids. *Journal of Molecular Liquids*, *255*(2017), 413–418. https://doi.org/10.1016/j.molliq.2018.01.180

Kim, J., Yoo, G., Lee, H., Lim, J., Kim, K., Kim, C. W., … Yang, J. W. (2013). Methods of downstream processing for the production of biodiesel from microalgae. *Biotechnology Advances*, *31*(6), 862–876. https://doi.org/10.1016/j.biotechadv.2013.04.006

Kim, Y., Choi, Y., Park, J., Lee, S., Yang, Y., Joo, H., … Hyun, S. (2012). Ionic liquid-

mediated extraction of lipids from algal biomass. *Bioresource Technology*, *109*, 312–315. https://doi.org/10.1016/j.biortech.2011.04.064

Knothe, G. (2005). Dependence of biodiesel fuel properties on the structure of fatty acid alkyl esters. *Fuel Processing Technology*, *86*(10), 1059–1070. https://doi.org/10.1016/j.fuproc.2004.11.002

Knothe, G., & Steidley, K. R. (2005). Kinematic viscosity of biodiesel fuel components and related compounds. Influence of compound structure and comparison to petrodiesel fuel components. *Fuel*, *84*, 1059–1065. https://doi.org/10.1016/j.fuel.2005.01.016

Ko1lle, P., & Dronskowski, R. (2004). Hydrogen Bonding in the Crystal Structures of the Ionic Liquid Compounds Butyldimethylimidazolium Hydrogen Sulfate , Chloride , and Chloroferrate ( II , III ). *Inorg. Chem*, *43*(9), 2803–2809.

Kore, R., & Srivastava, R. (2011). Synthesis and applications of highly efficient, reusable, sulfonic acid group functionalized Brönsted acidic ionic liquid catalysts. *Catalysis Communications*, *12*(15), 1420–1424. https://doi.org/10.1016/j.catcom.2011.05.030

Krasowska, A., Jabłoński, S., Biniarz, P., Płachetka, M., & Łukaszewicz, M. (2013). Microalgae – biodiesel potential producers : a review. *European Scientific Journal*, (3), 407–416. Retrieved from http://www.eujournal.net/index.php/esj/article/view/1476/1485

Kuan, D., Du, W., Dai, L., Ma, G., & Liu, D. (2016). Effect of solvent on the extraction of microalgae lipid for biodiesel production. *Chemical Research in Chinese Universities*, *32*(4), 625–629. https://doi.org/10.1007/s40242-016-5515-x

Kumar, R. R., Rao, P. H., & Arumugam, M. (2015). Lipid extraction methods from microalgae: A comprehensive review. *Frontiers in Energy Research*, *3*(JAN), 1–9. https://doi.org/10.3389/fenrg.2014.00061

Kumar, S. P. J., Prasad, S. R., Banerjee, R., Agarwal, D. K., Kulkarni, K. S., & Ramesh, K. V. (2017). Green solvents and technologies for oil extraction from oilseeds. *Chemistry Central Journal*, 1–7. https://doi.org/10.1186/s13065-017-0238-8

Lai, J. Q., Hu, Z. L., Wang, P. W., & Yang, Z. (2012). Enzymatic production of microalgal biodiesel in ionic liquid [BMIm][PF 6]. *Fuel*, *95*, 329–333. https://doi.org/10.1016/j.fuel.2011.11.001

Lam, M. K., & Lee, K. T. (2012). Microalgae biofuels: A critical review of issues, problems and the way forward. *Biotechnology Advances*, *30*(3), 673–690. https://doi.org/10.1016/j.biotechadv.2011.11.008

Lee, H., Shin, W. S., Jung, J. Y., Kim, C. W., Lee, J. W., Kwon, J. H., & Yang, J. W.

(2015). Optimization of variables affecting the direct transesterification of wet biomass from Nannochloropsis oceanica using ionic liquid as a co-solvent. *Bioprocess and Biosystems Engineering*, *38*(5), 981–987. https://doi.org/10.1007/s00449-014-1343-x

Lee, J. Y., Yoo, C., Jun, S. Y., Ahn, C. Y., & Oh, H. M. (2010). Comparison of several methods for effective lipid extraction from microalgae. *Bioresource Technology*, *101*(1 SUPPL.), S75–S77. https://doi.org/10.1016/j.biortech.2009.03.058

Leung, D. Y. C., Wu, X., & Leung, M. K. H. (2010). A review on biodiesel production using catalyzed transesterification. *Applied Energy*, *87*, 1083–1095. https://doi.org/10.1016/j.apenergy.2009.10.006

Lewis, N. S. (2007). Toward Cost-Effective Solar Energy Use. *Science*, *315*, 798–801. https://doi.org/10.1126/science.1137014

Li, M., Chen, J., Li, L., Ye, C., Lin, X., & Qiu, T. (2021). Novel multi–SO3H functionalized ionic liquids as highly efficient catalyst for synthesis of biodiesel. *Green Energy and Environment*, *6*(2), 271–282. https://doi.org/10.1016/j.gee.2020.05.004

Li, Y., Ghasemi Naghdi, F., Garg, S., Adarme-Vega, T. C., Thurecht, K. J., Ghafor, W. A., … Schenk, P. M. (2014). A comparative study: The impact of different lipid extraction methods on current microalgal lipid research. *Microbial Cell Factories*, *13*(1), 1–9. https://doi.org/10.1186/1475-2859-13-14

Liau, B. C., Shen, C. T., Liang, F. P., Hong, S. E., Hsu, S. L., Jong, T. T., & Chang, C. M. J. (2010). Supercritical fluids extraction and anti-solvent purification of carotenoids from microalgae and associated bioactivity. *Journal of Supercritical Fluids*, *55*(1), 169–175. https://doi.org/10.1016/j.supflu.2010.07.002

Liaw, H. J., & Chiu, Y. Y. (2003). The prediction of the flash point for binary aqueous-organic solutions. *Journal of Hazardous Materials*, *101*(2), 83–106. https://doi.org/10.1016/S0304-3894(03)00168-7

Lin, H. W., Yen, C. H., Hsu, H., & Tan, C. S. (2013). CO2 promoted hydrogenolysis of benzylic compounds in methanol and water. *RSC Advances*, *3*(38), 17222–17227. https://doi.org/10.1039/c3ra41717d

Lozano, P., Bernal, J. M., Gómez, C., Álvarez, E., Markiv, B., García-Verdugo, E., & Luis, S. V. (2020). Green biocatalytic synthesis of biodiesel from microalgae in one-pot systems based on sponge-like ionic liquids. *Catalysis Today*, *346*, 87–92. https://doi.org/10.1016/j.cattod.2019.01.073

Lu, W., Alam, M. A., Pan, Y., Wu, J., Wang, Z., & Yuan, Z. (2016). A new approach of microalgal biomass pretreatment using deep eutectic solvents for enhanced lipid

recovery for biodiesel production. *Bioresource Technology*, *218*, 123–128. https://doi.org/10.1016/j.biortech.2016.05.120

Luo, H., Fan, W., Li, Y., & Nan, G. (2013). Biodiesel production using alkaline ionic liquid and adopted as lubricity additive for low-sulfur diesel fuel. *Bioresource Technology*, *140*, 337–341. https://doi.org/10.1016/j.biortech.2012.11.112

Luo, H., Yin, H., Wang, R., Fan, W., & Nan, G. (2017). *Caprolactam-Based Brønsted Acidic Ionic Liquids for Biodiesel Production from Jatropha Oil*. *2*. https://doi.org/10.3390/catal7040102

Maaira, J., Santana, A., Recasens, F., & Angeles Larrayoz, M. (2011). Biodiesel production using supercritical methanol/carbon dioxide mixtures in a continuous reactor. *Fuel*, *90*(6), 2280–2288. https://doi.org/10.1016/j.fuel.2011.02.017

Majewski, A. W., & Jaaskelainen, H. (2004). Environmental Effects of Emissions. *Ecopoint*, Vol. 1, pp. 2–4.

Malekghasemi, S., Kariminia, H. R., Plechkova, N. K., & Ward, V. C. A. (2021). Direct transesterification of wet microalgae to biodiesel using phosphonium carboxylate ionic liquid catalysts. *Biomass and Bioenergy*, *150*(February), 106126. https://doi.org/10.1016/j.biombioe.2021.106126

Mandal, S., Patnaik, R., Singh, A. K., & Mallick, N. (2013). Comparative assessment of various lipid extraction protocols and optimization of transesterification process for microalgal biodiesel production. *Environmental Technology*, *34*(13–14), 2009–2018. https://doi.org/10.1080/09593330.2013.827730

Martínez, N., Callejas, N., Morais, E. G., Vieira Costa, J. A., Jachmanián, I., & Vieitez, I. (2017). Obtaining biodiesel from microalgae oil using ultrasound-assisted in-situ alkaline transesterification. *Fuel*, *202*, 512–519. https://doi.org/10.1016/j.fuel.2017.04.040

Mathimani, T., Beena Nair, B., & Ranjith kumar, R. (2016). Evaluation of microalga for biodiesel using lipid and fatty acid as a marker – A central composite design approach. *Journal of the Energy Institute*, *89*(3), 436–446. https://doi.org/10.1016/j.joei.2015.02.010

Mayers, J. J., Flynn, K. J., & Shields, R. J. (2013). Rapid determination of bulk microalgal biochemical composition by Fourier- Transform Infrared spectroscopy. *Bioresource Technology*, *148*, 215–220.

McCormick, R. L., Graboski, M. S., Alleman, T. L., Herring, A. M., & Tyson, K. S. (2001). Impact of biodiesel source material and chemical structure on emissions of criteria pollutants from a heavy-duty engine. *Environmental Science and Technology*, *35*(9), 1742–1747. https://doi.org/10.1021/es001636t

McKennedy, J., Önenç, S., Pala, M., & Maguire, J. (2016). Supercritical carbon dioxide treatment of the microalgae Nannochloropsis oculata for the production of fatty acid methyl esters. *Journal of Supercritical Fluids*, *116*, 264–270. https://doi.org/10.1016/j.supflu.2016.06.003

Mendes, R. L., Nobre, B. P., Cardoso, M. T., Pereira, A. P., & Palavra, A. F. (2003). Supercritical carbon dioxide extraction of compounds with pharmaceutical importance from microalgae. *Inorganica Chimica Acta*, *356*, 328–334. https://doi.org/10.1016/S0020-1693(03)00363-3

Molino, A., Larocca, V., Chianese, S., & Musmarra, D. (2018). Biofuels production by biomass gasification: A review. *Energies*, *11*(811), 1–31. https://doi.org/10.3390/en11040811

Moniruzzaman, M., Kamiya, N., & Goto, M. (2010). Activation and stabilization of enzymes in ionic liquids. *Organic and Biomolecular Chemistry*, *8*(13), 2887–2899. https://doi.org/10.1039/b926130c

Mostafa, S. S. M., & El-gendy, N. S. (2013). Evaluation of Fuel Properties for Microalgae Spirulina Platensis Bio-diesel and. *ARABIAN JOURNAL OF CHEMISTRY*. https://doi.org/10.1016/j.arabjc.2013.07.034

Mostafa, S. S. M., & El-Gendy, N. S. (2013). Evaluation of fuel properties for microalgae Spirulina platensis bio-diesel and its blends with Egyptian petro-diesel. *Arabian Journal of Chemistry*, S2040–S2050. https://doi.org/10.1016/j.arabjc.2013.07.034

Muhammad, N., Elsheikh, Y. A., Mutalib, M. I. A., Bazmi, A. A., Khan, R. A., Khan, H., … Khan, I. (2015). An overview of the role of ionic liquids in biodiesel reactions. *Journal of Industrial and Engineering Chemistry*, *21*, 1–10. https://doi.org/10.1016/j.jiec.2014.01.046

Murad, M. E., & Al-dawody, M. F. (2020). Biodiesel production from spirulina microalgae oil. *IOP Conference Series: Materials Science and Engineering PAPER*. https://doi.org/10.1088/1757-899X/928/2/022127

Nautiyal, P., Subramanian, K. A., & Dastidar, M. G. (2014). Production and characterization of biodiesel from algae. *Fuel Processing Technology*, *120*, 79–88. https://doi.org/10.1016/j.fuproc.2013.12.003

Ojha, N., & Das, N. (2017). A Statistical approach to optimize the production of Polyhydroxyalkanoates. *International Journal of Biological Macromolecules*. https://doi.org/10.1016/j.ijbiomac.2017.10.089

Olivier-Bourbigou, H., Magna, L., & Morvan, D. (2010). Ionic liquids and catalysis: Recent progress from knowledge to applications. *Applied Catalysis A: General*,

*373*(1–2), 1–56. https://doi.org/10.1016/j.apcata.2009.10.008

Olkiewicz, M. A. (2015). *Production Of Biodiesel From Sludge Generated In Municipal Sludge Generated In Municipal*.

Olkiewicz, M., Caporgno, M. P., Fortuny, A., Stüber, F., Fabregat, A., Font, J., & Bengoa, C. (2014). Direct liquid-liquid extraction of lipid from municipal sewage sludge for biodiesel production. *Fuel Processing Technology*, *128*, 331–338. https://doi.org/10.1016/j.fuproc.2014.07.041

Ong, H. C., Tiong, Y. W., Goh, B. H. H., Gan, Y. Y., Mofijur, M., Fattah, I. M. R., … Mahlia, T. M. I. (2021). Recent advances in biodiesel production from agricultural products and microalgae using ionic liquids: Opportunities and challenges. *Energy Conversion and Management*, *228*(November), 113647. https://doi.org/10.1016/j.enconman.2020.113647

Orr, V. (2016). *Direct Conversion of Wet Microalgae and Oleaginous Yeast to Biodiesel Using Ionic Liquids*. (August).

Pan, J., Muppaneni, T., Sun, Y., Reddy, H. K., Fu, J., Lu, X., & Deng, S. (2016). Microwave-assisted extraction of lipids from microalgae using an ionic liquid solvent [BMIM][HSO4]. *Fuel*, *178*, 49–55. https://doi.org/10.1016/j.fuel.2016.03.037

Park, J., Kim, B., Chang, Y. K., & Lee, J. W. (2017). Wet in situ transesterification of microalgae using ethyl acetate as a co-solvent and reactant. *Bioresource Technology*, *230*, 8–14. https://doi.org/10.1016/j.biortech.2017.01.027

Paudel, A., Jessop, M. J., Stubbins, S. H., Champagne, P., & Jessop, P. G. (2015). Extraction of lipids from microalgae using CO2-expanded methanol and liquid CO2. *Bioresource Technology*, *184*, 286–290. https://doi.org/10.1016/j.biortech.2014.11.111

Piemonte, V., Di, L., Iaquaniello, G., & Prisciandaro, M. (2015). Biodiesel production from microalgae : ionic liquid process simulation. *Journal of Cleaner Production*, 1–7. https://doi.org/10.1016/j.jclepro.2015.07.089

Plechkova, N. V., & Seddon, K. R. (2008). Applications of ionic liquids in the chemical industry. *Chemical Society Reviews*, *37*(1), 123–150. https://doi.org/10.1039/b006677j

Pohndorf, R. S., Camara, A. S., Larrosa, A. P. Q., Pinheiro, C. P., Strieder, M. M., & Pinto, L. A. A. (2016). Biomass and Bioenergy Production of lipids from microalgae Spirulina sp.: Influence of drying , cell disruption and extraction methods. *Biomass and Bioenergy*, *93*, 25–32. https://doi.org/10.1016/j.biombioe.2016.06.020

Popp, J., Lakner, Z., Harangi-Rákos, M., & Fári, M. (2014). The effect of bioenergy expansion: Food, energy, and environment. *Renewable and Sustainable Energy*

*Reviews*, *32*, 559–578. https://doi.org/10.1016/j.rser.2014.01.056

Poppe, J. K., Fernandez-Lafuente, R., Rodrigues, R. C., & Ayub, M. A. Z. (2015). Enzymatic reactors for biodiesel synthesis: Present status and future prospects. *Biotechnology Advances*, *33*(5), 511–525. https://doi.org/10.1016/j.biotechadv.2015.01.011

Pradana, Y. S., Azmi, F. A., Masruri, W., & Hartono, M. (2018). Biodiesel Production from Wet Spirulina sp . by One-Step. *MATEC Web of Conferences*, *156*, 1–4.

Pratas, M. J., Freitas, S., Oliveira, M. B., Monteiro, S. C., Lima, A. S., & Coutinho, J. A. P. (2010). Densities and viscosities of fatty acid methyl and ethyl esters. *Journal of Chemical and Engineering Data*, *55*(9), 3983–3990. https://doi.org/10.1021/je100042c

Qasim, M. K. (2019). Modified nanostructure MgO superbasicity with CaO in heterogeneous transesterification of sunflower oil. *Egyptian Journal of Chemistry*, *62*(3), 475–485. https://doi.org/10.21608/EJCHEM.2018.4321.1386

Qureshi, Z. S., Deshmukh, K. M., & Bhanage, B. M. (2014). Applications of ionic liquids in organic synthesis and catalysis. *Clean Technologies and Environmental Policy*, *16*(8), 1487–1513. https://doi.org/10.1007/s10098-013-0660-0

Rahman, A., & Nahar, K. (2016). Production and Characterization of Algal Biodiesel from Spirulina Maxima. *Global Journal of Researches in Engineering*, *16*(1), 35–39.

Rahman, M. A., Aziz, M. A., Al-khulaidi, R. A., Sakib, N., & Islam, M. (2017). Biodiesel production from microalgae S pirulina maxima by two step process : Optimization of process variable. *Journal of Radiation Research and Applied Sciences*, 1–8. https://doi.org/10.1016/j.jrras.2017.02.004

Ramírez-verduzco, L. F., Rodríguez-rodríguez, J. E., & Jaramillo-jacob, A. R. (2012). Predicting cetane number , kinematic viscosity , density and higher heating value of biodiesel from its fatty acid methyl ester composition. *Fuel*, *91*, 102–111. https://doi.org/10.1016/j.fuel.2011.06.070

Rangel-Basto, Y. A., García-Ochoa, I. E., Suarez-Gelvez, J. H., Zuorro, A., Barajas-Solano, A. F., & Urbina-Suarez, N. A. (2018). The effect of temperature and enzyme concentration in the transesterification process of synthetic microalgae oil. *Chemical Engineering Transactions*, *64*(May), 331–336. https://doi.org/10.3303/CET1864056

Rathnam, V. M., Modak, J. M., & Madras, G. (2020). Non-catalytic transesterification of dry microalgae to fatty acid ethyl esters using supercritical ethanol and ethyl acetate. *Fuel*, *275*(October 2019), 117998. https://doi.org/10.1016/j.fuel.2020.117998

Ratti, R. (2014). Ionic Liquids : Synthesis and Applications in Catalysis. *Advances in*

*Chemistry*, *2014*(3). https://doi.org/http://dx.doi.org/10.1155/2014/729842

Ren, Q., Zuo, T., Pan, J., Chen, C., & Li, W. (2014). *Preparation of Biodiesel from Soybean Catalyzed by Basic Ionic Liquids [Hnmm]OH*. 8012–8023. https://doi.org/10.3390/ma7128012

Rodriguez, M. del P., Brzezinski, R., Faucheux, N., & Heitz, M. (2016). Enzymatic transesterification of lipids from microalgae into biodiesel: a review. *AIMS Energy*, *4*(6), 817–855. https://doi.org/10.3934/energy.2016.6.817

Rogers, R. D., & Seddon, K. R. (2003). Ionic Liquids - Solvents of the Future? *Science*, *302*(5646), 792–793. https://doi.org/10.1126/science.1090313

Rull, F., & Sobron, F. (1994). Band Profile Analysis of the Raman Spectra of Sulphate Ions in Aqueous Solutions. *Journal of Raman Spectroscopy*, *25*(April), 693–698.

Saeedi Dehaghani, A. H., & Pirouzfar, V. (2018). Investigation on the Effect of Microalgae Chlorella sp. and Spirulina on Biodiesel Production. *Petroleum Chemistry*, *58*(8), 702–708. https://doi.org/10.1134/S0965544118080042

Sakthivel, R., Ramesh, K., Purnachandran, R., & Shameer, P. M. (2018). A review on the properties , performance and emission aspects of the third generation biodiesels A review on the properties , performance and emission aspects of the third generation biodiesels. *Renewable and Sustainable Energy Reviews*, *82*, 2970–2992. https://doi.org/10.1016/j.rser.2017.10.037

Salvo, R. D., Reich, A., Waite, H. Dykes, H., Teixeira, R. (2011). Lipid Extraction From Microalgae Using Asingle Ionic Liquid. *Patent Application Publication.US 2011/0130551A1*.

Salvo, R. D., Reich, A., Waite, H. Dykes, H., Teixeira, R. (2013). LIPID EXTRACTION FROM MICROALGAE USING ASINGLE IONIC LIQUID. *U.S. Patent .US 2011/0130551A1*.

Samorì, C., Pezzolesi, L., Barreiro, D. L., Galletti, P., Pasteris, A., & Tagliavini, E. (2013). Synthesis of new polyethoxylated tertiary amines and their use as Switchable Hydrophilicity Solvents. *RSC Advances*, *4*(12), 5999–6008. https://doi.org/10.1039/c3ra47144f

Samorì, C., Torri, C., Samorì, G., Fabbri, D., Galletti, P., Guerrini, F., … Tagliavini, E. (2010). Extraction of hydrocarbons from microalga Botryococcus braunii with switchable solvents. *Bioresource Technology*, *101*(9), 3274–3279. https://doi.org/10.1016/j.biortech.2009.12.068

Sánchez-Bayo, A., Morales, V., Rodríguez, R., Vicente, G., & Bautista, L. F. (2019). Biodiesel production (FAEEs) by heterogeneous combi-lipase biocatalysts using wet

extracted lipids from microalgae. *Catalysts*, *9*(3), 1–15. https://doi.org/10.3390/catal9030296

Santana, A., Jesus, S., Larrayoz, M. A., & Filho, R. M. (2012). Supercritical carbon dioxide extraction of algal lipids for the biodiesel production. *Procedia Engineering*, *42*(December), 1755–1761. https://doi.org/10.1016/j.proeng.2012.07.569

Sarf, F. (2019). Synthesis , Analysis and Thermoelectrochemical Applications of Ionic Liquids Nanomedicine & Nanotechnology Open Access. *Nanomed Nanotechnol*, *4*(2), 000159. https://doi.org/10.23880/nnoa-16000159

Sarin, A., Arora, R., Singh, N. P., Sarin, R., Malhotra, R. K., & Kundu, K. (2009). Effect of blends of Palm-Jatropha-Pongamia biodiesels on cloud point and pour point. *Energy*, *34*, 2016–2021. https://doi.org/10.1016/j.energy.2009.08.017

Sarin, A., Arora, R., Singh, N. P., Sarin, R., Malhotra, R. K., & Sarin, S. (2010). Blends of biodiesels synthesized from non-edible and edible oils: Effects on the cold filter plugging point. *Energy and Fuels*, *24*, 1996–2001. https://doi.org/10.1021/ef901131m

Sati, H., Mitra, M., Mishra, S., & Baredar, P. (2019). Microalgal lipid extraction strategies for biodiesel production: A review. *Algal Research*, *38*, 101413. https://doi.org/10.1016/j.algal.2019.101413

Schmidt, P., & Hendra, P. J. (1994). The application of Fourier-transform Raman spectroscopy to the determination of conformation in poly ( e-caprolactam ) chains. *Spectrochimica Acta, 50A*(11), 1999–2004.

Scurto, A. M., Hutchenson, K., & Subramaniam, B. (2009). *Gas-Expanded Liquids : Fundamentals and Applications*. 3–37.

Seki, S., Kobayashi, T., Kobayashi, Y., Takei, K., Miyashiro, H., & Hayamizu, K. (2010). Effects of cation and anion on physical properties of room-temperature ionic liquids. *Journal of Molecular Liquids*, *152*(1–3), 9–13. https://doi.org/10.1016/j.molliq.2009.10.008

Selaimia, R., Beghiel, A., & Oumeddour, R. (2015). The Synthesis of Biodiesel from Vegetable Oil. *Procedia - Social and Behavioral Sciences*, *195*, 1633–1638. https://doi.org/10.1016/j.sbspro.2015.06.221

Shakeela, K., Sinduri, V. L., & Rao, G. R. (2017). Hydrophobic supramolecular assemblies of Keggin anions with lactam-lactim cationic tautomers. *Polyhedron*, *137*(December), 43–51. https://doi.org/10.1016/j.poly.2017.07.023

Shankar, M., Chhotaray, P. K., Agrawal, A., Gardas, R. L., Tamilarasan, K., & Rajesh, M. (2017). Protic ionic liquid-assisted cell disruption and lipid extraction from fresh

water Chlorella and Chlorococcum microalgae. *Algal Research*, *25*(April), 228–236. https://doi.org/10.1016/j.algal.2017.05.009

Shankar, M., Chhotarayb, Pratap K. Gardasc, R. L., Tamilarasand, K., & Rajeshd, M. (2019). Application of carboxylate protic ionic liquids in simultaneous microalgal pretreatment and lipid recovery from marine Nannochloropsis sp . and. *Biomass and Bioenergy*, *123*(February), 14–24. https://doi.org/10.1016/j.biombioe.2019.02.005

Shartsaa, C. M., Gorelikb, V. S., Agoltsovb, A. M., Ziobinab, L. I., Sharts, O. N., & Diego, S. (1998). *Detection of carbon-fluorine bonds in organofinorine compounds by Raman spectroscopy using a coppervapor laser Auasthejç.* *3537*(November), 317–326.

Singh, A., Nigam, P. S., & Murphy, J. D. (2011a). Mechanism and challenges in commercialisation of algal biofuels. *Bioresource Technology*, *102*(1), 26–34. https://doi.org/10.1016/j.biortech.2010.06.057

Singh, A., Nigam, P. S., & Murphy, J. D. (2011b). Renewable fuels from algae: An answer to debatable land based fuels. *Bioresource Technology*, *102*(1), 10–16. https://doi.org/10.1016/j.biortech.2010.06.032

Singh, D. K., Rathke, B., Kiefer, J., & Materny, A. (2016). *Molecular Structure and Interactions in the Ionic Liquid 1 - Ethyl-3- methylimidazolium Tri fl uoromethanesulfonate.* https://doi.org/10.1021/acs.jpca.6b03849

Singh, H., Singh, S., Srivastava, A., Tandon, P., Bharti, P., Kumar, S., & Maurya, R. (2014). Conformational analysis and vibrational study of daidzein by using FT-IR and FT-Raman spectroscopies and DFT calculations. *Spectrochimica Acta - Part A: Molecular and Biomolecular Spectroscopy*, *120*, 405–415. https://doi.org/10.1016/j.saa.2013.10.045

Soh, L., & Zimmerman, J. (2011). Biodiesel production: The potential of algal lipids extracted with supercritical carbon dioxide. *Green Chemistry*, *13*(6), 1422–1429. https://doi.org/10.1039/c1gc15068e

Srivastava, G., Paul, A. K., & Goud, V. V. (2018). Optimization of non-catalytic transesterification of microalgae oil to biodiesel under supercritical methanol condition. *Energy Conversion and Management*, *156*(August 2017), 269–278. https://doi.org/10.1016/j.enconman.2017.10.093

Su, Y. C., Liu, Y. A., Diaz Tovar, C. A., & Gani, R. (2011). Selection of prediction methods for thermophysical properties for process modeling and product design of biodiesel manufacturing. *Industrial and Engineering Chemistry Research*, *50*, 6809–6836. https://doi.org/10.1021/ie102441u

Subramaniam, B. (2010). Gas-expanded liquids for sustainable catalysis and novel

materials: Recent advances. *Coordination Chemistry Reviews*, *254*(15–16), 1843–1853. https://doi.org/10.1016/j.ccr.2009.12.009

Sun, Y., Cooke, P., Reddy, H. K., Muppaneni, T., Wang, J., Zeng, Z., & Deng, S. (2017). 1-Butyl-3-methylimidazolium hydrogen sulfate catalyzed in-situ transesterification of Nannochloropsis to fatty acid methyl esters. *Energy Conversion and Management*, *132*, 213–220. https://doi.org/10.1016/j.enconman.2016.10.071

Taher, H., Al-Zuhair, S., Al-Marzouqi, A. H., Haik, Y., Farid, M., & Tariq, S. (2014). Supercritical carbon dioxide extraction of microalgae lipid: Process optimization and laboratory scale-up. *Journal of Supercritical Fluids*, *86*, 57–66. https://doi.org/10.1016/j.supflu.2013.11.020

Tan, Y. H., Abdullah, M. O., Kansedo, J., Mubarak, N. M., Chan, Y. S., & Nolasco-Hipolito, C. (2019). Biodiesel production from used cooking oil using green solid catalyst derived from calcined fusion waste chicken and fish bones. *Renewable Energy*, *139*(November 2014), 696–706. https://doi.org/10.1016/j.renene.2019.02.110

Tang, Y., Zhang, Y., Rosenberg, J. N., Sharif, N., Betenbaugh, M. J., & Wang, F. (2016). Efficient lipid extraction and quantification of fatty acids from algal biomass using accelerated solvent extraction (ASE). *RSC Advances*, *6*(35), 29127–29134. https://doi.org/10.1039/C5RA23519G

Teixeira, R. E. (2012). Energy-efficient extraction of fuel and chemical feedstocks from algae. *Green Chemistry*, *14*(2), 419–427. https://doi.org/10.1039/c2gc16225c

Teo, C. L., Jamaluddin, H., Zain, N. A. M., & Idris, A. (2014). Biodiesel production via lipase catalysed transesterification of microalgae lipids from Tetraselmis sp. *Renewable Energy*, *68*, 1–5. https://doi.org/10.1016/j.renene.2014.01.027

Tiong, Y. W., Yap, C. L., Gan, S., & Yap, W. S. P. (2018). Conversion of Biomass and Its Derivatives to Levulinic Acid and Levulinate Esters via Ionic Liquids. *Industrial and Engineering Chemistry Research*, *57*(14), 4749–4766. https://doi.org/10.1021/acs.iecr.8b00273

To, T. Q., Procter, K., Simmons, B. A., Subashchandrabose, S., & Atkin, R. (2018). Low cost ionic liquid-water mixtures for effective extraction of carbohydrate and lipid from algae. *Faraday Discussions*, *206*, 93–112. https://doi.org/10.1039/c7fd00158d

Torimoto, T., Tsuda, T., Okazaki, K. I., & Kuwabata, S. (2010). New frontiers in materials science opened by ionic liquids. *Advanced Materials*, *22*(11), 1196–1221. https://doi.org/10.1002/adma.200902184

Tran, D. T., Yeh, K. L., Chen, C. L., & Chang, J. S. (2012). Enzymatic transesterification of microalgal oil from Chlorella vulgaris ESP-31 for biodiesel synthesis using

immobilized Burkholderia lipase. *Bioresource Technology*, *108*, 119–127. https://doi.org/10.1016/j.biortech.2011.12.145

Triggs, N. E., Bonn, R. T., & Valentini, J. J. (1993). *Do All Solid Amides Hydrogen Bond ? Raman Evidence to the Contrary*. 5535–5540.

Tripathi, B. N., & Kumar, D. (2017). Prospects and challenges in algal biotechnology. In *Prospects and Challenges in Algal Biotechnology*. https://doi.org/10.1007/978-981-10-1950-0

Ullah, Z., Bustam, M. A., Man, Z., Muhammad, N., & Khan, A. S. (2015). Synthesis, characterization and the effect of temperature on different physicochemical properties of protic ionic liquids. *RSC Advances*, *5*(87), 71449–71461. https://doi.org/10.1039/c5ra07656k

Velasquez, S. F., Chan, M. A., Abisado, R. G., Traifalgar, R. F. M., Tayamen, M. M., Maliwat, G. C. F., & Ragaza, J. A. (2016). Dietary Spirulina (Arthrospira platensis) replacement enhances performance of juvenile Nile tilapia (Oreochromis niloticus). *Journal of Applied Phycology*, *28*(2), 1023–1030. https://doi.org/10.1007/s10811-015-0661-y

Ventura, S. P. M., E Silva, F. A., Quental, M. V., Mondal, D., Freire, M. G., & Coutinho, J. A. P. (2017). Ionic-Liquid-Mediated Extraction and Separation Processes for Bioactive Compounds: Past, Present, and Future Trends. *Chemical Reviews*, *117*(10), 6984–7052. https://doi.org/10.1021/acs.chemrev.6b00550

Viguera, M., Marti, A., Masca, F., Prieto, C., & Calvo, L. (2016). The process parameters and solid conditions that affect the supercritical CO2 extraction of the lipids produced by microalgae. *Journal of Supercritical Fluids*, *113*, 16–22. https://doi.org/10.1016/j.supflu.2016.03.001

Viner, K. J. (2017). Enhancing Triglyceride Production Using Carbon Dioxide. *Published MSc. Thesis.*, *Kingston,*(Queen's University).

Vyas, A. P., Verma, J. L., & Subrahmanyam, N. (2010). A review on FAME production processes. *Fuel*, *89*(1), 1–9. https://doi.org/10.1016/j.fuel.2009.08.014

Wahidin, S., Idris, A., Raehanah, S., & Shaleh, M. (2016). Ionic liquid as a promising biobased green solvent in combination with microwave irradiation for direct biodiesel production. *BIORESOURCE TECHNOLOGY*. https://doi.org/10.1016/j.biortech.2016.01.084

Wang, T. H., Hsu, C. L., Huang, C. H., Hsieh, Y. K., Tan, C. S., & Wang, C. F. (2016). Environmental impact of CO2-expanded fluid extraction technique in microalgae oil acquisition. *Journal of Cleaner Production*, *137*, 813–820. https://doi.org/10.1016/j.jclepro.2016.07.179

Ward, V. C. A., Munch, G., Cicek, N., & Rehmann, L. (2017). Direct Conversion of the Oleaginous Yeast Rhodosporidium diobovatum to Biodiesel Using the Ionic Liquid [C2mim][EtSO4]. *ACS Sustainable Chemistry and Engineering*, *5*(6), 5562–5570. https://doi.org/10.1021/acssuschemeng.7b00976

Wasserscheid, P., & Welton, T. (2003). Ionic Liquids in Synthesis. In *Synthesis* (Vol. 2003). https://doi.org/10.1055/s-2003-40869

Wilkes, J. S. (2002). A short history of ionic liquids - From molten salts to neoteric solvents. *Green Chemistry*, *4*(2), 73–80. https://doi.org/10.1039/b110838g

Winston, A., & Kemper, N. (1971). The split carbonyl band in the infrared spectra of halogen derivatives of 4-hydroxy-2,4-pentadienoic acid lactone. *Tetrahedron*, *27*(3), 543–548. https://doi.org/10.1016/s0040-4020(01)90723-9

Wu, X., Ruan, R., Du, Z., & Liu, Y. (2012). Current status and prospects of biodiesel production from microalgae. *Energies*, *5*(8), 2667–2682. https://doi.org/10.3390/en5082667

Xiao, J., Chen, G., & Li, N. (2018). Ionic liquid solutions as a green tool for the extraction and isolation of natural products. *Molecules*, *23*(7). https://doi.org/10.3390/molecules23071765

Xiaoli, L., Ruiqing, Z., Kaiwen, X., Xu, J., Juanjuan, J., Fang, H., & Yong, H. (2018). Rapid Determination of Chlorophyll and Pheophytin in Green Tea Using Fourier Transform. *Molecules Article*, *23*(1010). https://doi.org/10.3390/molecules23051010

Xing, H., Wang, T., Zhou, Z., & Dai, Y. (2005). Novel Brønsted-acidic ionic liquids for esterifications. *Industrial and Engineering Chemistry Research*, *44*(11), 4147–4150. https://doi.org/10.1021/ie0488703

Yang, H. Y., Lu, W. J., Chen, Y. C., Chen, K. T., Teng, J. C., & Wan, H. P. (2017). New algal lipid extraction procedure using an amphiphilic amine solvent and ionic liquid. *Biomass and Bioenergy*, *100*, 108–115. https://doi.org/10.1016/j.biombioe.2017.03.018

Young, G., Nippen, F., Titterbrandt, S., & Cooney, M. J. (2011). Direct transesterification of biomass using an ionic liquid co-solvent system. *Biofuels*, *2*(3), 261–266. https://doi.org/10.4155/bfs.11.18

Young, G., Nippgen, F., Titterbrandt, S., & Cooney, M. J. (2010). Lipid extraction from biomass using co-solvent mixtures of ionic liquids and polar covalent molecules. *Separation and Purification Technology*, *72*(1), 118–121. https://doi.org/10.1016/j.seppur.2010.01.009

Yuan, H., Yang, B., & Yang, J. (2009). Predicting properties of biodiesel fuels using mixture topological index. *JAOCS, Journal of the American Oil Chemists' Society*, *86*, 375–382. https://doi.org/10.1007/s11746-009-1354-y

Zabeti, M., Wan Daud, W. M. A., & Aroua, M. K. (2009). Activity of solid catalysts for biodiesel production: A review. *Fuel Processing Technology*, *90*(6), 770–777. https://doi.org/10.1016/j.fuproc.2009.03.010

Zaramello, L., Kuhnen, C. A., Dall'Oglio, E. L., & De Sousa, P. T. (2012). DFT study of gas phase acid-catalyzed ethanolysis of butyric acid triglyceride. *Fuel*, *94*, 473–479. https://doi.org/10.1016/j.fuel.2011.11.063

Zhang, B., Feng, H., He, Z., Wang, S., & Chen, H. (2018). Bio-oil production from hydrothermal liquefaction of ultrasonic pre-treated Spirulina platensis. *Energy Conversion and Management*, *159*(December 2017), 204–212. https://doi.org/10.1016/j.enconman.2017.12.100

Zhao, H., & Baker, G. A. (2013). Ionic liquids and deep eutectic solvents for biodiesel synthesis: A review. *Journal of Chemical Technology and Biotechnology*, *88*(1), 3–12. https://doi.org/10.1002/jctb.3935

Zheng, H., Yin, J., Gao, Z., Huang, H., Ji, X., & Dou, C. (2011). Disruption of chlorella vulgaris cells for the release of biodiesel-producing lipids: A comparison of grinding, ultrasonication, bead milling, enzymatic lysis, and microwaves. *Applied Biochemistry and Biotechnology*, *164*(7), 1215–1224. https://doi.org/10.1007/s12010-011-9207-1.

Zhong, L., Parker, S. F., & Parker, S. F. (2018). Structure and vibrational spectroscopy of methanesulfonic acid. *Royal Society Open Science*, *5*(12), 181363. https://doi.org/10.1098/rsos.181363.

Zhuanni, Y., Xiaolin, C., & Shuwei, X. I. A. (2016). The Mechanism of Lipids Extraction from Wet Microalgae Scenedesmus sp . by Ionic Liquid Assisted Subcritical Water. *J. Ocean Univ. China*, *15*(3), 549–552. https://doi.org/10.1007/s11802-016-2831-1

# APPENDICES

**Appendix A.** TGA curves of SO$_3$-CP/CPILs
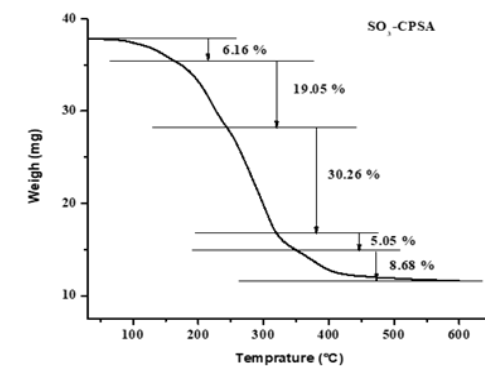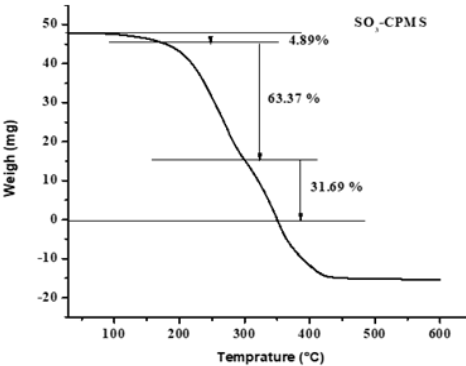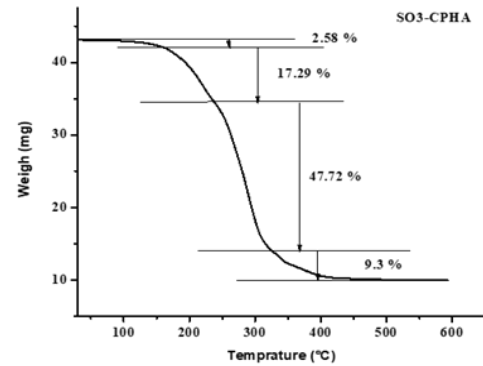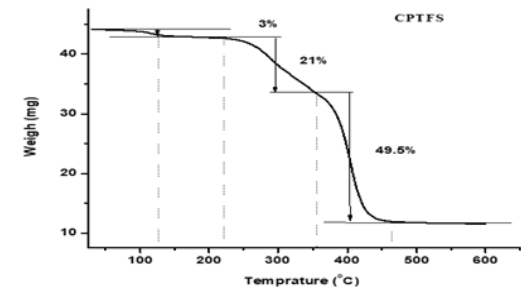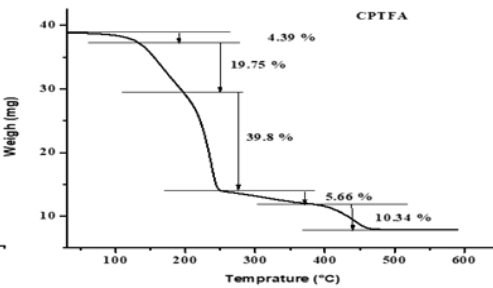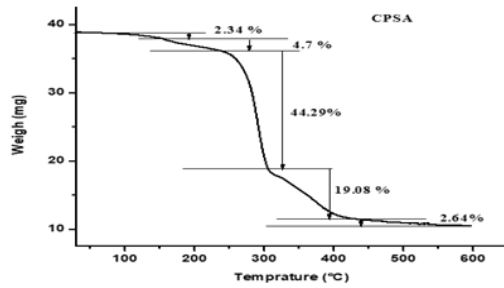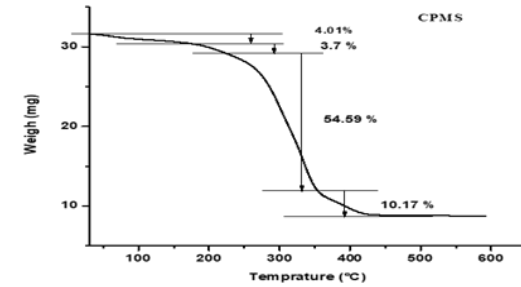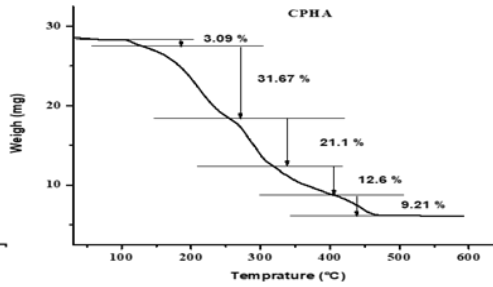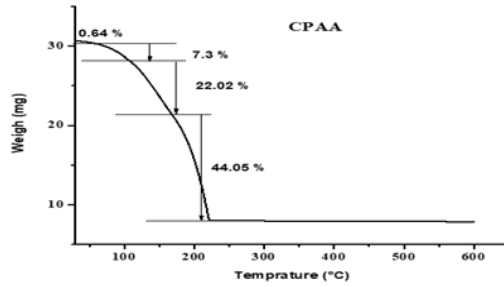
**Appendix B.** GC chromatogram of the FAMEs standard mixture
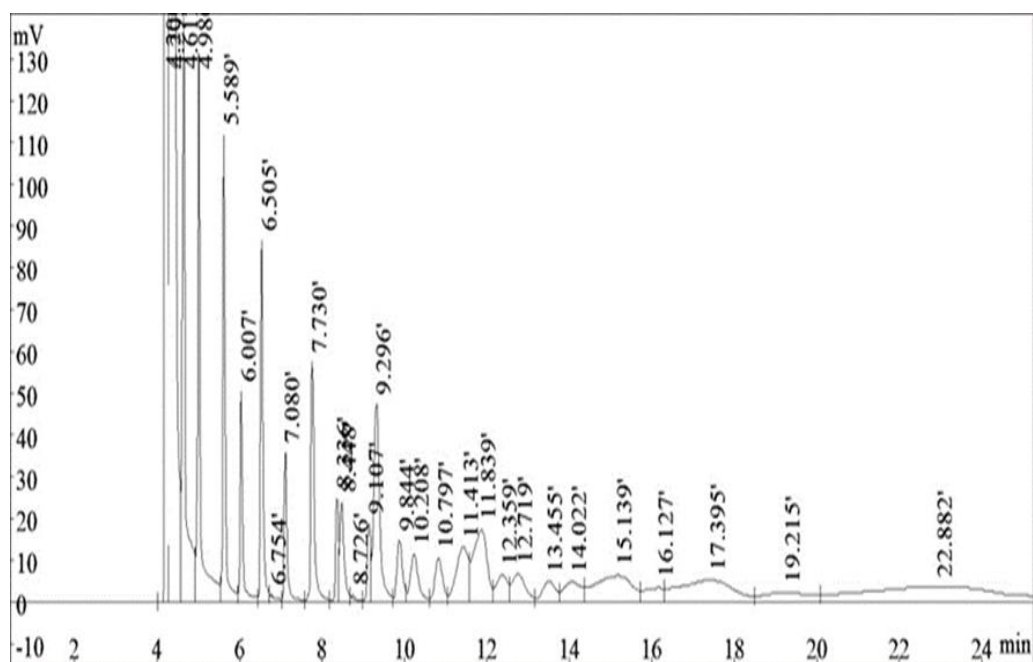


**Appendix C.** GC chromatogram of the FAMEs produced by conventional method

(indirect transesterification)
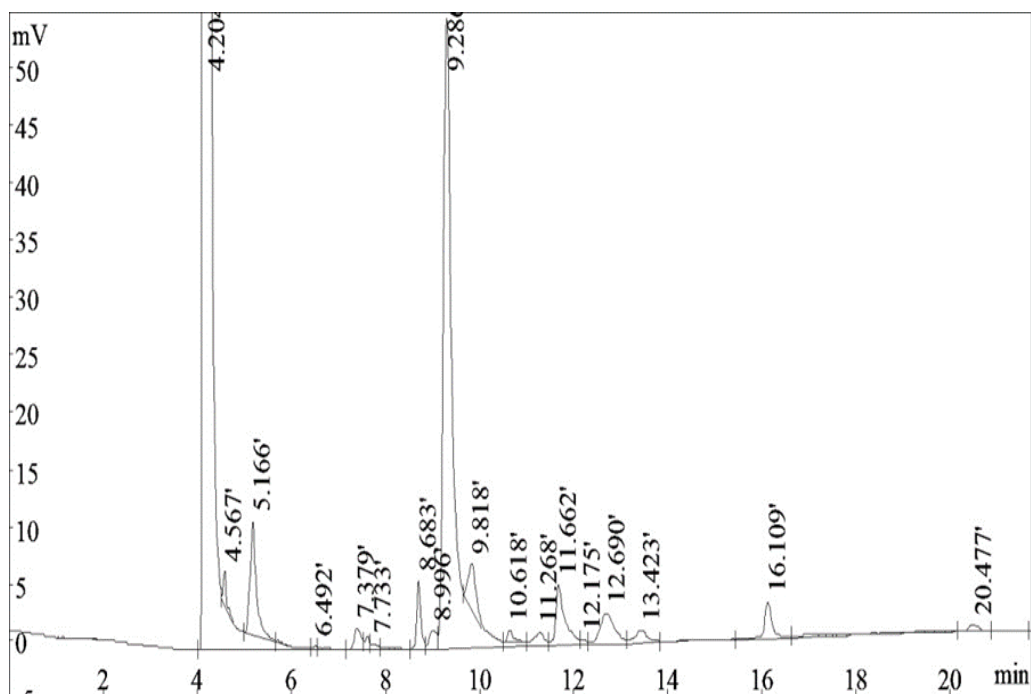
**Appendix D.** GC chromatogram of the FAMEs produced by CPAA (direct transformation)
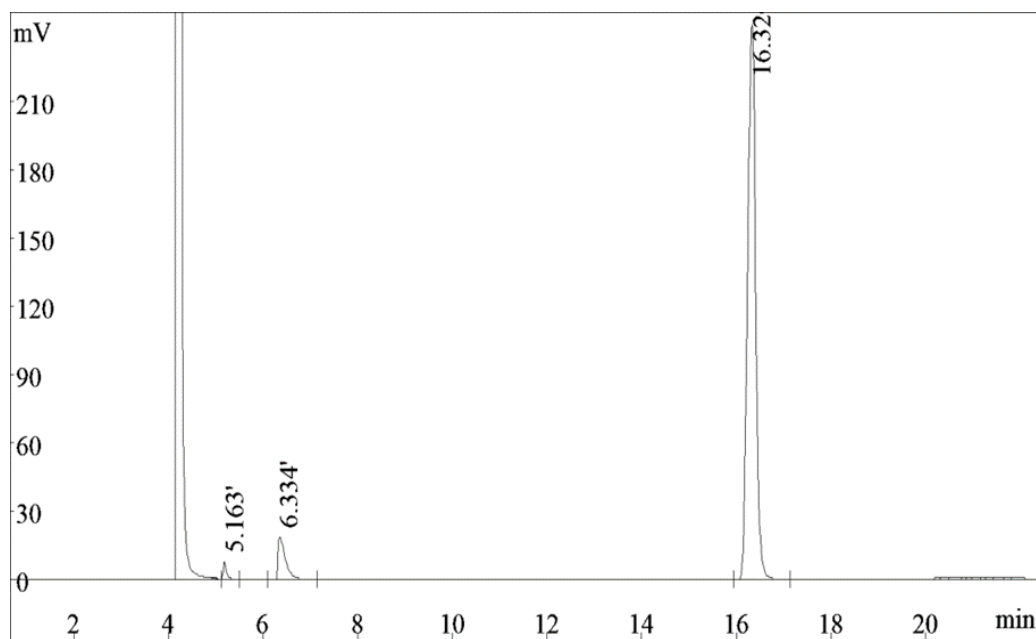


**Appendix E.** GC chromatogram of the FAMEs produced by CPHA (direct transformation)
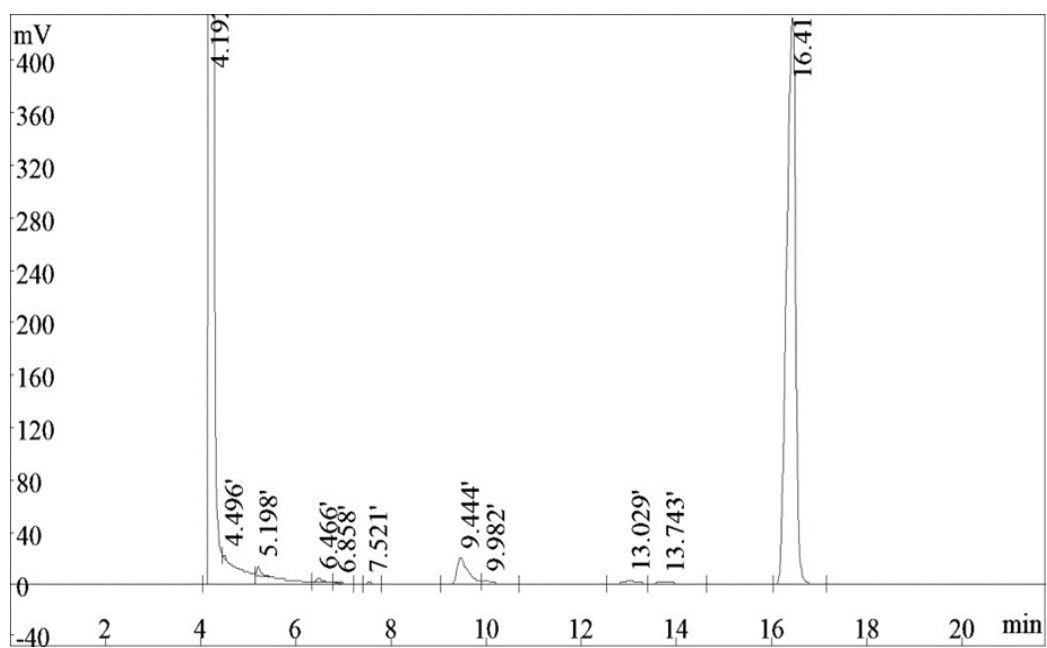
**Appendix F.** GC chromatogram of the FAMEs produced by CPTFA (direct transformation)
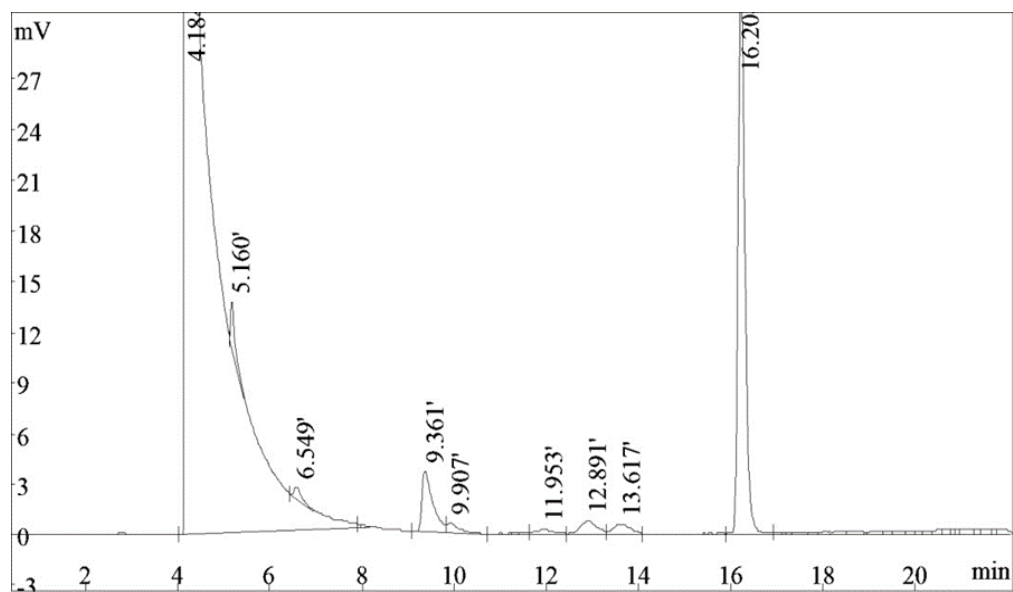


**Appendix G.** GC chromatogram of the FAMEs produced by CPSA (direct transformation)
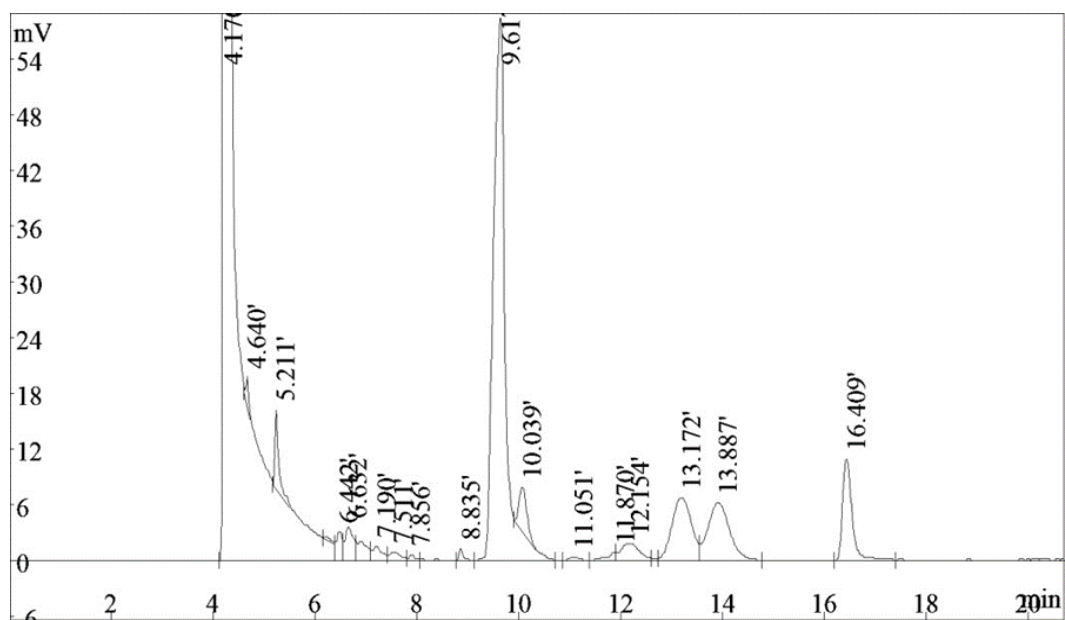
**Appendix H.** GC chromatogram of the FAMEs produced by CPMS (direct

transformation)
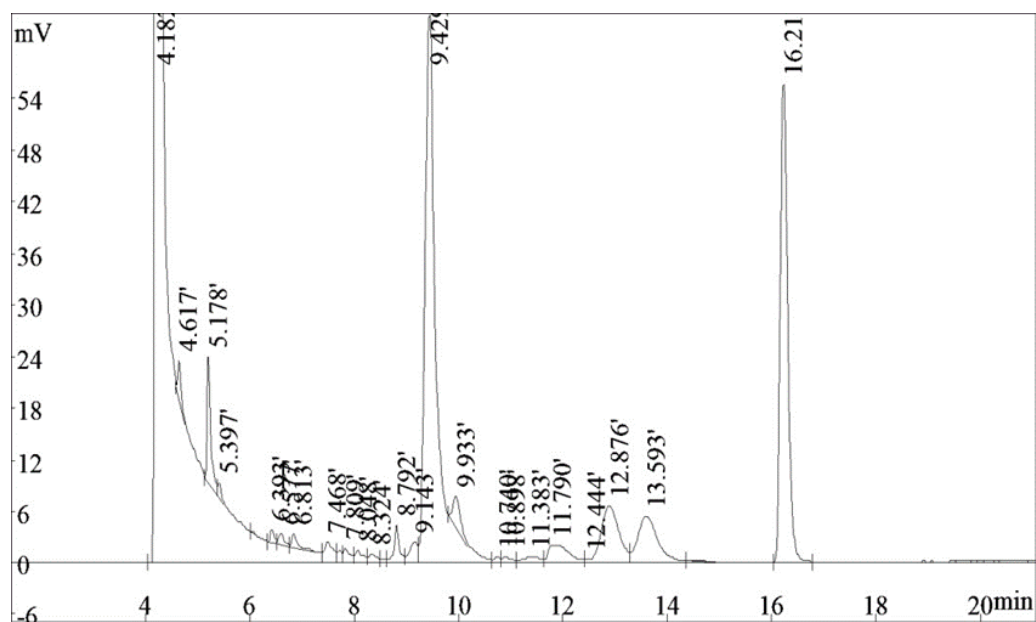


**Appendix I**. GC chromatogram of the FAMEs produced by CPTFS (direct

transformation)
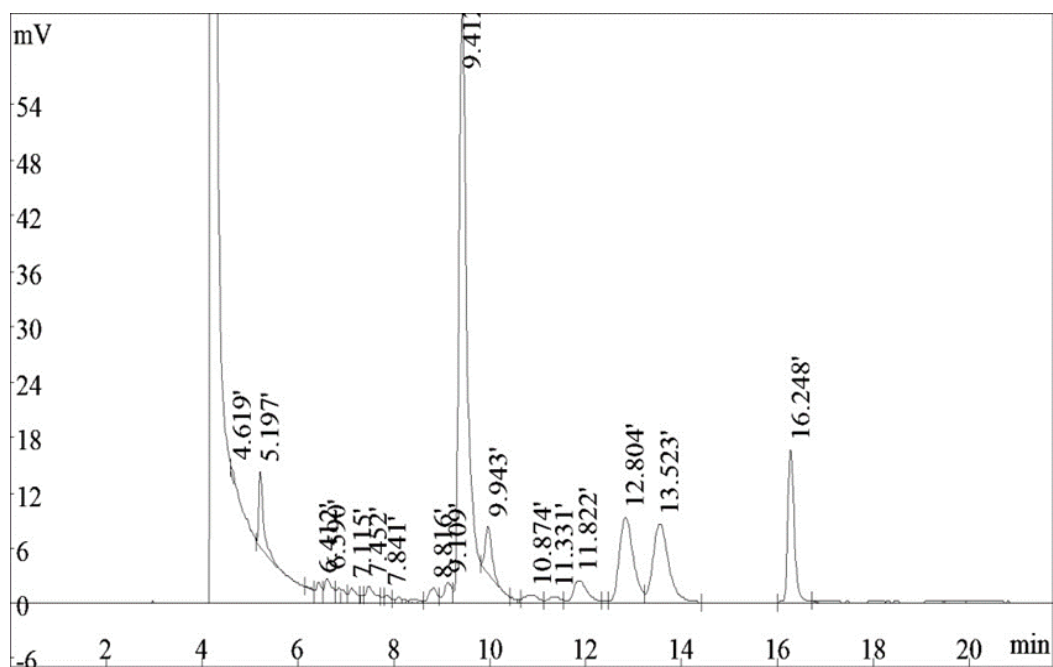
**Appendix J.** GC chromatogram of the FAMEs produced by SO$_3$-bCPHA (direct

transformation)
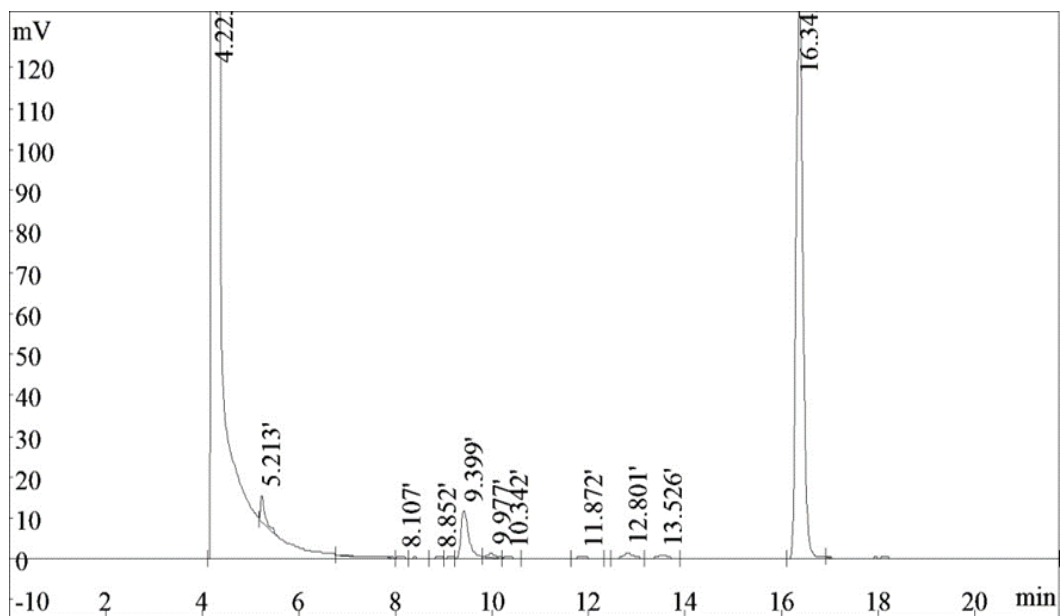


**Appendix K.** GC chromatogram of the FAMEs produced by SO$_3$-bCPMS (direct

transformation) from dry biomass
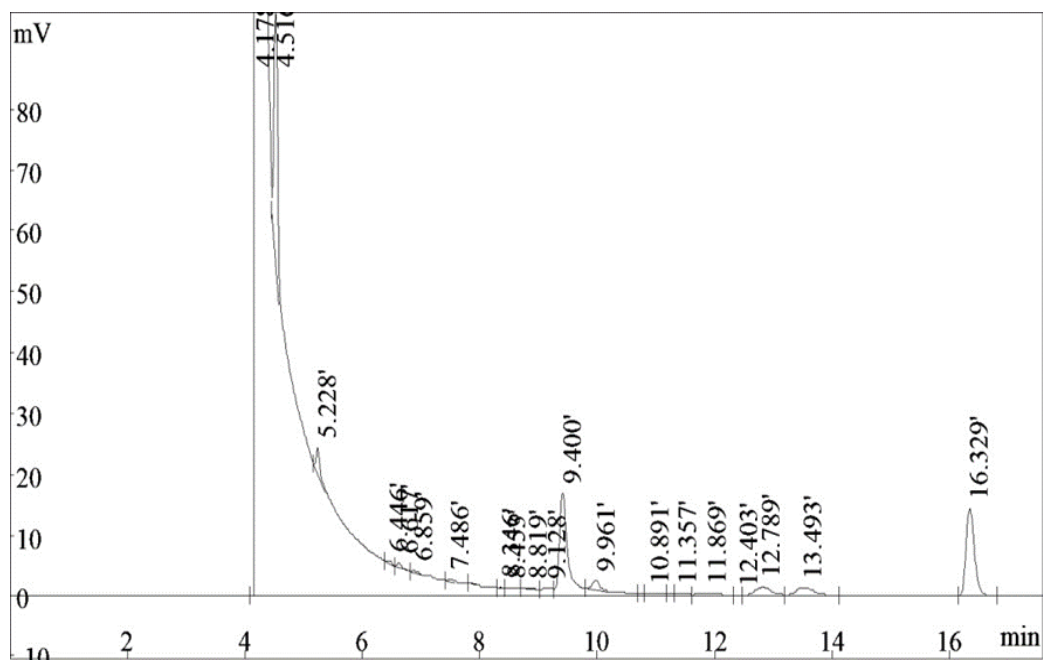
**Appendix L.** GC chromatogram of the FAMEs produced by SO$_3$-bCPMS (direct

transformation) from wet biomass
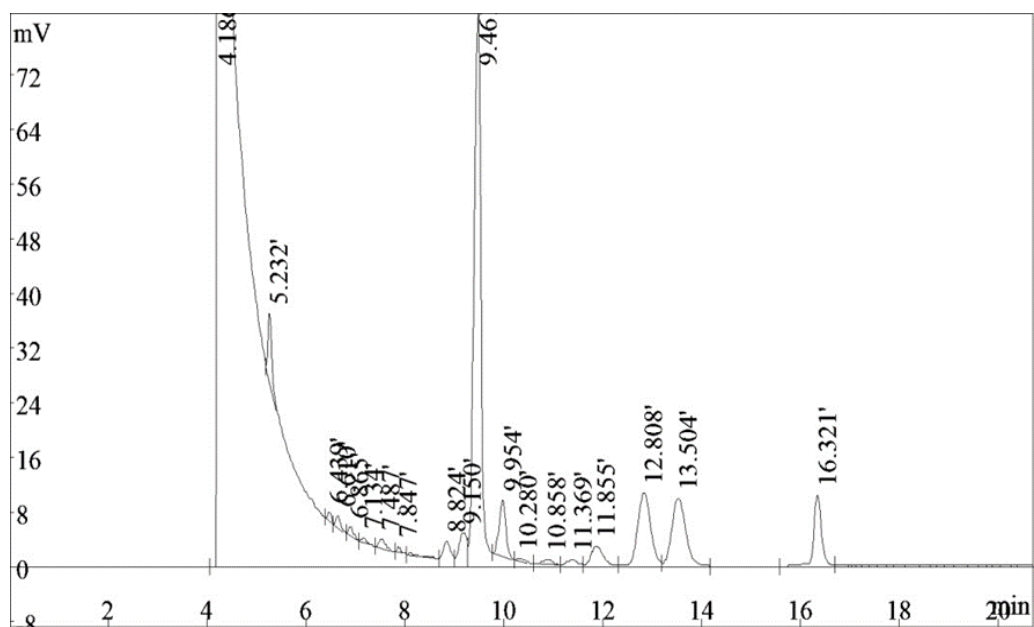


**Appendix M.** GC chromatogram of the FAMEs produced by SO$_3$-bCPSA (direct

transformation) from dry biomass
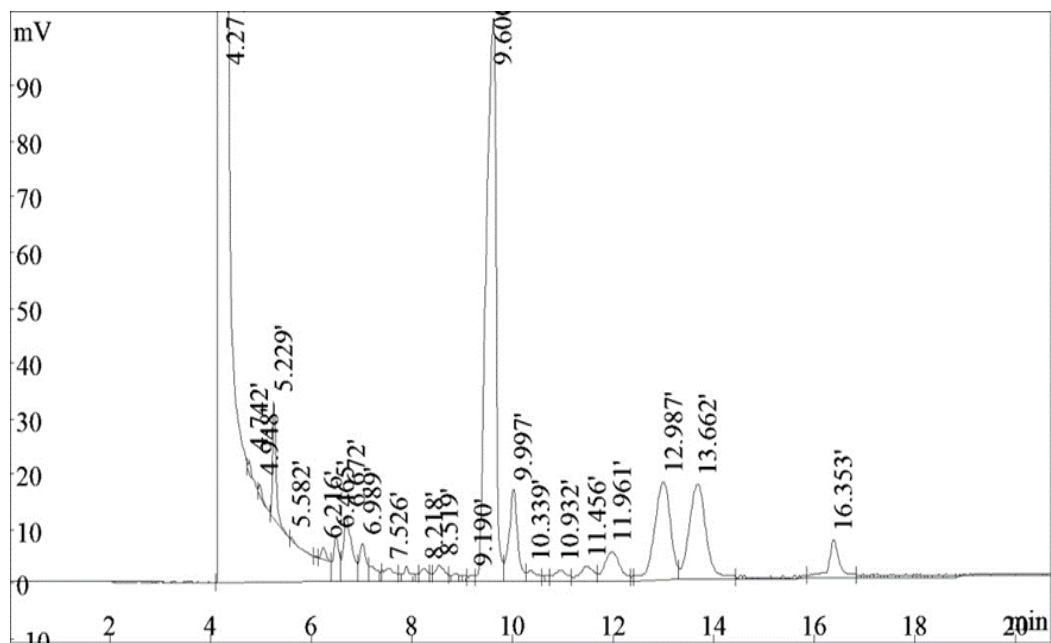
**Appendix N.** GC chromatogram of the FAMEs produced by SO₃-bCPSA (direct

transformation) from wet biomass
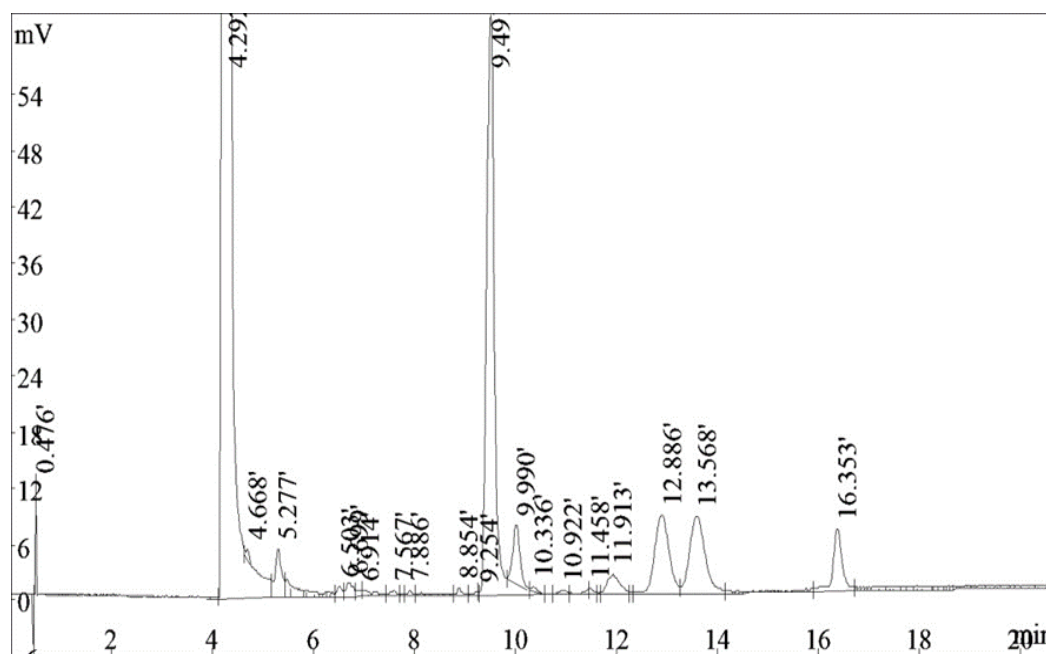


**Appendix O.** GC chromatogram of the FAMEs produced by CPAA (indirect

transformation)
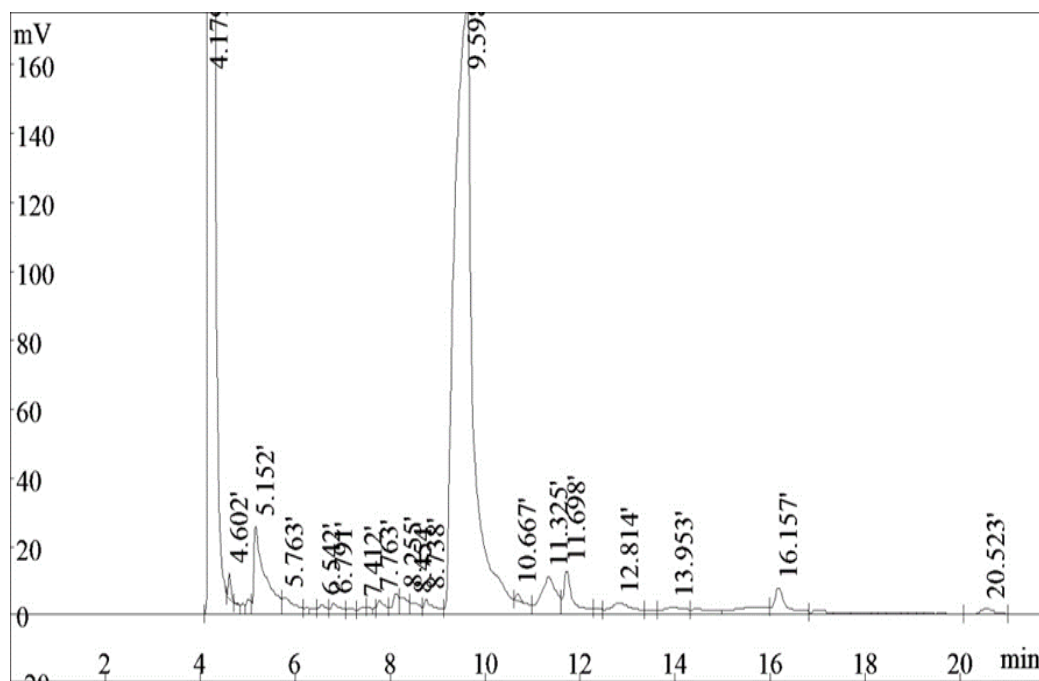
**Appendix P.** GC chromatogram of the FAMEs produced by CPHA (indirect

transformation)
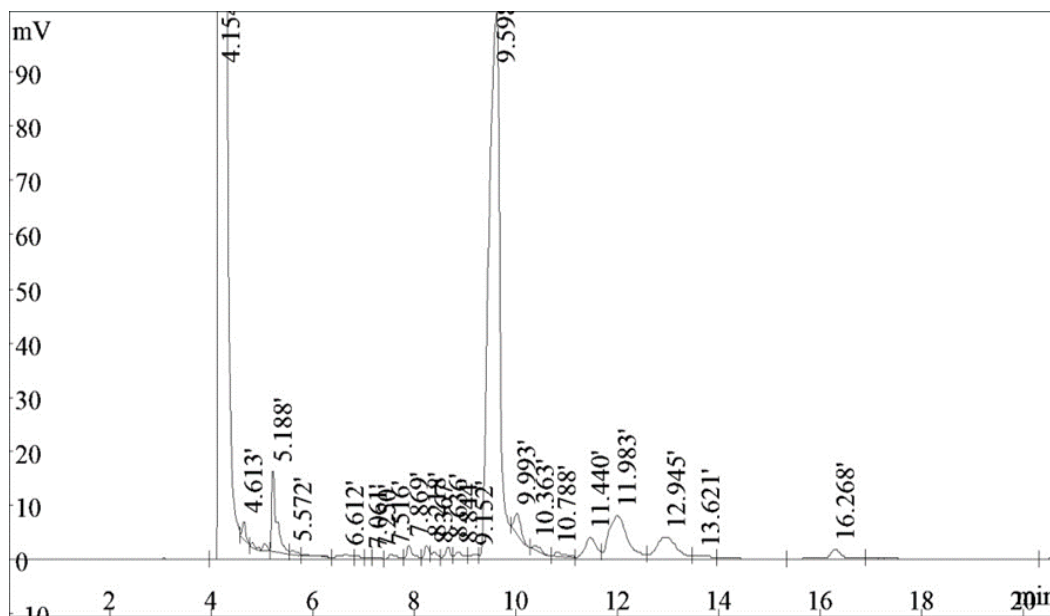


**Appendix Q.** GC chromatogram of the FAMEs produced by CPTFA (indirect

transformation)
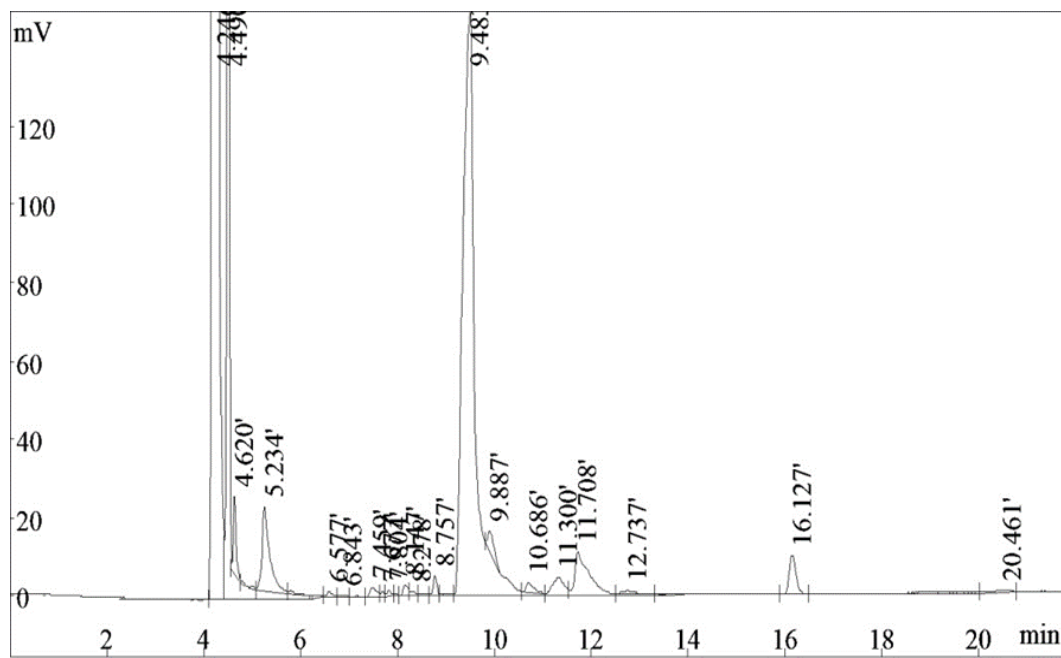
**Appendix R.** GC chromatogram of the FAMEs produced by CPSA (indirect transformation)
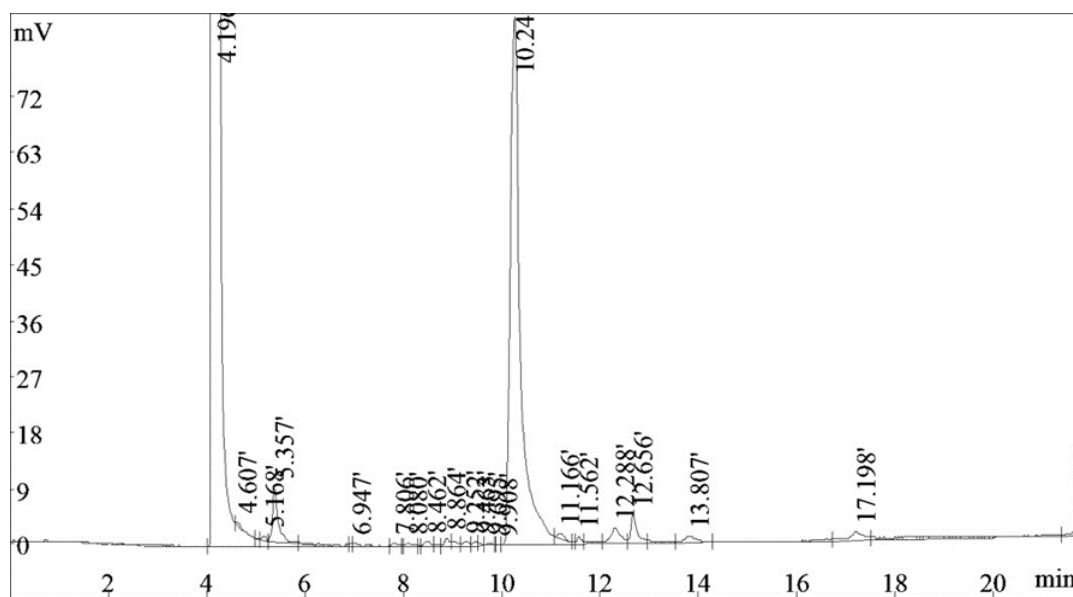


**Appendix S.** GC chromatogram of the FAMEs produced by CPMS (indirect transformation)
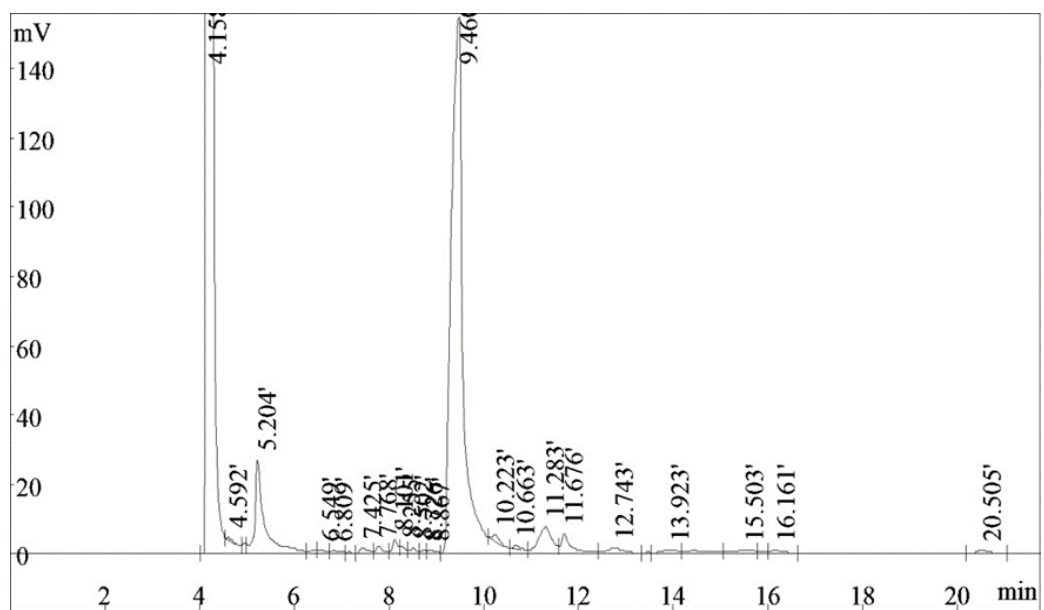
**Appendix T.** GC chromatogram of the FAMEs produced by CPTFS (indirect

transformation
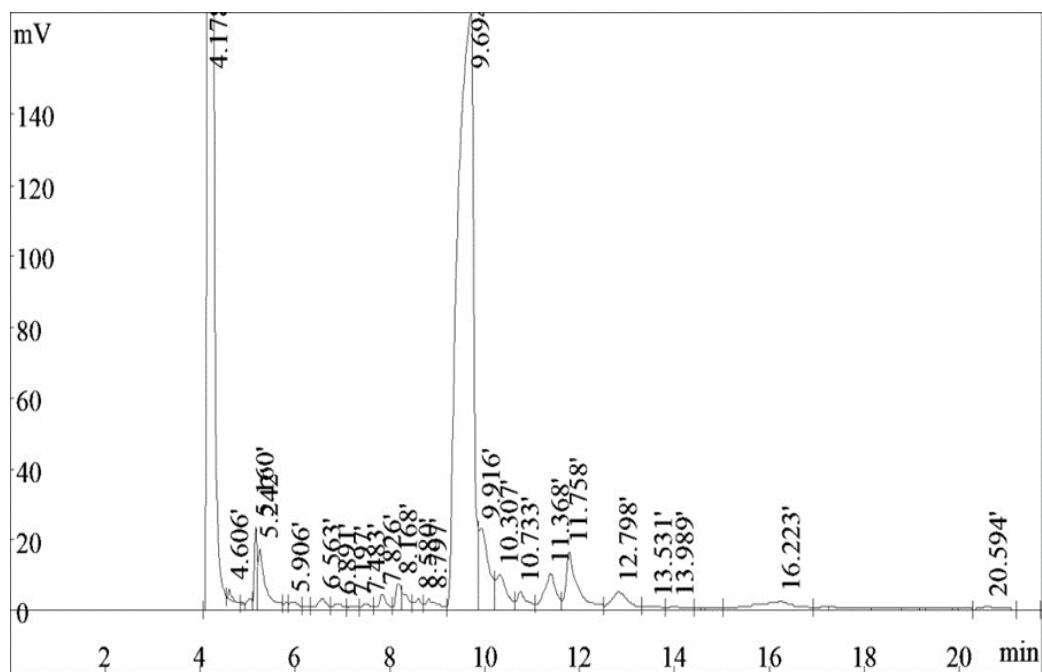
**Appendix U.** Raw data and statistical analysis of extracted lipids yields from dry and wet biomass using pure CPILs and their mixture with methanol

Raw data of extracted lipids yield % from dry biomass by CPIL at 75°C for 5h

| CPIL | Run1 | Run2 | Average | STD |
|---|---|---|---|---|
| CPAA | 9.88 | 10.45 | 10.165 | 0.40 |
| CPHA | 10.34 | 10.03 | 10.185 | 0.22 |
| CPSA | 4.5 | 5 | 4.75 | 0.35 |

Raw data of extracted lipids yield % from dry biomass by pure CPIL at 95°C for 2h

| Experimental Run | Control | | CPIL | | | | | |
|---|---|---|---|---|---|---|---|---|
| | MeOH | Hexane: MeOH | CPAA | CPTFA | CPHA | CPSA | CPTFS | CPMS |
| Run1 | 1.12 | 9.7 | 9.93 | 10.24 | 9.2 | 5 | 4.83 | 3.89 |
| Run2 | 1.5 | 9.37 | 10.33 | 9.89 | 9.33 | 5.33 | 5.61 | 4.48 |
| Average | 1.31 | 9.54 | 10.13 | 10.07 | 9.27 | 5.17 | 5.22 | 4.19 |
| STD | 0.27 | 0.23 | 0.28 | 0.25 | 0.09 | 0.23 | 0.55 | 0.42 |

Raw data of extracted lipids yield % from wet biomass by CPIL/MeOH mixture at 95°C for 2h

| CPIL | Run 1 | Run2 | Average | STD |
|---|---|---|---|---|
| Control | 4.1 | 4.18 | 4.14 | 0.06 |
| CPAA | 8.01 | 8.13 | 8.07 | 0.08 |
| CPTFA | 6 | 6.14 | 6.07 | 0.10 |
| CPHA | 5 | 5.11 | 5.06 | 0.08 |

Raw data of extracted lipids yield % from dry biomass by CPIL/MeOH mixture at 95°C for 2h

| Experimental Run | CPAA | CPTFA | CPHA | CPSA | CPTFS | CPMS |
|---|---|---|---|---|---|---|
| Run1 | 14.16 | 11.16 | 13.21 | 6.43 | 6.14 | 6.01 |
| Run2 | 14.32 | 10.97 | 13.12 | 6.23 | 6.32 | 6.11 |
| Average | 14.24 | 11.065 | 13.165 | 6.33 | 6.23 | 6.06 |
| STD | 0.11 | 0.13 | 0.06 | 0.14 | 0.13 | 0.07 |

T-test analysis of extracted lipids yield by pure CPIL compare to the control (Hexane: MeOH)

| CPIL | P-value |
|---|---|
| CPAA | 0.153218314 |
| CPTFA | 0.158850437 |
| CPHA | 0.32619118 |
| CPSA | 0.002839111 |
| CPTFS | 0.030786001 |
| CPMS | 0.010175062 |

T-test analysis of extracted lipids yield from wet biomass by CPIL/MeOH mixture compare to the control (Hexane: MeOH)

| CPIL | p-value |
|---|---|
| CPAA | 0.000805987 |
| CPTFA | 0.005044218 |
| CPHA | 0.007727526 |
| CPAA to dry control | 0.046833399 |

T-test analysis of extracted lipids yield by CPIL/MeOH mixture compare to the control (Hexane: MeOH)

| CPIL | P-value |
|---|---|
| CPAA | 0.006747991 |
| CPTFA | 0.02794087 |
| CPHA | 0.019759905 |
| CPSA | 0.007894538 |
| CPTFS | 0.009122529 |
| CPMS | 0.01911152 |

**Appendix V.** Raw data and statistical analysis of extracted lipids yields from dry and wet biomass using mixture of $SO_3$-CPILs with methanol

| Raw data of extracted lipids yield % from dry biomass by SO3-CPIL/MeOH at 95C for 2h | | | | | |
|---|---|---|---|---|---|
| IL | LIPID YIELD% | | Average | STD | |
| **SO3-CPSA** | 10 | 8 | 9 | 1.41 | |
| **SO3-CPMS** | 8 | 8 | 8 | 0 | |
| **SO3-CPHA** | 10 | 9.5 | 9.75 | 0.35 | |

| T-test analysis of extracted lipids yield by SO3-CPIL/MeOH /dry compare to the control (Hexane: MeOH) | |
|---|---|
| T TEST/ P-VALUE | |
| **SO3-CPSA** | 0.69 |
| **SO3-CPMS** | 0.07 |
| **SO3-CPHA** | 0.56 |

| Raw data of extracted lipids yield % from wet biomass by SO3-CPIL/MeOH at 95C for 2h | | | | | |
|---|---|---|---|---|---|
| IL | LIPID YIELD% | | Average | STD | |
| **SO3-CPSA** | 8 | 8 | 8 | 0.00 | |
| **SO3-CPMS** | 8 | 8 | 8 | 0 | |
| **SO3-CPHA** | 2 | 3 | 2.5 | 0.71 | |

| T-test analysis of extracted lipids yield by SO3-CPIL/MeOH /wet compare to the control (Hexane: MeOH) | |
|---|---|
| T TEST/ P-VALUE | |
| **SO3-CPSA** | 0.07 |
| **SO3-CPMS** | 0.07 |
| **SO3-CPHA** | 0.03 |

**Appendix W.** Raw data for fatty acid methyl esters (FAMEs) of the standard and which produced by CPILs (direct transesterification)

| FAME | standard | | CPAA | | | CPHA | | | CPTFA | | | CPSA | | | CPMS | | | CPTFS | | |
|---|---|---|---|---|---|---|---|---|---|---|---|---|---|---|---|---|---|---|---|---|
| | R.T | Area | R.T | Area | % | R.T | Area | % | R.T | Area | % | R.T | Area | % | R.T | Area | % | R.T | Area | % |
| C4:0 | | | | | | 4.496 | 9963 | 0.16993 | | | | | | | | | | | | |
| C6:0 | 4.612 | 626475 | | | | | | | | | | 4.64 | 7220 | 0.428145 | 4.617 | 12365 | 0.590433 | 4.619 | 1501 | 0.09244 |
| C8 | 4.98 | 519303 | 5.163 | 33491 | 1.144229 | 5.198 | 27577 | 0.470355 | 5.16 | 13483 | 3.265859 | | | | 5.178 | 57014 | 2.722438 | 5.197 | 45766 | 2.818513 |
| C10 | 5.589 | 345273 | | | | | | | | | | 5.211 | 33639 | 1.994786 | 5.397 | 7908 | 0.37761 | | | |
| C11 | 6.007 | 182952 | 6.334 | 196578 | 6.716138 | | | | | | | 6.442 | 26130 | 1.549504 | 6.393 | 30065 | 1.435614 | 6.412 | 18874 | 1.162361 |
| C12 | 6.505 | 305972 | | | | 6.466 | 24033 | 0.409908 | 6.549 | 7188 | 1.741081 | 6.632 | 41085 | 2.436333 | 6.577 | 38720 | 1.848893 | 6.59 | 31312 | 1.928359 |
| C13 | 7.08 | 156594 | | | | 6.858 | 15691 | 0.267627 | | | | 7.19 | 18590 | 1.102384 | 6.813 | 36111 | 1.724312 | 7.115 | 18807 | 1.158235 |
| C14 | 7.73 | 282067 | | | | 7.521 | 7050 | 0.120245 | | | | 7.511 | 12693 | 0.752693 | 7.809 | 28368 | 1.354582 | 7.841 | 7728 | 0.475931 |
| C14:1 | 8.336 | 106778 | | | | | | | | | | 7.856 | 5244 | 0.310968 | 8.048 | 14050 | 0.670892 | | | |
| C15 | 8.448 | 172834 | | | | | | | | | | 8.835 | 7529 | 0.446468 | 8.792 | 28556 | 1.363559 | | | |
| C15:1 | 9.107 | 102287 | | | | | | | | | | | | | 9.143 | 26530 | 1.266816 | 9.109 | 25408 | 1.564759 |
| C16 | 9.296 | 445206 | | | | 9.444 | 330330 | 5.634126 | 9.361 | 61005 | 14.77666 | 9.617 | 917868 | 54.4294 | 9.429 | 927725 | 44.29918 | 9.412 | 816612 | 50.2913 |
| C16:1 | 9.844 | 133031 | | | | 9.982 | 59981 | 1.023039 | 9.907 | 8771 | 2.124516 | 10.039 | 46026 | 2.729333 | 9.933 | 30235 | 1.443731 | 9.943 | 43568 | 2.683149 |
| C17 | 10.204 | 152333 | | | | | | | | | | 11.051 | 6539 | 0.387761 | 10.74 | 5124 | 0.244673 | | | |
| C17:1 | 10.797 | 132822 | | | | | | | | | | | | | 10.898 | 8239 | 0.393415 | 10.874 | 19318 | 1.189705 |
| C18 | 11.413 | 267306 | | | | | | | | | | | | | 11.383 | 10443 | 0.498657 | 11.331 | 14036 | 0.864411 |
| C18:1 | 11.837 | 390909 | | | | | | | 11.953 | 1277 | 0.309316 | 11.87 | 8634 | 0.511995 | 11.79 | 18758 | 0.895701 | 11.822 | 51253 | 3.156432 |
| C18:2 | 12.358 | 128877 | | | | | | | | | | 12.154 | 48880 | 2.898575 | | | | | | |
| C18:2 | 12.718 | 152969 | | | | 13.029 | 80517 | 1.373302 | 12.891 | 11586 | 2.806367 | | | | 12.876 | 153823 | 7.3451 | 12.804 | 185158 | 11.40301 |
| C18:3 | 13.473 | 113010 | | | | | | | | | | 13.172 | 180623 | 10.71091 | 13.593 | 141355 | 6.749749 | 13.523 | 195237 | 12.02373 |
| C18:3 | 14.008 | 144722 | | | | 13.743 | 66538 | 1.134876 | 13.617 | 5818 | 1.409239 | 13.887 | 185676 | 11.01055 | | | | | | |
| C20:0 | 15.137 | 395194 | | | | | | | | | | | | | | | | | | |
| C20:1 | | | 16.32 | 2696881 | 92.13963 | 16.418 | 5241341 | 89.39659 | 16.204 | 303719 | 73.56696 | 16.409 | 139970 | 8.300195 | 16.217 | 511954 | 24.44598 | 16.248 | 149186 | 9.187665 |
| C22:0 | 17.396 | 501236 | | | | | | | | | | | | | | | | | | |
| C23:0 | 19.192 | 204064 | | | | | | | | | | | | | | | | | | |
| C24:0 | | | | | | | | | | | | | | | 20.623 | 6883 | 0.328666 | | | |
| C24:1 | 22.625 | 900303 | | | | | | | | | | | | | | | | | | |
| Total | | 6862517 | | 2926950 | 7.860367 | | 5863021 | 1.438064 | | 412847 | 5.00694 | | 1686346 | 9 | | 2094226 | 14 | | 1623764 | 10 |

R.T = Retention time. % = percentage yield of each FAME based on total area.

**Appendix X.** Raw data for fatty acid methyl esters (FAMEs) produced by $SO_3$-CPILs (direct transesterification)

| FAME | standard R.T | Area | SO3-CPHA R.T | Area | % | SO3-CPMS/DRY R.T | Area | % | SO3-CPMS/WET R.T | Area | % | SO3-CPSA/DRY R.T | Area | % | SO3-CPSA/WET R.T | Area | % |
|---|---|---|---|---|---|---|---|---|---|---|---|---|---|---|---|---|---|
| C4:0 | | | | | | | | | | | | | | | | | |
| C6:0 | 4.612 | 626475 | | | | 4.516 | 138983 | 23.4 | | | | 4.742 | 4093 | 0.135992 | 4.668 | 3010 | 0.23901124 |
| C8 | 4.98 | 519303 | | | | | | | | | | 4.948 | 6503 | 0.216066 | | | |
| C10 | 5.589 | 345273 | 5.213 | 27429 | 1.906989 | 5.228 | 14355 | 2.4 | 5.232 | 40628 | 2.453044 | 5.229 | 79925 | 2.655557 | 5.277 | 47556 | 3.77621878 |
| C11 | 6.007 | 182952 | | | | 6.446 | 1664 | 0.3 | 6.439 | 6441 | 0.388896 | 6.465 | 62965 | 2.092051 | 6.503 | 9930 | 0.78849887 |
| C12 | 6.505 | 305972 | | | | 6.617 | 3432 | 0.6 | 6.61 | 9870 | 0.595932 | 6.672 | 139775 | 4.64411 | 6.699 | 16901 | 1.3420362 |
| C13 | 7.08 | 156594 | | | | 6.859 | 2444 | 0.4 | 6.865 | 7544 | 0.455493 | 6.989 | 62606 | 2.080123 | 6.914 | 6317 | 0.50160598 |
| C14 | 7.73 | 282067 | | | | 7.486 | 1823 | 0.3 | 7.487 | 11754 | 0.709685 | 7.526 | 40807 | 1.355838 | 7.567 | 7294 | 0.57918538 |
| C14:1 | 8.336 | 106778 | | | | 8.346 | 4339 | 0.7 | 7.847 | 8656 | 0.522633 | 8.218 | 25760 | 0.855892 | | | |
| C15 | 8.448 | 172834 | 8.852 | 2907 | 0.002021 | 8.453 | 14674 | 2.5 | 8.824 | 46567 | 2.81163 | 8.519 | 40421 | 1.343013 | 8.854 | 7117 | 0.56513056 |
| C15:1 | 9.107 | 102287 | | | | 9.128 | 18815 | 3.2 | 9.15 | 58223 | 3.515398 | 9.19 | 8725 | 0.002899 | 9.254 | 719 | 0.05709272 |
| C16 | 9.296 | 445206 | 9.399 | 126728 | 8.810706 | 9.4 | 161763 | 27 | 9.461 | 777183 | 47 | 9.6 | 1281049 | 42.56364 | 9.491 | 640689 | 50.8743762 |
| C16:1 | 9.844 | 133031 | 9.977 | 17177 | 1.194223 | 9.961 | 34751 | 6 | 9.954 | 69357 | 4 | 9.997 | 185405 | 6.160195 | 9.99 | 56172 | 4.46037853 |
| C17 | 10.204 | 152333 | 10.342 | 2854 | 0.198423 | | | | 10.28 | 18345 | 1.107637 | 10.339 | 25333 | 0.841705 | 10.336 | 3136 | 0.24901636 |
| C17:1 | 10.797 | 132822 | | | | | | | 10.858 | 21374 | 1.290523 | 10.932 | 32859 | 1.091761 | 10.922 | 7018 | 0.5572694 |
| C18 | 11.413 | 267306 | | | | | | | 11.369 | 19271 | 1.163548 | 11.456 | 48014 | 1.595295 | 11.458 | 4999 | 0.39694923 |
| C18:1 | 11.837 | 390909 | 11.872 | 4403 | 0.3 | 11.869 | 3324 | 1 | 11.855 | 53581 | 3.235122 | 11.961 | 103583 | 3.441609 | 11.913 | 37093 | 2.94539665 |
| C18:2 | 12.358 | 128877 | | | | | | | | | | | | | | | |
| C18:2 | 12.718 | 152969 | 12.801 | 14866 | 1 | 12.789 | 27463 | 5 | 12.808 | 195152 | 11.78292 | 12.987 | 376150 | 12.49782 | 12.886 | 161864 | 12.8529287 |
| C18:3 | 13.473 | 113010 | 13.526 | 17411 | 1.2 | 13.493 | 32464 | 5 | 13.504 | 196071 | 11.83841 | 13.662 | 385460 | 12.80715 | 13.568 | 168127 | 13.3502468 |
| C18:3 | 14.008 | 144722 | | | | | | | | | | | | | | | |
| C20:0 | 15.137 | 395194 | | | | | | | | | | | | | | | |
| C20:1 | | | 16.343 | 1224566 | 85 | 16.329 | 134790 | 23 | 16.321 | 116211 | 7.016606 | 16.353 | 100293 | 3.332297 | 16.353 | 81413 | 6.4646585 |
| C22:0 | 17.396 | 501236 | | | | | | | | | | | | | | | |
| C23:0 | 19.192 | 204064 | | | | | | | | | | 54 | | | | | |
| C24:0 | | | | | | | | | | | | | | | | | |
| C24:1 | 22.625 | 900303 | | | | | | | | | | | | | | | |
| Total | | 6862517 | | 1438341 | 2 | | 595084 | 34 | | 1656228 | 13.85087 | | 3009726 | 17.31501 | | 1259355 | 8.65506549 |

**Appendix Y.** Comparisons between experimental and predicted values of physicochemical properties of *S. platensis* biodiesel by means of the average absolute deviation (AAD).

| Methods | Calculated Values | | | | | | | | AAD | | | | | | | | | | | | |
|---|---|---|---|---|---|---|---|---|---|---|---|---|---|---|---|---|---|---|---|---|---|
| | CP | PP | CFPP | Ø | ή | ρ | δ | FP | CP | PP | Ø | ή | ρ | | | | Reproducibility(ρ) | δ | | | Reproducibility (δ) | FP |
| CPAA | -4.99 | -12.24 | -7.82 | 67.7 | 0.24 | 0.87 | 40 | 444 | 66.3 | 36 | 3.29 | 94.4186 | 1.16 | 2.25 | 0 | | 1.12382 | 3.382 | 2.83 | 4.17 | 0.67276873 | 134.92 |
| CPHA | 0.96 | -5.79 | -2.05 | 68.6 | 0.33 | 0.87 | 40.2 | 457 | 132 | 35.67 | 2 | 92.32558 | 1.16 | 2.25 | 0 | | 1.12382 | 2.899 | 3.34 | 4.69 | 0.931623428 | 141.8 |
| CPSA | -1.46 | -8.39 | -4.39 | 58.9 | 2.67 | 0.87 | 39.3 | 382 | 51.3 | 6.778 | 2.97 | 37.90698 | 1.16 | 2.25 | 0 | | 1.12382 | 5.072 | 1.03 | 2.34 | 2.06283736 | 102.12 |
| CPMS | -1.98 | -8.97 | -4.9 | 63 | 2.33 | 0.87 | 39.3 | 383 | 34 | 0.333 | 3.79 | 45.81395 | 1.16 | 2.25 | 0 | | 1.12382 | 5.072 | 1.03 | 2.34 | 2.06283736 | 102.65 |
| CPTFA | 1.67 | -5.01 | -1.35 | 66.64 | 0.85 | 0.87 | 39.8 | 430 | 156 | 44.33 | 9.79 | 80.23256 | 1.16 | 2.25 | 0 | | 1.12382 | 3.865 | 2.31 | 3.65 | 0.839507652 | 127.51 |
| CPTFS | -1.2 | -8.13 | -4.14 | 60.06 | 2.46 | 0.87 | 39.3 | 381 | 60 | 9.667 | 1.05 | 42.7907 | 1.16 | 2.25 | 0 | | 1.12382 | 5.072 | 1.03 | 2.34 | 2.06283736 | 101.59 |
| SO3-CPHA | 0.76 | -6 | -2.24 | 68.68 | 0.52 | 0.87 | 40.2 | 452 | 125 | 33.33 | 1.89 | 87.90698 | 1.16 | 2.25 | 0 | | 1.12382 | 2.899 | 3.34 | 4.69 | 0.931623428 | 139.15 |
| SO3-CPMS/dry | -1.15 | -8.07 | -4.09 | 49.4 | 1.42 | 0.84 | 35.1 | 277 | 61.7 | 10.33 | 0.9 | 66.97674 | 2.33 | 5.62 | 3.4 | 1.2 | 1.88355 | | | | | 46.561 |
| SO3-CPMS/wet | -1.78 | -8.76 | -4.7 | 60.27 | 2.44 | 0.87 | 39.4 | 387 | 40.7 | 2.667 | 0.71 | 43.25581 | 1.16 | 2.25 | 0 | | 1.12382 | 4.831 | 1.29 | 2.6 | 1.792055554 | 104.76 |
| SO3-CPSA/dry | -1.98 | -8.97 | -4.9 | 58.52 | 2.4 | 0.87 | 39.2 | 375 | 34 | 0.333 | 3.59 | 44.18605 | 1.16 | 2.25 | 0 | | 1.12382 | 5.314 | 0.77 | 2.08 | 2.337947345 | 98.413 |
| SO3-CPSA/wet | -1.7 | -8.67 | -4.63 | 59.55 | 2.49 | 0.87 | 39.3 | 383 | 43.3 | 3.667 | 1.89 | 42.09302 | 1.16 | 2.25 | 0 | | 1.12382 | 5.072 | 1.03 | 2.34 | 2.06283736 | 102.65 |
| Kenyan standard | | | | | | | 40.5 | | | | | | | | | | | 2.174 | 5.47 | 4.11 | 1.656412888 | |
| SUM | | | | | | | | | 804 | 183.11 | 31.86 | 677.91 | 46.70 | | | | 13.12 | 104.48 | | | 17.41 | 1202.12 |
| AVERAGE | | | | | | | | | 73.12 | 16.65 | 2.90 | 61.63 | 1.37 | | | | 1.19 | 3.17 | | | 1.58 | 109.28 |

**Appendix Z.** Raw data for (FAMEs) produced by conventional method and CPILs (indirect transesterification)

| FAME | standard R.T | standard Area | conventional R.T | conventional Area | conventional % | CPAA R.T | CPAA Area | CPAA % | CPHA R.T | CPHA Area | CPHA % | CPTFA R.T | CPTFA Area | CPTFA % | CPSA R.T | CPSA Area | CPSA % | CPMS R.T | CPMS Area | CPMS % | CPTFS R.T | CPTFS Area | CPTFS % |
|---|---|---|---|---|---|---|---|---|---|---|---|---|---|---|---|---|---|---|---|---|---|---|---|
| C4:0 | | | | | | | | | | | | 4.49 | 1202440 | 25.75255 | | | | | | | | | |
| C6:0 | 4.612 | 626475 | 4.567 | 9503 | 0.757939 | 4.602 | 20844 | 0.33014482 | 4.613 | 10633 | 0.469565 | 4.62 | 56896 | 1.218537 | 4.607 | 2574 | 0.179955 | 4.592 | 3314 | 0.093133 | 4.606 | 6418 | 0.114905 |
| C8 | 4.98 | 519303 | 5.166 | 116176 | 9.265949 | 5.152 | 406076 | 6.43177348 | 5.188 | 58522 | 2.584395 | 5.234 | 214796 | 4.600267 | 5.168 | 3519 | 0.246023 | 5.204 | 362296 | 10.18155 | 5.16 | 74194 | 1.328332 |
| C10 | 5.589 | 345273 | | | | 5.763 | 94643 | 1.49903549 | 5.573 | 62005 | 2.738208 | | | | 5.357 | 65130 | 4.553412 | | | | 5.242 | 170348 | 3.049824 |
| C11 | 6.007 | 182952 | | | | | | | | | | | | | | | | | | | | | |
| C12 | 6.505 | 305972 | 6.492 | 2029 | 0.161829 | 6.542 | 37284 | 0.59053537 | 6.612 | 6296 | 0.278038 | 6.577 | 15342 | 0.328578 | | | | 6.549 | 14172 | | 6.563 | 44823 | 0.802488 |
| C13 | 7.08 | 156594 | 7.379 | 20455 | 1.631447 | 6.791 | 50035 | 0.79249644 | | | | 6.843 | 7523 | 0.001611 | 6.947 | | | 7.425 | 21181 | 0.595246 | 7.197 | 9887 | 0.177012 |
| C14 | 7.73 | 282067 | 7.733 | 7106 | 0.566759 | 7.763 | 54097 | 0.85683382 | 7.869 | 16762 | 0.740228 | 7.456 | 27259 | 0.583804 | 7.806 | 10199 | 0.713039 | 7.768 | 20295 | 0.570347 | 7.826 | 46808 | 0.838027 |
| C14:1 | 8.336 | 106778 | | | | 8.255 | 56519 | 0.89519549 | 8.218 | 17991 | 0.794502 | 8.147 | 21458 | 0.459564 | | | | 8.101 | 30114 | 0.846289 | 8.168 | 60774 | 1.088067 |
| C15 | 8.448 | 172834 | 8.683 | 32204 | 2.568522 | 8.454 | 50641 | 0.00802095 | 8.367 | 10236 | 0.452033 | 8.278 | 11558 | 0.247537 | | | | 8.249 | 17750 | 0.498826 | 8.58 | 32764 | 0.58659 |
| C15:1 | 9.107 | 102287 | 8.996 | 18304 | 1.459888 | | | | 9.152 | 12037 | 0.531567 | 8.757 | 26334 | 0.563993 | 9.252 | 6185 | 0.43241 | | | | | | |
| C16 | 9.296 | 445206 | 9.286 | 767106 | 61.18273 | 9.598 | 4727324 | 74.8753364 | 9.598 | 1560071 | 68.89443 | 9.483 | 2553604 | 54.69031 | 10.248 | 1176146 | 82.2275 | 9.46 | 2658898 | 74.72261 | 9.694 | 3716468 | 66.53776 |
| C16:1 | 9.844 | 133031 | 9.818 | 40977 | 3.268238 | | | | 9.993 | 28429 | 1.255456 | 9.887 | 42581 | 0.911954 | | | | | | | 9.916 | 310848 | 5.565265 |
| C17 | 10.204 | 152333 | | | | | | | 10.363 | 9228 | 0.407519 | | | | 11.166 | 8155 | 0.570138 | 10.223 | 15179 | 0.426573 | 10.307 | 164661 | 2.948007 |
| C17:1 | 10.797 | 132822 | 10.618 | 9967 | 0.794947 | 10.667 | 13011 | 0.20607917 | 10.788 | 22333 | 0.98625 | 10.686 | 23790 | 0.509508 | 11.562 | 9598 | 0.671022 | 10.663 | 6820 | 0.191661 | 10.733 | 77263 | 1.383278 |
| C18 | 11.413 | 267306 | 11.268 | 18834 | 1.502159 | 11.325 | 246737 | 3.90802828 | 11.44 | 69272 | 3.059127 | 11.3 | 82622 | 1.769508 | 12.288 | 41906 | 2.92976 | 11.283 | 159246 | 4.475266 | 11.368 | 180307 | 3.228125 |
| C18:1 | 11.837 | 390909 | 11.662 | 72794 | 5.805893 | 11.698 | 176793 | 2.80019634 | 11.983 | 207684 | 9.171551 | 11.708 | 252130 | 5.399846 | 12.656 | 42958 | 3.003308 | 11.676 | 81331 | 2.285633 | 11.758 | 279124 | 4.997295 |
| C18:2 | 12.358 | 128877 | 12.175 | 3920 | 0.312651 | | | | | | | | | | | | | | | | | | |
| C18:2 | 12.718 | 152969 | 12.69 | 59458 | 4.742243 | 12.814 | 120451 | 1.90780432 | 12.945 | 120465 | 5.319865 | 12.737 | 20141 | 0.431358 | | | | 12.743 | 46755 | 1.313949 | 12.798 | 135155 | 2.419747 |
| C18:3 | 13.473 | 113010 | 13.423 | 23064 | 1.839535 | | | | 13.621 | 20639 | 0.911441 | | | | | | | | | | 13.531 | 37927 | 0.679026 |
| C18:3 | 14.008 | 144722 | | | | 13.953 | 74343 | 1.17750701 | | | | | | | 13.807 | 25389 | 1.775013 | 13.923 | 32377 | 0.909886 | 13.989 | 23723 | 0.424725 |
| C20:0 | 15.137 | 395194 | | | | | | | | | | | | | | | | 15.503 | 37971 | 1.067093 | | | |
| C20:1 | 16.127 | 118325 | 16.109 | 37139 | 2.962127 | 16.157 | 135885 | 2.152261 | 16.268 | 31834 | 1.405824 | 16.127 | 90912 | 1.947054 | | | | 16.161 | 23689 | 0.665728 | 16.223 | 175395 | 3.140183 |
| C22:0 | 17.396 | 501236 | | | | | | | | | | | | | 17.198 | 29919 | 2.091717 | | | | | | |
| C23:0 | 19.192 | 204064 | | | | | | | | | | | | | | | | | | | | | |
| C24:0 | | | 20.477 | 14759 | 1.177146 | 20.523 | 48910 | 0.77467775 | | | | 20.461 | 19821 | 0.424505 | 21.613 | 8678 | 0.606702 | 20.505 | 26970 | 0.757934 | 20.594 | 38615 | 0.691343 |
| C24:1 | 22.625 | 900303 | | | | | | | | | | | | | | | | | | | | | |
| Total | | 6980842 | | 1253795 | | | 6313593 | | | 2264437 | | | 4669207 | | | 1430356 | | | 3558358 | | | 5585502 | |

**Research Outputs of this Study**

**<u>Patents</u>**

1.  Synthesis of novel caprolactam ionic liquids (KE/P/2021/3907).

2.  Production of biodiesel from microalgae in a single extraction and transesterification step using caprolactam-based ionic liquids (KE/P/2021/3909).

**<u>Publications</u>**

1.  Naiyl R. A., Kengara F. O., Kiriamiti K. H., Ragab Y. A. 2022. Lipid extraction from microalgae using pure caprolactam-based ionic liquids and with organic co-solvent. PeerJ Analytical Chemistry 4:e13 DOI 10.7717/peerj-achem.13.

2.  Naiyl R. A., Kengara F. O., Kiriamiti K. H., Ragab Y. A. 2021. Synthesis and characterization of caprolactam-based ionic liquids as green solvents. Asian Journal of Applied Chemistry Research 8(May):74–87 DOI 10.9734/AJACR/2021/v8i430201.

**<u>Workshop</u>**

1.  Attended and presented a paper at the Royal Society-DFID Africa Capacity Building Initiative workshop under the theme "Advances in Sustainable Energy Materials for Africa II", at Kisumu Hotel in Kisumu from $19^{th}$ – $20^{th}$ Sept. 2019.